Transport boundaries for pneumatic conveying [manuscipt]

Jianglin Yi
University of Wollongong

TRANSPORT BOUNDARIES FOR PNEUMATIC CONVEYING

A thesis submitted in fulfilment of the requirements

for the award of the degree of

DOCTOR OF PHILOSPHY

from

UNIVERSITY OF WOLLONGONG

bY

JIANGLIN YI

B.Sc.(U.TSINGHUA), M.Sc.(U.TSINGHUA)

FACULTY OF ENGINEERING, WOLLONGONG UNIVERSITY

2001

CERTIFICATION

I, Jianglin Yi, declare that this thesis, submitted in fulfilment of the requirements for the award of Doctor of Philosophy, in the Faculty of Engineering, University of Wollongong, is wholly my own work unless otherwise referenced or acknowledged. The document has not been submitted for qualifications at any other academic institution.

Jianglin Yi

9 July, 2001

ACKNOWLEDGMENTS

" I believe you will make an excellent contribution to this Centre", I still very clearly remember what my supervisor told me when I commenced my PhD candidate. Now my PhD candidate is approaching the end and I am quite confident and proud to say:" Yes I did it". Also it is with great pleasure and gratitude that I acknowledge the excellent supervision and constant encouragement of my supervisor, A/Prof. P W Wypych, throughout the duration of this work.

I gratefully acknowledge that University of Wollongong provided UPA scholarship and Australian Government provided OPRS scholarship.

Acknowledgement also is made to the staff of the Centre of Bulk Solids and Particulate Technologies, especially David Hastie, who conducted the conveying tests of this project.

I would like to thank Dr. Renhu Pan, who helped me come to Australia and gave me a lot of support during my PhD candidate.

Finally, special acknowledgement is made to my family for their love, encouragement and unfailing support.

SUMMARY

Pneumatic conveying is being selected for an increasing number of industrial applications and products and is playing a more vital and integral role in the transportation of solid materials such as plastic pellets, grain and chemicals. However, despite all the minimum conveying velocity research (one of the operating boundaries for pneumatic conveying) that has been undertaken for several decades, the wide scatter and contradictions in the predictions of the minimum conveying velocity for dilute phase pneumatic conveying exist yet, determination of the operating boundaries for pneumatic conveying (mainly maximum conveying velocity for dense phase and minimum conveying velocity for dilute phase) still has been one of the most important tasks to be solved for the design, optimising and upgrade of pneumatic conveying systems as a consequence of that the mechanisms involved in the formation of boundaries between dilute-phase and dense-phase pneumatic conveying through a horizontal pipeline have not been well explored.

Saltation velocity was investigated initially in this thesis and then the emphasis was placed on the transition between dilute-phase and dense-phase. With careful observations, it is found that pneumatic conveying of granular solid materials through a horizontal pipeline can exhibit five different flow modes (as the air velocity is decreased): fully suspended flow; strand flow; stable or unstable strand flow over a stationary layer for low solid mass flow rates; stable or unstable strand flow over a slowly moving bed for high solid mass flow rates; low-velocity slug-flow. The pressure fluctuations within the unstable zone result from the flow mode alternation

between a strand flow over a stationary layer (or slowly moving bed) and slug flow starting at the inlet due to a decrease in air velocity. The first slug moves quickly at a relatively high velocity and picks up a relatively thick stationary layer in front of it but only deposits a small amount of the material behind it. The increase in slug length and large increase in pressure cause severe pressure fluctuations and pipeline vibrations. Two different flow modes may exist simultaneously in the conveying pipeline: strand flow over a stationary layer or slowly moving bed near the feed point followed by the dilute-phase (suspension) flow of particles. For the latter, material erodes away from the end of the stationary layer or slowly moving bed and is conveyed in the form of small dunes (or pulsating strand flow).

Based on the mass balance, force balance, momentum balance and the unstable flow forming mechanism, a theoretical three-layer model for the prediction of the transition zone boundaries has been established. With stability analysis, the boundaries of the transition zone in the state diagram have been identified, and have been found to agree very well with experimental data. According to the model established, the discussion on the influence of design parameters of particle and bulk properties of the material being conveyed and pipe wall properties on boundaries in the state diagram has been conducted.

The discussion on the operating boundaries for pneumatic conveying of granular materials has been extended to conveying of powder materials and a principle for classification of granular materials and powder materials, which have different flow mode in PCC, has been proposed.

The research also has been carried out on the pressure drop prediction for pneumatic conveying of granular materials in the form of low-velocity slug-flow in order to have

a perfect PCC state diagram. A new approach for the direct measurement of stress transmission factor has been developed in this thesis. The effect of the weight of the granular material in the slug on pressure drop is taken in account according to the experimental test results. The model for pressure drop prediction also includes a modified equation for the frontal force of the moving slug – allowing for momentum balance of accelerating particles and the additional force from the stationary layer to resist the movement. The modelling predictions agree very well with test results obtained on poly pellets conveyed through 98 mm and 60.3 mm ID horizontal stainless steel pipelines, each 21m in length.

TABLE OF CONTENTS

LIST OF FIGURES

LIST OF TABLES

NOMENCLATURE

A	cross-sectional area of pipe, m^2
B	Model constant for Equation 2.3.15
c	Constant
C_1	Constant for Equation 12.8.4
C_2	Constant for Equation 12.8.4
d_p	Particle diameter, m
D	Pipe internal diameter, m
f_r	Friction factor in Equation 2.3.9
f_p	Particle-particle friction factor
f_w	Particle-wall friction factor
F	Force, N
F_{meter}	Output of force meter, N
F_{min}	Froude number at minimum transport velocity, $F_{min}=U_{min}\,(g\,D)^{-0.5}$
$F_{lateral}$	Lateral force along slug, N
F_{ri}	Non-dimension friction number

F_{slug} Total resistance force on slug, N

F_{weight} Weight force of slug, N

g Gravitational acceleration, m s^{-2}

G_s Solids mass flow rate per unit area, kg s^{-1} m^{-2}

H Height, m

ΔJ Change in momentum for Equation 5.2.12, kg m s^{-1}

ΔH Height of element, m

L Length, m

L_s Length of slug, m

L_{st} Total length of slugs within pipeline, m

L_t Length of pipeline, m

ΔL Length of element, m

l Length of spring, m

l_0 Length of spring in free state, m

l_w Width of stationary layer or strand layer, m

K Model constant for Equation 2.3.15

K_w Stress transmission coefficient

K_{spring}	Spring constant, N m^{-1}
m	mass of particle, kg
m_f	Air mass flow rate, kg s^{-1}
m_s	Solids mass flow rate, kg s^{-1}
m^*	Mass flow rate ratio of solids to gas
n	number flow rate of particles per unit of cross-sectional area, m^{-2} s^{-2}
N_1	Axial stress on a slug element, Pa (spring above material)
N_2	Axial stress on a slug element, Pa (spring underneath material)
N_{Slug}	Number of slugs in pipeline
Δp_f	Pressure drop due to air, Pa
Δp_p	Pressure drop due to particles, Pa
Δp_t	Total pipeline pressure drop, Pa
ΔP	Pressure difference, Pa
P_z	Axial stress on slug, Pa
$\overline{P_z}$	Average axial stress on slug, Pa
P_r	Radial stress on slug, Pa
R	Friction force, N

S	Shear force exerted at the strand, N
S_{Δ}	Particle size distribution parameter in Equation 2.3.1
U_{criti}	Critical velocity, m s^{-1}
U_{gp}	Interstitial air velocity, m s^{-1}
U_{min}	Minimum transport velocity, m s^{-1}
U_p	article velocity, m s^{-1}
U_s	Saltation velocity, m s^{-1}
U_{s0}	Single particle saltation velocity, m s^{-1}
U_{slug}	slug velocity, m s^{-1}
U_{slip}	Superficial slip velocity, m s^{-1}
U_t	Single particle terminal velocity, m s^{-1}
W_{plate}	Weight of plate, N
W_{rig}	Weight of rig, N
W_{slug}	Weight of slug, N
Z	Height, m

Subscripts

st	Strand section

su Suspension section

Greek letter

α Relative area of stationary bed

α_{cri} critical relative area occupied by stationary bed for Equation 7.3.1

γ_b Bulk specific gravity with respect to water at 4 °C

ε Voidage

η Viscosity of air, Pas

θ Angle

θ_r Angle of repose for equation 2.3.15

λ_h Momentum transfer factor

μ Mass flow rate ratio of solids to gas, $\mu = m_s/m_f$

v Air velocity, m s^{-1}

ρ' Superficial bulk density, kg m^{-3}

ρ_f Air density, kg m^{-3}

ρ_b Loose-poured bulk density, kg m^{-3}

ρ_p Particle density, kg m^{-3}

σ_f Axial stress at front of slug, Pa

σ_{f1} Axial stress at front of slug caused by force balance of stationary layer, Pa

σ_{f2} Axial stress at front of slug caused by momentum balance of stationary layer, Pa

τ Shear stress, N m^{-2}

ϕ Section of pipe cross-sectional area not occupied by strand and stationary bed

ϕ_s Static internal friction angle, °

ϕ_w Wall friction angle, °

ω Angle defined by Equation 10.1.3

CHAPTER 1: INTRODUCTION

1.1 Features of Pneumatic Conveying of Solid Materials

Pneumatic conveying involves the transportation of a wide range of powdered and granular solid materials in an air stream within and/or among bulk solids handling or processing operating units. In recent decades, pneumatic conveying has been selected for an increasing number of industrial applications and products and plays a more vital and integral role in the transportation of materials such as flour, catalysts, granular chemicals, lime, soda, plastic pellets, coal, wheat and corn.

The main features that make pneumatic conveying of solid materials attractive to industries are:

(i) Isolation from the environment. Products can be kept separate without polluting the environment and being contaminated by products (e.g. hot catalyst can be transported pneumatically between reactor and regenerator within the hydrocarbon re-forming operating unit).

(ii) Flexibility of layout. Materials can be transported vertically and horizontally by the addition of a bend in the pipeline (especially important for limited head room). Also, materials can be distributed to, and picked up, from different areas in the plant (e.g. fly ash from several combustors within a power station can be transported pneumatically through one conveying pipeline to a fly ash collecting location).

(iii) Security. A pipeline can be used to transport high-value products (e.g. those in a diamond recovery plant).

(iv) Ease of control and automation.

(v) Low installation, maintenance and manpower cost.

(vi) Greater capacity. Solid products such as pulverised coal, cement and corn can be transported efficiently at large conveying rates (e.g. 100 to 400 t/h).

Offset against the advantages, there are some disadvantages for pneumatic conveying such as:

(i) Relatively high power consumption. Pneumatic conveying is not economical for conveying solid materials over long distances compared with that by vehicle on the road. The optimal range is a few hundred metres.

(ii) Wear and tear of the equipment.

(iii) Damage to products. This may occur during conveying even with proper and optimal design.

(iv) High levels of skills to design, operate and maintain a system. Because of the complexity of flow behaviour during the conveying, experienced and competent staff must be on hand.

1.2 Modes of Pneumatic Conveying

Pneumatic conveying exhibits different performance and flow patterns for different particle properties and operating conditions. The most acceptable classification so far is based on the average particle concentration in the pipeline and is separated into two categories: dilute-phase pneumatic conveying and dense-phase pneumatic conveying.

Dilute-phase pneumatic conveying generally employs a large amount of gas and the gas stream carries the materials as discrete particles by means of lift and drag forces

acting on individual particles. With a high gas velocity, particles are uniformly distributed over the pipe cross-section and this state is referred to as a fully suspended flow. As the gas velocity decreases, a segregation of particle concentration occurs across the cross-section of the conveying pipeline and a strand flow occurs with high solids concentration on the lower part and suspended flow on upper part of the cross-section of the pipeline. Dilute-phase pneumatic conveying systems are very common in industry and in many applications can produce a wide range of problems such as excessive system erosion and/or product damage due to the relatively high velocities required for transport, and excessive power consumption due to high air flows especially for coarse and/or heavy particles.

Dense-phase pneumatic conveying generally employs less gas and is attractive because of the potential for high capacities within smaller diameter pipelines, less breakage of products, less wear on the pipeline systems, lower overall energy consumption and smaller dust-separating requirements. Dense-phase pneumatic conveying has three main forms according to the particle and pipeline properties. They are:

(i) Low-velocity slug-flow (LVSF) of free-flowing granular bulk solids (e.g. plastic granules, grain, beans, wheat, rice).

(ii) Fluidised dense-phase (FDP) conveying of powder materials that can fluidise well and retain aeration (e.g. cement, fly ash, skim milk powder, carbon fines, pulverised coal)

(iii) Low-velocity plug-flow (LVPF) of more cohesive and/or sticky solid materials (e.g. full-cream milk powder, instant coffee powder, drinking chocolate).

1.3 Transition between Dilute-Phase and Dense-Phase Pneumatic Conveying

In conveying granular materials, there is a transition regime between dilute-phase and dense-phase located between Boundary B and D in the state diagram shown in Figure 1.3.1. A strand flow over a stationary layer or a slowly moving bed and sometimes violent long slug flow with strong pressure fluctuations have been observed when operation is in the transition regime. For powder materials there is also a transition regime in the state diagram, where the gas-solids flow exhibits the form of a strand flow over a stationary layer or a direct transformation from dilute-phase pneumatic conveying to dense-phase pneumatic conveying is achieved. For some conveying conditions, the transition flow does not occupy the whole conveying pipeline and usually it takes place near the inlet of the conveying pipeline with a flow mode of a strand over a stationary layer or slowly moving bed of certain length and strand flow afterwards. In such a situation for the conveying of granular materials, strand flow in the form of pulsating or moving dune flow will appear.

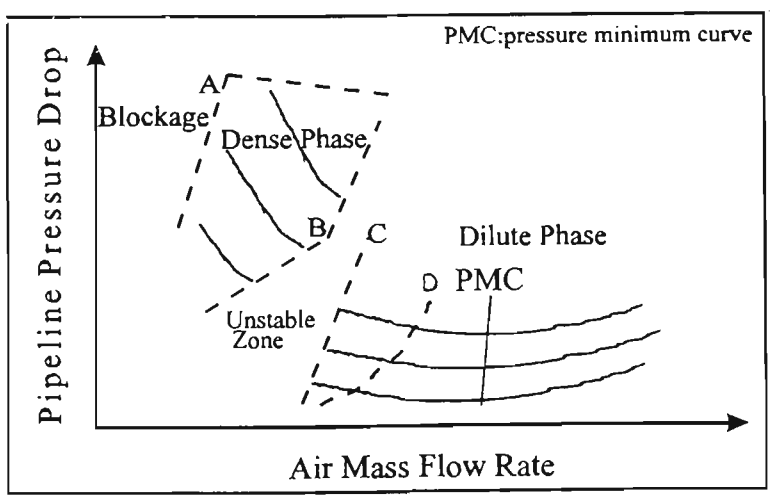

Figure 1.3.1 Pneumatic conveying characteristics for granular products.

Usually the unstable zone is located at the left side within the transition zone and operation in the unstable zone, which may result in severe pipeline vibrations and

pressure fluctuations even pipeline blockage, should be avoided. The transition zone between dilute-phase and dense-phase is also considered as the most important region in the state diagram and considerable effort has been made over several decades to identify the boundaries of transition zone for two reasons. Firstly, during dense-phase or dilute-phase, lower pressure drop can be achieved if operation is close to the transition zone in the state diagram. Secondly, blockage or instability or even failure in conveying may take place in the transition region.

Many investigations into pneumatic conveying have been connected with the transition between dilute-phase and dense-phase. Minimum conveying velocity for dilute-phase pneumatic conveying, which can be also considered as the upper boundary of the unstable or transition zone, is one of the major parameters required for the design/optimisation of pneumatic conveying systems and has been a popular or well-researched topic for several decades. The existing procedures to predict the minimum conveying velocity still contain numerous flaws, limitations and contradictions [109, 110] and this situation can be attributed to that the fact that research on the minimum conveying velocity has not considered the mechanism of the formation of the unstable zone and the single-particle concept has been believed to be fundamental to a study on saltation velocity. On the other hand, the lower boundary of the transition zone that is also considered as the maximum conveying velocity of dense-phase pneumatic conveying has never been researched.

The transition behaviours between dilute-phase and dense-phase pneumatic conveying also can be considered as one of the criteria to classify the different modes of pneumatic conveying. The classification of bulk solid materials for different modes of pneumatic conveying has been made in order to determine the connection between

flow modes and the properties of solid materials [17, 27, 41, 80]. However, the classification of solid materials proposed by many researchers based on the solid properties of fluidisation is not generally applicable as the gravity force acting on the moving particle is in different directions for horizontal pneumatic conveying and fluidised bed.

Since the precise mechanism by which dense-phase pneumatic conveying transforms to dilute-phase conveying has never been well understood, such a situation will limit the further application of pneumatic conveying to industries.

1.4 Thesis Objectives

One part of the task in the design of a pneumatic conveying system is to establish models for predicting overall pressure drop across the conveying pipeline reliably and accurately. This can be based on conveying test results from a pilot plant or a series of simple tests on the properties of the solid materials and pipeline wall surface. The other part of the task is to determine the conveying operating region in the state diagram so that pneumatic conveying of solid materials can be conducted steadily and pressure fluctuations or pipeline blockage can be avoided. So far, industrial design still relies mainly on past experience and the problem of scaling-up laboratory data is still significant.

Since the complexity of the mechanism involved in the formation of the transition regime in the state diagram and the particle properties play an important role for the different characteristics of the transition performance of gas-solids two-phase flow, plastic pellets were selected as the testing particles for the purpose of alleviating the influence of particle properties on the flow behaviour in the transition regime and simplifying parameters for model establishment. The ultimate objective of this

research is to explore the mechanism involved in the formation of the unstable zone for pneumatic conveying of granular materials and establish a model for the prediction of the boundaries of the transition zone. Further, a new approach is required to establish for the prediction of pipeline pressure for low-velocity slug -flow pneumatic conveying of granular materials so as to provide a reliable and accurate design strategy and method for dense-phase pneumatic conveying of granular materials.

To achieve the ultimate goal of this research, work has been concentrated on the following aspects:

(i) Evaluating existing correlations for the upper boundary of the transition zone or minimum conveying velocity for dilute-phase pneumatic conveying.

(ii) Experimentally investigating the influence of feeding device, pipe diameter and materials, particle properties on saltation velocity

(iii) Exploring the mechanism involving the formation of the unstable zone investigating the flow behaviour of plastic pellets in the unstable zone and.

(iv) Establishing a physical model to describe the observed three-layered flow structure of gas-solid flow in the transition regime based on mass balance, force balance and momentum balance.

(v) Carrying out stability analysis of the three-layered flow structure and explaining the formation of the unstable flow and corresponding critical conditions, together with explaining the relationship between the different boundary lines in the state diagram.

(vi) Discussing the influence of particle properties and pipeline properties on the unstable zone for pneumatic conveying of granular materials based on the model established.

(vii) Extending the application of the model to powder materials and discussing the transition regime in the state diagram for powder materials. Trying to determine the main parameters to identify granular materials and powder materials that have different transition boundaries in the state diagram.

(viii) Developing a test rig for the measurement of the stress transmission coefficient and measuring this coefficient for plastic pellets.

(ix) Developing a test rig for the measurement of the sliding friction coefficient and measuring this coefficient for plastic pellets and the actual conveying pipelines.

(x) Establishing a model for the prediction of pipeline pressure for low-velocity slug -flow pneumatic conveying of plastic pellets.

(xi) Combining the boundary model and pressure drop model to provide full information about the unstable boundary in the state diagram and comparing the predictions between models and the experimental results.

(xii) Further discussing the influence of particle properties, operating conditions and pipeline properties on the transition flow performance between dilute-phase and dense-phase pneumatic conveying.

(xiii) Developing a design model for the dense-phase pneumatic conveying of granular materials and providing a framework of computer program for calculating the boundaries and pressure.

As the research strategy, saltation velocity was investigated initially and mainly by experimental approach. Theoretical approach to explore saltation velocity was not going smoothly because of the lack of an understanding of mechanistic complexities involved in pneumatic conveying of solid materials within the transition zone at the primary stage. Hence the emphasis was then placed on exploration to the transition zone and the dense-phase pneumatic conveying. As it is impossible for all the research on this topic to be fully explored in one thesis, some problems related to this research topic may only be addressed to a certain depth and further research to solve such problems is suggested later.

1.5 Definitions for Some Basic Concepts

Before addressing the research topic in the detail, it is necessary to define some basic concepts.

Suspension Flow: this refers to solid-air flow in a dilute condition. The particle density or concentration across the whole suspension flow region in the cross-section seems even. Suspension flow can occupy the whole pipe cross-section or just the upper part of the pipe cross-sectional area.

Strand and Strand Flow: strand refers to solids moving with a variation in particle concentration that is higher than suspension flow. It can occur on the bottom of a conveying pipeline or a stationary layer or a slowly moving bed with suspension flow above it. The voidage of the strand is higher than that of bulk materials and tends to be equal to that of bulk materials as its condition approaches the unstable zone Boundary B shown in Figure 1.3.1. Strand flow consists of a moving strand and a suspension flow over the strand in a horizontal pipeline. Balling or duning can be considered as kinds of discrete strand flow.

Dilute-Phase Pneumatic Conveying: this refers to that air-solid flow in the form of suspension flow only or suspension flow and strand flow together.

Dense-Phase Pneumatic Conveying: this refers to air-solid flow in a form of congregation of particles occupying the whole or at least the upper part of the cross-sectional area of pipeline. The difference from the moving bed is that the moving bed usually exists on the bottom of the pipeline.

Low-Velocity Slug-Flow (horizontal): this refers to particles moving in the form of slug. Particle velocity in the slug is the same and the moving slug occupying the whole cross-sectional area of the pipeline will pick up the stationary layer in front of it and deposit a certain amount of particles behind it, determined by slug velocity.

Slowly Moving Bed: this represents solid materials with a voidage similar to a loose-poured condition on the bottom of the pipeline moving with very low velocity driven by the shear force from the strand flow above it. All particles contacting each other in the moving bed have the same velocity both in value and direction. The moving bed and stationary layer can be changed into each other according the shear force from the strand flow.

Stationary Layer: this refers to solid materials depositing on the bottom of the pipeline and usually under a strand. Its voidage is equal to that of loose-poured bulk materials. The thickness of the stationary layer varies with the conveying condition.

Unstable Flow Zone: this represents operation in the region of the state diagram where in a horizontal pipeline the flow mode alternates between long violent slug flow and strand flow over a stationary layer or slowly moving bed on the bottom of the pipeline.

Transition Flow Zone: this refers to operation in a horizontal pipeline where the flow mode can be either strand flow over a stationary layer or slowly moving bed on the bottom of pipeline or alternation between long violent slug flow and strand flow over a stationary layer or slowly moving bed on the bottom of the pipeline.

CHAPTER 2: REVIEW OF RESEARCH TO DETERMINE OPERATING BOUNDARIES FOR PNEUMATIC CONVEYING

2.1 Introduction

Determination of the operating boundaries for pneumatic conveying has been a popular research topic for some decades. Most attention however, has been paid to the determination of the minimum conveying velocity for dilute-phase pneumatic conveying while little interest has been shown in the lower boundary of the unstable zone or the maximum conveying velocity for dense phase pneumatic conveying. Since it is desirable to operate dilute-phase pneumatic conveying systems reliably with velocities close to the boundary in order to minimise energy consumption, pipeline wear and particle degradation, considerable effort has been made to determine the minimum conveying velocity accurately and reliably for a wide range of products and system characteristics.

For example, numerous theoretical and/or empirical correlations for the prediction of minimum conveying velocity have been developed over the past few decades [42, 83, 110, 111]. These correlations have been developed by different researchers around the world and are based on different bulk solid materials, test rigs conveying conditions/techniques and measurement principles. However, the mechanism for the formation of the unstable zone has never been really considered. To provide guidance on the "best" of these correlations, some interesting statistical comparisons also have been carried out [42, 83]. However, when applied to several industrial systems and large-scale test rigs, even the "best" correlations have been found to contain numerous flaws and limitations and they also display unexpected and contradictory results, especially for larger G_s, larger D and/or smaller d_p [110, 111].

To gain a better appreciation and understanding of these discrepancies and contradictions, it is important to appreciate the different flow modes that can occur in

conventional pipelines and also the various definitions of minimum conveying velocity used by researchers, to evaluate and compare the recommended correlations, the influence of particle properties, pipeline configurations and conveying conditions at minimum conveying velocity.

2.2 General Forms of Pneumatic Conveying

Numerous bulk solid materials with dramatically different particle properties (e.g. size, size distribution, shape and density) are transported pneumatically in conventional pipeline systems. For powders and granules, two general forms of conveying characteristic are observed, and these are described in detail below.

2.2.1 Smooth Transition from Dilute-Phase to Dense-Phase

This flow mode usually occurs for powder materials (e.g. flyash, cement and pulverised coal). A typical set of pneumatic conveying characteristics (PCC) for solid materials of this kind is shown in Figure 2.2.1.

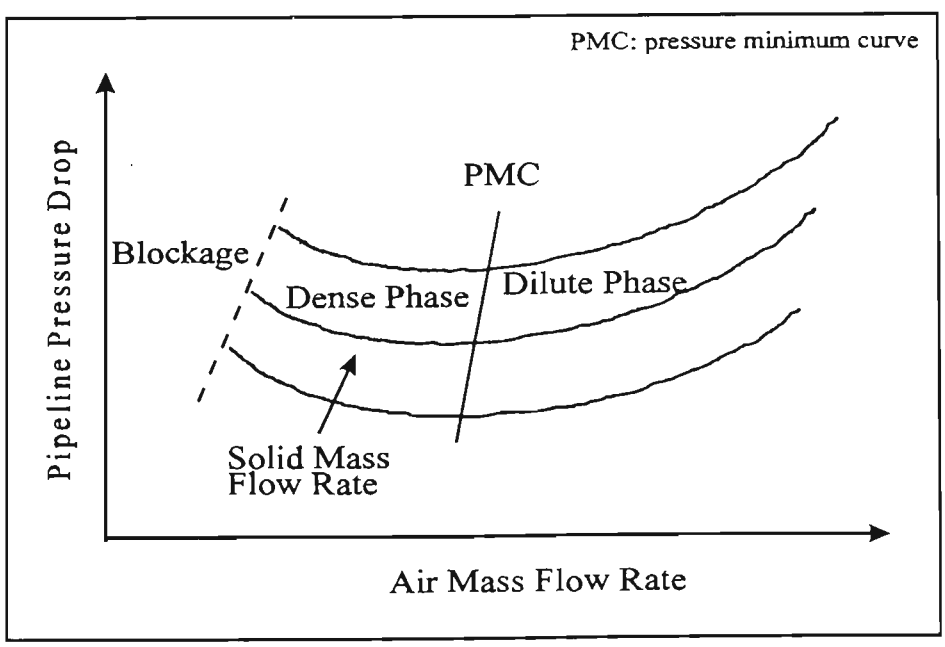

Figure 2.2.1 General form of pneumatic conveying characteristics for fine powders.

For a high and constant solid mass flow rate, when the air mass flow rate is decreased from high to low, the pressure drop also decreases and reaches a minimum value. The region to the right of this pressure minimum point in the PCC usually is referred to as dilute-phase pneumatic conveying. As the air mass flow rate is decreased further, the pressure drop usually increases. This region in the PCC is generally called dense-phase pneumatic conveying. The locus of pressure minima is referred to as the pressure minimum curve (PMC) and is often used to define minimum conveying velocity for dilute-phase. Actually, operating at the minimum conveying velocity for dilute-phase for fine powder materials does not mean that further reductions in gas velocity will induce unstable operation or pipeline blockage.

When conveying with a solid mass flow rate reducing to certain value, suspension and/or a strand flow over a stationary layer will be observed when the air mass flow rate is in between dilute-phase and dense phase in PCC (This will be further discussed in Chapter Six). For light powder materials such as flyash, the solids mass flow rate must be very low to allow the stationary layer to form on the bottom of the conveying pipeline and such low solids mass flow rate normally will not be selected for system operation. It was observed during PVC conveying tests that for a certain solids mass flow rate, the transition from dilute-phase to dense-phase may involve moving large amounts of stationary material on the bottom of the conveying pipeline and hence unstable flow with violent pressure fluctuation in the transition zone will take place. For relatively heavy powder materials such as PVC, the stationary layer on the bottom of the conveying pipeline will form with relatively high solids mass flow rate. The minimum conveying velocity for such powder materials still has significance and should be taken into account in the design of pneumatic conveying systems because a smooth transition can not be achieved between dilute-phase and dense-phase.

2.2.2 Dilute-Phase, Unstable-Zone and Dense-Phase

This flow mode characteristic usually occurs for granular products (e.g., plastic pellets, wheat and rice). Figure 1.3.1 shows a typical set of pneumatic conveying characteristics for this flow mode. In dilute-phase with high air velocity, the particles are distributed evenly over the entire cross section of the pipe. When conveying takes place along a line of constant solid mass flow rate in the direction of decreasing air mass flow rate, the pressure decreases gradually and the air-solid two-phase flow exhibits the suspension of particles over a strand. With lower air mass flow rates, some particles will drop out of the strand and form a stationary layer or a slowly moving bed along the bottom of pipeline from the inlet of the conveying pipeline. Here, most of the material is transported in the form of a strand over a stationary layer or a slowly moving bed, or in the form of small clusters or dunes along the conveying pipeline where the stationary layer or slowly moving bed has not been achieved. With further decrease in air mass flow rate, the air-solid flow will be in the form of a strand over a stationary layer or a slowly moving bed that can extend to end of relatively short conveying pipelines. If the air mass flow rate is lowered even further, the air-solid flow will be in the form of unstable flow with pressure fluctuations. If the air mass flow rate is reduced further, the particles will be conveyed gently and in the form of slugs. The state diagram or conveying characteristics for granular materials is shown in Figure 1.3.1 and consists of three boundary lines A, B and C and two other line PMC and D. Line A represents the minimum air mass flow rate to convey granular materials in the form of low-velocity slug flow with a given solids mass flow rate. Line B depicts the maximum air mass flow rate for conveying granular materials in the form of low-velocity slug-flow. Line C represents the maximum air mass flow rate for conveying granular materials in the form of unstable flow with violent pressure fluctuations. Line

D delineates the points at which particles begin to deposit from a strand or suspension along the bottom of the pipeline.

2.3 Review of Existing Minimum Conveying Velocity Correlations

Numerous theoretical and empirical correlations have been developed for the prediction of saltation or minimum conveying velocity for dilute-phase pneumatic conveying. In this section, eleven well-known correlations are presented with their minimum velocity definition and experimental conditions, such as test materials and pipelines.

Zenz [116] conducted experiments with pipelines of 31.75 mm and 63.5 mm inner diameter. The test materials used were rice krispies, glass beads, sand, salt, cracking catalyst, soybeans and tenite with different ranges in size. The effect of particle size distribution was the main focus of his work and a special constant, S_Δ was used to characterise the influence of particle size and size distribution. The air velocity required to carry solids at a certain loading without allowing them to settle in any horizontal pipe runs is defined as the minimum conveying velocity corresponding to the line D in Figure 1.3.1. Zenz proposed the following correlation to calculate the minimum conveying velocity.

$$\frac{G_s}{\rho_p} = 0.213 S_\Delta^{1.5} \cdot (U_s - U_{s0}) / U_{s0} \qquad (2.3.1)$$

Where S_Δ and U_{SO} are determined graphically [116].

Rose and Duckworth [89, 90, 91] investigated the minimum conveying velocity with a pipeline of 32 mm diameter. The test materials were mustard seed, glass bead, steel bead and lead bead. The minimum conveying velocity was defined as the air velocity

at which particles settled out of suspension and the flow became unstable. The correlation developed for minimum conveying velocity was:

$$\frac{U_{min}}{U_t} = 3.2 \cdot (m^*)^{0.2} \cdot \left(\frac{D}{d_p}\right)^{0.6} \cdot \left(\frac{\rho_p}{\rho_f}\right)^{-0.7} \cdot \left(\frac{U_{min}^2}{g \cdot D}\right)^{0.25} \qquad (2.3.2)$$

Duckworth [19] conducted further experiments looking at the influence of particle and fluid properties and inclination of pipe on the minimum conveying velocity with pipelines of 12.7 mm and 25.4 mm diameter. The test materials were glass, mustard seed and polystyrene. The minimum conveying condition corresponding to line C in Figure 1.3.1 was determined by visual observation and noting the onset of violent oscillations of static pressure. The developed correlation for the minimum conveying velocity was:

$$\frac{U_{min}}{U_t} = f_1\left(\frac{d_p}{D}\right) \cdot f_2(\theta) \cdot (m^*)^{0.3} \qquad (2.3.3)$$

Where $f_1\left(\frac{d_p}{D}\right)$ and $f_2(\theta)$ are determined graphically [19].

Rizk [86, 87, 88] carried out experiments on minimum conveying velocity using pipelines of 50 mm, 100 mm, 200 mm and 400 mm diameter. Styropor and polystyrol were used as the test materials. The minimum pressure drop curve corresponding to line PMC in Figure 1.3.1 was considered as the boundary between "safe" steady flow and a region of stationary particles. The correlation of the minimum conveying velocity was:

$$m^* = \left(\frac{1}{10^{\delta}}\right) \cdot Fr_{min}^{\ x} \qquad (2.3.4)$$

Where $\delta = 1.44\ d_p + 1.96$, $x = 1.1\ d_p + 2.5$ and d_p in mm.

Matsumoto [61, 62] investigated the minimum conveying velocity with pipelines of 26 mm and 49 mm diameter, using glass bead, copper bead and polystyrene as the test materials. The velocity at which the pressure drop reached a minimum value was defined as the saltation velocity corresponding to line PMC in Figure 1.3.1 [61], while the minimum conveying velocity was defined as the velocity at which material began to settle out on the bottom of pipeline and a stationary bed was formed corresponding to line D in Figure 1.3.1 [62]:

Saltation velocity [60]:

$$m^* = 0.448 \cdot \left(\frac{\rho_p}{\rho_f}\right)^{0.5} \cdot \left(\frac{U_t}{10\sqrt{g \cdot d_p}}\right)^{-1.75} \cdot \left(\frac{U_s}{10\sqrt{g \cdot D}}\right)^{3.0} \qquad (2.3.5)$$

Minimum conveying velocity [61]:

$$m^* = 0.373 \cdot \left(\frac{\rho_p}{\rho_f}\right)^{1.06} \cdot \left(\frac{U_t}{10\sqrt{g \cdot d_p}}\right)^{-3.70} \cdot \left(\frac{U_s}{10\sqrt{g \cdot D}}\right)^{3.61} \qquad (2.3.6)$$

In the later paper [62], the influence of particle size on minimum conveying velocity was also investigated and separate expressions for fine and coarse bulk solid materials were achieved:

For $d_p > 1.39D \cdot \left(\frac{\rho_p}{\rho_f}\right)^{-0.74}$

$$m^* = 0.373 \cdot \left(\frac{\rho_p}{\rho_f}\right)^{1.06} \cdot \left(\frac{U_t}{10\sqrt{g \cdot d_p}}\right)^{-3.70} \cdot \left(\frac{U_s}{10\sqrt{g \cdot D}}\right)^{3.61} \qquad (2.3.7)$$

For $d_p < 1.39D \cdot \left(\frac{\rho_p}{\rho_f}\right)^{-0.74}$

$$m^* = 5560\left(\frac{d_p}{D}\right)^{1.43} \cdot \left(\frac{U_{min}}{10\sqrt{g \cdot D}}\right)^{4} \qquad (2.3.8)$$

Wirth [104, 105, 106] defined the minimum conveying velocity as that prevailing at the appearance of the first plug (slug) corresponding to line C in Figure 1.3.1. The pipelines used in his experiments were 10 mm and 40 mm in diameter. The test materials were silica sand, glass bead and polystyrene. The correlation for calculating the minimum conveying velocity was:

$$\frac{\rho_f}{\rho_p \cdot (1.0 - \varepsilon)} \cdot m^* = 0.018 F_n^{-4} \qquad (2.3.9)$$

Where $F_n = \dfrac{U_f}{\sqrt{\left(\frac{\rho_p}{\rho_f} - 1\right)(1-\varepsilon) D \cdot g \cdot f_r}}$

Schade [92] investigated minimum conveying velocity in a wide range of pipe diameters (D = 50, 60, 80, 100, 120 and 150 mm) and the test materials used in the experiments were granule, sand, styropor, rubber and polystyrol. Capacitive plates built into the wall of the pipes were used to measure the deposition of material at the bottom of the pipeline. The definition of the minimum conveying velocity in Schade's work was the air velocity at which the particle velocity became zero and should be located between line B and D in Figure 1.3.1. Hence, the value of Schade's critical

velocity is lower than a practical minimum conveying velocity (i.e. if particle deposition is to be avoided). Schade's correlation was:

$$\frac{U_{min}}{\sqrt{g \cdot D}} = (m^*)^{0.11} \cdot \left(\frac{D}{d_p}\right)^{0.025} \cdot \left(\frac{\rho_p}{\rho_f}\right)^{0.34} \qquad (2.3.10)$$

Weber's correlation for minimum conveying velocity [102] was presented without verification and without reference to pipe and material details:

For $U_t \leq 3\ m\ s^{-1}$

$$Fr_{min} = \left(7 + \frac{8}{3}U_t\right) \cdot (m^*)^{0.25} \cdot \left(\frac{d_p}{D}\right)^{-0.1} \qquad (2.3.11)$$

For $U_t \bullet 3\ m\ s^{-1}$

$$Fr_{min} = 15(m^*)^{0.25} \cdot \left(\frac{d_p}{D}\right)^{0.1} \cdot \qquad (2.3.12)$$

Geldart [26] conducted experiments on minimum conveying velocity with high gas pressures (up to 82.5 bar) and the pipelines were 9.19 mm and 12.52 mm in diameter. The test material was fine coal with average particle sizes of 8, 18 and 26 μm. The minimum conveying velocity was obtained by setting a pressure differential between the feeder and receiver and measuring the solids flow rate at different gas velocities. The minimum conveying velocity defined by Geldart corresponds to line PMC in Figure 2.2.1. The expressions were:

For $\frac{G_s}{D} > 4700$

$$U_{min} = 1.5 G_s^{0.465} \cdot D^{-0.01} \cdot \eta^{0.55} \cdot \rho_f^{-0.42} \qquad (2.3.13)$$

For $\frac{G_s}{D} < 4700$

$$U_{min} = 8.7 G_s^{0.302} \cdot D^{0.153} \cdot \eta^{0.55} \cdot \rho_f^{-0.42} \qquad (2.3.14)$$

Ochi [72, 73] conducted experiments on minimum conveying velocity with pipelines of 40 mm, 50 mm and 60 mm diameter. The test materials used in the experiments were wheat, rape seed and polyethylene pellets. The minimum conveying velocity was defined as the limiting fluid velocity at which conveying is possible in a state in which particles are not stagnant on the bottom of wall of the pipe, corresponding to the line D in Figure 1.3.1 The expression of minimum conveying velocity was:

$$U_{min} = 1.41K \cdot U_t \cdot \cos\theta_r \cdot \sqrt{\sin\theta_r} + B \qquad (2.3.15)$$

where K and B are model constants and θ_r is the angle of repose obtained from the gradient angle method using a cylinder.

Cabrejos and Klinzing [9] investigated minimum conveying velocity for a wide range of parameters using a pipeline of 50 mm diameter. The test materials used in the experiments were alumina, glass beads and polyester polymers. The definition for minimum conveying velocity was the air velocity at which the particles start to drop out of suspension and settle on the bottom of the pipe. The expression for the minimum conveying velocity was:

$$\frac{U_{min}}{\sqrt{g \cdot d_p}} = \frac{U_{s0}}{\sqrt{g \cdot d_p}} + 0.00224 \left(\frac{\rho_p}{\rho_f}\right)^{1.25} \cdot (m^*)^{0.5} \qquad (2.3.16)$$

where U_{so} is single particle saltation velocity and was found experimentally to be 2.5 m s^{-1} for alumina, 2.8 m s^{-1} for glass bead and 3.2 m s^{-1} for polyester polymers.

2.4 Correlation Trends and Comparisons

The values and trends of minimum conveying velocity, which are calculated by the correlations mentioned above based on the "common" particle density of 1000kg/m^3, air temperature of 20 °C and air pressure of 101 KPa abs except it is stated, are discussed and compared graphically in this sub-chapter.

2.4.1 Effect of Particle Diameter

The effect of particle diameter on the minimum conveying velocity of dilute-phase pneumatic conveying is shown in Figure 2.4.1. For a small pipe diameter, low solid mass flow rate and large particle diameter (e.g., $d_p \geq 0.5$ mm), as shown in the left side of Figure 2.4.1, the minimum conveying velocities for all correlations show almost the same trend of decreasing for decreasing particle size. For finer particles ($d_p < 0.5$ mm), the influence of particle diameter on the minimum conveying velocity is complicated, and three different trends can be seen (ie minimum conveying velocity decreasing, increasing or almost constant). With the differences in properties, different fine particles may display different trends experimentally and hence, existing correlations are not considered reliable enough for the prediction of trends for fine particles. The right side of Figure 2.4.1 shows the trends of different correlations of minimum conveying velocity for the conditions of large pipe bore and high solids mass flow rate per unit area. The deviations in minimum conveying velocity shown on the right side in Figure 2.4.1 are greater than those on left side and the three trend "categories" are far more pronounced.

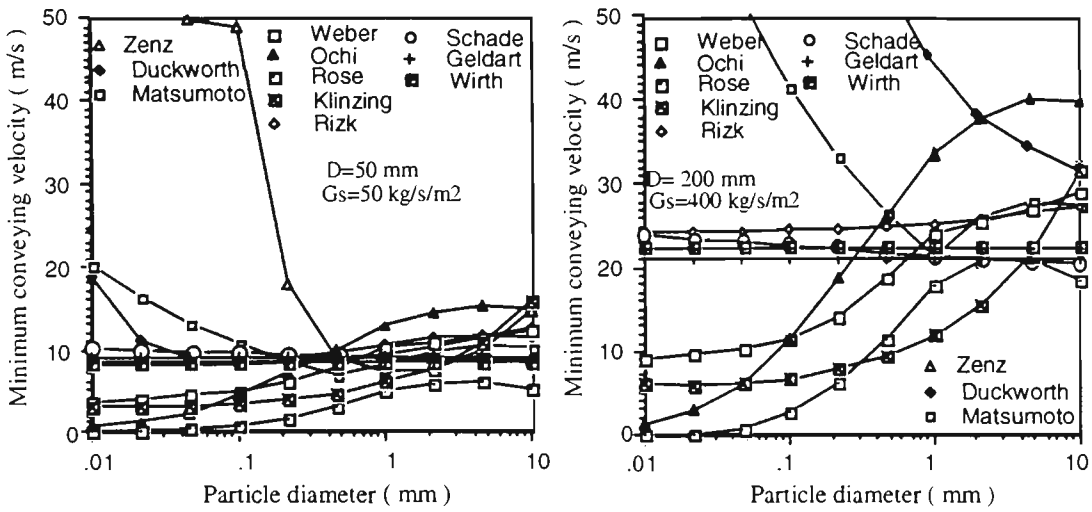

Fig. 2.4.1 Minimum conveying velocity with respect to particle diameter

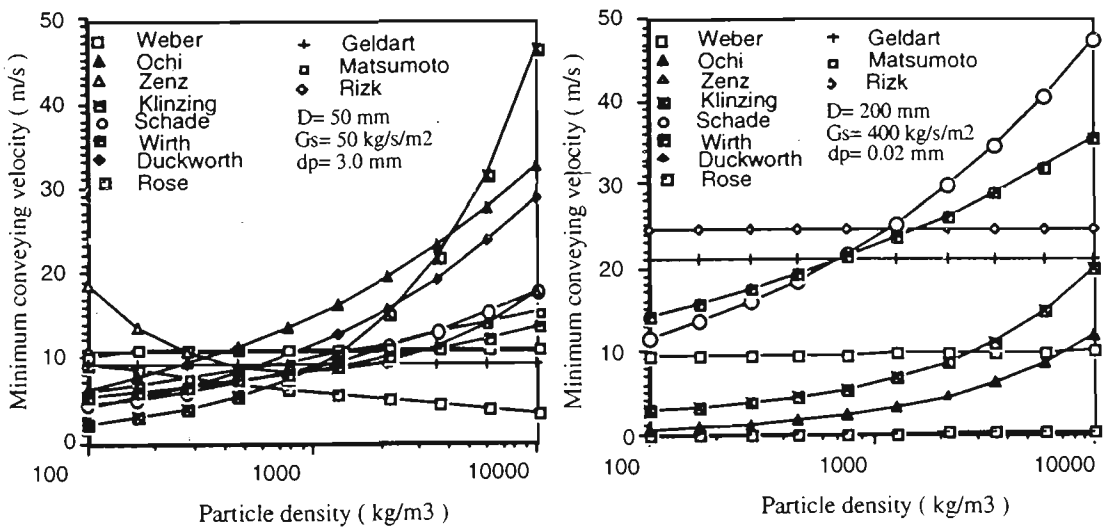

Fig. 2.4.2 Minimum conveying velocity with respect to particle density

2.4.2 Effect of Particle Density

The predicted results of the minimum conveying velocities of the eleven correlations with respect to the variation in particle density are shown in Figure 2.4.2. The predicted minimum conveying velocities generally display the trend of increasing with increasing particle density. It is found that the scatter on the left side of Figure 2.4.2 is

minimal at around a density of 1000 kg m^{-3} and this can be attributed to the fact that most particles tested had a density of about 1000 kg m^{-3} (such as plastic pellets). For a large pipe diameter and high solid mass flux, the predictions of minimum conveying velocity from the eleven correlations are rather more scattered as the results of less experimental data support. However the trends of the predictions from the eleven correlations are similar under the influence of particle density (i.e. velocity increasing with density).

2.4.3 Effect of Pipe Diameter

The minimum conveying velocities predicted by the eleven correlations mentioned above always increase as the pipe diameter increases as shown in Figure 2.4.3.

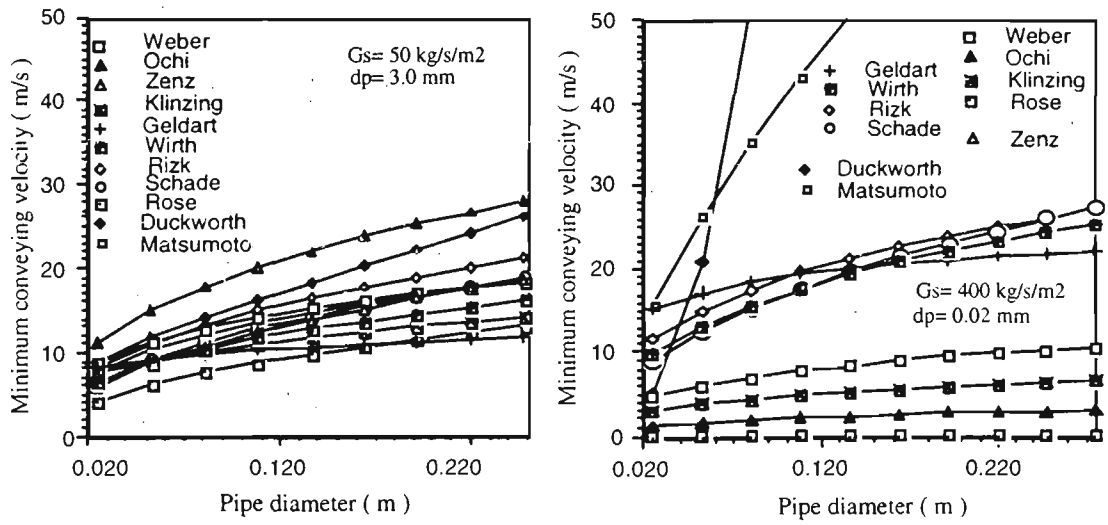

Fig. 2.4.3 Minimum conveying velocity with respect to pipe diameter

Because most of these correlations were based on test results obtained on pipe bores from 25 mm to 100 mm, the predictions of minimum conveying velocity agree fairly well in this region. The predictions of minimum conveying velocity for finer particles and higher solid mass flux are more complicated and scattered as shown on the right side of Figure 2.4.3.

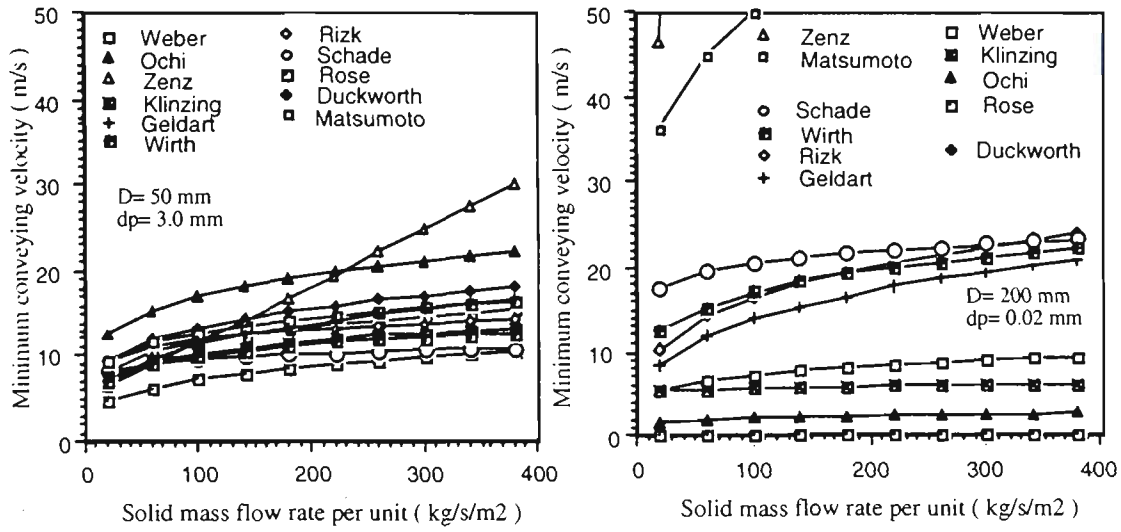

Fig. 2.4.4 Minimum conveying velocity with respect to solid mass flow rate

2.4.4 Effect of Solid Mass Flux

The influence of solid mass flow rate per unit area on the minimum conveying velocity of dilute-phase pneumatic conveying is quite easy to confirm by experiment. This results in the predictions of the eleven correlations that display the same trend, even though wide scatter still exists in the value of velocity as shown in Figure 2.4.4. The deviations can be attributed to: the different definitions of the minimum conveying velocity used by the different correlations, subjectivity of the researchers and the structure of the experimental rigs. For finer particles and larger pipe bore, the predictions of minimum conveying velocity show similar trends but with much greater scatter as shown on the right side in Figure 2.4.4. Chapter Four describes later that for the conveying of granular materials, there are different flow modes for high solids mass flow rate and low solids mass flow rate, and that the flow in the unstable zone involves two different mechanisms. For powder materials with high solids mass flow rate, normally there is no obvious and sharp change in conveying pressure gradient as

the pneumatic conveying transfers from dilute-phase to dense-phase. Since investigations conducted previously have never addressed the mechanism involved in the formation of the unstable zone in the state diagram, correlations for minimum conveying velocity for dilute-phase pneumatic conveying so far have not included any suggestion of it [109, 110].

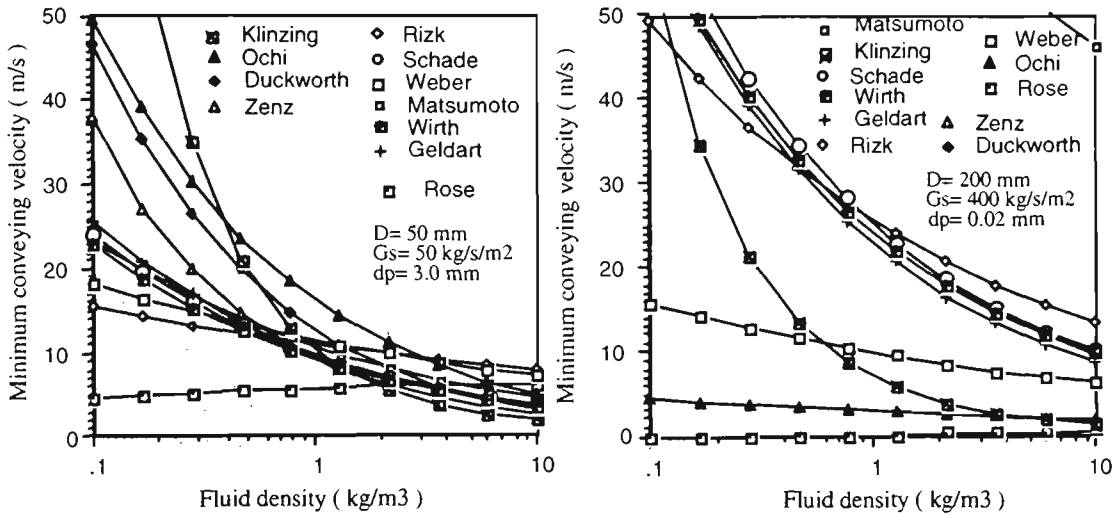

Fig. 2.4.5 Minimum conveying velocity with respect to fluid density

2.4.5 Effect of Fluid Density

The gas used in most pneumatic conveying systems is air. As sometimes other gases with different fluid densities and viscosities are used for pneumatic conveying, it is necessary to consider the influence of fluid properties on predictions of the minimum conveying velocity. Also, gas pressure and density can vary considerably from high positive values for pneumatic conveying of solid materials over a long distance to extremely low vacuums for some very special pneumatic conveying situations. The trends of predicted minimum conveying velocities generally show a decrease in velocity with increasing gas density, as shown in Figure 2.4.5. The deviations of the predictions from the eleven correlations become less when the gas density is similar to

that of atmospheric conditions (for D=50 mm) and much greater when the gas density is reduced to a vacuum condition. As the results of most of the correlations lack the support from experiment data in vacuum conditions, predictions of existing correlations are not reliable for conveying systems design for the pneumatic conveying conducted in vacuum conditions, especially for fine powders and large pipe bores.

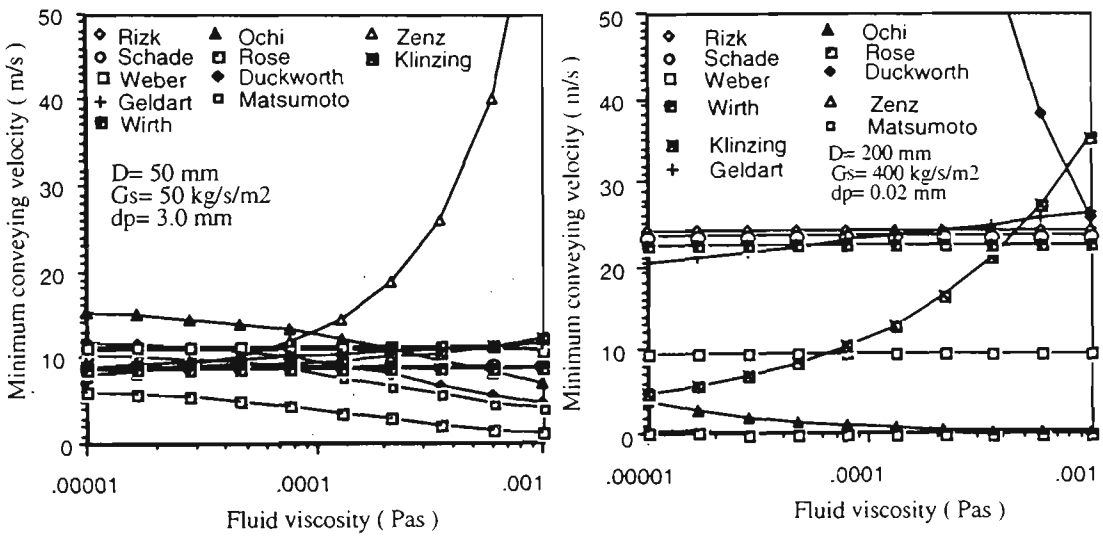

Fig. 2.4.6 Minimum conveying velocity with respect to fluid viscosity

2.4.6 Effect of Fluid Viscosity

In most of the eleven correlations for minimum conveying velocity of dilute-phase pneumatic conveying, fluid viscosity is not formally considered as one of the key parameters. The relationship between fluid viscosity and minimum conveying velocity mainly exists in the equations for single particle terminal velocity. This is a very popular and important parameter in the correlations for dilute-phase pneumatic conveying minimum conveying velocity predictions. The contradictions in the trends of minimum conveying velocity with respect to fluid viscosity are shown clearly in Figure 2.4.6. While the fluid viscosity is increased from 10^{-5} to 10^{-3} Pas, there are three basic trends: velocity increasing, decreasing or changing very little. Since the

viscosity of the fluid (usually air) does not vary with pressure (and is considered as a constant), it has seldom been taken into account directly when correlations have been established. From fluid dynamics theory, the drag force acting on the particles increases as the fluid viscosity increases. As a result, the minimum conveying velocity for dilute-phase pneumatic conveying should decrease as the fluid viscosity increases.

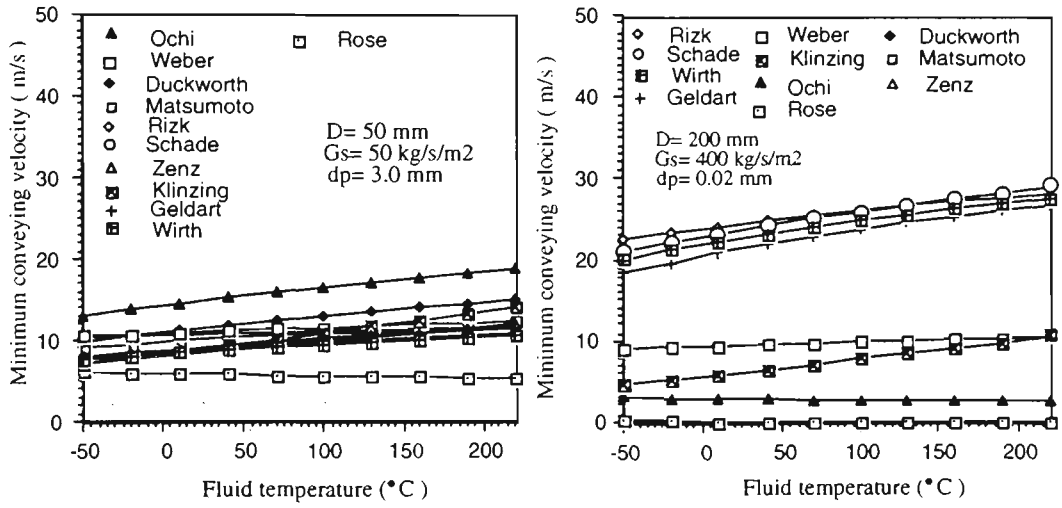

Fig. 2.4.7 Minimum conveying velocity with respect to fluid temperature

2.4.7 Effect of Gas Temperature

In many cases, solid materials conveyed through the pipeline system are at temperatures different from the external environment but will finally be equal to temperatures in the environment as the result of heat transfer between them, especially if the conveying pipelines are long enough. Some processes such as cooling, heating and drying may be coupled with the pneumatic conveying process, so that the temperature may change as the result of heat transfer. Hence the effect of gas temperature on the minimum conveying velocity for dilute-phase pneumatic conveying must be considered. Temperature affects fluid properties such as density and viscosity and they directly influence the flow behaviour of gas and solid particles in the pipe.

Considering an increase in gas temperature, the density decreases and viscosity increases for constant pressure. In Figure 2.4.7, it can be seen that as the gas temperature is increased from -50 °C to + 220 °C, almost all the minimum conveying velocities predicted by the eleven correlations increase except that of Rose, but the extent of increase is very limited.

2.5 Summary

Despite minimum conveying velocity research being undertaken for several decades, the wide scatter and contradictions in the predictions trends demonstrated in this chapter show that more effort still is in this area. The mechanisms involved in the formation of unstable flow for different solid materials with different particle properties (and different operating conditions) in the transition between dilute-phase and dense-phase have not been well explored. Hence, different definitions of minimum conveying velocity have been used by the researchers and all the correlations have not been related to the various mechanisms displaced by different powder and granular materials for the formation of unstable flow. The approach of modifying single particle flow behaviour to simulate the pneumatic conveying of solid materials though a pipeline so far has not produced reasonable predictions of the minimum conveying velocity. Direct application of some concepts for a particle flow in the vertical direction to air-solid flow in horizontal direction resulted in confusion during research on minimum conveying velocity. Also the testing rigs and procedures used by all researchers are different and can have an influence on the results.

Notwithstanding the corresponding doubts associated with these models, some clear trends can be seen (namely, minimum conveying velocity increasing with G_s and D). However, significant research still is needed before any model predictions can be used

directly in the design or optimisation of pneumatic conveying systems. Test work should be carried out in a pilot plant to verify design and operating parameters.

CHAPTER 3: PNEUMATIC CONVEYING TESTING FACILITY AND PROCEDURE

3.1 Introduction

Even though pneumatic conveying tests have been conducted and repeated through different conveying pipelines for a wide variety of particle properties, pipeline configurations and operating conditions and numerous PCC are available from the literature, agreement among individual researchers still can not be achieved. It is believed that the conveying test facility is one of the important aspects attributing to such a situation of investigation and understanding for the pneumatic conveying of solid materials. Many considerations have been taken into account in the design of the conveying system to ensure the experimental approach works properly and avoid problems such as the air mass flow rate not being maintained constant during the conveying test when the pressure drop across the conveying pipeline is fluctuating, the feeding rate not being kept steady during the conveying tests, the influence of the air (e.g. air temperature, humidity of the air, oil contained in the air).

3.2 General Arrangement of the Pneumatic Conveying Test Rig

The pneumatic conveying testing system was designed and established for the purpose of testing air-solid flow activities covering both dense-phase and dilute-phase pneumatic conveying regions in the state diagram. It was designed to provide visual observation and all necessary operating information, such as pressure gradient along the conveying pipeline, solids mass flow rate, air mass flow rate, particles retained in the pipeline, and primarily consisted of five components: feeding system, conveying pipeline, receiving system, air supply and a data acquisition system. A schematic layout of the testing system is shown in Figure 3.2.1.

3.2.1 Feeding system

The feeding system performed the function of feeding the solid materials from atmospheric pressure into high pressure accurately and steadily during the tests. Related measurements included the feeding rate of solids and air leakage from the rotary valve. The system consisted of a feeding bin, a filter / orifice plate, load cells and a rotary valve feeder.

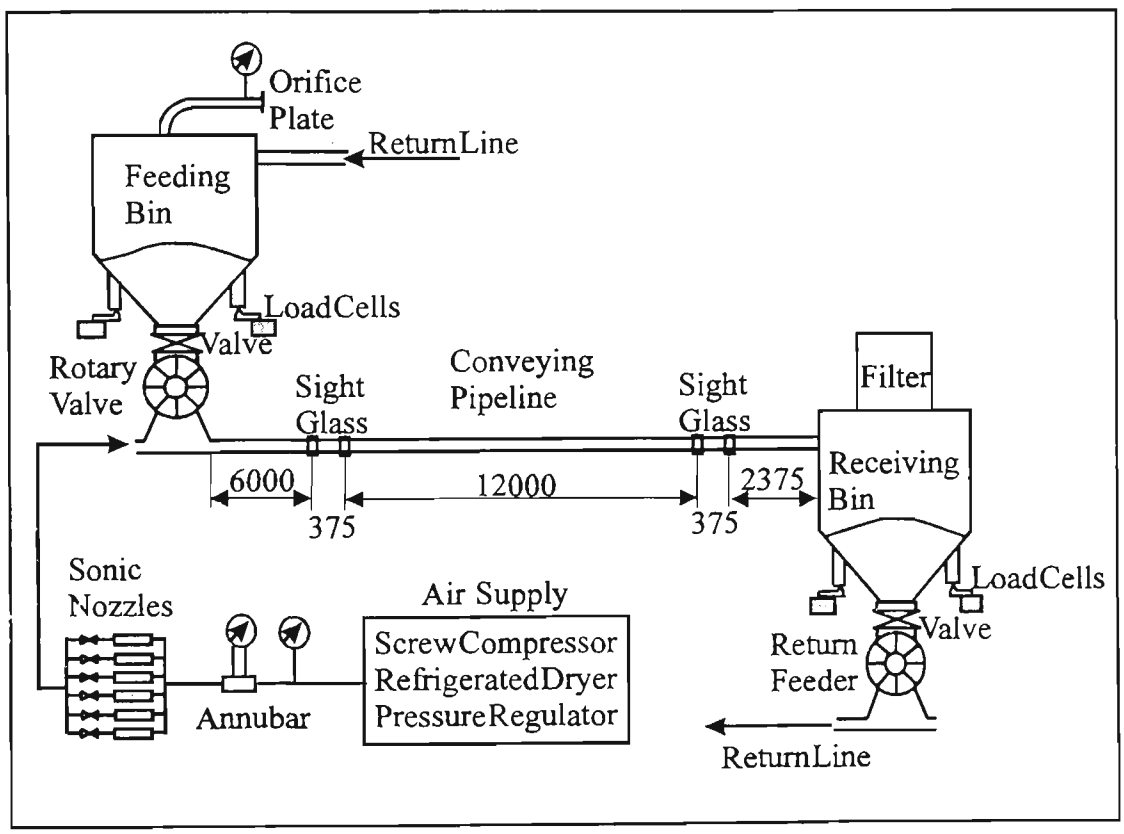

Figure 3.2.1 Schematic layout of testing rig

- Feeding bin. The feeding bin comprised a conical mass-flow hopper. It's holding capacity was approximately 0.665 m^3. The bin was mounted with four shear-beam load cells used to monitor the mass of material entering the conveying pipeline.

- Filter / orifice plate. Initially a filter was located on top of the feeding bin, however due to the white plastic pellets producing very little dust there was no need for it.

Also a modification was required to allow recording of rotary valve air leakage and this was carried out by removing the filter and placing a lid on the top of the feed bin with an orifice plate mounted on it. Air lost through the rotary valve discharged to the atmosphere via this orifice plate and the differential pressure across it was recorded for the measurement of rotary valve leakage.

- Feeding rotary valve - the valve was a Waeschle ZGR 250 rotary valve, with a swept volume of 8 litres per rev and ten separate pockets. Two of the main rotary valve functions were to minimise the loss of pressured air to atmosphere and control the feeding rate by varying the rotor speed.

It was very important to feed the test materials into the pipeline continuously and evenly. To control the feeding rate, it was found that continuous and even feeding of the test material into the pipeline could not be achieved at low feeding rates due to the occurrence of product pulses and pressure fluctuations along the test pipeline.

Also a Waeschle ZGR 320 drop-through rotary valve was used to determine the difference in maximum feed rate achievable and investigate the amount of air leakage this rotary valve produced in order to identify the influence of the structure of the rotary valve on the air-solid flow behaviour through the pipeline.

3.2.3 Testing Pipeline System

The objectives for the design of the pipeline system were to provide an experimental approach to address the influence of the pipe internal diameter and the pipe inner wall surface properties on the unstable zone boundaries and obtain visual observation of the air-solid flow behaviour through the horizontal pipeline. This was particularly important for exploring the mechanisms involved in the formation of the unstable

zone. The test pipelines used were horizontal, connecting the feeding shoe of the Waeschle rotary valve to the receiving bin. The total length of the horizontal pipeline was 21 m, (the distance from the first pipeline pressure tapping to the receiving bin). Several pipe diameters and wall materials were used for this testing, Table 3.2.1 and 3.2.2 show the details.

Table 3.2.1 Pipeline Specifications for Saltation

Pipeline Material	Internal Diameter, mm	Wall Thickness, mm
Mild Steel	105.3	4.5
Glass	105	5.0
Glass	155	7.5

Table 3.2.2 Pipeline Specifications for Dense-phase

Pipeline Material	Internal Diameter, mm	Wall Thickness, mm
Stainless Steel 304	60.3	1.6
Stainless Steel 304	98.4	1.6
Aluminium	55.8	3.2

Two short sight glasses were also present in each horizontal pipeline, at approximately 6 and 18 m, so that observations of the flow of product from two different locations

could be recorded and compared. The sight glasses were of a short length to minimise the frictional difference between the glass and the pipeline wall materials. A number of pressure tappings were present along the pipeline to monitor the pressure drop along the conveying pipeline.

3.2.4 Air Supply System

The air supply system was designed to provide sufficient cooled, dried and oil-free pressurised air with an adjustable and stable air mass flow rate for all conveying experiments covering both dilute-phase and dense-phase through pipelines with different internal diameter.

Air with a maximum pressure of 800 kPag was supplied from the following combination of rotary screw compressors:

- Atlas Copco electrical-powered Model GA-308, 3.1m^3 min^{-1} free air delivery.
- Ingersoll Rand diesel-powered Model P374-WP, 10.6 m^3 min^{-1} free air delivery.
- Ingersoll Rand diesel-powered Model P840-WGM, 24.1 m^3 min^{-1} free air delivery.

A wide range of air mass flow rates was provided by a combination of three rotary screw compressors. The pressurised air from the compressors passed through an after-cooler, two refrigerated air dryers and two air receivers (1.74 and 6.0 m^3 volumetric capacity) before entering the conveying pipeline to ensure a dry and oil-free air supply.

The measurement of air mass flow rate during the conveying tests was obtained by annubars. Because of the fluctuations in air supply and downstream conveying pipeline pressure, a pressure regulator and sonic nozzles were used to control air mass flow rate. The pressure regulator ensured a stable downstream air pressure with a range

between 500 kPag and 300 kPag. Each sonic nozzle was manufactured to have an accurate internal diameter so that the air mass flow rate through a nozzle would be constant regardless of downstream air pressure in the conveying pipeline up to 83% of absolute upstream pressure. With a combination of nozzles and a certain downstream air pressure after the pressure regulator, a desired stable air mass flow rate for conveying tests was achieved.

3.2.5 Receiving System

The receiving system performed the functions of collecting the solid materials from the conveying pipeline during the conveying tests, measuring the solid receiving rate, separating the solid materials from the air and sending the solid materials back to the feeding bin. It consisted of a receiving bin, a filter, returning rotary valve and returning pipeline:

- Receiving bin. The receiving bin also used a conical mass-flow hopper. The total volume of the bin was approximately 0.437 m^3 and it was mounted on four shear-beam load cells to monitor the mass of material entering the receiving bin.

- Return rotary valve. A 200 mm diameter BMH drop-through rotary valve attached to the base of the receiving bin was used to feed the bulk solid material from the receiving bin into the return line, which sent the product back to the feeding bin. The return pipeline was not monitored so the rotary valve speed and air mass flow rate were set to a condition which achieved good low-velocity slug-flow conveying so as to minimise product damage.

- Return pipeline. The return pipeline was constructed with 81 mm ID mild steel. It consisted of one vertical rise and three bends.

3.2.6 Data Acquisition System

A data acquisition system, DataTaker, combined with a PC with real-time display was used to record all the necessary conveying parameters such as solids mass flow rate, conveying air mass flow rate and pressures along the test pipeline. These raw data were then analysed to produce the relevant test results.

3.3 Conveying Test Procedures

3.3.1 Checks

To ensure the experiment results were accurate, a check of the test rig such as leakage along the pipeline as well as the working condition of the instruments was conducted before the commencement of the conveying. The air leakage check was carried out using the procedure below:

- Block the end of the conveying pipeline with a block flange.
- Pressurise the conveying pipeline and keep a pressure constant.
- Drop soapy water on each tapping point and connection and observe whether bubbles appear.
- If no bubbles appear, there is no leakage along the pipeline; if the bubbles do appear, de-pressurise the system, fix the leakage and repeat the last step.

3.3.2 Calibration

The load cells sensing the weight of the bin containing solid materials and the pressure transducers sensing the air pressure at testing points generate electrical output that a data acquisition system could process. The electrical output of a good sensor should provide a stable linear relationship between the electrical output and the actual

measuring quantity. However, variations in some environmental factors such as temperature, pressure, electric field and humidity may affect the characteristics of a sensor. Hence, it was necessary to calibrate the sensors periodically to ensure the measurements were accurate and correct. Standardised calibration procedures had been developed by the Centre for Bulk Solids and Particulate Technologies for load cells and pressure transducers.

3.3.3.1 Load Cell Calibration

Load cells installed under the supporters of the feeding bin or the receiving bin monitoring the variation in the weight of the feeding bin or receiving bin representing the discharging or receiving rate of solid mass of the bins. Calibration of load cells was carried out by feeding a given amount of solid materials into the bin and measuring the electrical output. The detailed procedures are as follows:

(i) Clean the feeding bin, receiving bin and conveying pipeline and then record the voltage output of all load cells.

(ii) Load a given mass of a product (say 40 kg) into the feeding bin and then record the voltage output of the load cells of the feeding bin.

(iii) Send the product from the feeding bin to receiving bin through the conveying pipeline and then record the voltage output of the load cells of the receiving bin.

(iv) Send all products from the receiving bin to the feeding bin, add another given mass of the product into the feeding bin and then record the voltage output of the load cells of the feeding bin.

(v) Repeat steps (iii) and (iv) until the mass of product in the feeding bin is more than that for a batch test. Then a linear relationship between the electrical output of the load cells and the actual measuring mass of product is achieved.

3.3.3.2 Pressure Transducer Calibration

To ensure the accurate measurement of the pressures along the conveying pipeline, the pressure transducers used in the conveying test program were calibrated by maintaining a given constant pressure in the conveying pipeline and recording simultaneously the voltage output from the transducers. The detailed calibration procedures applied in the Centre for Bulk Solids and Particulate Technologies are summarised as follows:

(i) Connect pressure transducers and a high accuracy pressure gauge to the conveying pipeline via pressure tapping.

(ii) Clean the conveying pipeline with a high flow rate of air and block the two ends of conveying pipeline with blind plate.

(iii) Open the air supply valve, blow air into the conveying pipeline until the pressure reaches a designated value (e.g. 40 kPag), then close the air supply valve.

(iv) Record the pressure value and the voltage response of all the pressure transducers and the output of the pressure gauge when the air pressure in the conveying pipeline becomes stable.

(v) Repeat (iii) and (iv) until the pressure higher than that expected in the conveying tests is obtained. Remove the blind plates from the conveying pipeline.

Hence, the calibration lines of the pressure transducers can be achieved and used for processing the electrical signals by a data acquisition system.

3.4 Conveying Test Procedures

The objective of conducting pneumatic conveying of solid particles tests is to obtain the pressure drop along the conveying pipeline for different air and solids mass flow rates and observations of the flow behaviours for different operating conditions along the conveying pipeline. With the databases of pressure gradient as well as observations of flow behaviours, the mechanisms involved in the formation of unstable zone in the state diagram and influence of pipeline properties, particle properties and operating conditions on the boundaries of the unstable zone will be explored. Normally the conveying tests are conducted with a constant solids mass flow rate and gradually decreasing air mass flow rate until the solids mass flow can not be maintained because air mass flow rate is too low to move so much solid materials into the conveying pipeline. Hence, a curve in PCC with a constant solids mass flow rate is obtained. Then one should conduct the tests with a change in solids mass flow rate to have another a constant solids mass flow rate curve in PCC. The main procedure for the conveying tests is designed as follows:

(i) Adjust the feeding rotary valve to a certain speed to have a designated solids mass flow rate. Conduct the conveying tests with a maximum air mass flow rate that is higher than at saltation condition.

(ii) With the same solids mass flow rate, conduct more conveying tests with decreasing value of air mass flow rates. The conveying tests should cover both dilute-phase and dense-phase until the rotary stops because solid materials building up inside the feeding shoe and the conveying pipeline blocks.

(iii) Change the rotor speed of the feeding rotary valve, repeat steps (i) and (ii).

The procedure mentioned above is for the group tests and each single conveying test conducted should follow the procedure below:

(i) Load a certain amount of product, sufficient for a batch test, into the feeding bin.

(ii) Adjust the speed of the feeding rotary valve to have a designated solids mass flow rate.

(iii) Select the combination of sonic nozzles and the pressure output from the pressure regulator to achieve a designated air mass flow rate.

(iv) Prepare the data acquisition system to scan the required channels at a suitable sampling rate.

(v) Start the data acquisition system.

(vi) Ten seconds later, open the conveying air valve to introduce the air into the conveying pipeline.

(vii) Start the feeding rotary valve and feed the solid materials into the conveying pipeline.

(viii) After enough data has been obtained, stop the feeding rotary valve, stop the data acquisition system, increase the air mass flow rate to clean the conveying pipeline and maintain the air flow rate until the pipeline is clean.

(ix) Send the solid materials from the receiving bin to the feeding bin and prepare for the next conveying test.

CHAPTER 4: EXPERIMENTAL INVESTIGATION ON SALTATION VELOCITY AND TRANSITION MECHANISM

4.1 Introduction

As mentioned before, saltation velocity was investigated initially and the investigation on saltation velocity was focused on the effect of feeding device, pipe properties and particle properties on the PCC. Then the emphasis of experimental work was placed on exploration of the transition mechanism of pneumatic conveying of granular materials for three reasons. Firstly, while many previous experimental tests have covered both dilute-phase and dense-phase pneumatic conveying, little has previously been published on experimental tests focused on the determination of the boundaries for the whole unstable zone. Secondly, in what has been published, there is a lack of full assessment and understanding of the accurate performance of pneumatic conveying of particle materials in the unstable zone or between the dense-phase and dilute-phase. Thirdly, saltation velocity can not solely explain the mechanism involved in minimum conveying velocity for dilute-phase pneumatic conveying even though it has been an interesting research topic for several decades. Without careful observations and data measurement on the conveying tests conducted in the unstable zone and well exploration of the mechanism for the formation of unstable flow, theoretical approaches are impossible to be applied to predict the boundaries of the unstable zone as well as the saltation velocity.

4.2 Experimental Investigation on Saltation Velocity

The experimental work on saltation velocity in this thesis was to install a full-scale test rig with different straight pipelines and feeding devices to investigate the mechanism of saltation and set up a good database of saltation for analysis, comparison and establishment of model. The physical properties of two solid materials for testing saltation velocity are listed in the Table 4.2.1 bellow:

Table 4.2.1 Physical Properties of test materials

Material	ρ_p (kg/m^{-3})	ρ_b (kg/m^{-3})	d_p (μm)
White Plastic Pellets	897	507	3800#
Corvic Vinyl	1487	512	116+

#Equivalent volume diameter, + Median diameter (laser particle sizer)

4.2.1 Pneumatic Conveying Characteristic Curves

At the stage of research on saltation velocity, conveying tests were conducted on three pipeline (one mild steel pipeline, ID=105 mm and two glass pipelines, ID=105 mm and 155 mm) and two test materials (white plastic pellets and corvic vinyl). From the data obtained, and ignoring rotary valve air leakage that is expected relatively low due to the low pressures involved, pneumatic conveying characteristic (PCC) curves were produced and shown as follows:

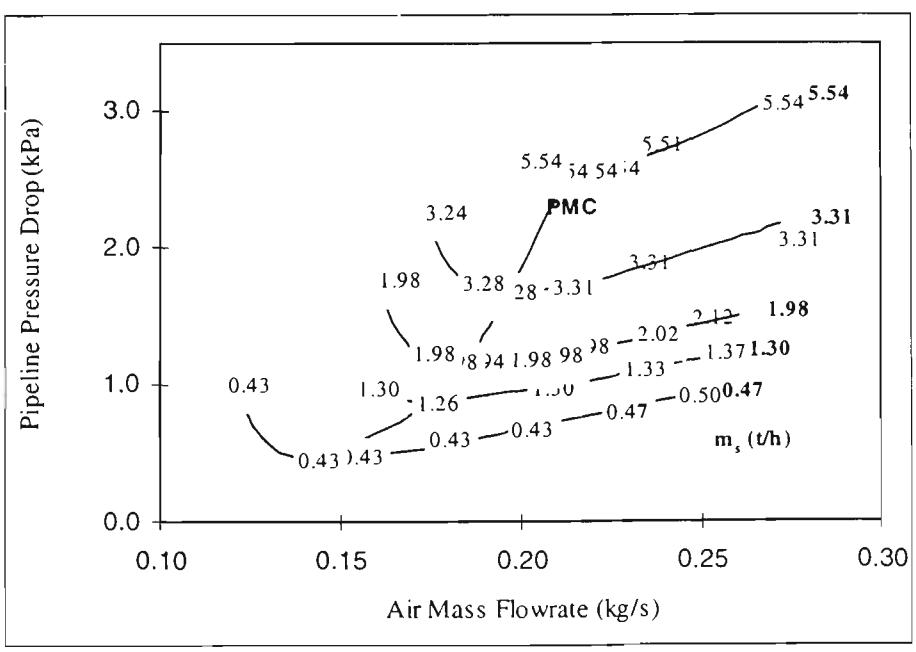

Figure 4.2.1 PCC for white plastic pellets, mild steel pipeline, unmodified feeding shoe, L=17.2m, ID=105mm

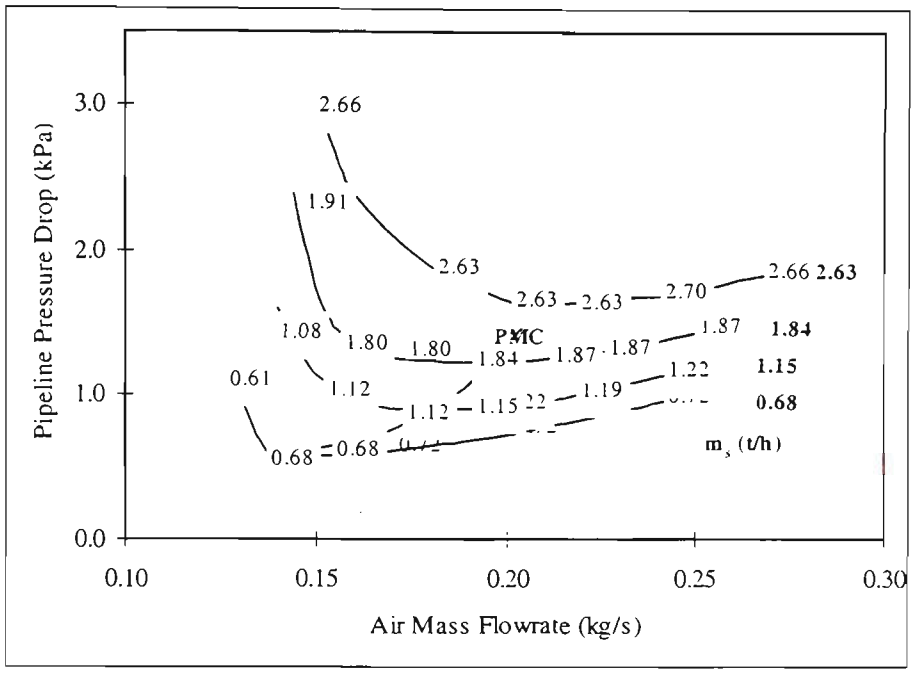

Figure 4.2.2 PCC for white plastic pellets, mild steel pipeline, modified feeding shoe, L=17.2m, ID=105mm

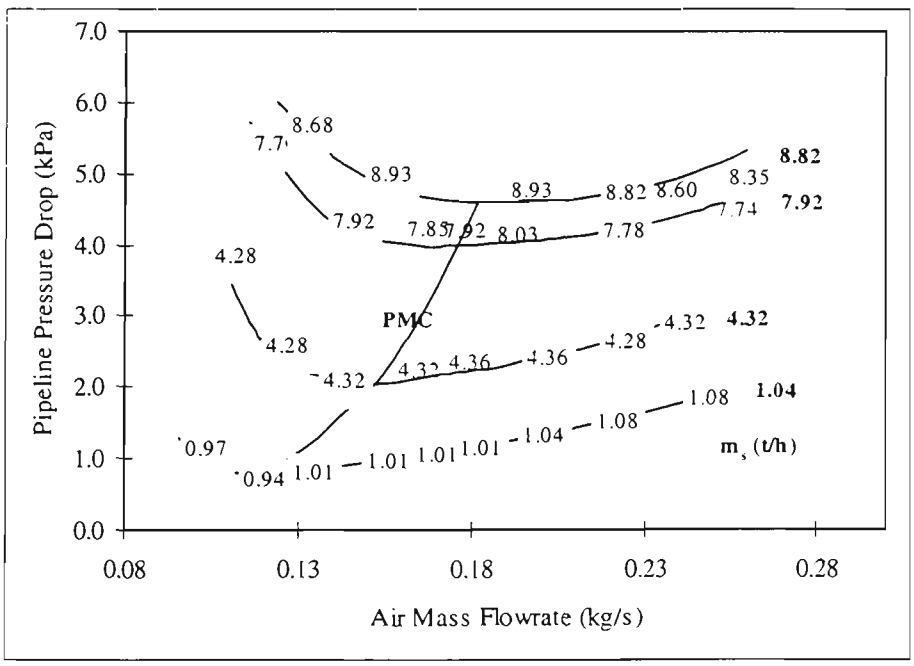

Figure 4.2.3 PCC for white plastic pellets, glass pipeline, unmodified feeding shoe, L=17.2m, ID=105mm

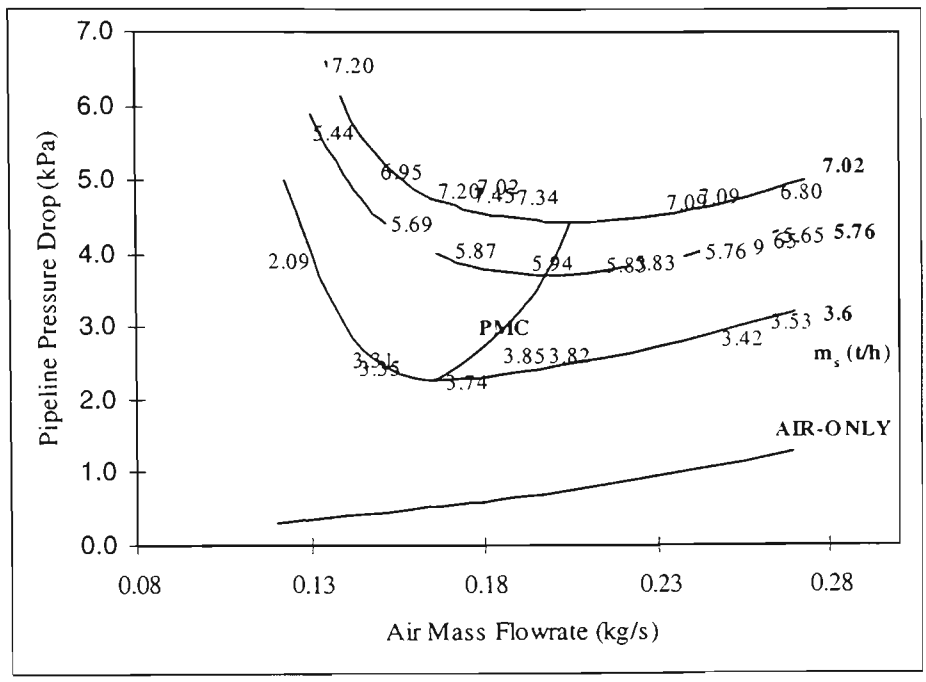

Figure 4.2.4 PCC for white plastic pellets, glass pipeline, modified feeding shoe, L=17.2m, ID=105mm

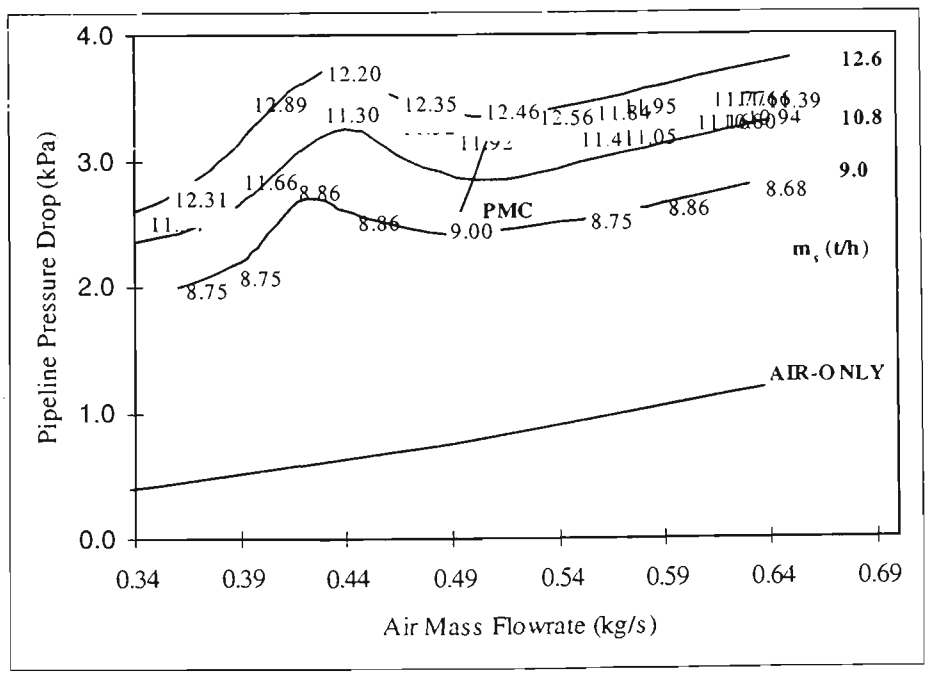

Figure 4.2.5 PCC for white plastic pellets, glass pipeline, modified feeding shoe, L=17.2m, ID=155mm

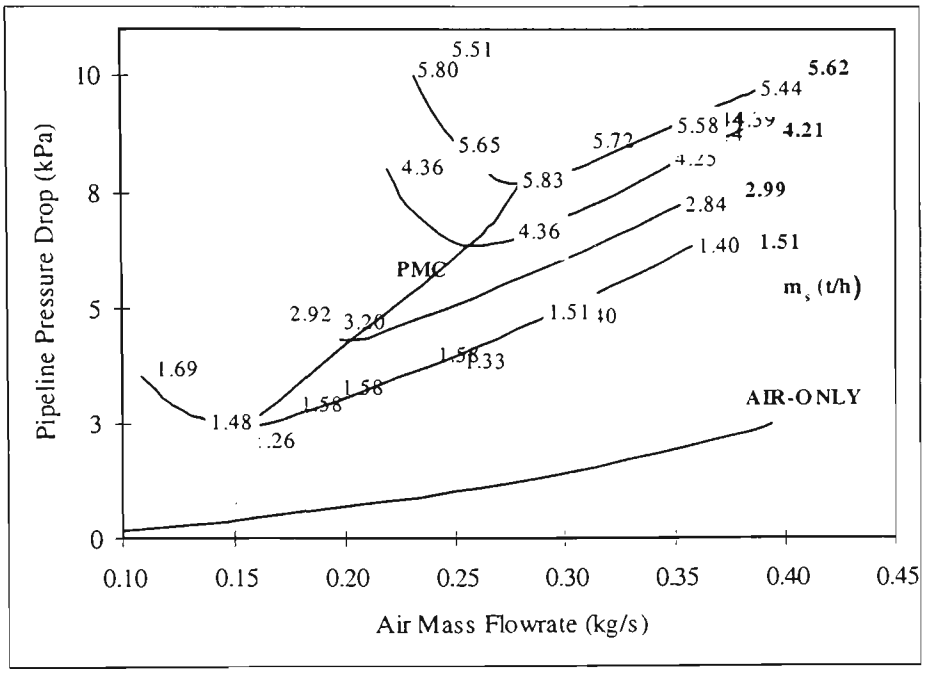

Figure 4.2.6 PCC for Corvic Vinyl powder, glass pipeline, unmodified feeding shoe, L=17.2m, ID=105mm

4.2.2 Comparison of Different PCCs Obtained

The following graphs directly compare various combinations of PCCs from different test pipelines and solid materials to show similarities and difference present. Direct comparisons can not be made between the 105 mm ID mild steel pipelines and the 105 mm ID glass pipelines due to the total pipeline pressure being measured at a different point. For the mild steel pipelines the total pipeline pressure was measured at 17.2 m from outlet and for the glass pipelines the total pipeline pressure was measured at 19.48 m from outlet.

Figure 4.2.7 shows the comparison of PCCs for pneumatic conveying of white plastic pellets through mild steel pipelines with different feeding shoes. It can be seen that by varying only the feeding shoe, the 2 sets of data show a distinct difference in the

behaviour of conveying. For high air mass flow rates, conveying with a constant solids mass flow rate for both the unmodified and modified feeding shoes produces similar pressure drops. The pressure minimum curve for the tests using the unmodified feeding shoe is situated at lower m_f values. The curves for the modified feeding shoe are quite flat around the PMC zone compared with a visible curve for the unmodified feeding shoe. For low air mass flow rates, both sets of data indicate a steady increase in pressure.

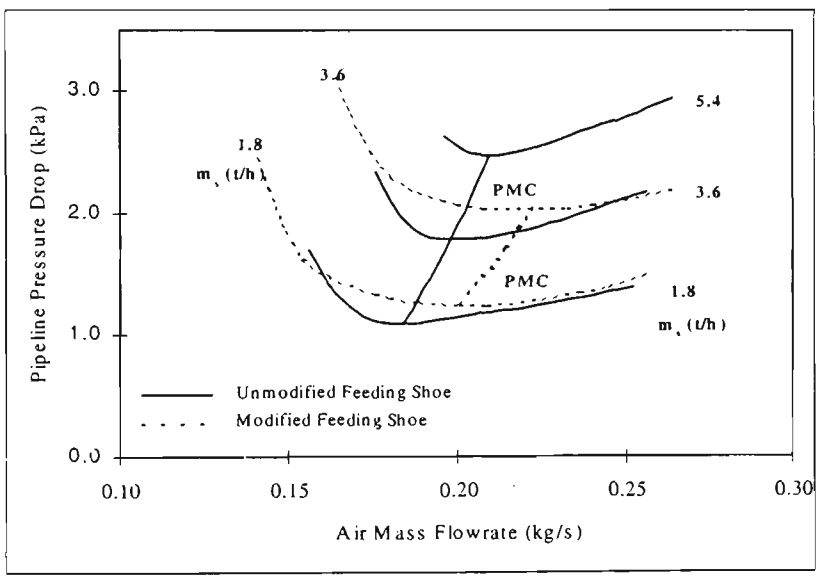

Figure 4.2.7 Comparison of white plastic pellets in 105mm ID mild steel pipeline L=17.2m with unmodified feeding shoe and white plastic pellets in 105mm ID mild steel pipeline L=17.2m with modified feeding shoe

Figure 4.2.8 shows the comparison of PCCs for pneumatic conveying of white plastic pellets through glass pipelines with different feeding shoes. Again there is a visible difference between the two sets of data. In general, the conveying with a constant solids mass flow rate through the pipeline with the modified feeding shoe has higher pressure drops than that for pipeline with the unmodified feeding shoe. The PMC for the test rig with the modified feeding shoe occurs at higher air mass flow rates than that for the test rig with the unmodified feeding shoe.

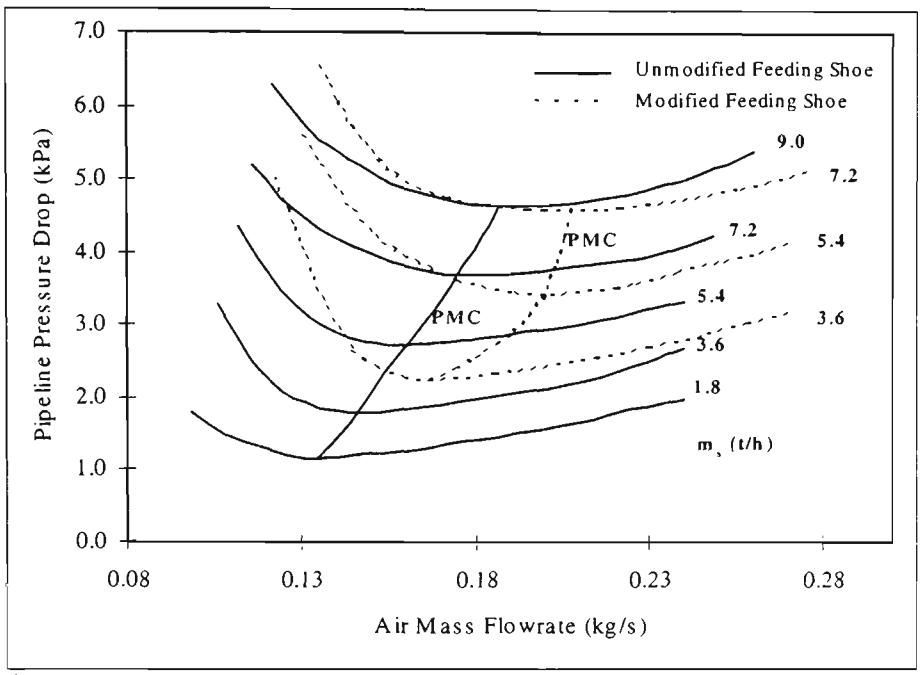

Figure 4.2.8 Comparison of white plastic pellets in 105mm ID glass pipeline L=19.48m with unmodified feeding shoe and white plastic pellets in 105mm ID glass pipeline L=19.48m with modified feeding shoe

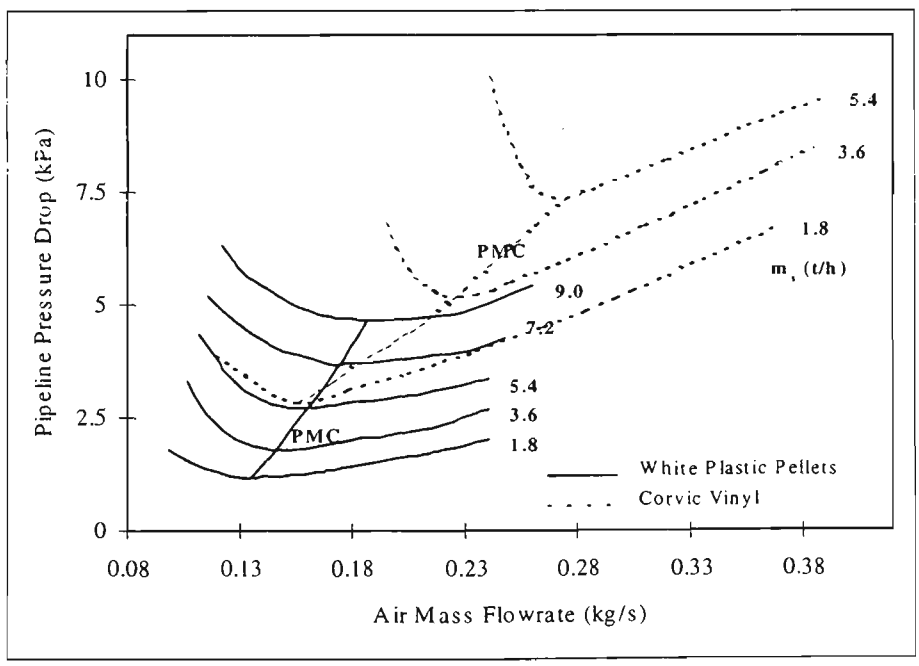

Figure 4.2.9 Comparison of white plastic pellets in 105mm ID glass pipeline L=19.48m with unmodified feeding shoe and corvic vinyl in 105mm ID glass pipeline L=19.48m with unmodified feeding shoe

Figure 4.2.9 shows the comparison of conveying characteristics for white plastic pellets and corvic vinyl in the same pneumatic conveying system. It can clearly be seen that to obtain the same solids mass flow rate for the corvic vinyl, there is a significant increase in the pressure required and also a significantly larger air mass flow rate.

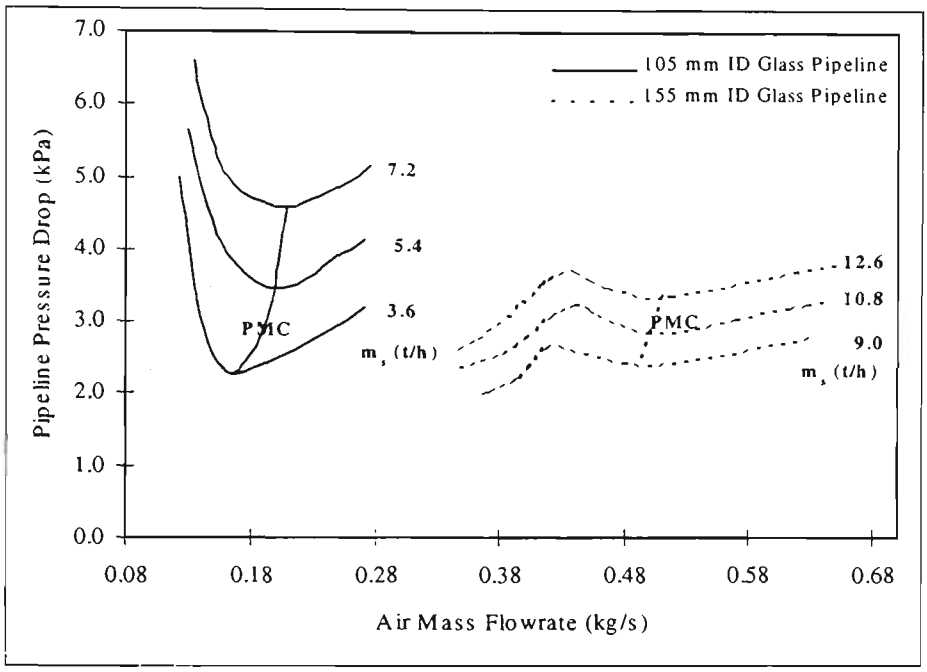

Figure 4.2.10 Comparison of white plastic pellets in 105mm ID glass pipeline L=19.48m with modified feeding shoe and white plastic pellets in 155mm ID glass pipeline L=19.48m with modified feeding shoe

Figure 4.2.10 shows the comparison of PCCs for white plastic pellets through a 105 mm ID glass pipeline and a 155 mm ID glass pipeline. It is clearly visible that there is a large difference in pressure drops and air mass flow rate required to convey the product in a 155 mm ID pipeline. There was an unexpected "hump" in the curves for the 155 mm ID glass pipeline as shown in Figure 4.2.5 and Figure 4.2.10. Initially it was thought that there was an error with the data logger but on further investigation the "hump" was still present. The hump in pressure drop may be attributed to the formation of a stationary layer along the conveying pipeline after feeding shoe. As the

stationary bed became deeper, the effective conveying area of the pipeline reduced, affecting the pressure drop across the pipeline. For both the 105 mm ID glass pipeline and the 155 mm ID glass pipeline, the pressure tapping point was located after the first 1.5 m glass tube. The stationary bed forming in the 105 mm pipeline was not as distinct, due to the feeding shoe being modified, but the stationary bed in the 155 mm pipeline was unavoidable even with the modified feeding shoe. The results demonstrate a potential problem with large-diameter pipeline conveying systems fed by rotary valves.

4.2.3 Conclusions for Experimental Investigation on Saltation Velocity

With analysis and comparison of the PCCs obtained from the conveying tests, the following conclusion can be achieved:

(i) Pipeline wall properties have an effect on the location of the minimum pressure curve and saltation velocity in the state diagram due to the difference in wall friction.

(ii) Products conveyed showed a marked difference in the location of the minimum pressure curve and saltation velocity in the state diagram also. For plastic pellets, air mass flow rate at the minimum pressure curve is higher than that of saltation while for corvic vinyl the situation is contrary.

(iii) Pipe diameter effects the location of the minimum pressure curve and saltation velocity in the state diagram.

(iv) Feeding structure effects the location of the minimum pressure curve and saltation velocity in the state diagram.

The experimental results of minimum conveying velocity or saltation velocity were compared with the predictions of eleven correlations established by different researchers [111] and shown in Figure 4.2.11. From Figure 4.2.11, it can be seen that the trends of the predictions of the different correlations are the same as that of the experiment, that is minimum conveying velocity increasing with solids mass flow rate. The differences in the prediction values can be attributed to the different definitions of minimum conveying velocity and the different experiment methods.

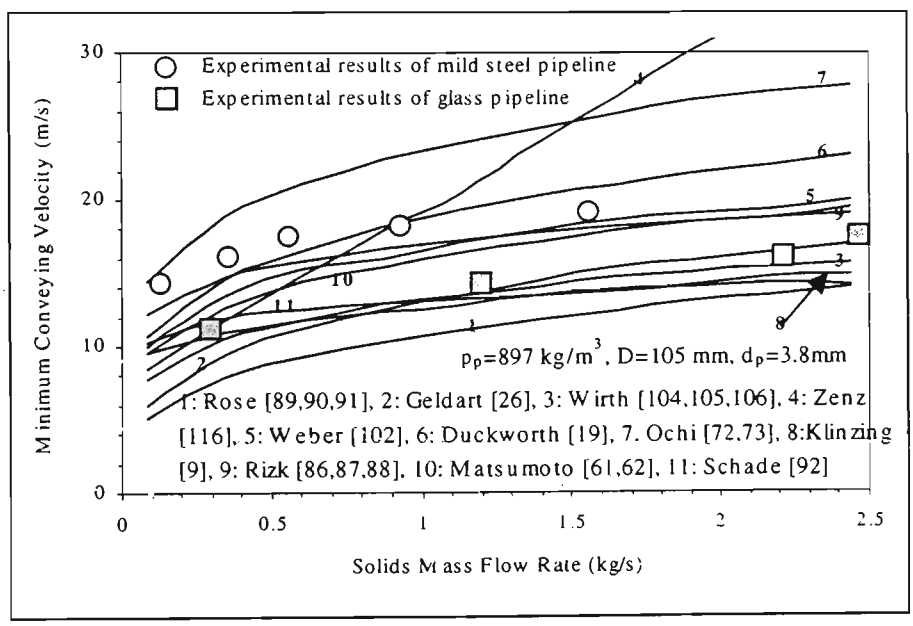

Figure 4.2.11. Comparison of experimental results of minimum conveying velocity for dilute-phase and correlation predictions

4.3 Visual Observations of Air-Solid Flow and Unstable Flow Mechanism

Descriptions of air-solid two-phase flow behaviours through horizontal pipeline have been made by many researchers in different locations around the world. But what largely overlooked is visual observation highlighting the flow phenomena within the unstable zone in the state diagram for pneumatic transportation of granular materials. The influence of solid mass flow rate on the flow behaviours in the unstable zone did

not raise enough attention from researchers. Hence it is worthwhile to carry out visual observation on the pneumatic transportation of plastic pellets with particle density of 897 kg/m^3, bulk density of 546 kg/m^3 and particle diameter of 4.7 mm through a 98.4 mm internal diameter, 21m long horizontal stainless steel pipeline. For the convenience of making a comparison, a low and a high solids mass flow rate were selected and kept constant with a wide range of variation in air mass flow rate.

4.3.1 Visual Observations of Air-Solid Two-Phase Flow through a Horizontal Pipeline with Low Solids Mass Flow rate

For a conveying with a solids mass flow rate of about 0.37 kg/s, as the air mass flow rate decreasing, the following flow phenomena were observed through the sight-glass 6.0 m from the feeding point of conveying pipeline and some conveying parameters were also measured. Note: air leakage of the rotary valve for feeding has been allowed for.

- Test 1, m_f=0.189 kg/s or v=19.9 m/s; average pressure drop across the conveying pipeline was 1.31 kPa. Very lean flow, visible segregation of the two phases with a slightly higher concentration of particles (strand flow) near the bottom of the pipe could be observed.

- Test 2, m_f=0.1689 kg/s or v=17.8 m/s; average pressure drop across the conveying pipeline was 1.21 kPa. Observations are as above and the concentration of particles near the bottom of the conveying pipeline increased slightly.

- Test 3, m_f=0.156 kg/s or v=16.5 m/s; average pressure drop across the conveying pipeline was 1.14 kPa. Observations were as above and the concentration of particles near the bottom of the conveying pipeline increased slightly.

- Test 4, m_f=0.139 kg/s or v=14.7 m/s; average pressure drop across the conveying pipeline was 1.07 kPa. Observations were as above and the concentration of particles near the bottom of the conveying pipeline increased slightly.

- Test 5, m_f=0.133 kg/s or v=14.0 m/s; average pressure drop across the conveying pipeline was 1.03 kPa. Observations were as above and the concentration of particles near the bottom of the conveying pipeline increased slightly.

- Test 6, m_f=0.122 kg/s or v=12.8 m/s; average pressure drop across the conveying pipeline was 1.02 kPa. Very faint balling at very fast speed was seen.

- Test 7, m_f=0.114 kg/s or v=12.0 m/s; average pressure drop across the conveying pipeline was 1.11 kPa. The strand became thicker with balling more pronounced.

- Test 8, m_f=0.109 kg/s or v=11.4 m/s; average pressure drop across the conveying pipeline was 1.24 kPa. More balling was observed and the strand started to thicken.

- Test 9, m_f=0.0966 kg/s or v=10.2 m/s; average pressure drop across the conveying pipeline was 1.87 kPa. More balling was observed and the strand became thicker.

- Test 10, m_f=0.0913 kg/s or v=9.6 m/s; average pressure drop across the conveying pipeline was 2.76 kPa. Deposited dunes formed about 40 to 50 mm in height, and then the dune moved again.

- Test 11, m_f=0.0844 kg/s or v=8.9 m/s; average pressure drop across the conveying pipeline was 3.38 kPa. A stationary layer formed about 20 mm in height. There was a strand flow over the stationary layer.

- Test 12, m_f=0.0783 kg/s or v=8.2 m/s; average pressure drop across the conveying pipeline was 4.67 kPa. The stationary layer was observed, it was not as thick as previously.

- Test 13, m_f=0.0672 kg/s or v=7.0 m/s; average pressure drop across the conveying pipeline was 6.95 kPa. A strand flow over a stationary layer about 30~35 mm high observed.

- Test 14, m_f=0.0586 kg/s or v=6.2 m/s; average pressure drop across the conveying pipeline was 7.70 kPa. A strand flow over a stationary layer about 40 mm high observed.

- Test 15, m_f=0.0491 kg/s or v=5.2 m/s; an unstable flow alternated between a strand flow over a stationary layer and a long and violent slug with a pressure drop peak of 61 kPa and a pressure drop trough of 0.5 kPa.

- Test 16, m_f=0.0418 kg/s or v=4.4 m/s; an unstable flow alternated between a strand flow over a stationary layer and a long slug with a pressure drop peak of 34 kPa and a pressure drop trough of 0.8 kPa. The time period became shorter than in Test 15.

- Test 17, m_f=0.0385 kg/s or v=4.0 m/s; an unstable flow alternated between a strand flow over a stationary layer and a long slug with a pressure drop peak of 20 kPa

and a pressure drop trough of 1.0 kPa. The time period became shorter than in Test 16.

- Test 18, m_f=0.0322 kg/s or v=3.4 m/s; still an unstable flow alternated between a strand flow over a stationary layer and a long slug with a pressure drop peak of 16 kPa and a pressure drop trough of 1.0 kPa. The time period became shorter than in Test 17.

- Test 19, m_f=0.0234 kg/s or v=2.5 m/s; average pressure drop across the conveying pipeline was 9.46 kPa. Gentle slug flow with about 25mm thickness stationary layer on the bottom of conveying pipeline was observed.

- Test 20, m_f=0.0204 kg/s or v=2.1 m/s; average pressure drop across the conveying pipeline is 11.4 kPa. Gentle slug flow with about 35 mm thickness stationary layer on the bottom of the conveying pipeline was observed.

- Test 21, m_f=0.0156 kg/s or v=1.6 m/s; average pressure drop across the conveying pipeline was 13.6 kPa. Gentle slug flow with about 50 mm thickness stationary layer on the bottom of the conveying pipeline was observed.

- Test 22, m_f=0.0107 kg/s or v=1.1 m/s; average pressure drop across the conveying pipeline was 19.8 kPa. Gentle slug flow with about 55 mm thickness stationary layer on the bottom of the conveying pipeline was observed. The feeding rate was kept 0.38 kg/s while the receiving rate dropped to 0.35 kg/s.

- Test 23, m_f=0.0085 kg/s or v=0.87 m/s; the solids mass flow rate could not be maintained because of the lower air mass flow rate.

4.3.2 Visual Observations of Air-Solid Flow through the Horizontal Pipeline with High Solids Mass Flow rate

For conveying with a solids mass flow rate of about 1.8 kg/s, as the air mass flow rate decreasing, the following flow phenomena were observed through the sight-glass 6.0 m from the feeding point of the conveying pipeline and also the conveying parameters were measured:

- Test 1, m_f=0.185 kg/s or V=19.5 m/s; average pressure drop across the conveying pipeline was 5.1 kPa. Very lean fully suspension flow could be observed.

- Test 2, m_f=0.1649 kg/s or V=17.4 m/s; average pressure drop across the conveying pipeline was 5.0 kPa. Observations were as above.

- Test 3, m_f=0.152 kg/s or V=16.0 m/s; average pressure drop across the conveying pipeline was 4.9 kPa. Visible segregation of the two phases with a slightly higher concentration of particle (strand flow) near the bottom of the pipe was observed.

- Test 4, m_f=0.135 kg/s or V=14.2 m/s; average pressure drop across the conveying pipeline was 5.6 kPa. Observations were as above with the strand flow on the bottom of the pipe observed.

- Test 5, m_f=0.129 kg/s or V=13.5 m/s; average pressure drop across the conveying pipeline was 6.4 kPa. Observations were as above with the slightly thick strand flow on the bottom of the pipe and very faint balling observed.

- Test 6, m_f=0.117 kg/s or V=12.3 m/s; average pressure drop across the conveying pipeline was 7.1 kPa. A thicker strand flow on the bottom of the pipe and minor balling observed.

- Test 7, m_f=0.109 kg/s or v=11.5 m/s; average pressure drop across the conveying pipeline was 9.1 kPa. A thicker strand flow on the bottom of the pipe and more balling was observed.

- Test 8, m_f=0.104 kg/s or v=10.9 m/s; average pressure drop across the conveying pipeline was 9.7 kPa. A strand flow over a slowly moving bed with a thickness of 10~15 mm was observed.

- Test 9, m_f=0.092 kg/s or v=9.6 m/s; average pressure drop across the conveying pipeline was 13.7 kPa. A strand flow over a slowly moving bed with a thickness of 20~25 mm was observed.

- Test 10, m_f=0.086 kg/s or v=9.1 m/s; average pressure drop across the conveying pipeline was 14.7 kPa. A strand flow over a slowly moving bed with a thickness about 25 mm was observed.

- Test 11, m_f=0.079 kg/s or v=8.3 m/s; average pressure drop across the conveying pipeline was 16.3 kPa. A strand flow over a slowly moving bed with a thickness about 35 mm was observed.

- Test 12, m_f=0.074 kg/s or v=7.8 m/s; average pressure drop across the conveying pipeline was 17.3 kPa. A strand flow over a slowly moving bed with a thickness of 35~40 mm was observed.

- Test 13, m_f=0.0655 kg/s or v=6.9 m/s; an unstable flow alternated between a strand flow over a moving bed and a long and violent slug with a pressure drop peak of 96 kPa and a pressure drop trough of about 2.0 kPa.

- Test 14, m_f=0.0632 kg/s or V=6.6 m/s; an unstable flow alternated between a strand flow over a moving bed and a long and violent slug with a pressure drop peak of 75 kPa and a pressure drop trough of about 4.0 kPa. The time period for building a slowly moving layer and sweeping it into receiving bin became shorter than Test 13

- Test 15, m_f=0.0595 kg/s or V=6.3 m/s; an unstable flow alternated between strand flow over a moving bed and a long slug with a pressure drop peak of 65 kPa and a pressure drop trough of about 6.0 kPa. Very close to the unstable/dense-phase boundary. m_f=0.0542 kg/s or V=5.7 m/s and slug flow with average pressure drop across the conveying pipeline was 27.8 kPa was also observed.

- Test 16, m_f=0.041 kg/s or V=4.3 m/s; average pressure drop across the conveying pipeline was 32.9 kPa. Gentle slug flow with stationary layer about 15 mm thick left on the bottom of conveying pipeline was observed.

- Test 17, m_f=0.033 kg/s or V=3.5 m/s; average pressure drop across the conveying pipeline was 36.1 kPa. Gentle slug flow with stationary layer about 20 mm thick left on the bottom of conveying pipeline was observed.

- Test 18, m_f=0.027 kg/s or V=2.8 m/s; average pressure drop across the conveying pipeline is 41.2 kPa. Gentle slug flow with stationary layer about 30 mm thick left on the bottom of conveying pipeline was observed. Solids mass flow rate could not be maintained for lower air mass flow rates.

4.4 Solids Contained in Conveying Pipeline and Pressure Drop during Conveying

To highlight the flow phenomena especially within the unstable zone for pneumatic transportation of granular materials, with the load cells installed on the feeding bin and receiving bin of the test rig, the mass of solid materials entering the feeding rotary valve and receiving bin could be monitored and hence the mass of solid materials contained in the conveying pipeline could be obtained. The solid materials contained in the conveying pipeline could flow in suspension, strand or slowly moving bed, deposited near the inlet or along the conveying pipeline or feeding shoe. Corresponding to solid materials contained in the conveying pipeline, the pressure drop across the conveying pipeline showed a very similar variation as the air mass flow rate changed. For the convenience of making a comparison, a low solids mass flow rate (0.37 kg/s) and a high solids mass flow rate (1.8 kg/s) were selected and kept constant with a wide range variations in air mass flow rate for the display of conveying tests. Analysis of the pressure drop across the conveying pipeline and the solid materials contained in the conveying pipeline provided some important information for flow phenomena identification and flow mechanism exploration.

4.4.1 Solids Contained in Pipeline and Pressure Drop for Low Solids Mass Flow Rate:

With a solids mass flow rate of 0.37 kg/s and decreasing air mass flow rate from 0.189 kg/s to 0.109 kg/s where the stationary layer could not be observed through sight-glass, the measurement of the solid materials contained in the conveying pipeline for the air mass flow rates of 0.189, 0.122, 0.109 kg/s is shown in Figure 4.4.1 for comparison. It was very clear that as the air mass flow rate decreased from 0.189 kg/s to 0.122 kg/s, there was almost no variation in amount of solid materials contained in the conveying pipeline. When the air mass flow rate was further decreased to 0.109 kg/s, a significant

increase in the amount of mass of solid materials contained in the conveying pipeline implied that the flow structure in the conveying pipeline began to change. Even though the formation of a stationary layer had not been observed through sight-glass that was located 6.0 m from the inlet of the conveying pipeline, a stationary layer with a length less than 6.0 m could have formed at the inlet of the conveying pipeline where the particle velocity was lower and extended forwards. Also solid materials became more concentrated in the strand on the bottom of the conveying pipeline and the strand velocity being lower induced the increase in mass of solid materials contained in the conveying pipeline.

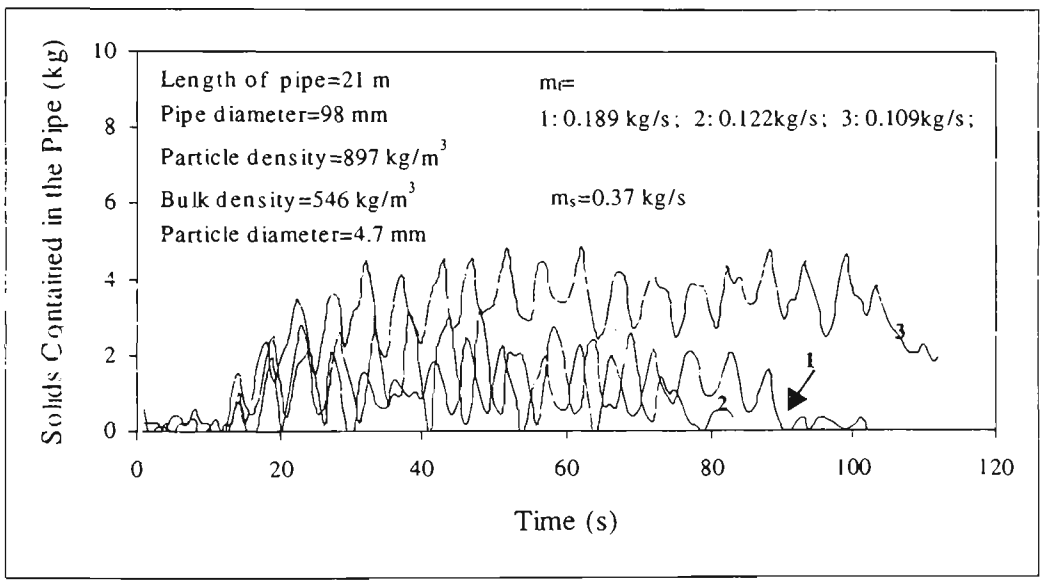

Figure 4.4.1 Material contained in conveying pipeline with respect to air mass flow rate

Corresponding to the mass of solid materials contained in the conveying pipeline with low solids mass flow rate and variation in air mass flow from 0.189 kg/s to 0.109 kg/s, the curves of pressure drop across the conveying pipeline in Figure 4.4.2 showed the same trend that indicates the clear relationship between the pressure drop across the conveying pipeline and the mass for solid materials contained in it. As the air mass

flow rate decreased from 0.189 kg/s to 0.122 kg/s, there was almost no variation in pressure across the conveying pipeline. When the air mass flow rate was further decreased to 0.109 kg/s, the significant increase in the pressure across the conveying pipeline occurred as shown in Figure 4.4.2. The fluctuation in the amount of the mass of solid materials contained in the conveying pipeline may be caused by unsteady flow of materials from the feeding hopper and/or the pulsing nature of the rotary valve. Since the amount of solid material contained in the conveying pipeline was small, the fluctuation seemed to be very pronounced and as the mass of solid materials contained in the conveying pipeline reached a certain value, the fluctuation looked to be negligible as shown in Figure 4.4.3.

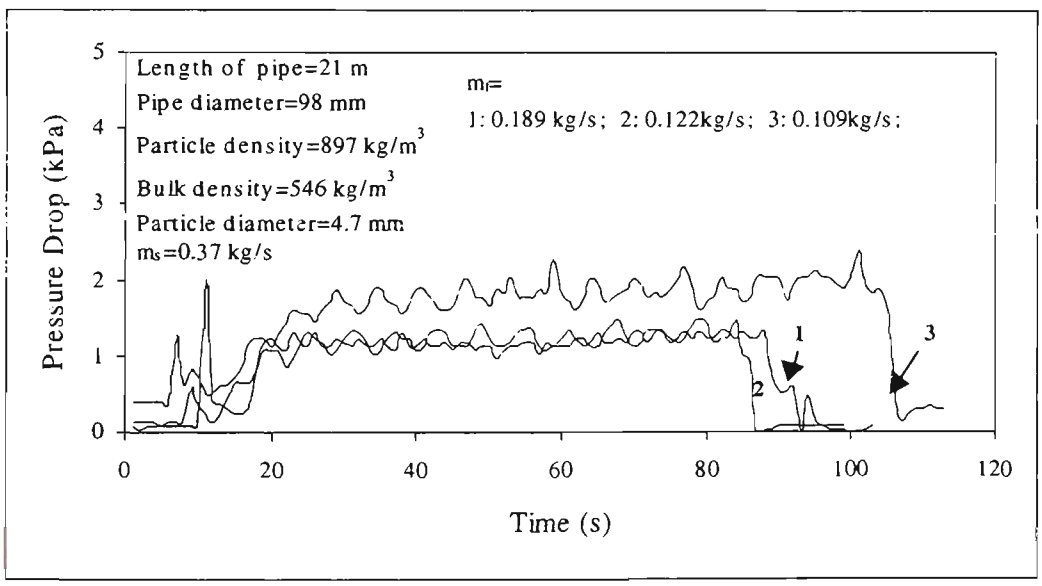

Figure 4.4.2 Pressure drop across conveying pipeline with respect to air mass flow rate

Figure 4.4.3 shows the mass of solid materials contained in the conveying pipeline when air-solid two-phase in the form observed as strand flow over stationary layer with solid mass flow rate of 0.37 kg/s and a variation in air mass flow from 0.096 kg/s to 0.076 kg/s. Three curves in the Figure 4.4.3 represent mass of solids contained in

the conveying pipeline when the air mass flow rates are 0.096, 0.083, 0.076 kg/s respectively. As the air mass flow rate decreased, the amount of solids contained in the conveying pipeline increased significantly as a result of the increase in the thickness and extension in length of the stationary layer. Corresponding to the trend of the amount of the mass of solid materials contained in the conveying pipeline, the pressure drop across the conveying pipeline also increased considerably as the air mass flow rate was decreasing as shown in Figure 4.4.4.

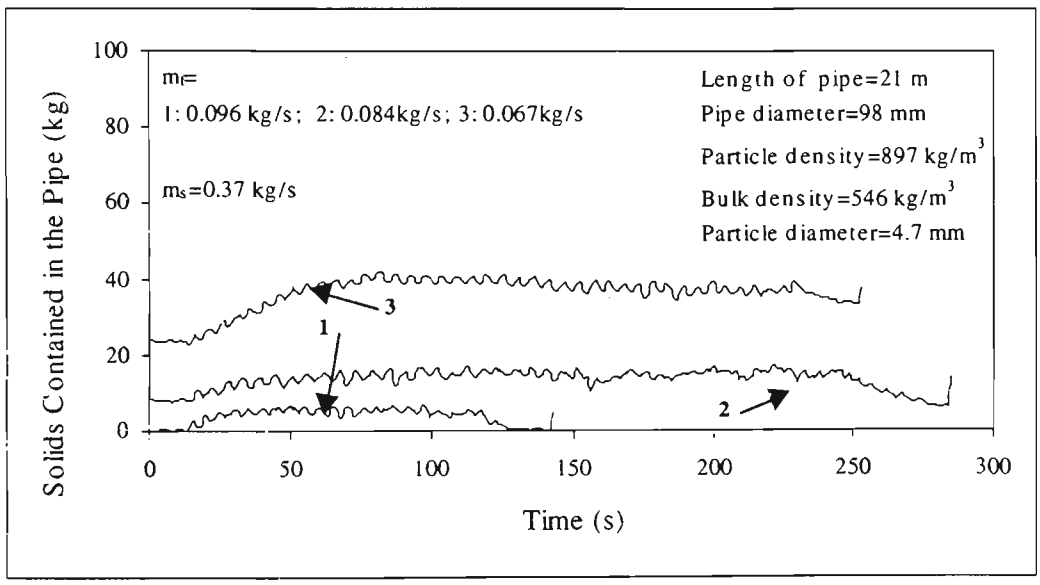

Figure 4.4.3 Materials contained in conveying pipeline with respect to air mass flow rate

The increase in the pressure drop across the conveying pipeline may be attributed to the increase in friction force between the moving strand and the stationary layer that was much higher than the friction force between the moving strand and the pipe wall, and to the increase in the amount of solid materials in the strand. Even though the pneumatic conveying of solid materials can be stable in the form of a strand flow over a stationary layer if the air mass flow rate is well controlled, the quick increase in pressure drop across the conveying pipeline caused by the increase of the friction

between the stationary layer and the strand as well as the possibility of unstable flow proves that such a mode of conveying is not suitable for industry.

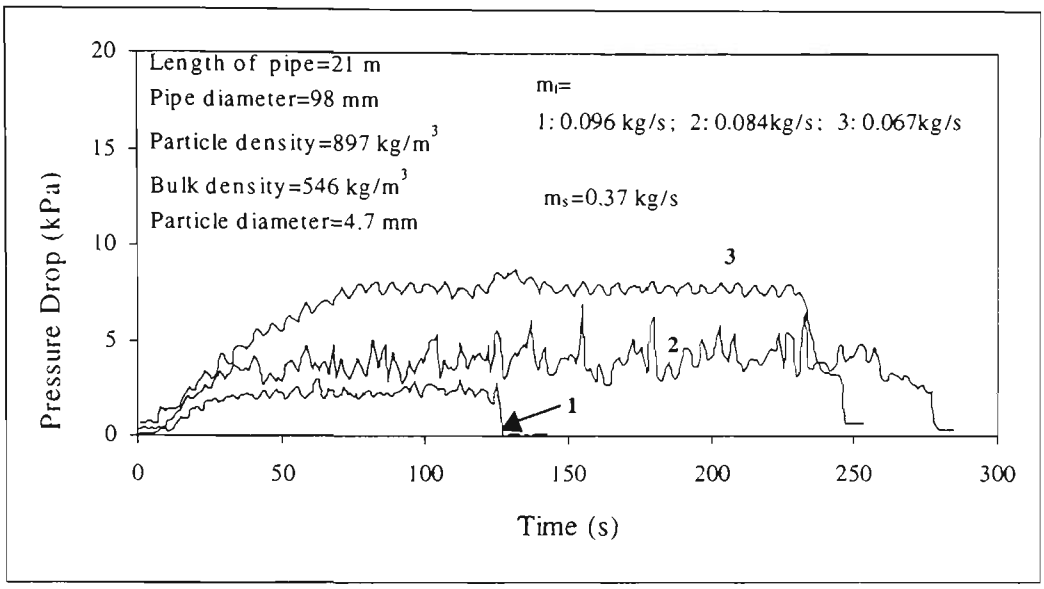

Figure 4.4.4 Pressure drop across conveying pipeline with respect to air mass flow rate

Figure 4.4.5 and Figure 4.4.6 show the mass of solid materials contained in the pipe and the pressure drop across the conveying pipeline when the conveying tests were conducted in the unstable zone. In Figure 4.4.5, the sloping segments of curve-1 clearly shows the building up and extension of a stationary layer along the conveying pipeline and the vertical segments show that the solid materials deposited on the bottom of the conveying pipeline had been swept into receiving bin as the result of the transition from the strand flow over stationary layer to long slug flow. When the transition happened, the first slug was formed at the inlet of the conveying pipeline where the velocity of the strand was lowest, then the slug picked up very thick stationary layer in front of it and deposited very thin layer behind and became longer and longer until it entered the receiving bin. Such unstable flow behaviours were also reflected by the fluctuation of the pressure drop across the conveying pipeline shown in Figure 4.4.6. When the stationary layer building up and extending from inlet of the

conveying pipeline, the increase in pressure drop across the conveying pipeline is represented by a slope straight line like curve-1 in Figure 4.4.6. When the transition of flow mode occurred, a slug formed at the inlet of the conveying line, moved forward and became longer, pressure drop across the conveying pipeline suddenly increased at a very high rate corresponding to the increase in the length of slug. This is represented by the vertical parts of curve-1 in Figure 4.4.6. The curve-2 in both Figures 4.4.5 and 4.4.6 is quite different from the curve-1 as the effect of transition of flow mode was not so pronounced as that of curve-1. Since the air mass flow rate was quite low for the conveying condition represented by curve-2, once the long slug form, it will move at relatively low velocity and deposit more thicker layer of solid materials behind and hence cause less pressure drop fluctuation across the conveying pipeline compared with that in high air mass flow rate.

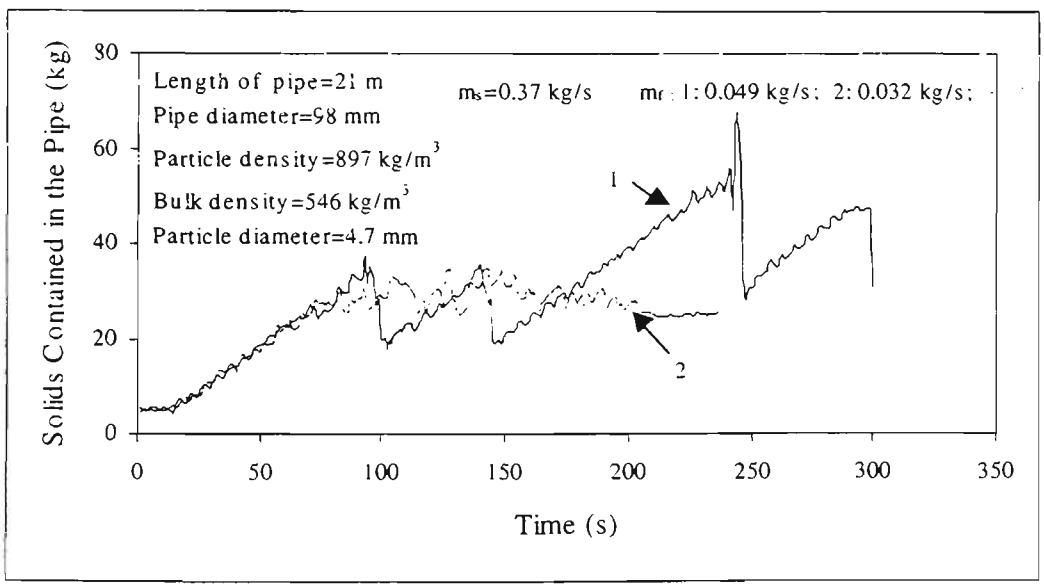

Figure 4.4.5 Material contained in conveying pipeline with respect to air mass flow rate

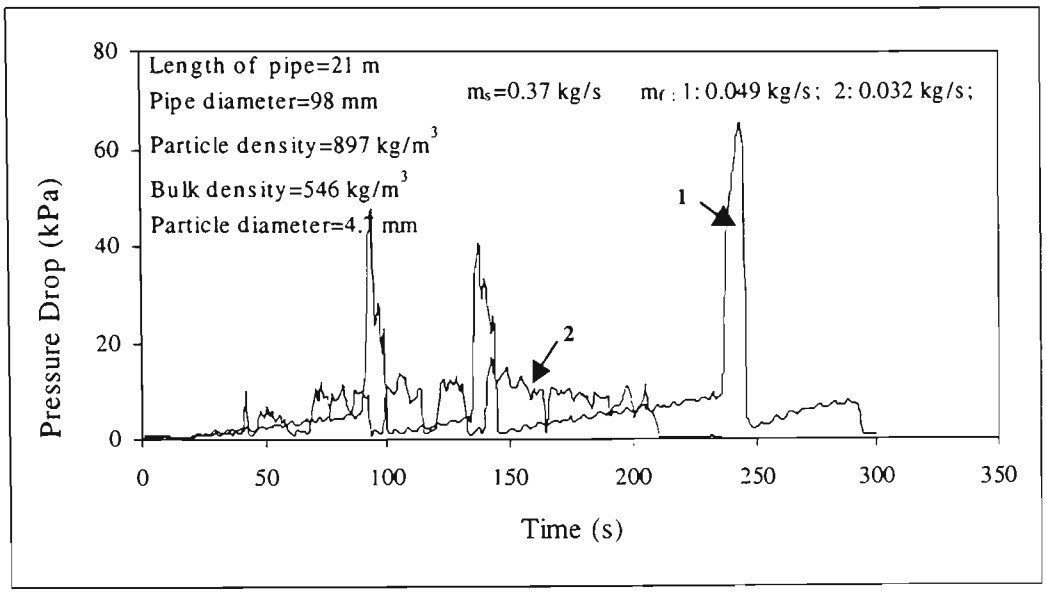

Figure 4.4.6 Pressure drop across conveying pipeline with respect to air mass flow rate

The curves in Figures 4.4.7 and 4.4.8 represent the mass of solid materials contained in the conveying pipeline and the pressure drop across it for the pneumatic conveying in the form of low-velocity slug-flow. As the air mass flow rate decreased from 0.02 kg/s to 0.011 kg/s, the mass of solid materials contained in the conveying pipeline significantly increased as the result of the decrease in slug velocity, an increase in the thickness of the stationary layer deposited by the slug and the number of slug contained in the conveying pipeline when the solids mass flow rate kept constant. Corresponding to the increase in the mass of solid materials contained in the conveying pipeline, the pressure drop across the conveying pipeline was no so significant. Curve-3 in both Figures 4.4.7 and 4.4.8 represents that the steady state low-velocity slug flow could not be maintained for more solid materials entering the conveying pipeline and less solid materials could be moved out into the receiving bin. Solid materials retained in the conveying pipeline increased and hence the whole conveying pipeline would block as the conveying continued.

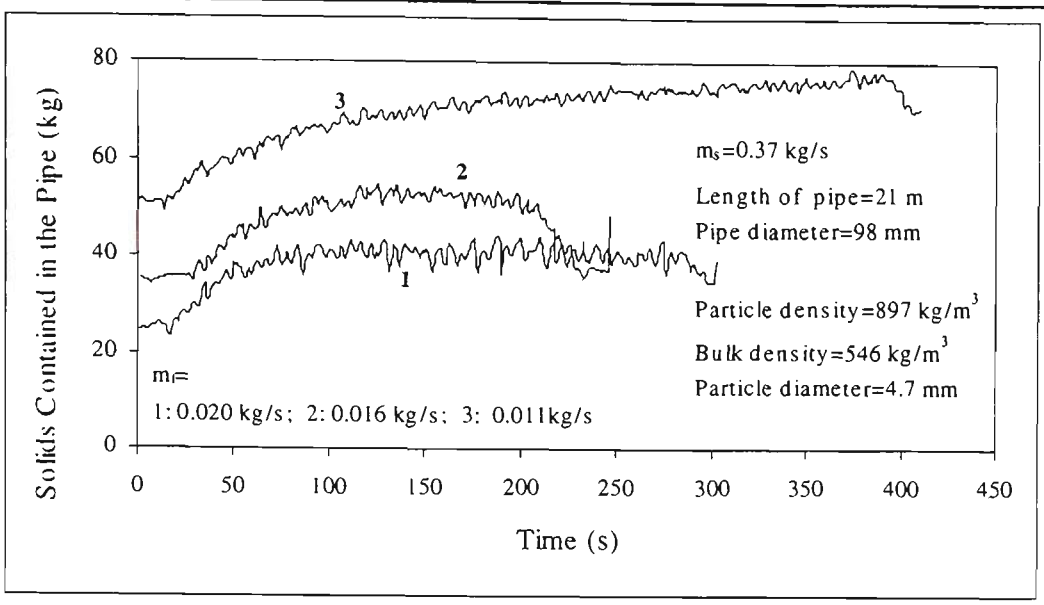

Figure 4.4.7 Material contained in conveying pipeline with respect to air mass flow rate

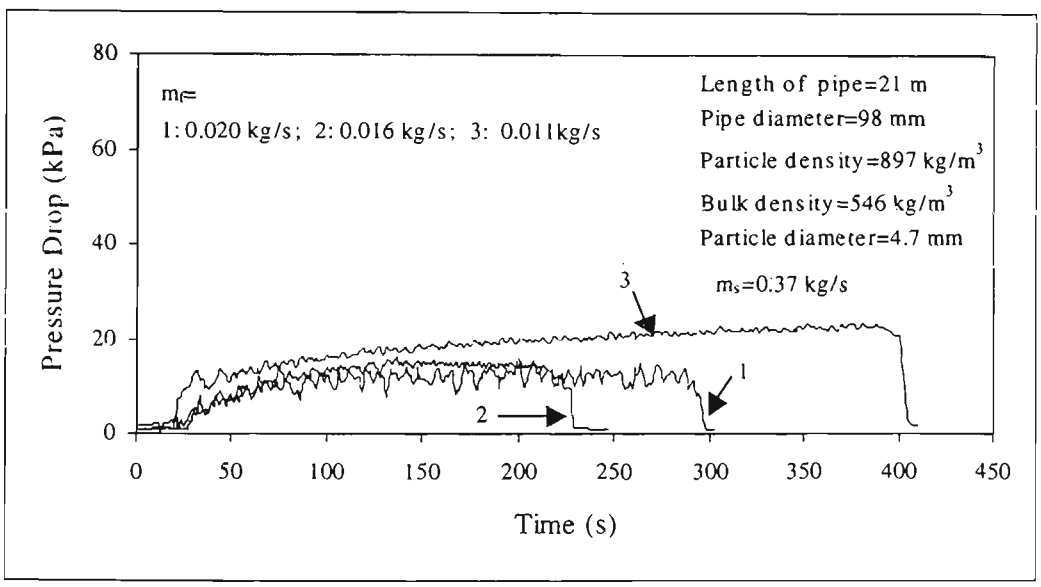

Figure 4.4.8 Pressure drop across conveying pipeline with respect to air mass flow rate

4.4.2 Solids Contained in Pipeline and Pressure Drop for High Solids Mass Flow Rate:

In order to explore in detail the air-solid two-phase flow structure and the mechanisms for the formation of the unstable zone in the state diagram, the pressure drop across the

conveying pipeline and the mass of the solid materials contained in it with high and low solids mass flow rates were addressed separately for pneumatic conveying of granular materials. The following paragraphs are devoted to discussion of the pressure drop across the conveying pipeline and the mass of solid materials contained in it with a solids mass flow rate of about 1.8 kg/s for pneumatic conveying of granular materials.

Figure 4.4.9 shows the measurement of the mass of solid materials contained in the conveying pipeline for the air mass flow rates of 0.185, 0.129, 0.109 kg/s respectively. It was clear that as the air mass flow rate decreased from 0.185 kg/s to 0.129 kg/s, there was a very slightly increase in amount of mass of solid materials contained in the conveying pipeline. When the air mass flow rate was further decreased to 0.109 kg/s, the mass of solid materials contained in the conveying pipeline began to increase significantly implying that the flow structure in the conveying pipeline had began to change. The formation of the stationary layer still had not been observed at sight-glass that was located 6.0 m from the inlet of the conveying pipeline. A slowly moving bed on the bottom of conveying pipeline with a length less than 6.0 m could have began to form at the inlet of the conveying pipeline where the particle velocity was lower and extended forwards. Also solid materials became more concentrated in the strand over the bottom of the conveying pipeline and the strand velocity was lowered to increase the mass of solid materials contained in the conveying pipeline.

Corresponding to mass of solid materials contained in the conveying pipeline with solids mass flow rate of 1.8 kg/s and variation in air mass flow from 0.185 kg/s to 0.109 kg/s, the curves of pressure drop across the conveying pipeline in Figure 4.4.10 show the same trend that indicates the definite relationship between the pressure drop

across the conveying pipeline and mass of solid materials contained in it. As the air mass flow rate decreased from 0.185 kg/s to 0.129 kg/s, there was a slight variation in pressure across the conveying pipeline. When the air mass flow rate was further decreased to 0.109 kg/s, there was a greater pressure drop across the conveying pipeline as shown in Figure 4.4.10.

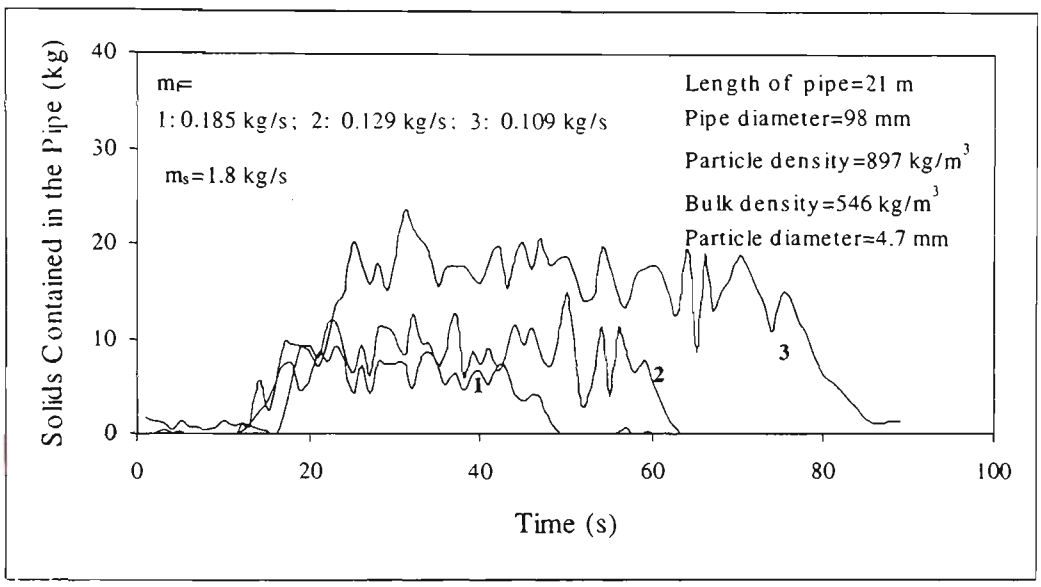

Figure 4.4.9 Material contained in the pipeline with respect to air mass flow rate

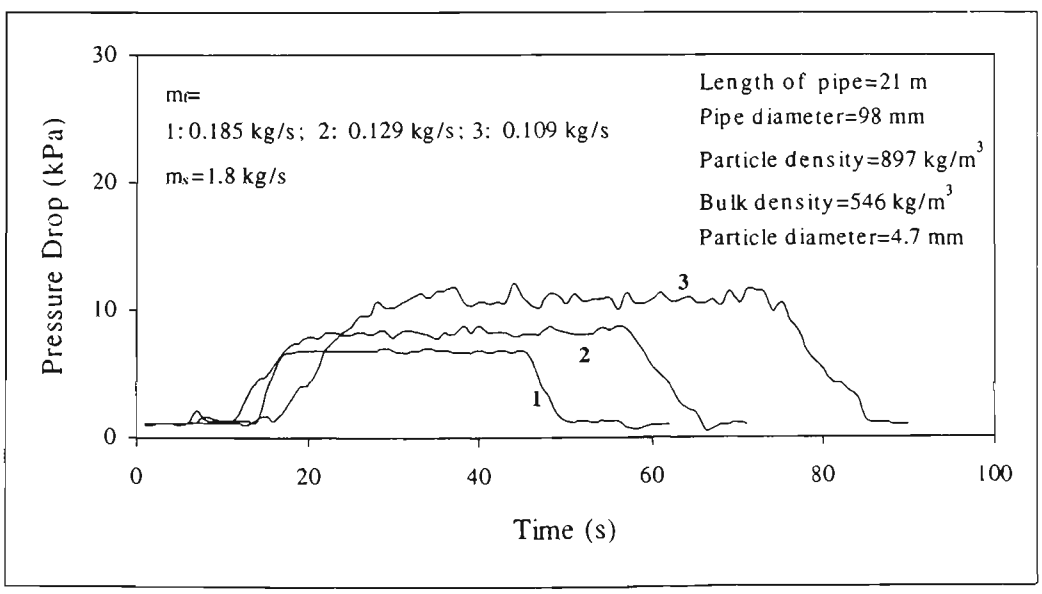

Figure 4.4.10 Pressure drop across conveying pipeline with respect to air mass flow rate

As was the situation with the low solids mass flow rate, so the fluctuation in the mass of solid materials contained in the conveying pipeline might have been caused by the unsteady flow of mass solids in the feeding bin or pulsing flow of solid materials entering the receiving bin. As the mass of the solid materials contained in the conveying pipeline was small, the fluctuation of mass of the solid materials contained in the conveying pipeline seemed to be very pronounced and when the mass of solid materials contained reached a certain value, the fluctuation looked to be negligible.

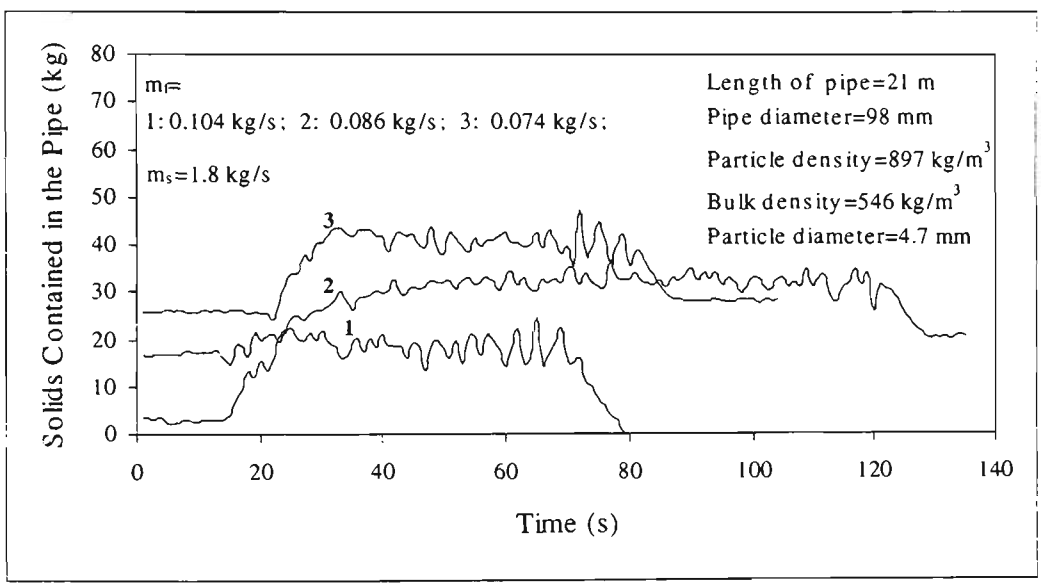

Figure 4.4.11 Material contained in conveying pipeline with respect to air mass flow rate

Figures 4.4.11 and 4.4.12 show the testing results of pneumatic conveying of solid materials in the form observed as strand flow over a slowly moving bed. When the air flow rate decreased from 0.104 to 0.074 kg/s, the mass of solid materials contained in the conveying pipeline increase significantly as a result of the slowly moving bed building up and extending. Corresponding to the trend of the amount of solids contained in the conveying pipeline as shown in Figure 4.4.11, the pressure drop across the conveying pipeline shown in Figure 4.4.12 also increased considerably as

the air mass flow rate was decreasing. The increase in the pressure drop across the conveying pipeline could also be attributed to the increase in friction force between the strand and the slowly moving bed compared with the friction force between the strand and the pipe wall, and the increase in the amount of solid materials in the strand. Since the air mass flow rate is not easy to control accurately and the high pressure drop caused by the stationary layer and the pulsating flow results in shattering or erosion of the slowly moving bed at its end, such a mode of pneumatic conveying is not accepted by industry.

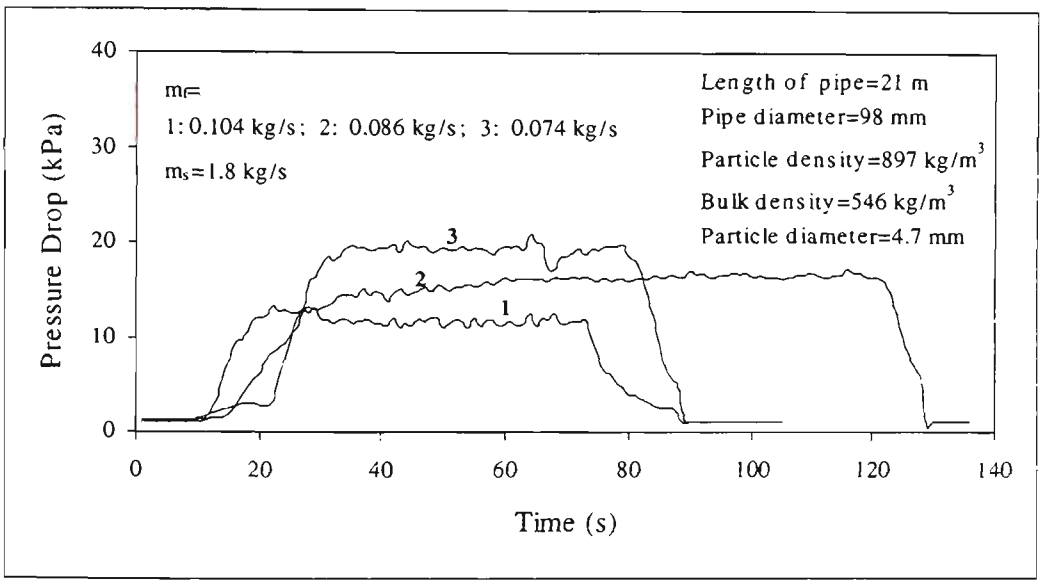

Figure 4.4.12 Pressure drop across conveying pipeline with respect to air mass flow rate

Figure 4.4.13 and Figure 4.4.14 show the results of the mass of solids contained in the conveying pipeline and the pressure drop across it when the conveying tests were conducted in the unstable zone in state diagram. In Figure 4.4.13, the segments of curves with a positive slope represent the building up and extending of a slowly moving bed along the conveying pipeline and the segments of curve with negative slope show the transition from the strand flow over a slowly moving bed to a long and

violent slug flow and long slugs entering the receiving bin. When the transition occurred, the slug first formed near the inlet of the conveying pipeline, then swept the slowly moving bed on the bottom of the conveying pipeline and became longer and longer until entered the receiving bin.

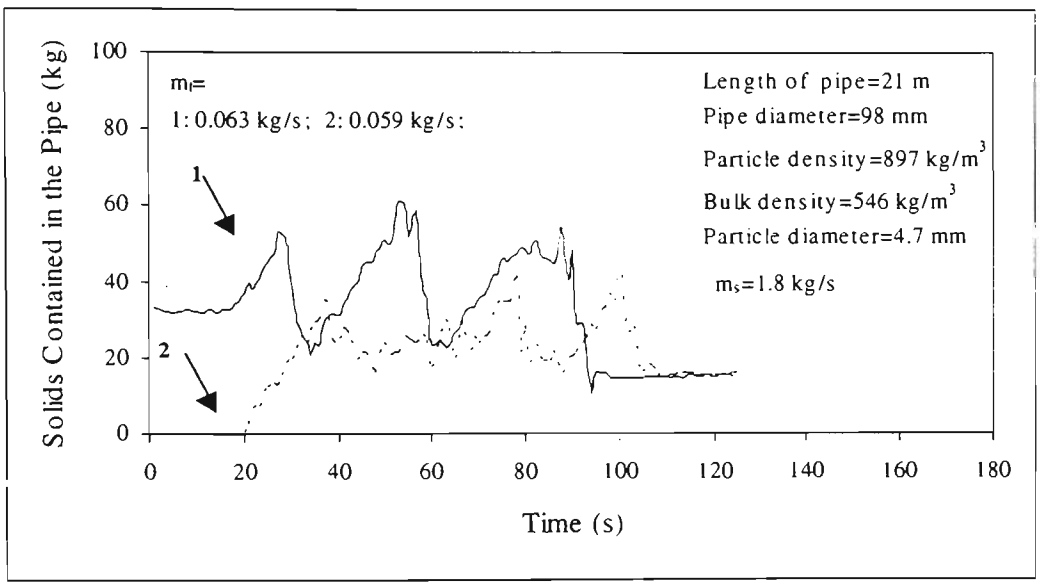

Figure 4.4 13 Material contained in conveying pipeline with respect to air mass flow rate

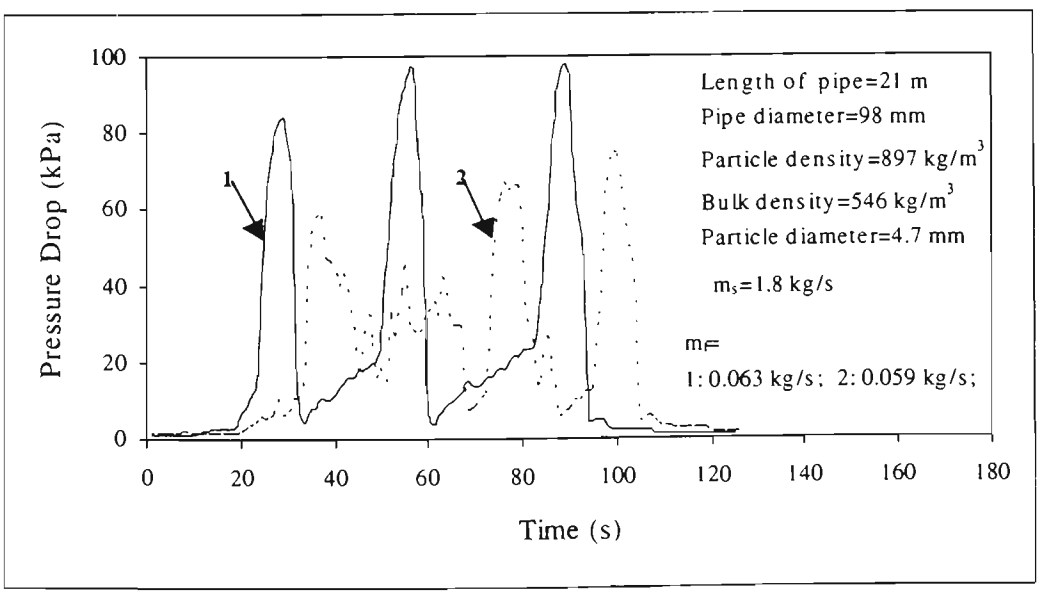

Figure 4.4.14 Pressure drop across conveying pipeline with respect to air mass flow rate

Such unstable flow behaviours were also reflected by the fluctuation of the pressure drop across the conveying pipeline shown in Figure 4.4.14. When the slowly moving bed was building up and extending, the pressure drop across the conveying pipeline increased gradually. When the transition of flow mode happened, a long slug formed and moved forward, a sudden huge peak in pressure drop appeared.

The curves in Figures 4.4.15 and 4.4.16 represent pneumatic conveying in the form of low-velocity slug-flow with a solids mass flow rate of about 1.8 kg/s. As air mass flow rate decreased, the slug velocity decreased. The particles in the layer deposited by the slugs increased and the number of slugs contained in the conveying pipeline increased, as the solids mass flow rate kept constant. As a result, the mass of the solid materials contained in the conveying pipeline and pressure drop across the pipeline increased.

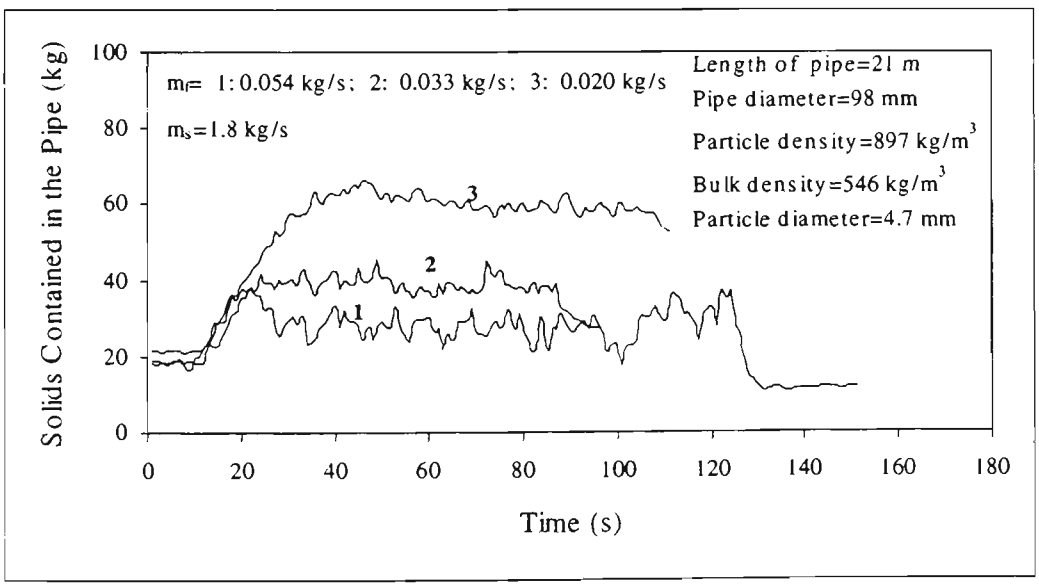

Figure 4.4.15 Material contained in conveying pipeline with respect to air mass flow rate

Curve-1 in both Figures 4.4.15 and 4.4.16 represents the operation of the pneumatic conveying on the boundary between the dense phase low-velocity slug flow zone and

the unstable zone in the state diagram. The characteristics of unstable flow can still be seen through the curve-1 in Figure 4.4.16.

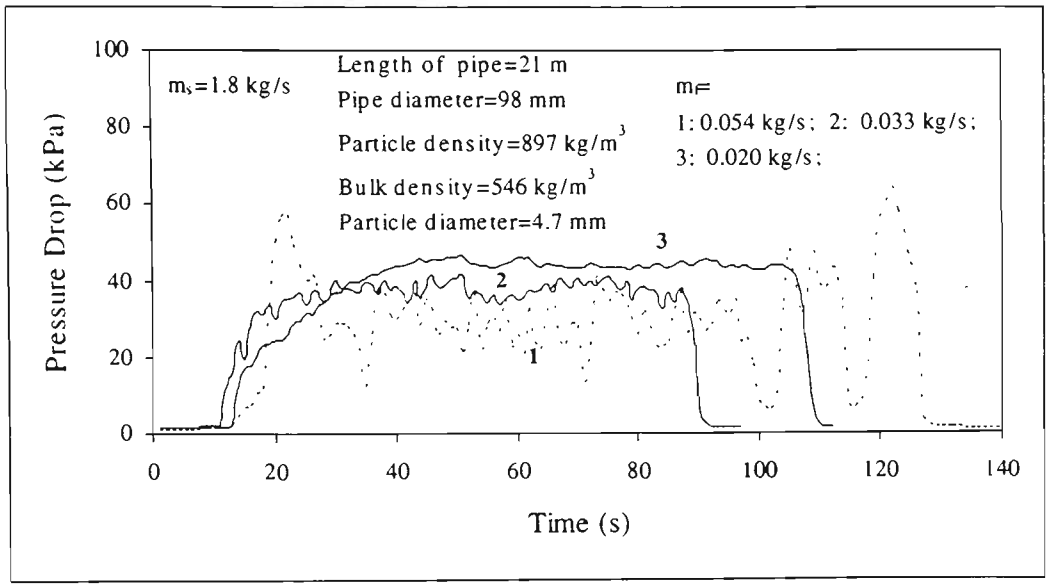

Figure 4.4.16 Pressure drop across conveying pipeline with respect to air mass flow rate

4.5 Pneumatic Conveying Characteristics of Plastic Pellets through 98.4 mm and 60.3 mm ID 21m Long Stainless Steel Pipelines

The pneumatic conveying characteristics of plastic pellets through the test rig with a 98.4 mm and 60.3 mm ID 21m long stainless steel pipelines are shown in Figures 4.5.1 and 4.5.2. While the operations conducted with a very low air mass flow rate in the dense-phase pneumatic conveying zone, the air mass flow rates reached the point where the solids mass flow rate could not be maintained constantly at a low air mass flow rate. Because the operations in the unstable zone were subjected to violent fluctuations in the pressure, the operating points representing the unstable flow alternating between long violent slug flow and a strand over a stationary layer or a slowly moving bed could not be located in the PCC diagrams.

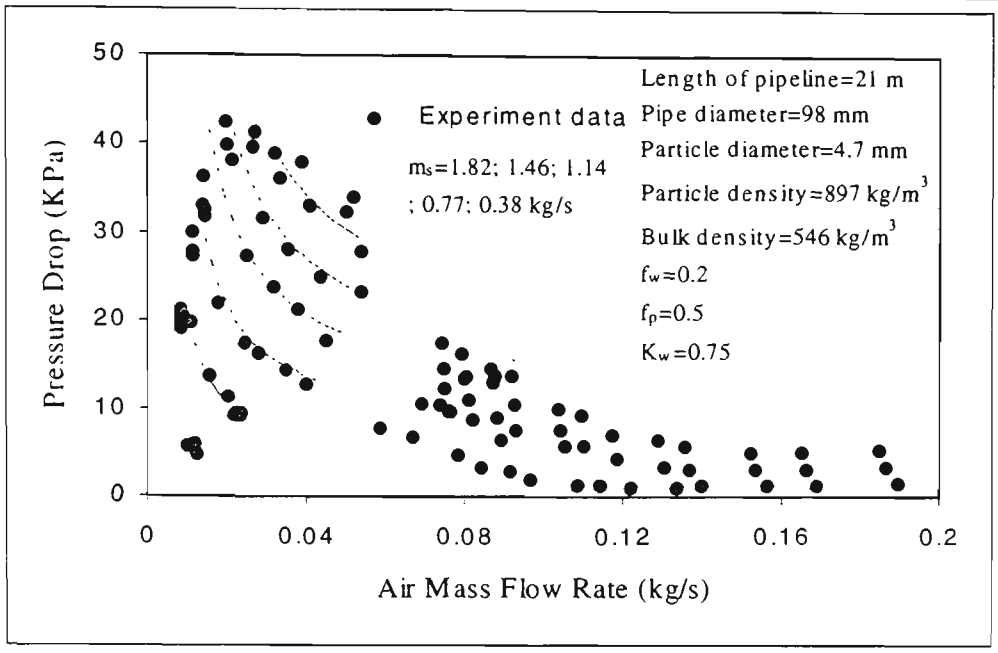

Figure 4.5.1 PCC for plastic pellets through the test rig with 98.4 mm ID stainless steel pipeline

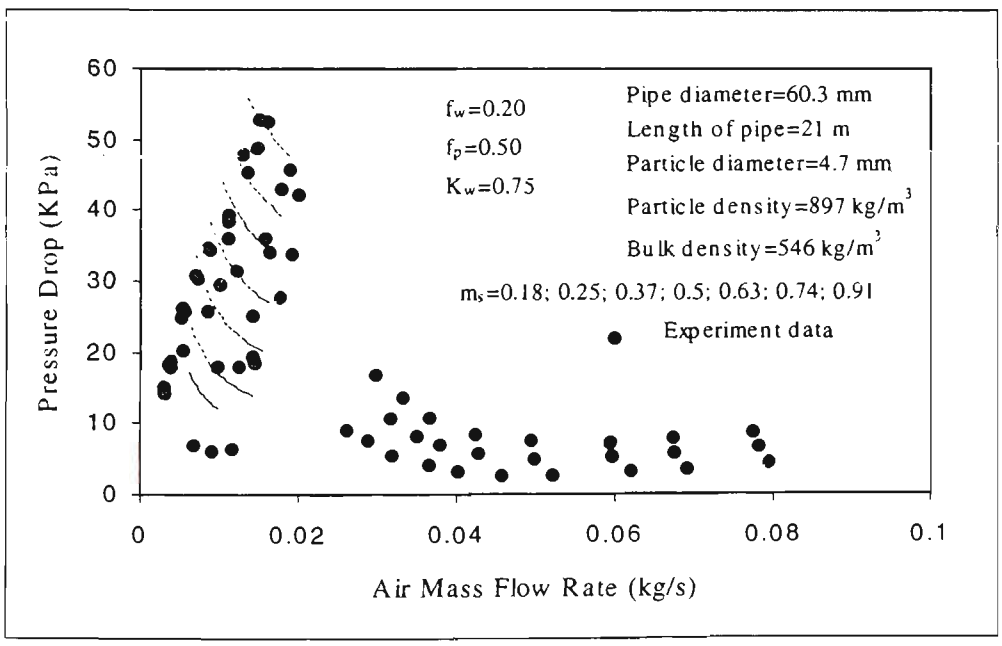

Figure 4.5.2 PCC for plastic pellets through the test rig with 60.3 mm ID stainless steel pipeline

4.6 Discussion on Visual Observations of Air-Solid Two-Phase Flow through 98.4 mm 21m Long Stainless Steel Horizontal Pipeline

Based on tests of pneumatic conveying of plastic pellets with particle diameter of 4.7 mm, particle density of 897 kg/m^3 through the stainless steel conveying pipeline with a 98 mm inner diameter and 21 m in length, the following conclusions can be achieved after careful observation and the analysis of the flow behaviours, the pressure drop across the conveying pipeline and the mass of solid materials contained in the pipeline for conveying conditions covering dilute-phase, unstable zone and low-velocity slug flow dense phase in the state diagram:

(i) Pneumatic conveying of granular plastic pellets exhibits different flow modes: low-velocity slug-flow, dilute-phase flow with suspended particles and/or strands, strand flow over a layer (stationary or moving).

(ii) Solids mass flow rate has an important influence on the air-solid two-phase flow behaviours when the operation is in or close to the unstable zone in state diagram. The layers under the strand flow were in two different conditions on the bottom of conveying pipeline according to the solids mass flow rate. A stationary layer over which the strand flow was going on for low solid mass flow rates and a slowly moving bed over which strand flow was going on for high solid mass flow rates indicate the main difference.

(iii) If the conveying pipeline is long enough, there may be two flow modes existing in it: a strand flow over the stationary layer or slowly moving bed near the inlet, and dilute-phase flow with suspended particles and/or strands afterwards. For such conveying conditions, pulsating strand flow such as moving dune or balling will appear as the shattering or erosion of the front end of stationary layer or slowly moving bed occurs.

(vi) The pressure fluctuations within the unstable zone result from the flow mode transition from strand flow over a stationary layer (or slowly moving bed) to slug flow starting near the inlet due to the decrease in air velocity (increase in pressure drop and air density). As the first slug moves quickly at a relatively high velocity and picks up a relatively thick stationary layer in front of it, it only deposits a small amount of the material behind it. The great increase in slug length and pressure drop causes severe pressure fluctuations and pipeline vibrations.

(v) In the unstable zone, the time period for building up the stationary layer or slowly moving bed and then forming a long slug quickly moving into the receiving bin will be reduced as the air mass flow rate approaches to the boundary between the unstable and low-velocity slug-flow operating zones. If the second slug already forms before the first slug enters the receiving bin, then the pressure fluctuations across the conveying pipeline will be alleviated. In the other words, the difference between the peak and the trough of pressure drop across the conveying pipeline, which is used to distinguish the unstable flow from low-velocity slug flow in the tests, will be smaller.

(vi) During operations in the unstable zone with high solids mass flow rate, a strand flow over the slowly moving bed appears in the cross-section of the conveying pipeline near the inlet of it. As the conveying continues, the slowly moving bed stops just before the slug forms at the inlet of the conveying pipeline. With a low solids mass flow rate, a strand flow over the stationary layer appears in the cross-section of the conveying pipeline as the conveying begins. As the conveying continues, the thickness of the stationary layer on the bottom of

conveying pipeline gradually increases until the first slug forms at the inlet of conveying pipeline.

CHAPTER 5: MODEL FOR PREDICTION OF TRANSITION ZONE

5.1 Introduction

The air-solid two-phase flow of granular plastic pellets through the horizontal conveying pipeline in the operating regime of unstable zone of state diagram has been well explored in Chapter Four. It has been shown that there is a three-layer flow structure (suspension flow, strand flow and stationary layer or slowly moving bed) across the cross-section of the conveying pipeline for pneumatic conveying of granular plastic pellets through the horizontal pipeline operated in the unstable zone of state diagram. Further observations on the flow behaviors in the unstable zone indicate that with high solids mass flow rate, suspension flow and strand flow over the slowly moving bed appear in the cross-section of the conveying pipeline as the conveying begins and continues, the slowly moving bed stops just before the slug forms at the inlet of the conveying pipeline. For conveying of granular plastic pellets in the unstable zone of state diagram with low solids mass flow rate, suspension flow and strand flow over the stationary layer appear in the cross-section of the conveying pipeline as the conveying begins. As the conveying continues the thickness of the stationary layer on the bottom of the conveying pipeline gradually increases until the first slug forms at the inlet of conveying pipeline.

Following observations of the air-solid two-phase flow of granular plastic pellets through the horizontal conveying pipeline in the operating regime of unstable zone of state diagram, a three-layer flow structure in the unstable zone of the state diagram is assumed for the flow structure of the model. Based on this three-layer flow structure, a theoretical model for illustrating the force balance, mass balance and momentum balance between two adjacent layers is established. By analysing the relationships between the three layers, the mechanisms for the formation of the boundaries of unstable zone in the state diagram are explored. The approach for the predictions of the

boundaries of the unstable zone in the state diagram for pneumatic conveying of granular materials through the horizontal pipeline is developed.

5.2 Theoretical Model

There are three basic assumptions for the establishment of the model: all the particles moving in suspension above the strand are at the superficial velocity of the air; all the particles moving in the strand are at the superficial velocity of air in the strand; and the velocity of the slowly moving bed is negligible. There is a steady state particle exchange between the suspension flow and the strand. The suspended particles impinging the strand will slow down to the strand velocity and be expelled from the suspension. Other particles will be displaced from the strand and accelerated by the air to the same velocity as the air in the suspension. The force balance, mass balance and momentum balance are set up. The pressure drop is subdivided into additional pressure drop and single-phase (airflow) pressure drop that is negligible compared with solids pressure drop (Note: derivation based on Wirth [104, 105, 106] but extended to three-layer flow structure as shown in Fig. 5.2.1)

$$\frac{\Delta P}{\Delta L} = \frac{\Delta P_p}{\Delta L} + \frac{\Delta P_g}{\Delta L} \tag{5.2.1}$$

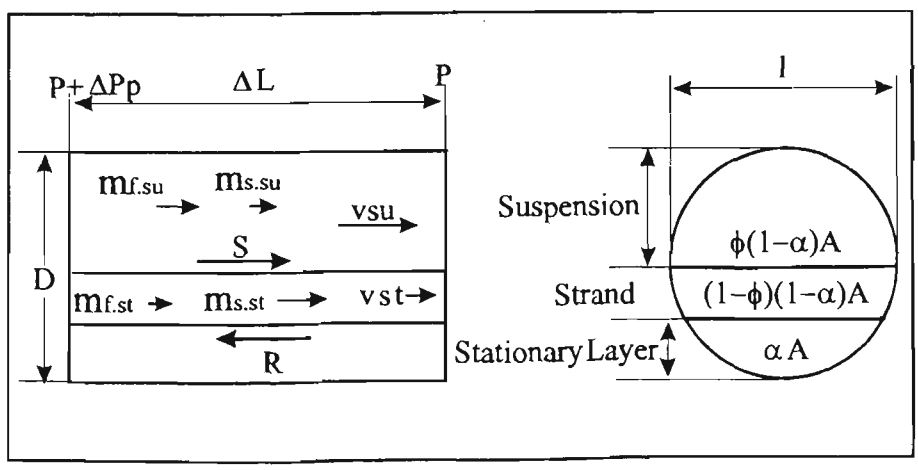

Figure 5.2.1 Flow structure in pipe element

5.2.1 Force Balance

In the layer of suspension, the force balance between the shear force S and the solid pressure drop can be represented by the equation below:

$$\Delta P_p \cdot (1-\alpha) \cdot \phi \cdot A = S \tag{5.2.2}$$

In the middle layer of the strand, the friction force R between the strand and stationary layer or slowly moving bed is equal to the pressure drop and shear force S :

$$\Delta P_p \cdot (1-\alpha) \cdot (1-\phi) \cdot A + S = R \tag{5.2.3}$$

The friction between the strand and the stationary layer or slowly moving bed is equal to the weight of the strand less the buoyancy multiplied by the coefficient of the particle internal friction:

$$R = f_p \cdot (\rho_p - \rho_f) \cdot (1-\varepsilon_{st}) \cdot (1-\phi) \cdot (1-\alpha) \cdot A \cdot \Delta L \cdot g \tag{5.2.4}$$

From the above three equations, the following equation can be obtained:

$$\frac{\Delta P_p}{f_p \cdot \rho_p \cdot \left(1 - \rho_f / \rho_p\right) \cdot (1-\varepsilon_{st}) \cdot g \cdot \Delta L} = (1-\phi) \tag{5.2.5}$$

The left side of the equation 5.2.5 is defined as the non-dimensional pressure drop [67, 104, 105, 106].

5.2.2 Mass Balance

Mass balance of air and solids exists in the three layers across the cross-section of conveying pipeline. It is assumed that the air mass flow through the stationary layer or slowly moving bed region of the cross-section of the conveying pipeline is negligible

and hence the mass flow of air through the whole conveying pipeline is equal to the air mass flow through the suspension region plus air mass flow through the strand region of the cross-section of the conveying pipeline and can be presented by the equation:

$$m_f = \rho_f \cdot v_{su} \cdot \phi \cdot (1-\alpha) \cdot A + \rho_f \cdot (1-\phi) \cdot \varepsilon_{st} \cdot v_{st} \cdot (1-\alpha) \cdot A \qquad (5.2.6)$$

For the solid materials, it is assumed that the solids mass flow through the stationary layer or slowly moving bed region of the cross-section of the conveying pipeline is negligible and hence the mass flow of solids through the whole conveying pipeline is equal to the solids mass flow through the suspension region plus solids mass flow through the strand region of the cross-section of the conveying pipeline and can be presented by the equation:

$$m_s = \rho_p \cdot (1-\phi) \cdot (1-\varepsilon_{st}) \cdot v_{st} \cdot (1-\alpha) \cdot A + \rho_p \cdot \phi \cdot (1-\varepsilon_{su}) \cdot v_{su} \cdot (1-\alpha) \cdot A \qquad (5.2.7)$$

There are three mass-flow ratios of solids to air for the strand and suspension regions of the cross-section and the whole cross-section of conveying pipeline then can be defined as:

$$\mu_{st} = \left[\rho_p \cdot (1-\phi) \cdot (1-\varepsilon_{st}) \cdot v_{st} \cdot (1-\alpha) \cdot A\right] / \left[\rho_f \cdot v \cdot (1-\alpha) \cdot A\right] \qquad (5.2.8)$$

$$\mu_{su} = \left[\rho_p \cdot \phi \cdot (1-\varepsilon_{su}) \cdot v_{su} \cdot (1-\alpha) \cdot A\right] / \left[\rho_f \cdot v \cdot (1-\alpha) \cdot A\right] \qquad (5.2.9)$$

$$\mu = M_s / M_f \qquad (5.2.10)$$

An overwhelming majority of particles is moving in the form of strand through the strand region of cross-section of conveying pipeline hence it is reasonable to consider

$\mu = \mu_{st}$. A combination of the mass of air and solids balance Equations 5.2.6 and 5.2.7 leads to the following equation:

$$\frac{v_{st}}{v_{su}} = \frac{\phi}{1-\phi} \cdot \left[\frac{\rho_p \cdot (1-\varepsilon_{st})}{\rho_f \cdot \mu} - \varepsilon_{st} \right]^{-1} \tag{5.2.11}$$

5.2.3 Momentum Balance

The shear stress acting on the interface between the strand and suspension regions is caused by the exchange of the moving particles with different velocities. It was assumed previously that the particles moving in suspension are at the velocity of the air in the suspension and the particles in the strand are at the velocity of the air in strand.

For a single particle, the momentum change between the strand and suspension zone is given as follows:

$$\Delta J = m \cdot (v_{su} - v_{st}) \tag{5.2.12}$$

The shear stress at the interface of the strand and suspension results from the number of particle exchanges and can be expressed as follows:

$$\tau = n \cdot \Delta J \tag{5.2.13}$$

n is the number flow rate of particles per unit area. It is considered that the exchanging number of particles per unit interface area is proportional to the solids mass flow rate in the suspended flow region divided by the mass of a single particle and the cross-section area of the suspended flow channel.

$$n \propto \frac{m_{s.su}}{m \cdot \phi \cdot (1-\alpha) \cdot A} \tag{5.2.14}$$

Combining the Equations 5.2.12, 5.2.13 and 5.2.14 results in:

$$\tau = \frac{K \cdot m_{s.su} \cdot (v_{su} - v_{st})}{\phi \cdot (1-\alpha) \cdot A} \tag{5.2.15}$$

The relationship between the strand width, the relative cross-sectional area of strand region and relative area of stationary layer or slowly moving bed region is provided by [67]:

$$l_w = \left[4 \cdot \phi \cdot (1-\alpha) \cdot \left(1 - \phi \cdot (1-\alpha)\right)\right]^{1/3} \cdot D \tag{5.2.16}$$

Using the above equations, shear stress S can be written as:

$$S = \tau \cdot \Delta L \cdot l_w =$$

$$K \cdot \mu_{su} \cdot \rho_f \cdot v^2 \cdot D \cdot \Delta L \frac{\left[4 \cdot \phi \cdot (1-\alpha) \cdot \left(1 - \phi \cdot (1-\alpha)\right)\right]^{1/3}}{\phi^2} \left(1 - \frac{v_{st}}{v_{su}}\right)\left[1 - \frac{\rho_f \cdot \varepsilon_{st} \cdot \mu}{\rho_p \cdot (1-\varepsilon_{ST})}\right] \tag{5.2.17}$$

It is assumed that the air can carry a certain amount of particles in suspension and the mass flow ratio μ_{su} in suspension is constant. So $K \cdot \mu_{su}$ is constant and can be replaced by λ_h [67]. Combining the equations of mass balance and force balance, the momentum balance gives:

$$\frac{v^2}{f_p \cdot (\rho_p / \rho_f) \cdot (1 - \rho_f / \rho_p) \cdot (1 - \varepsilon_{st}) \cdot D \cdot g} =$$

$$\frac{1}{\lambda_h}\cdot\frac{\pi}{4}\cdot\frac{1}{1-\dfrac{\rho_f\cdot\mu\cdot\varepsilon_{st}}{\rho_p\cdot(1-\varepsilon_{st})}}\cdot\frac{1}{1-\dfrac{v_{st}}{v_{su}}}\cdot\frac{\phi^3\cdot(1-\phi)\cdot(1-\alpha)}{\left[4\cdot(1-\alpha)\cdot\phi\cdot\left(1-(1-\alpha)\cdot\phi\right)\right]^{1/3}}. \qquad (5.2.18)$$

Where λ_h=0.0826 [67]. Equations 5.2.5, 5.2.11 and 5.2.18 make up the model of the three-layer structure flow for pneumatic conveying of granular materials and are used the prediction of unstable zone boundaries. The left side of the Equation 5.2.18 is defined as a non-dimension friction number [67, 104, 105, 106]:

$$Fri^2=\frac{v^2}{f_p\cdot(\rho_p/\rho_f)\cdot(1-\rho_f/\rho_p)\cdot(1-\varepsilon_{st})\cdot D\cdot g} \qquad (5.2.19)$$

5. 3 Stability Analysis for State Diagram of Strand Flow

From the Equations 5.2.5, 5.2.11 and 5.2.18, the diagram that depicts the non-dimensional pressure gradient versus the non-dimension friction number with the volumetric flow ratio $(\rho_f\cdot\mu)/(\rho_p\cdot(1-\varepsilon_{st}))$ and velocity ratio v_{st}/v_{su} as parameters is shown in Figure 5.3.1 for the convenience of stability analysis.

For conveying with constant solids and air mass flow rates through a horizontal conveying pipeline, a disturbance during stable strand flow through an empty pipe or over a stationary layer or slowly moving bed may result in a reduction of the strand velocity and hence the velocity ratio v_{st}/v_{su}. The decrease in strand velocity results in an increase in the amount of solid materials contained in the pipeline, if the disturbance results in an increase of solid mass flow rate and hence volumetric flow ratio $(\rho_f\cdot\mu)/(\rho_p\cdot(1-\varepsilon_{st}))$, then the extra solid materials contained in the conveying pipeline can be removed and conveying can be stable and maintained. On the other hand, if the disturbance results in an decrease of solid mass flow rate and hence volumetric flow ratio $(\rho_f\cdot\mu)/(\rho_p\cdot(1-\varepsilon_{st}))$, then the extra solid materials contained in the conveying

pipeline can be accumulated on it and the blockage of the conveying pipeline or the formation of slug will be induced. According to Figure 5.3.1 three different types of operating points are discerned with respect to stability analysis.

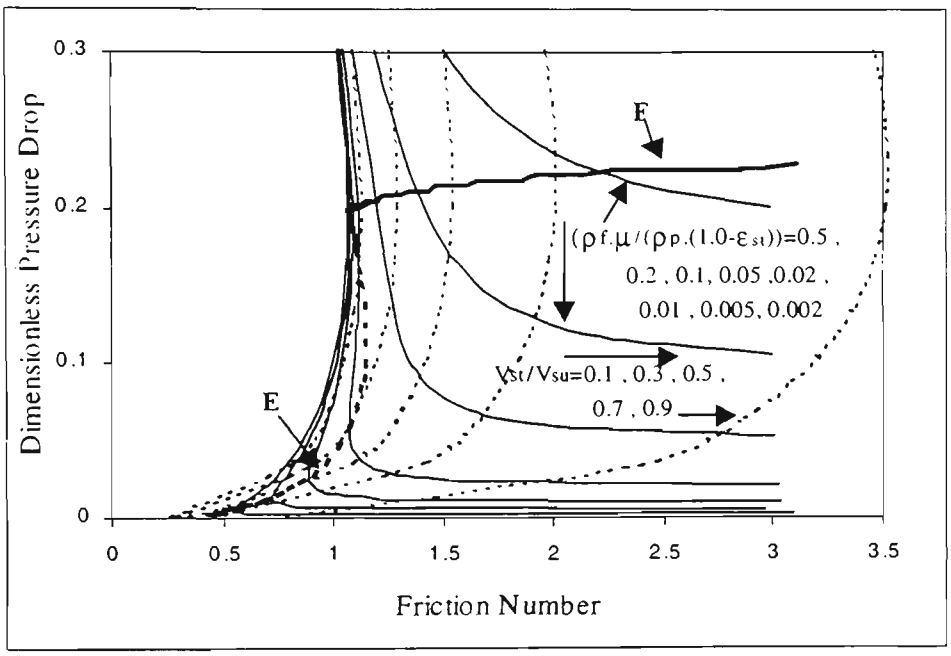

Figure 5.3.1 State diagram based on Equations 5.2.5, 5.2.11 and 5.2.18

5.3.1 Type A

Type A operating points are those at which the curves of $(\rho_f \cdot \mu)/(\rho_p \cdot (1-\varepsilon_{st}))$=constant and v_{st}/v_{su}=constant have a positive slope and the slope of curve $(\rho_f \cdot \mu)/(\rho_p \cdot (1-\varepsilon_{st}))$=constant is higher than that of curve of v_{st}/v_{su}=constant at operating points in the diagram. In pneumatic conveying of granular materials through the horizontal pipeline, type A operating points represent the mode of air-solid two-phase flow in the form of a strand flow over a stationary layer with low solids mass flow rate. A schematic representation of type A operating points is shown in Figure 5.3.2.

Assuming that a disturbance causes a decrease in the velocity ratio v_{st}/v_{su} and shifts the operating point A to point A1 with a lower volumetric flow ratio $(\rho_f \cdot \mu)/(\rho_p \cdot (1-\varepsilon_{st}))$,

then an increase in the amount of extra solid materials accumulated in the pipeline will take place. An increase amount of solid materials in the pipeline results in an increase of the thickness of the stationary layer and the decrease of the intersectional channel area of the flow. With constant air mass flow rate and almost constant air pressure, the air velocity through the flow channel will increase and hence the F_{ri}. As a result, F_{ri} keeps increasing until the operating point A1 is shifted to A2 where the volumetric flow ratio can be retained and hence the solid mass flow rate. For type A operating points, stable strand flow over a stationary layer for pneumatic conveying of granular materials is feasible with an increase in the thickness of the stationary layer.

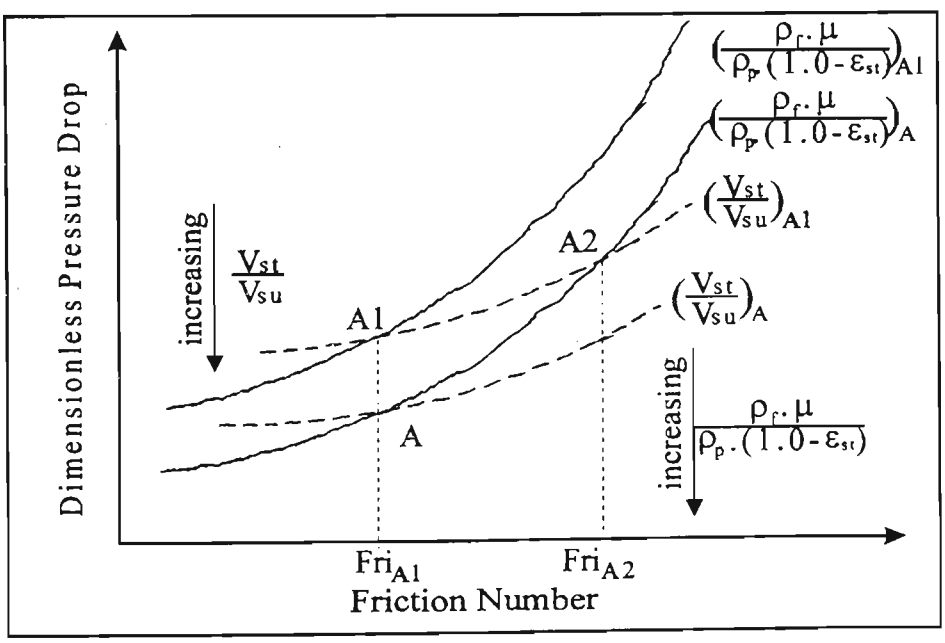

Figure 5.3.2 Schematic representation of type A operating points

The thickness of the stationary layer for type A operating points can not increase forever without limitation. When the air velocity and the solids mass flow rate per unit area through the flow channel increase to certain value as the result of reduction of flow channel area, type A operating points will transfer into type C operating points. In such a situation, a disturbance causing a decrease in the velocity ratio v_{st}/v_{su} can not

result in increase in the thickness of the stationary layer and finally induce the formation of the slug that will be further discussed later.

5.3.2 Type B

Type B operating points are those at which the curves $(\rho_f \cdot \mu)/(\rho_p \cdot (1-\varepsilon_{st}))$=constant have a negative slope while the curves v_{st}/v_{su}=constant have a positive slope. Type B operating points represent the mode of air-solid two-phase flow through a horizontal pipeline in the form of the strand flow without the stationary layer or slowly moving bed on the bottom of conveying pipeline. Figure 5.2.3 provides a schematic representation of this type of operating points in the diagram.

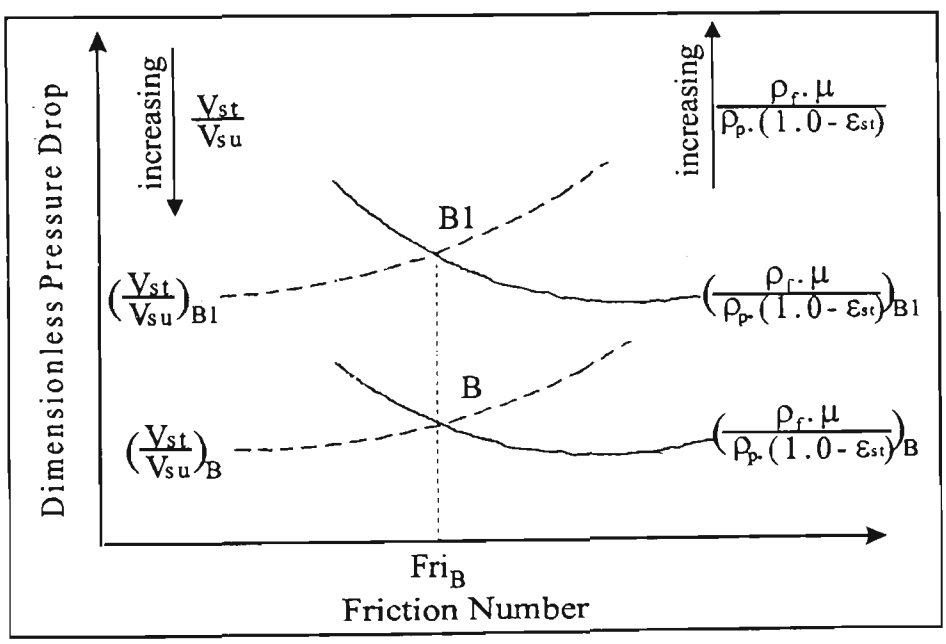

Figure 5.3.3 Schematic representation of type B operating points

A disturbance causing a decrease in the velocity ratio v_{st}/v_{su} and shifts point B onto point B1. At point B1, a higher volumetric flow ratio $(\rho_f \cdot \mu)/(\rho_p \cdot (1-\varepsilon_{st}))$ is attained. This means that the system is able to remove the extra solid materials contained in the conveying pipeline and go back to point B. Type B operating points represent the

steady-state strand flow of pneumatic conveying of granular materials through a horizontal pipeline

5.3.3 Type C

Type C operating points are those at which the curves $(\rho_f \cdot \mu)/(\rho_p \cdot (1-\varepsilon_{st}))$=constant and v_{st}/v_{su}= constant have negative slopes. In the pneumatic conveying of granular materials through a horizontal pipeline, type C operating points represent the mode of air-solid two-phase flow in the form of the strand flow over a slowly moving bed with high solids mass flow rate. A schematic representation of type C operating points is shown in Figure 5.3.4.

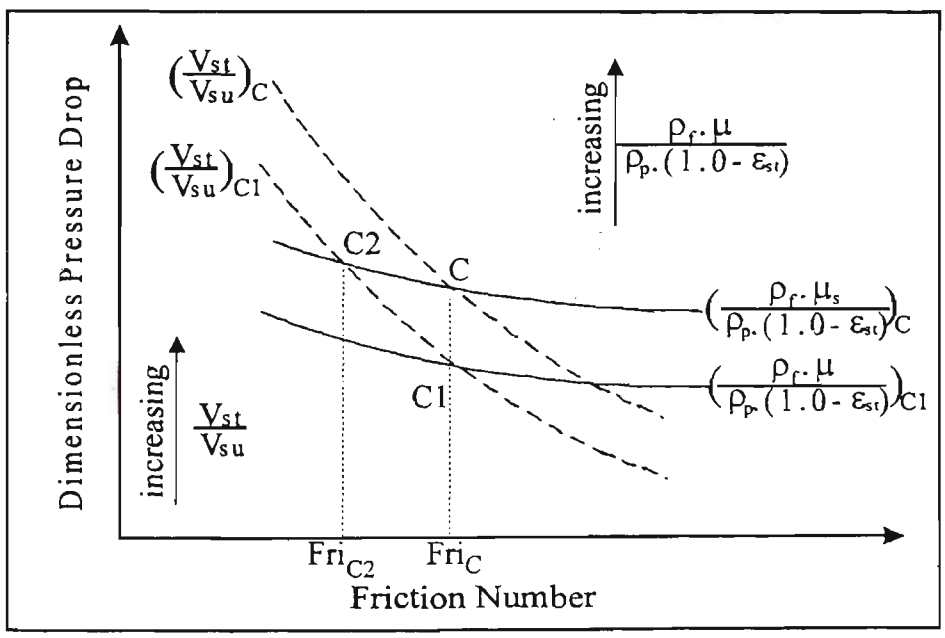

Figure 5.3.4 Schematic representation of type C operating points

Assuming that a disturbance causes a decrease in the velocity ratio v_{st}/v_{su} and shifts the operating point C to point C1 with a lower volumetric flow ratio $(\rho_f \cdot \mu)/(\rho_p \cdot (1-\varepsilon_{st}))$, then an increase in the amount of extra solid materials accumulated in the pipeline will take place, further occupy the whole pipeline intersection and finally induce the

formation of slug flow. Stable strand flow over a layer is not feasible for type C operating points unless the friction force between the strand and the layer is high enough to push the layer to move and reduce its thickness, and then the conveying area becomes larger and the F_{ri} becomes lower. As shown in Figure 5.3.4, keeping the same v_{st}/v_{su} and reducing the F_{ri}, the volumetric flow ratio $(\rho_f \cdot \mu)/(\rho_p \cdot (1-\varepsilon_{st}))$ can be retained and the result is a stable strand flow type of pneumatic conveying over a slowly moving bed. If the friction force between the strand and the layer is not high enough to keep the layer moving because the layer is too thick, then the formation of a slug will occur and the flow mode of a strand flow over a slowly moving bed can not be maintained.

5.3.4 The Limiting Curves E and F

To separate the points having a positive slope of the curves v_{st}/v_{su}=constant from that having a negative slope, the limiting curve **F** in Figure 5.3.1 is defined by a vertical slope of the respective curves v_{st}/v_{su}=constant, as follows:

$$\left\{\partial\left[\frac{\Delta P_p}{f_r \cdot \rho_p \cdot (1-\rho_f/\rho_p)\cdot(1-\varepsilon_{st})\cdot g \cdot \Delta L}\right]\Big/\partial F_{ri}\right\}_{\frac{V_{st}}{V_{su}}=const} = \infty \qquad (5.3.1)$$

Note f_r is equal to f_w for an empty pipe and equal to f_p for strand flow over a stationary bed. Also to separate the points having a negative slope of curves $(\rho_f \cdot \mu)/(\rho_p \cdot (1-\varepsilon_{st}))$=constant from those having a positive slope, the limiting curve **E** is defined by a vertical slope of the respective curves $(\rho_f \cdot \mu)/(\rho_p \cdot (1-\varepsilon_{st}))$=constant as follows:

$$\left\{\partial\left[\frac{\Delta P_p}{f_r \cdot \rho_p \cdot (1-\rho_f/\rho_p)\cdot(1-\varepsilon_{st})\cdot g \cdot \Delta L}\right]\Big/\partial F_{ri}\right\}_{\frac{\rho_f \mu}{\rho_s(1-\varepsilon_{st})}=const} = \infty \qquad (5.3.2)$$

As the results, curve **F** separates the type C operating points from type B operating points and curve **E** separates type A operating points from type B operating points. In Figure 5.3.1, the region on the right side of curve **E** and below the curve **F** in the diagram are type B operating points which represent the pneumatic conveying of granular materials through a horizontal pipeline in the mode of steady-state strand flow without stationary layer or slowly moving bed on the bottom of the conveying pipeline. The region on the left side of curve **E** in the diagram is type A operating point, which represent the pneumatic conveying of granular materials through a horizontal pipeline in the mode of limited stable strand flow over a stationary layer. The upper region of curve **F** in the diagram is type C operating points which represent the pneumatic conveying of granular materials through a horizontal pipeline in the mode of limited stable strand flow over a slowly moving bed. The stability of the strand flow over a slowly moving bed is determined by the friction force between the strand and the slowly moving bed or the thickness of the layer over which the strand flow is going. It is worth pointing out that in the moving stationary bed, there is no velocity difference and movement between particles, while in the moving strand velocity difference and movement between particles exist.

5.3.5 Unreal Stable Operating Points in the State Diagram

In the state diagram based on the Equations 5.2.5, 5.2.11 and 5.2.18 shown in Figure 5.3.1, mathematical stability analysis confirms that the stable operating region without limitations is outlined by curve **E** separating type A operating points from type B operating points and **F** separating the type C operating points from type B operating points. Further mathematical exploration of the state diagram shown in Figure 5.3.5, reveals that in a special region in the diagram there are two different operating points

in the state diagram with the same air mass flow rate or F_{η} and the volumetric flow ratio $(\rho_f \cdot \mu)/(\rho_p \cdot (1-\varepsilon_{st}))$.

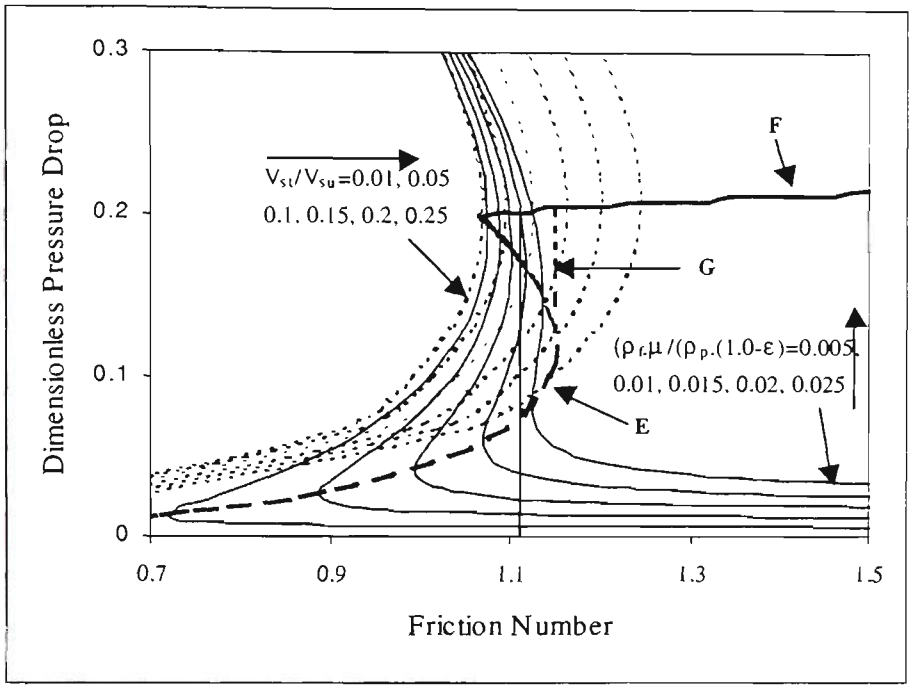

Figure 5.3.5 State diagram based on Equations 5.2.5, 5.2.11 and 5.2.18

In Figure 5.3.5, for instance, with the volumetric flow ratio $(\rho_f \cdot \mu)/(\rho_p \cdot (1-\varepsilon_{st}))=0.02$ at $F_{\eta}=1.112$, there are two stable operating points located within the stable operating region outlined by curve E and F with different dimensionless pressure drop of 0.038 and 0.20 respectively. The velocity ratio v_{st}/v_{su} for two operating points are 0.51 and 0.092 separately. The two stable operating points are the two solutions from the Equations 5.2.5, 5.2.11 and 5.2.18 with $(\rho_f \cdot \mu)/(\rho_p \cdot (1-\varepsilon_{st}))=0.02$ and only one can exist in the real pneumatic conveying of granular materials. In mathematics, they represent two different conveying situations. One has a close velocity in strand and suspension, so that the strand moves at a velocity close to that in suspension occupying less area in cross-section of the pipeline so causing less pressure drop. The other has about ten times velocity difference in the strand and suspension, and strand moves in the velocity

much lower than that in suspension occupying more area in the cross-section of the pipeline and causes much more pressure drop. According to the law of nature, the second conveying condition is not easy to maintain and can not exist in real pneumatic conveying. All the operating points considered as the second solution of the equations and will not exist in real conveying are in the triangle region in the state diagram outlined by lines E, F and G shown in Figure 5.3.5. The true stable operating points without conditions for pneumatic conveying of granular materials through a horizontal pipeline are on the left of lines E and G, below the line F in the state diagram. The line G can be considered as part of the line of $(\rho_f \cdot \mu)/(\rho_p \cdot (1-\varepsilon_{st}))=C$ in the diagram established by the Equations 5.2.5, 5.2.11 and 5.2.18 and the constant C is decided by such mathematical condition that C is the largest value for $(\rho_f \cdot \mu)/(\rho_p \cdot (1-\varepsilon_{st}))$ to make the Equation 5.3.3 have only one solution.

$$\left\{\partial\left[\frac{\Delta P_p}{f_r \cdot \rho_p \cdot (1-\rho_f/\rho_p) \cdot (1-\varepsilon_{st}) \cdot g \cdot \Delta L}\right] \Big/ \partial F_{ri}\right\}_{\frac{\rho_f \mu}{\rho_p (1-\varepsilon st)}=C} = \infty \qquad (5.3.3)$$

5.4 Explanation of the Model Results

5.4.1 Explanation of the Different Boundaries in the State Diagram

For the model established in this chapter, the state diagram for pneumatic conveying of plastic pellets through a horizontal stainless steel pipeline 21 m in length and 98 mm in diameter is presented in Figure 5.4.1. In the state diagram, the ordinate is the solids mass flow rate and the abscissa is the air mass flow rate. The curves in the state diagram presented in Figure 5.4.1 are the mathematical results from Equations 5.2.5, 5.2.11 and 5.2.18 for different conditions. The pressure drop across the conveying pipeline, which is the result of conveying operation and can be calculated by different

models for different flow modes, is not presented in this diagram that is specially design for description of operating conditions

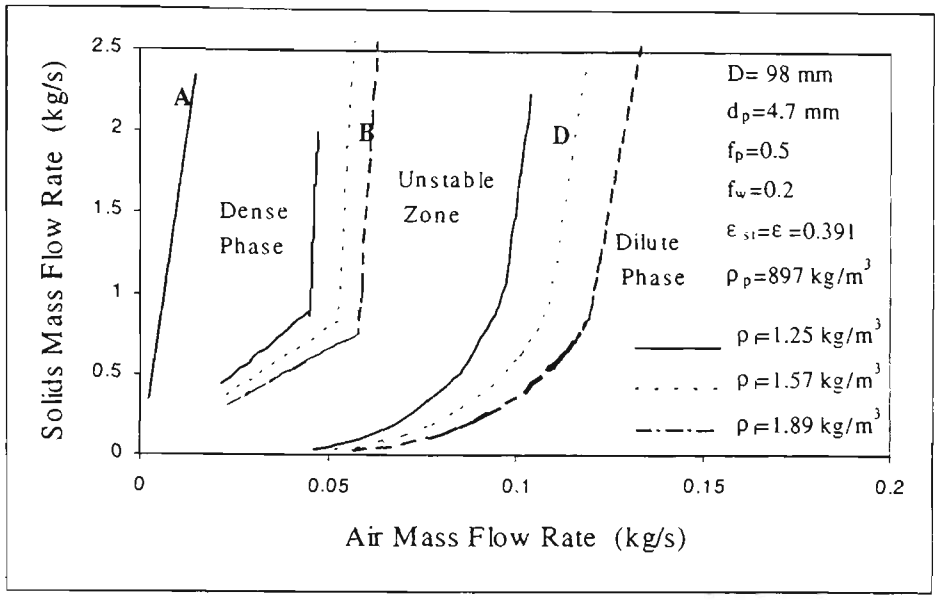

Figure 5.4.1 Predicted state diagram for pneumatic conveying of plastic pellets through 98.4 mm ID pipe

5.4.2 Boundary A

Boundary A, which is not the focus in this study, is derived from the Ergun Equation, powder mechanics, force balance with consideration for air passing through the voidage of solid materials and accelerating the solid materials to a certain velocity that is determined by solids mass flow rate within the feeding shoe. It is determined by particle properties, pipe wall properties, fluid properties (e.g. air density), structure of feeding design and the length of the pipeline. Boundaries A and B should cross because there is a limitation of solids mass flow rate for a certain air mass flow rate. Normally pneumatic conveying would not be conducted close to Boundary A in the state diagram for reasons of economics and safety. For the design of a dense-phase pneumatic conveying system, it must be ensured that at the feeding point or the location the pipeline diameter is stepped-up where the air velocity may be the lowest

locations along the conveying pipeline, and the air mass flow rate must be in the right side of Boundary A in state diagram.

5.4.3 Boundary B:

Boundary B is a broken line and consists of two parts, the upper part is from the limiting curve F in Figure 5.3.5 for stand flow over a slowly moving layer with critical thickness α_{cri}. The critical thickness of the slowly moving layer is defined as the maximum thickness of layer that can be driven by the friction between the strand and the layer:

$$\begin{aligned} &f_p \cdot \rho_p \cdot (1-\varepsilon_{st}) \cdot (1-\phi) \cdot (1-\alpha_{cri}) \cdot g \cdot A = \\ &f_w \cdot \left[\rho_p \cdot (1-\varepsilon_{st}) \cdot (1-\phi) \cdot (1-\alpha_{cri}) \cdot g \cdot A\right] + f_w \cdot \rho_p \cdot (1-\varepsilon) \cdot \alpha_{cri} \cdot g \cdot A \end{aligned} \qquad (5.4.1)$$

For the conveying of granular materials with relatively high solids mass flow rate, if the thickness of the layer is greater than α_{cri}, then the layer can not be moved by friction force from the strand flow over it. Hence, the thickness of the layer will increase and the formation of a slug will be induced. According to the stability analysis, the operating point should be located on the left side of Boundary B and flow in the mode of slow-velocity slug-flow. For the conveying with a thickness of layer less than α_{cri}, then the layer will be moved by friction force from the strand flow over it and the operating point should be located on the right side of Boundary B and flow in the mode of strand flow over a slowly moving bed. It may alternate between long violent slug flow and strand flow over a slowly moving bed if the conveying pipeline is long enough to generate a high pressure drop along the conveying pipeline and make the air velocity at the inlet of the conveying pipeline pass Boundary B and enter low-velocity slug-flow zone in the state diagram.

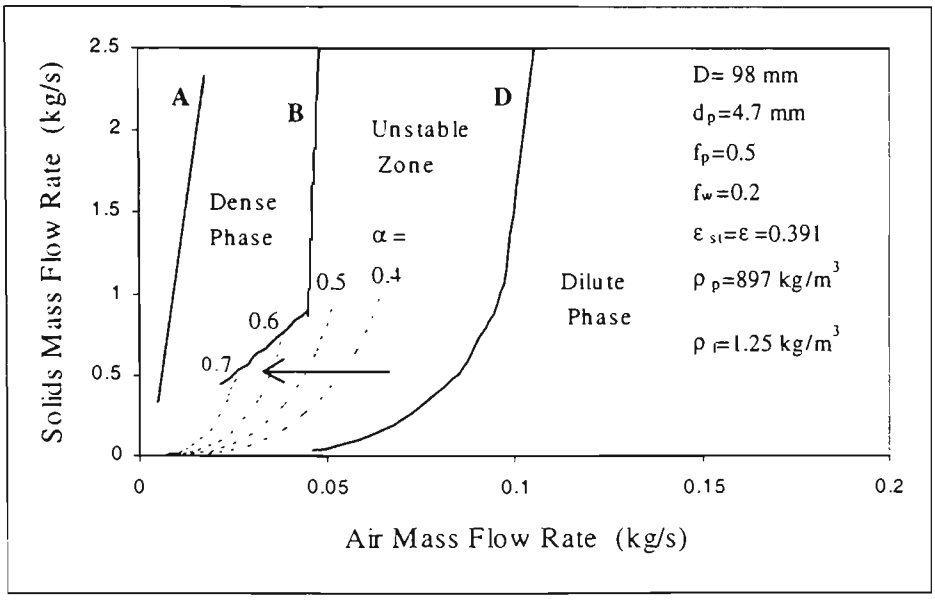

Figure 5.4.2 Predicted state diagram for pneumatic conveying of plastic pellets through 98 mm ID pipe

The lower part of the line of Boundary B is derived from the intersection points of curves F and E for different thicknesses of stationary layers. For a conveying with relatively low solids mass flow rate in the unstable zone (e.g. m_s=0.5 kg/s in Figure 5.4.2), the air-solid two-phase flow will be in the form of a strand over a stationary layer initiating at the inlet and then extending forward. Keeping the solids mass flow rate constant and decreasing the air mass flow rate, the thickness of the stationary layer along the conveying pipeline will increase (e.g. α=0.4, 0.5, 0.6, 0.7 as air mass rate decreasing in the direction of arrow shown in Figure5.4.2) and the flow channel of the cross-section area will decrease, and the air velocity can actually increase. Finally, with an increasing stationary layer along the conveying pipeline, the air-solid two-phase flow will eventually reach Boundary B in the state diagram where type A operating points turn into type C operating points and the friction between the strand and the layer is not high enough to move the layer. As a result, a slug will form at the

inlet of conveying pipeline, sweeping the layer on the bottom of the conveying pipeline as it moves forwards and then enters the receiving bin.

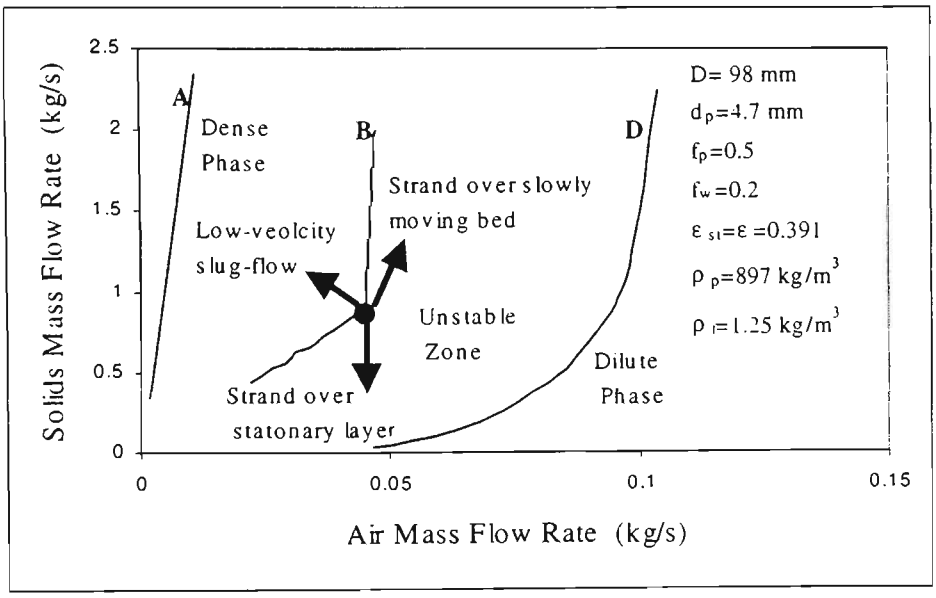

Figure 5.4.3 Predicted state diagram for pneumatic conveying of plastic pellets through 98 mm ID pipe

5.4.4 Turning Point on Line B

Along Boundary B there is a turning point with a very special meaning based on the theoretical model developed in this chapter. It has never been explored by the researchers in the state diagram before as it is not easy to be observed by the conveying experiment. In the state diagram, the turning point on line B represents a conveying condition that it may turn into three different conveying states or flow modes, namely low-velocity slug-flow, strand flow over a stationary layer and strand flow over a slowly moving bed along three directions as shown in Figure 5.4.3. If the air mass flow rate and solid mass flow rate vary upwards and to the right, the conveying may in form of strand flow over a moving bed layer. If the air mass flow rate and solid mass flow rate solid vary to the left and downwards, it may show the strand flow over a stationary layer. If the air mass flow rate and the solid mass flow

rate vary upwards and to the left, the conveying may be in the form of low-velocity slug-flow.

5.4.5 Boundary D

Wirth [67] defined the critical velocity for dilute-phase pneumatic conveying as that prevailing at the appearance of the first plug or the velocity for transition from conveying with constant pressure drop to strong fluctuation in pressure drop. It should be Line C in the state diagram shown in Figure 1.3.1. Actually the Lines E and F in Figure 5.3.5 or Boundary D in Figure 5.4.3 were used as the critical velocity. While Boundary D in Figure 5.4.3 is also the saltation velocity defined by some other researchers. On the right side of Boundary D in the state diagram, the air-solid two-phase flow will be in the form of suspended particles and/or strands without any particles deposited on the bottom of the conveying pipeline. On the left side of Boundary D in the state diagram, the air-solid two-phase flow will be in the form of a strand flow over a slowly moving bed for high solids mass flow rate and a strand flow over a stationary layer for low solids mass flow rate.

5.4.6 Boundary C:

This boundary is located between lines B and D and separates the stable strand flow over a stationary layer or slowly moving bed from the unstable strand flow that alternates between a strand flow over a stationary layer or slowly moving bed and violent long slug flow. Boundary C can also be considered to be the line separating operating points presenting pneumatic conveying of granular materials with a stable pressure drop across the conveying pipeline from those with unstable pressure drops across the conveying pipeline in the state diagram. The location of Boundary C in state diagram also depends on the length of the conveying pipeline. For a short conveying

pipeline, the location of Boundary C will be close to Boundary B while, for a long conveying pipeline, it will be close to Boundary D.

5.4.7 Fix Bed Zone:

This zone is located to the left of boundary A in the state diagram in Figures 5.4.1, 5.4.2 and 5.4.3. Pneumatic conveying of granular materials in the fix bed zone is usually in a state of blockage of the conveying pipeline.

5.4.8 Dense Phase Zone:

This zone is located between Boundaries A and B. Every point in the dense phase zone in the state diagram in Figures 5.4.1, 5.4.2 and 5.4.3 represents the flow mode of the low-velocity slug flow through the conveying pipeline.

5.4.9 Dilute Phase Zone

This zone is located to the right of Boundary D in the state diagram in Figures 5.4.1, 5.4.2 and 5.4.3 and conveying in this zone is in the form of dilute phase pneumatic transportation. The points far away from boundary D may be more in a state of full suspension. The points close to Boundary D may be in a mode of strand flow along the lower part of the pipeline and suspension flow in the upper part of the pipeline. The points closer to Boundary D may in a mode of a strand flow over a stationary layer for low solids mass flow rate, and a strand flow over a slowly moving bed for high solids mass flow rate.

5.4.10 Unstable Zone

This zone is located between Boundaries B and C and actually consists of upper and lower parts which represent different flow states. The points in the lower part of unstable zone represent air-solid two-phase flow alternates between violent long slug

flow and the flow of a strand over a stationary layer. The points in the upper part of the unstable zone represent air-solid two-phase flow alternating between the violent long slug flow and the flow of a strand over a slowly moving bed. For pneumatic conveying in the Unstable Zone, the pressure drop across the conveying pipeline is not stable.

5.5 Further Discussion on the Unstable Zone in the State Diagram of Pneumatic Conveying of Granular Materials

Boundary B of the Transition Zone predicted by the model that has been established in this chapter is actually the boundary for the first slug to form according to the force balance and stability analysis. Normally when the air velocity is reduced and just enters the zone representing the flow mode of low-velocity slug flow in the state diagram as the result of pressure drop across the conveying pipeline increases and air density increases, a long stationary layer or a slowly moving bed has already built along the conveying pipeline from the inlet. The length of stationary layer or slowly moving bed along the conveying pipeline depends on the difference in air velocity between the operating point and the Boundary B in the state diagram. Great quantities of solid particles contained in the conveying pipeline provide the materials to form a long slug or a group of slugs when the first slug is formed at the location along the pipeline where the air velocity is lowest. For some operations in the unstable zone with a very high solids mass flow rate and a long conveying pipeline, the second long slug or group of slugs has been formed before the first long slug or group of slugs enter the receiving bin. For such an operating situation, pressure fluctuation still exists which may induce the vibration of pipeline system but the level of the violence is much lower. Usually the bigger the difference in air velocity between the operating point and Boundary B in the state diagram, the longer the length of stationary layer or slowly moving bed along the conveying pipeline. Also the higher the solids mass flow rate

and the longer the length of conveying pipeline, the smaller the difference in air velocity between the operating point and Boundary B in the state diagram and then the more the possibility to have more than one long slug or group of slugs in the conveying pipeline. As a results, it is better to select a smaller pipe bore and have a relatively high solids mass flow rate for a certain amount of solid materials transportation for the industry using low-velocity slug-flow. When the air mass flow rate is kept constant and within the Boundary B in the state diagram, at the beginning of conveying when the solids particle is introduced into the conveying pipeline, even if the operating system is well designed, it is also very easy to cause unstable flow or pressure fluctuation as the air pressure at the beginning may be lower and the air velocity may be higher so that a long stationary layer or slowly moving bed may be built up along the conveying pipeline from the inlet. Hence a gradual increase in air mass flow rate according corresponding to the increase of the pressure drop across the conveying pipeline is recommended for beginning of operation of the conveying system if the flow is in the mode of low-velocity slug-flow.

5.6 Comparison between Experimental and Predicted Boundaries

Comparisons of the boundaries for pneumatic conveying of plastic pellets through the test rig with 98mm and 60.3 mm ID, 21m in length stainless steel pipelines are shown in Figures 5.6.1 and 5.6.2. Note air leakage has been taken into account in determining the air mass flow rate values shown in those figures. There is a good agreement between the experimental results and the model predictions. It is necessary to mention that the air pressure or air density has been taken into account for the prediction of Boundaries B and D both in Figures 5.6.1 and 5.6.2 and the pressure drops across the conveying pipeline are provided by the model for pressure drop prediction developed in Chapter Twelve.

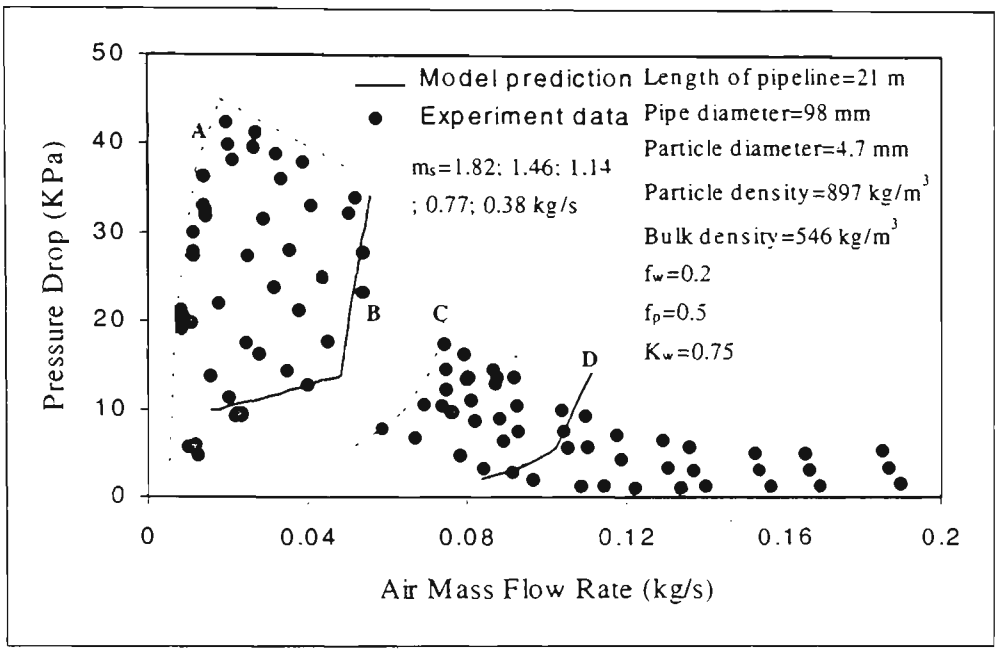

Figure 5.6.1 Comparison between experimental and predicted boundaries in PCC for 98 mm ID stainless steel pipeline

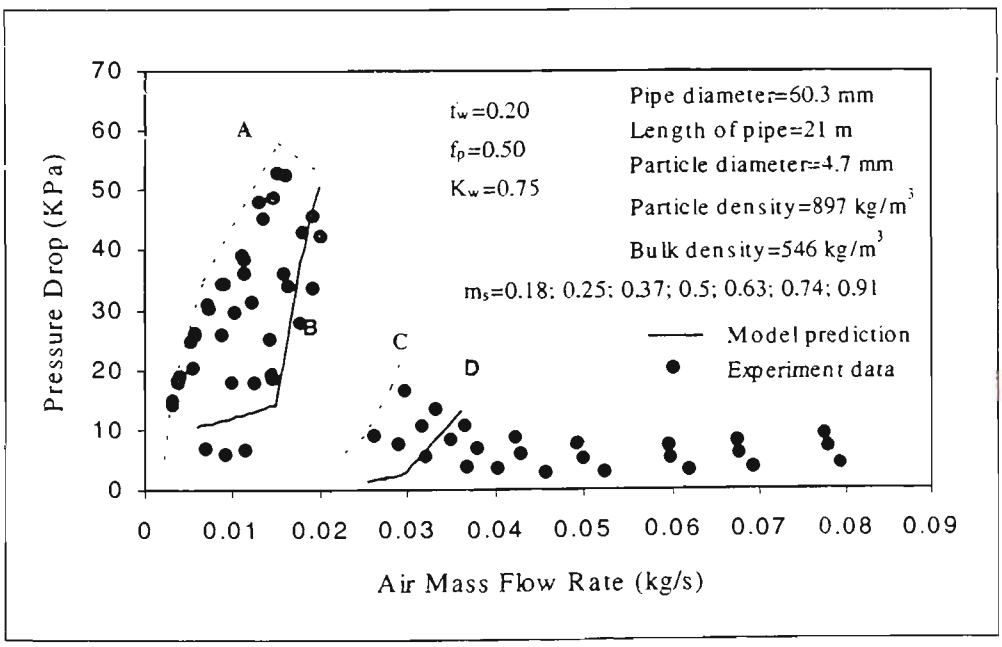

Figure 5.6.2 Comparison between experimental and predicted boundaries in PCC for 60.3 mm ID stainless steel pipeline

5.7 Original Nature of the Model Compared with Wirth's Model

It is undeniable that Wirth's model [67, 104, 105, 106] provided important theoretical support in establishing the model. The force balance, mass balance and momentum balances were first applied in his model established for the determination of minimum conveying velocity or saltation velocity of dilute phase pneumatic conveying. Some non-dimensional groups used in Wirth's model were transplanted to this model building. Since so many similarities exist between the two models, it is necessary to mention the original qualities of this model and the difference between the two models. The main differences may be listed as follows:

- Difference in objectives: Wirth's model considers the boundary of dilute-phase pneumatic conveying while this model considers the boundaries of the unstable zone between dilute-phase and dense-phase pneumatic conveying.

- Wirth's model has a two-layer flow structure while this model has a three-layer flow structure involving the mechanisms for the formation of the unstable zone.

- In stability analysis, being limited by two-layer structure, Wirth's model considers only type B operating points are only stable operating points. This model provides the conditions for stable flow of type A and C operating points.

- Wirth's model mentions the stationary layer on the bottom of the conveying pipeline, the slowly moving bed was treated as a strand.

- Wirth's model also puts forwards the limitations of plugging (plug flow or strand flow over stationary layer) based on its stability analysis while this model provides the boundary for slug formation based on force balance.

- Wirth's model can not provide the predictions that this model can, while the predictions from this model can cover all the results Wirth's model can provide.

CHAPTER 6: INFLUENCE OF DESIGN PARAMETERS ON BOUNDARIES OF TRANSITION ZONE FOR PNEUMATIC CONVEYING OF GRANULAR PELLETS

6.1 Introduction

Low-velocity slug flow pneumatic conveying of free-flowing granular bulk solids is one of the most common and popular modes of dense-phase pneumatic conveying used in industry. It has the advantages of lower power consumption, product damage and pipe wall wear. The state diagram or conveying characteristics for typical low-velocity slug flow conveying consists of four Boundaries A, B, C and D. The unstable zone is in between lines B and C and operation of pneumatic conveying in the unstable zone will result in severe pipeline vibrations and fluctuations in pressure. To avoid any abnormal pneumatic conveying operation, it is necessary to appreciate the influence of design parameters on the boundaries of transition zone and predict the boundaries reliably allowing for changes in design parameters.

The main purpose of this chapter is to discuss the factors that influence the boundaries of the transition zone based on the model developed in Chapter Five. It is generally accepted that the factors that should be decisive for the formation and change of the boundaries of the transition zone for pneumatic conveying of granular materials through horizontal pipelines are pipeline properties, particle properties and fluid properties. According to the model, the main pipeline properties are internal pipe diameter, wall friction factor; the particle properties are particle density, particle voidage and the factor of friction between particles; the air density will be considered regarding to the conveying with high pressure and negative air pressure.

The discussion which follows will focus mainly on the prediction of operating boundaries for industrial design purposes, especially for the design of long distance dense phase pneumatic conveying with step-up pipeline diameter. Some guideline will be provided for the scaling up design parameters from the pilot scale test unit to

industrial scale. Line A is to describe the initiation of the movement of the slug of granular solids through a conveying pipeline and is decided not only by features of particle and pipeline diameter and pipe wall surface but also by the length of the pipeline and operating condition. Also the operation of the low-velocity slug flow pneumatic conveying systems should be far away from the boundary A for economic reasons. Hence, the discussion concerning the transition zone in this chapter will not cover Line A. In order to have a comparison with the experimental results that will be provided in the later chapters, all the factors or parameters will be kept constant and equal to those of the experimental condition if applicable. The particle density is 897kg/m3, bulk voidage is 0.391, particle diameter is 4.7 mm, pipeline inner diameters are 60.3 mm and 98.4 mm, f_w=0.20, f_p=0.5. Also the ordinate of the state diagram is solids mass flow rate per unit area (kg $s^{-1}m^{-2}$) and the abscissa is air velocity (ms^{-1}).

6.2 Influence of Pipeline Diameter on Boundaries of Transition Zone

For pneumatic conveying of granular solids in industrial applications, there is a wide variation in pipeline diameter from a few centimetres to forty centimetres, corresponding to the quantity of solid materials to be transported and the distance to be covered. In most situations, pipe diameters of the pilot scale test unit are smaller than those in industrial applications. To predict the operating boundaries accurately and reliably is vital to the success of applications of pneumatic conveying in industry. Based on the model established in Chapter Five, an approach to assess the variance of the operating boundaries with respect to the variation in pipeline diameter is provided.

Figure 6.2.1 and 6.2.2 show comparisons of the boundaries of transition zone in the state diagram for pneumatic conveying of granular materials through a horizontal pipeline with pipeline diameters of 40, 60 and 98 mm respectively. From these figures,

it is clear that the diameter of the conveying pipeline significantly affect the location of the boundaries of the transition zone in the state diagram. As the diameter of the conveying pipeline is increased, Boundary D considered as the minimum conveying (saltation) velocity for dilute-phase pneumatic conveying of granular solids move forwards and so does the upper part of Boundary B that is the maximum conveying velocity for low-velocity slug-flow with high solids mass flow rate. The lower part of Boundary B that is the maximum conveying velocity for low-velocity slug-flow with low solids mass flow rate is kept at the same location in the state diagram and extend forwards as the pipe diameter is increased. Also the area of the transition zone in the state diagram is enlarged as the pipe diameter increases.

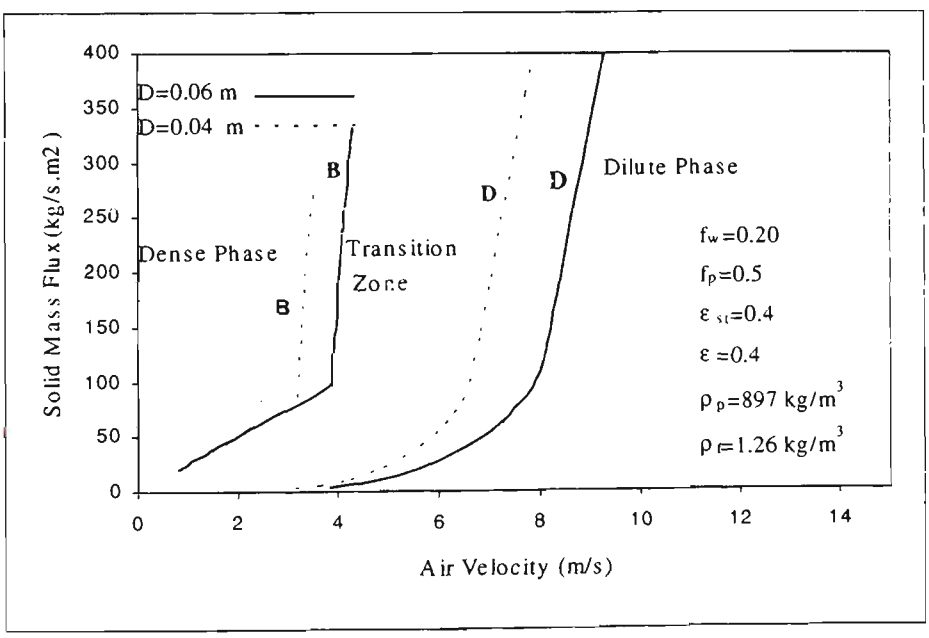

Figure 6.2.1 Predicted state diagram with respect to pipeline diameter

As a result, the traditional concept of the operating region for low-velocity slug-flow, which was defined only by air velocity (from 1 m/s to 4.0 m/s) and accepted by many pneumatic conveying system designers without consideration on the pipeline diameter and solids mass flow rate, is not applicable. In the design of the conveying velocity for

dense-phase pneumatic conveying of granular materials, to ensure the operation is within the low-velocity slug-flow zone in the state diagram, the diameter of the conveying pipeline must be determined first. According to the pipeline diameter as well as solids mass flow rate, a optimal conveying velocity can then be selected. Any design of conveying velocity without full evaluation on which conveying modes the conveying will be in or which operating zones in the state diagram the conveying will be in with respect to different pipeline diameters and solid mass flow rates will induce serious results in the operations.

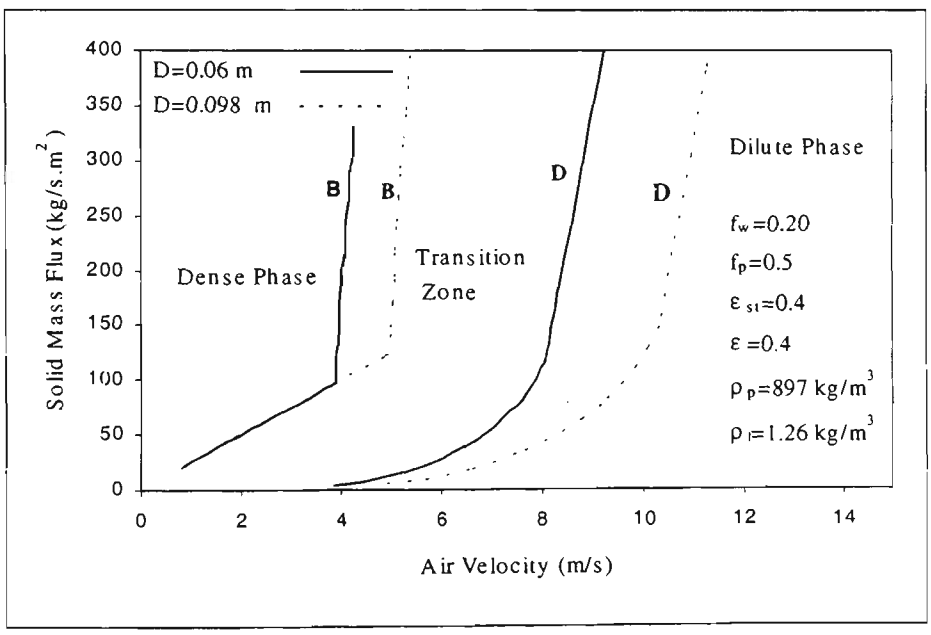

Figure 6.2.2 Predicted state diagram with respect to pipeline diameter

In the selection of a diameter of conveying pipeline during the design of conveying system for a certain conveying task, it should be borne in mind that a smaller pipeline diameter is more optimal for the pipeline system design if the conveying load is less than the maximum slugging rate or the capacity of the pipeline for slugging flow for a given pipeline diameter and product. According to the state diagram, for a given conveying load (kg/s) with the same air velocity, the operation may be in the dense-

phase zone for a suitable pipe bore and in the unstable zone for a large pipe bore. Also if the pneumatic conveying of granular materials through the pipeline is with large bore, both boundaries D and B moves forward. Hence the minimum conveying velocity for dilute-phase and maximum conveying velocity for dense-phase increase and the pipeline wear and particle degradation will increase especially for the conveying of fragile granular solids. Large pipe bore also means a wider unstable zone. When operations in conveying of granular materials over a long distance in unstable condition, the length of the stationary layer over which the strand flow goes will be longer for a wider unstable zone in the state diagram. Once a long slug is formed and the transition of the flow takes place, the fluctuation in pressure will be much greater.

6.3 Influence of Pipeline Wall Sliding Friction Factor on Boundaries of Transition Zone

The roughness of the pipe wall inner surface has been taken into account in the establishment of many models for prediction of pressure drop of dense-phase pneumatic conveying. Some researchers also have considered it in the models for predicting the minimum conveying velocity of dilute-phase pneumatic conveying. So far the influence of the roughness of pipe wall surface on the mode of air-solid two-phase flow has been ignored by the researchers in this area, so exploration or appreciation of this topic may begin with this thesis. Since Boundary B has not been addressed so far, the relationship between pipe wall roughness and the maximum conveying velocity for low-velocity slug-flow pneumatic conveying of granular materials is still unknown. With the model established in Chapter Five and assuming its applicability can extend to all pipe wall surface, an effort will be made here to explore the relationship between the roughness of pipe wall surface and the mode of air-solid two-phase flow and appreciate the significance of pipe wall roughness to a

determination of the boundaries of the transition zone in the state diagram for pneumatic conveying of granular materials through a horizontal pipeline.

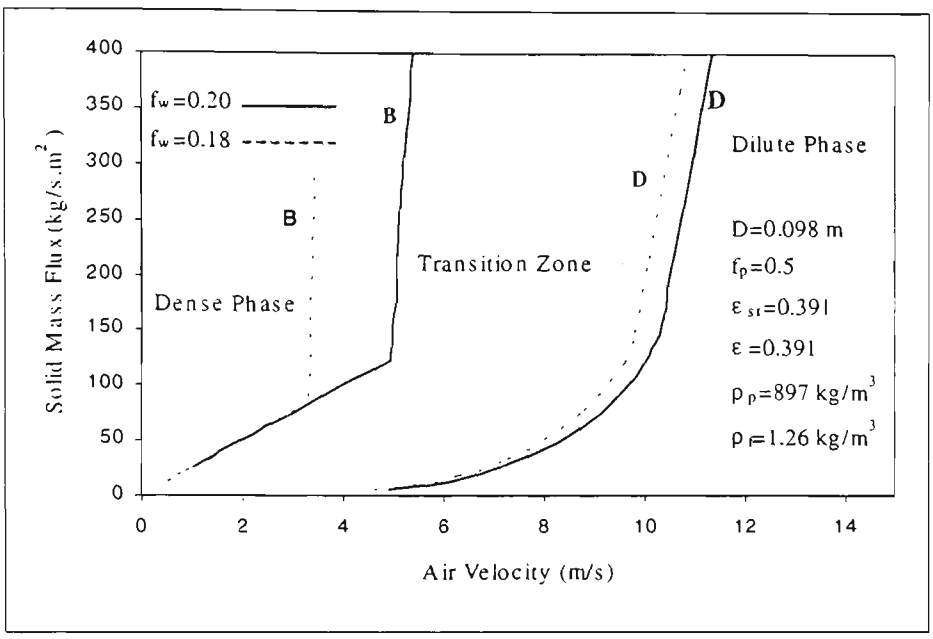

Figure 6.3.1 Predicted state diagram with respect to pipe wall roughness

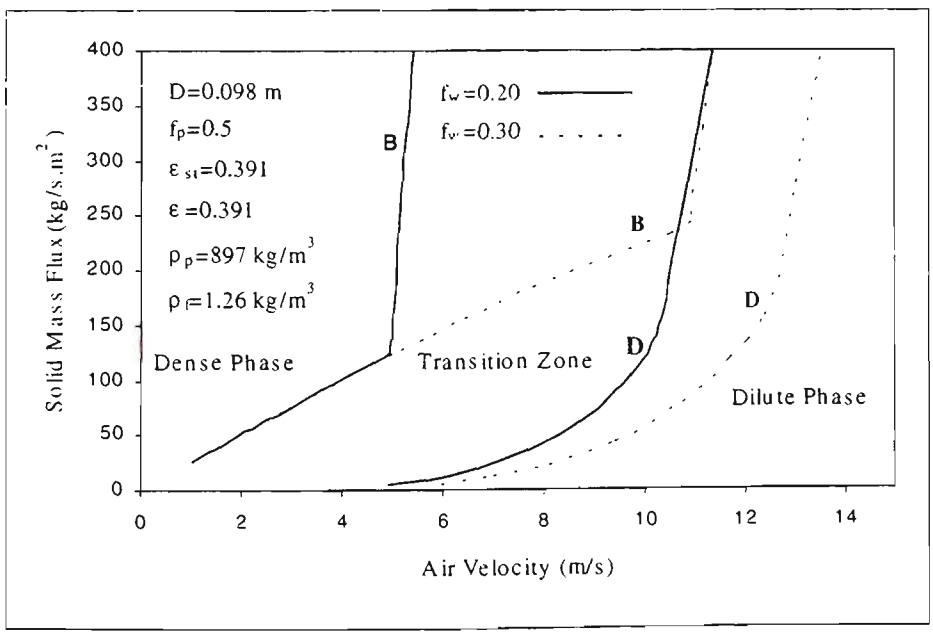

Figure 6.3.2 Predicted state diagram with respect to pipe wall roughness

The comparison in Figures 6.3.1 and 6.3.2 for the conveying of certain granular solids though a horizontal pipeline with the same inner diameter of the conveying pipeline shows that transition zone in the state diagram will change its location and area according to the variation in pipe wall roughness or the pipe wall sliding friction factor. As the pipe wall roughness or wall sliding friction factor increases, both maximum conveying velocity for low-velocity slug flow and minimum conveying velocity for dilute-phase flow increase. The upper area of the transition zone presenting the mode of air-solid two-phase flow in the form of a strand over a slowly moving bed (if a slug does not form) in the state diagram contracts while the lower part of transition zone presenting the mode of air-solid two-phase flow in the form of a strand over a stationary layer (if a slug does not form) in the state diagram becomes enlarged. As the pipe wall roughness or wall sliding friction factor decreases, both maximum conveying velocity for dense-phase flow and minimum conveying velocity for dilute-phase flow decrease; the upper area of transition zone presenting the mode of air-solid two-phase flow in the form of a strand over a slowly moving bed (if a slug does not form) in the state diagram expands while the lower part of transition zone presenting the mode of air-solid two-phase flow in the form of a strand over a stationary layer (if a slug did not form) in the state diagram becomes smaller.

In the design of a conveying pipeline system, the concept that the pipe wall roughness can change the flow mode of air-solid two-phase flow provides an approach to avoid unstable flow for the conveying of granular solids over a long pipeline for industrial applications. Pipe with a smooth wall surface can be selected to lower the resistance to the moving slug and lessen the pressure gradient if the conveying velocity is within the low-velocity slug-flow zone in the state diagram. As the air velocity increases, pipe

with a rough inner wall surface can be selected to keep the conveying of granular materials in the flow mode of low-velocity slug-flow.

In the model established in Chapter Five, one of extreme situations of the wall roughness of conveying pipeline to be explored is what will happen in the state diagram when the sliding friction factor keeps decreasing.

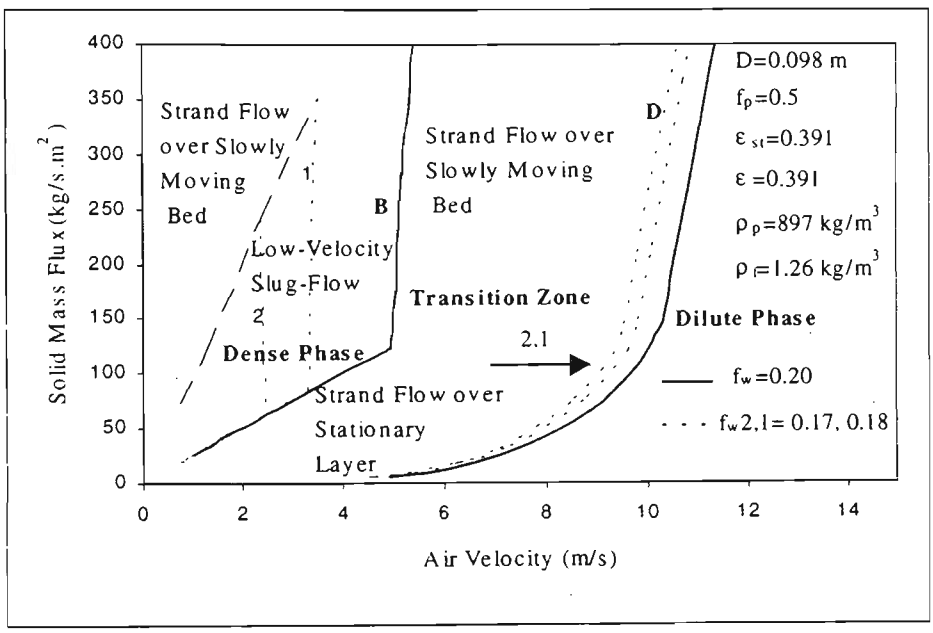

Figure 6.3.3 Predicted state diagram with respect to pipe wall roughness

Figure 6.3.3 shows the state diagram for pneumatic conveying of plastic pellets through a horizontal pipeline with a decreasing sliding friction factor of the pipe wall. For Boundary D, as f_w is decreased from 0.20 to 0.17, a slight change takes place for the minimum conveying velocity for dilute-phase pneumatic conveying shown as curves D in the state diagram. For Boundary B, as f_w is decreased from 0.20 to 0.17, the area presenting flow mode of a strand over a slowly moving bed is enlarged and gradually occupies most of the area in the transition zone in the state diagram. The area presenting the flow mode of strand over a stationary layer contracts and gradually occupies a very small area of the transition zone in the state diagram. The area

representing flow mode of low-velocity slug-flow becomes smaller as the f_w is decreases from 0.2 to 0.17. Further decrease in sliding friction factor of the pipe wall (e.g. reducing to 0.15) will finally induce the disappearance of the mode of low-velocity slug-flow for pneumatic conveying of granular materials in the state diagram. According to the stability analysis in Chapter Five, a strand flow over a slowly moving bed can be kept stable if the friction between the strand and the layer is high enough to move the layer. As the air velocity decreases, the thickness of the layer on the bottom of the pipeline increases and finally the thickness of the layer will reach such value that friction between the strand and the layer can not move the layer, so the first slug forms. If the sliding friction factor of the pipe wall is at a very low value compared with the friction factor between particles, then the layer under the strand can be kept moving and formation of slug can be prevented in the conveying pipeline if solids mass flow rate is higher than certain value.

For industrial applications of pneumatic conveying of granular materials over a long distance, a new approach to avoid unstable operation is provided by a selecting the conveying pipeline with a very smooth wall surface. For the research of air-solid two-phase flow through a horizontal pipeline, the concept that mode of low-velocity slug flow for pneumatic conveying of granular materials may not exist in the pipeline with a very smooth wall surface is established and has very important theoretical significance for the research on air-solid two-phase flow through a horizontal pipeline and should be examined by experimental approaches.

Another extreme situation of wall roughness to be explored is what will happen in the state diagram for pneumatic conveying of granular materials through a horizontal

pipeline when the sliding friction factor or roughness of pipe wall continues to increase.

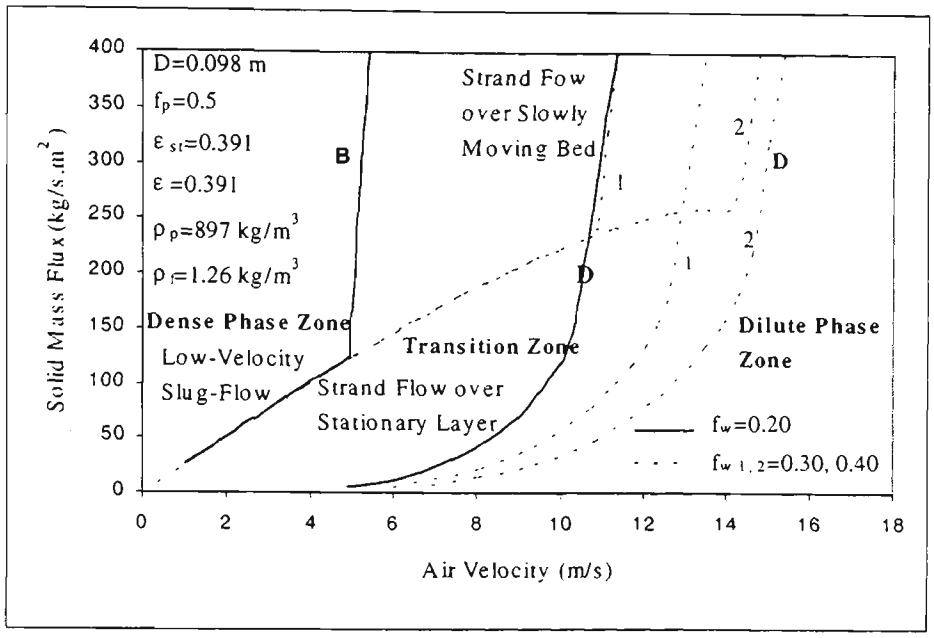

Figure 6.3.4 Predicted state diagram with respect to pipe wall roughness

Figure 6.3.4 shows the state diagram for pneumatic conveying of plastic pellets through a horizontal pipeline with an increasing sliding friction factor of the pipe wall. As f_w is increased from 0.20 to 0.40, Boundary D or the minimum conveying velocity for dilute-phase pneumatic conveying increases; Boundary B or the maximum conveying velocity for low-velocity slug-flow also increases; the area and the location of the Transition Zone in the state diagram change. The area presenting flow mode of a strand over a slowly moving bed in the state diagram moves forward and gradually occupies less area in the Transition Zone in the state diagram; the area presenting flow mode of a strand over a stationary layer in the state diagram enlarges and gradually occupies most of the Transition Zone in the state diagram. The area representing flow mode of low-velocity slug-flow becomes larger as the f_w increases from 0.20 to 0.40. Further increase in the sliding friction factor of the pipe wall (e.g., increase to 0.425)

will finally induce the disappearance of the mode of a strand over a slowly moving bed for pneumatic conveying of granular materials in the state diagram. According to the stability analysis in Chapter Five, flow mode of a strand flow over a slowly moving bed can be kept stable if the friction between the strand and the layer is high enough to move layer. As the sliding friction factor increases, finally friction between the strand and the layer can not move the layer any more, hence flow mode of a strand flow over a slowly moving bed can not be maintained and the Transition Zone with high solids mass flow rate can not exist in the state diagram any longer.

For industrial applications of pneumatic conveying of granular materials over a long distance, a new approach to avoid unstable operation, which induces pressure fluctuation and even blockage of pipeline, is provided by selecting a conveying pipeline with a very rough wall surface and a relatively small pipe bore, but the overall pressure drop is much higher as the result of high wall friction. For the research of air-solid two-phase flow through a horizontal pipeline, the concept that flow mode of a strand flow over a slowly moving bed for pneumatic conveying of granular materials may not exist in the pipeline with a very rough wall surface and relatively small pipe bore is established even though it lacks of experimental demonstration so far.

6.4 Influence of Particle Density on Boundaries of Transition Zone

As one of the key parameters of particle properties, particle density is employed in many correlations for the prediction of the minimum conveying velocity of dilute-phase pneumatic conveying and in the classification of solid materials for the purpose of flow mode determination. The influence of particle density on the flow mode as well as the location and boundaries of the transition zone in the state diagram for pneumatic conveying of granular materials through a horizontal pipeline has never

been explored well. Hence it is necessary to conduct such a discussion based on the model established in Chapter Five.

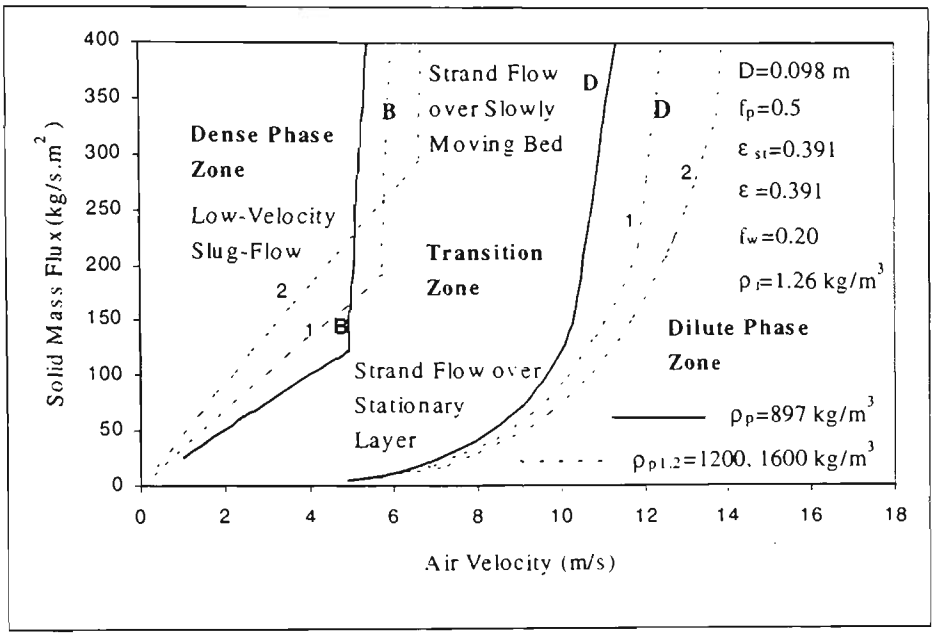

Figure 6.4.1 Predicted state diagram with respect to particle density

Figure 6.4.1 shows the comparison of the Transition Zones in the state diagram for pneumatic conveying of granular materials as the particle density increases. Both Boundary B as the maximum conveying velocity of low-velocity slug-flow and Boundary D as the minimum conveying velocity for dilute-phase pneumatic conveying move forward and the area of the Transition Zone is enlarged with increase in particle density. Within the Transition Zone, the area representing the flow mode of strand flow over a stationary layer extends into the area normally representing the flow mode of strand flow over a slowly moving bed as the particle density increases.

For the design of industrial application, it is necessary not only to be aware that the maximum conveying velocity of low-velocity slug-flow and the minimum conveying velocity for dilute-phase pneumatic conveying are increased as particle density increases, but also understand that when the dense-phase pneumatic conveying of high

particle density granular solids through a horizontal pipeline, lowering the solid mass flow rate usually makes the operation of conveying in the unstable condition more easier than that with low particle density materials. The gap between maximum conveying velocity of low-velocity slug-flow and minimum conveying velocity for dilute-phase pneumatic conveying in the state diagram is larger and greater pressure fluctuation may develop if unstable flow takes place.

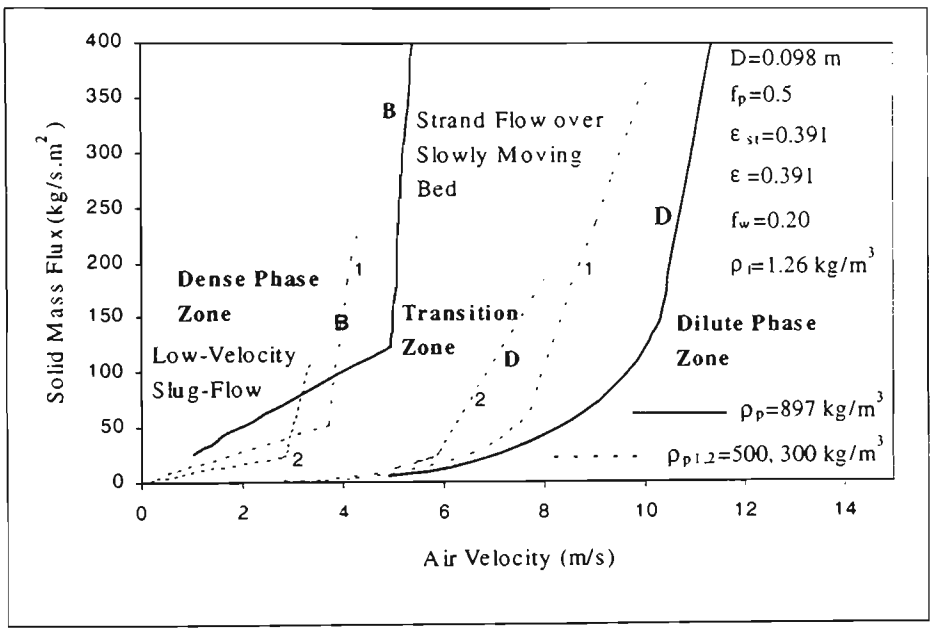

Figure 6.4.2 Predicted state diagram with respect to particle density

Figure 6.4.2 shows that as the particle density decreases, Boundaries B and D move backward, the Transition Zone in the state diagram shrinks and the flow behaviours become complicated. The complexities of the flow behaviours for conveying very light granular materials are that the area in the state diagram representing the flow mode of a strand flow over a stationary layer becomes smaller and only exists for very low solids mass flow rate, the area in the state diagram representing the flow mode of a strand flow over a slowly moving bed becomes larger and extends to the area where normally the air-solid two-phase flow is in the mode of low-velocity slug-flow for a very high

solids mass flow rate (e.g., for ρ_p=300 kg m^{-3}, G_s is high than 100 $kg.s^{-1}m^{-2}$, low-velocity slug-flow will not display).

For industrial application, pneumatic conveying of light granular materials is easy to handle according to the state diagram. With respect to research, the concept that the flow mode of low-velocity slug-flow for pneumatic conveying of light granular materials will not display in the conveying operation with high solids mass flow rate still needs some experimental demonstrations.

6.5 Influence of Voidage of Bulk Granular Solids on Boundaries of Transition Zone

To characterise and classify the solid materials for pneumatic conveying, the density difference between fluid and particle, particle diameter and distribution, permeability and air retention ability have been directly taken into account as the key parameters in the determination of the flow mode in previous research. The voidage of bulk solid materials has not been directly considered as a key parameter in conveying behaviours through the pipeline system but was used indirectly in the Pan's [80] classification of three modes of pneumatic conveying and has achieved some success in applications. The significance of the voidage of bulk granular solid materials to the determination of the mode of pneumatic conveying or flow behaviours will be addressed according to the model established in Chapter Five.

Figure 6.5.1 shows the comparison in the state diagram for pneumatic conveying of granular materials through a horizontal pipeline with bulk voidage of 0.391, 0.6, 0.7 and 0.8 respectively. As the voidage increases, the transition zone in the state diagram becomes smaller, the minimum conveying velocity for dilute-phase pneumatic delineated by Boundary D became less and so does the maximum conveying velocity

for low-velocity slug flow delineated by Boundary B. The shrinkage in the lower part of the transition zone representing the flow mode of a strand over a stationary layer projects more than that of the upper part representing the flow mode of a strand over a slowly moving bed. This means that the higher the voidage of bulk granular materials, the less the solids mass flow rate per unit area to keep the flow in the mode of a strand over a slowly moving bed in the transition zone. For pneumatic conveying of granular materials with high voidage, the area in the state diagram representing the flow mode of a strand flow over a slowly moving bed will extend to an area where normally the air-solid two-phase flow is in the mode of low-velocity slug-flow for relatively high solids mass flow rate (e.g. for ε=0.6, G_s>272 $kg.s^{-1}m^{-2}$; ε=0.7, G_s>169 $kg.s^{-1}m^{-2}$; ε=0.8, G_s>87 $kg.s^{-1}m^{-2}$) and low-velocity slug-flow will not display during the conveying operation. Line H in the state diagram in Figure 6.5.1 delineates the area where low-velocity slug-flow is replaced by the flow mode of a strand over a slowly moving bed or strand flow only for granular materials with variation in bulk voidages.

The comparisons suggest to the designers of pneumatic conveying systems that granular products are easier to transport pneumatically through a horizontal pipeline with high voidage. The voidage of granular solids should be taken into account for the determination of operating condition in order to ensure that the operation points are within the appropriate area in the state diagram for pneumatic conveying. For some granular materials whose voidage is effected by compression, some kind of feeding device that will cause compression for solid materials such as screw-feeding blow tank should be avoided to be used for pneumatic conveying of such kind of solid materials.

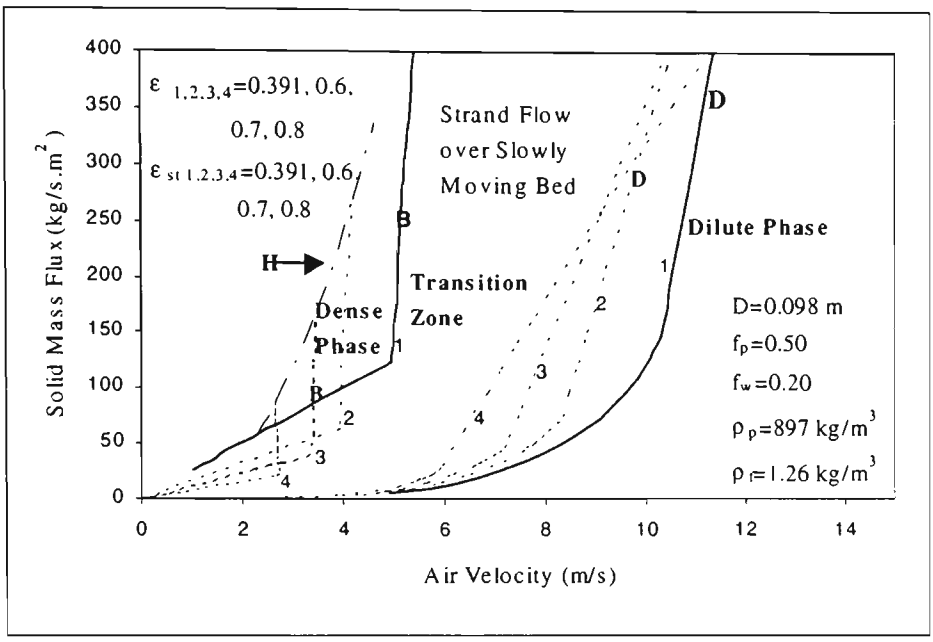

Figure 6.5.1 Predicted state diagram with respect to bulk voidage

6.6 Influence of Friction between Particles on Boundaries of Transition Zone

The friction between particles that is considered equal to the internal friction of particles is a key factor in bulk solid mechanism for silo design and has never been taken into account in any determination of the transition zone in the state diagram for pneumatic conveying of granular materials through a horizontal pipeline. The predictions of the model established in Chapter Five show that the factor of friction between particles is one of the most important parameters for determining the maximum conveying velocity for pneumatic conveying of granular materials in the mode of low-velocity slug flow.

Figure 6.6.1 shows the comparisons of flow regimes in the state diagram with the variation of decreasing particle friction factor. It is clear that the friction between particles mainly defines the gap between Boundaries B and D of the upper part of the transition zone representing the flow mode of a strand over a slowly moving bed in the state diagram. The gap will disappear as the friction between particles further

approaches to the friction between particle and pipe wall. The decrease in fiction between particles has no effect on the location of boundary D delineating the minimum conveying velocity for dilute-phase pneumatic conveying. Also the location of area representing the flow mode of a strand over a stationary layer in the state diagram is not affected.

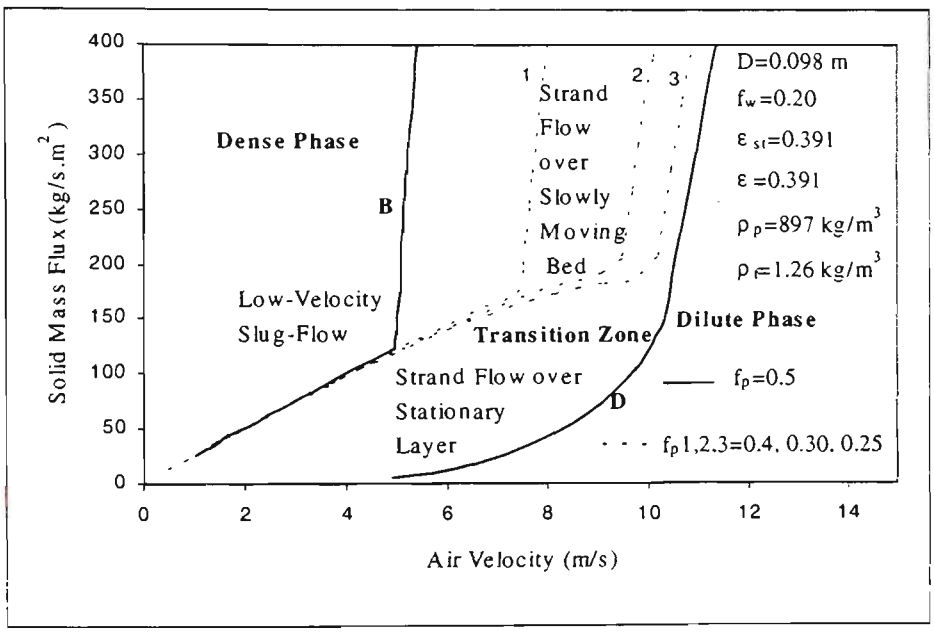

Figure 6.6.1 Predicted state diagram with respect to friction between particles

For the design of industrial applications, a smaller particle fiction factor means a wider operating zone of low-velocity slug flow and a narrower transition zone in the state diagram for pneumatic conveying of granular materials with a relatively high solids mass flow rate. For the conveying with a relative low solids mass flow rate, the situation is almost the same. In most situation of conveying of granular solids, the friction between particles is higher than that between particle and pipe wall and the friction between particles can be reflected by a deposed angle. Hence the granular solids with a smaller deposed angle will exhibit higher maximum conveying velocity in dense phase pneumatic conveying and possess a narrow gap between Boundaries B

and D in the state diagram if other factors that influence air-solid two-flow are similar and the solid mass flow rate is relatively higher. For the design of pneumatic conveying of granular solids with a low solid mass flow rate, the friction between particles will not matter much in the location of boundaries of the transition zone in the state diagram.

Figure 6.6.2 shows the comparisons of flow regimes in the state diagram with the variation of particle friction factors increasing. The upper part of the transition zone representing the flow mode of a strand over a slowly moving bed in the state diagram is enlarged and extends to the area where normally the air-solid two-phase flow is in the mode of low-velocity slug-flow for relatively high solids mass flow rate (e.g. for f_p=0.55, G_s>391 kg.s^{-1}m^{-2}; f_p=0.6 G_s>213 kg.s^{-1}m^{-2}; f_p=0.625, G_s>138 kg.s^{-1}m^{-2}; f_p=0.65, G_s>213 kg.s^{-1}m^{-2}). Line H in the state diagram in Figure 6.6.2 delineates the area where low-velocity slug-flow is replaced by the flow mode of a strand over a slowly moving bed for pneumatic conveying of granular materials with variation in friction between particles. The increase in friction between particles has no effect on the location of Boundary D delineating the minimum conveying velocity for dilute-phase pneumatic conveying.

The concept that friction between particles influences the maximum conveying velocity for pneumatic conveying of granular materials in the mode of low-velocity slug-flow and the gap between Boundaries B and D in state diagram provides a guideline for the surface design of products in industries. To achieve an easy handling ability that is important for safety and stability in the process of transportation and storage, granule of products can be made with certain shapes and diameters so that friction between particles can be lower.

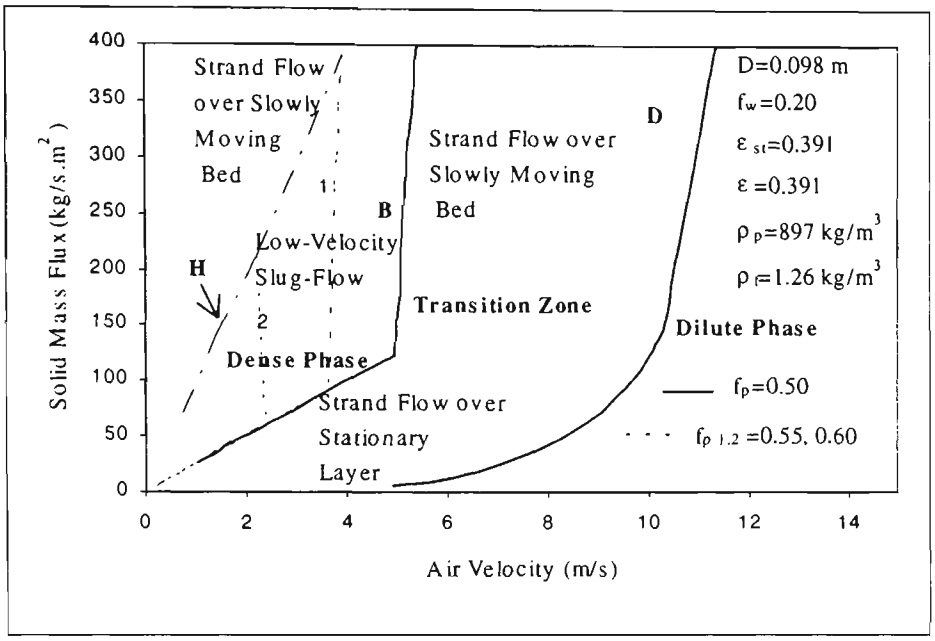

Figure 6.6.2 Predicted state diagram with respect to friction between particles

6.7 Influence of Air Pressure on Boundaries of Transition Zone

In many industrial applications, pneumatic conveying of granular solids covers long distances and hence high-pressure air is employed. The determination of boundaries for pneumatic conveying with high pressure is usually not directly achieved easily by conducting pilot-scale tests. Even though the experimental rig is equipped for high pressure conveying test, there is still no method for scaling up the experiment results from pilot-scale to industrial scale. As a result, pneumatic conveying of granular materials over long distances is more popular in the form of dilute-phase pneumatic conveying rather than in dense-phase which has the advantages of lower power consumption, product damage and pipe wall wear. With the model established in Chapter Five, an approach for the assessment of the influence of air-pressure or air density on the boundaries of the Transition Zone in the state diagram for pneumatic conveying of granular materials through a long horizontal pipeline is provided.

Figure 6.7.1 shows the comparison in the state diagram of three conveying conditions with absolute air pressure of 1.0, 2.0 and 4.0 kgf/cm^2 respectively. For the convenience of discussion and comparison, in Figure 6.7.1, the ordinate of the state diagram is kept the same as that used in previous sub-chapters while the abscissa is the air mass flow rate with units in kg/s. In Figure 6.7.1, as the air density increases, the transition zone in the state diagram becomes larger and moves forwards, the area representing the flow mode of a strand over a slowly moving bed becomes larger and the area representing the flow mode of a strand over a stationary layer becomes constricted and limited to a lower solids mass flow rate per unit area.

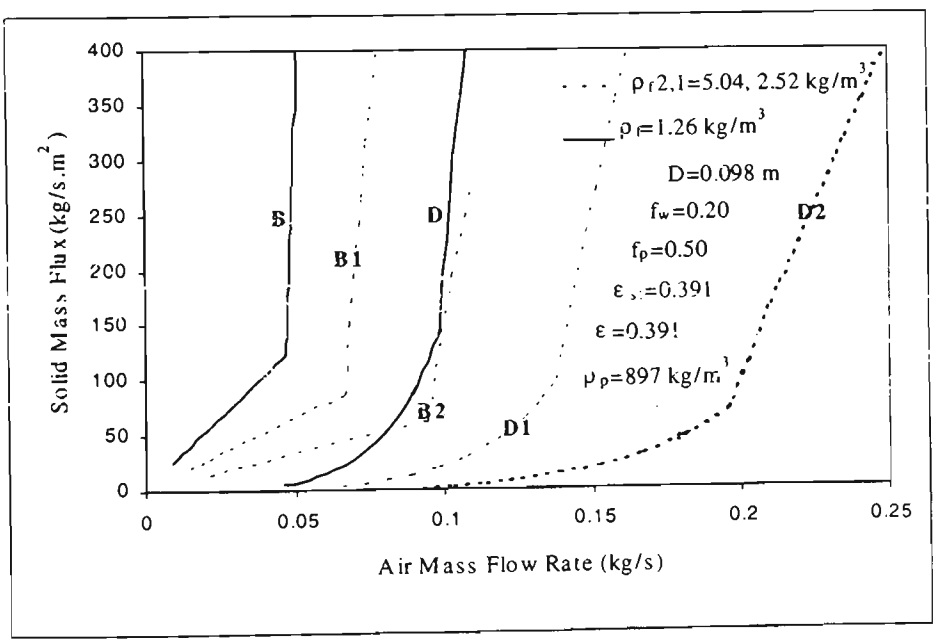

Figure 6.7.1 Predicted state diagram with respect to air density

In Figure 6.7.2, with air velocity as the abscissa and as the air density increases, the transition zone in the state diagram becomes smaller and moves backwards. The area representing the flow mode of a strand over a slowly moving bed occupies more of the transition zone and the area representing the flow mode of a strand over a stationary layer becomes constricted and limited to a lower solids mass flux.

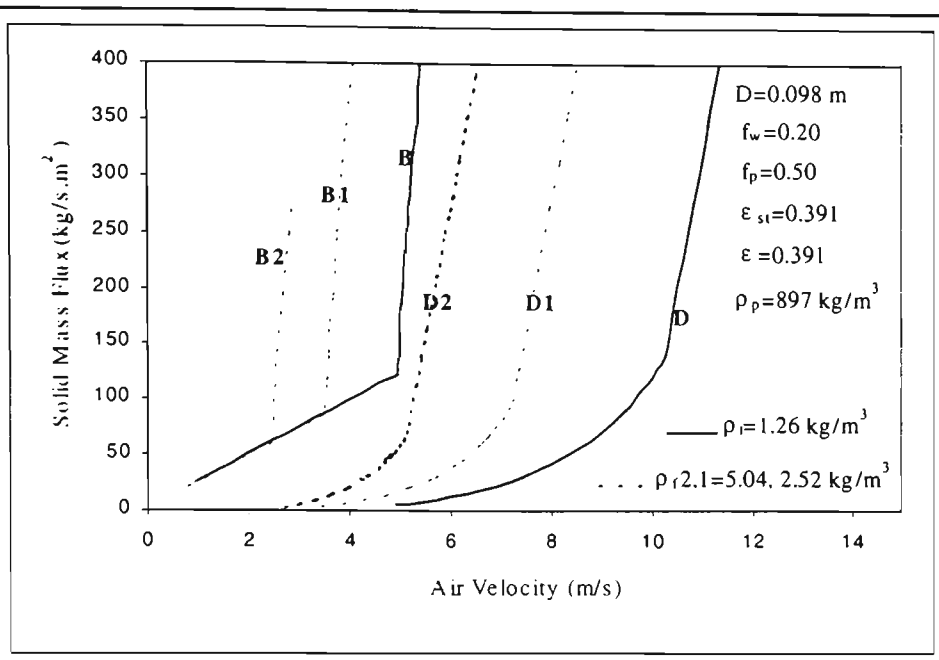

Figure 6.7.2 Predicted state diagram with respect to air density

For pneumatic conveying of granular solids over a long distance in the form of low-velocity slug-flow, high air pressure is employed at the inlet of the conveying pipeline, and the air pressure will decrease along the pipeline and reach atmospheric pressure at the exit. With a constant air mass flow rate along the conveying pipeline, a step-up pipe bore is necessary to keep the air velocity in the pipeline within the dense-phase zone in the state diagram in order to ensure the conveying operation is stable and the low-velocity slug-flow can be maintained through the whole pipeline system. For a well-designed dense-phase pneumatic conveying long pipeline system, low-velocity slug-flow may be maintained through the whole pipeline during steady state operations. At the beginning of the conveying when the granular materials start to enter the conveying pipeline, the operation with constant air mass flow rate may be in the unstable zone in the state diagram since the pressure at the inlet may not have reached the required value. Hence pressure fluctuation takes place and then becomes normal as the pressure at the inlet of the conveying pipeline reaches the required value

and such prediction has been demonstrated in many industrial applications for long-distance dense-phase pneumatic conveying of granular materials. For the same reason, pressure fluctuations also take place during the end of the operation of dense-phase pneumatic conveying systems.

Pneumatic conveying of granular materials in the form of low-velocity slug flow at negative pressure is seldom selected for industrial applications. This is because the distance of dense-phase pneumatic conveying under negative pressure is very limited for the restricted pressure drop available and the vacuum system is not very convenient to handle compared with pressured system. The transition boundaries for low-velocity slug flow in the state diagram under negative pressure are still worth considering.

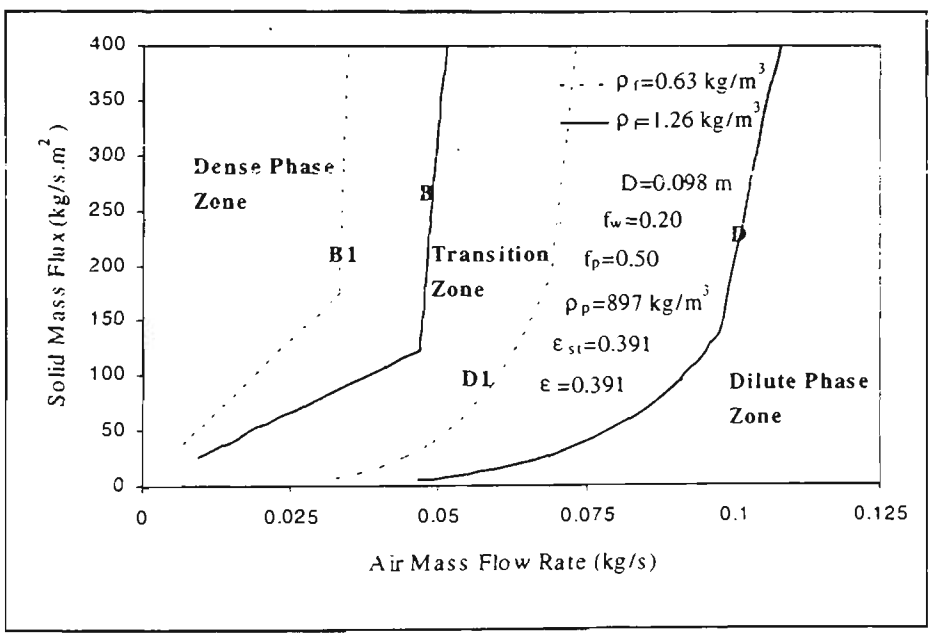

Figure 6.7.3 Predicted state diagram with respect to air density

Figure 6.7.3 shows a comparison in the state diagram for conveying conditions with absolute air pressure of 1.0 and 0.5 kgf/cm^2 respectively. For the convenience of discussion and comparison, the ordinate of the state diagram has been kept the same as that used in previous sub-chapters while the abscissa is the air mass flow rate with

units in kg/s. As the air density decreases, the transition zone in the state diagram becomes smaller and moves backwards and the area representing the flow mode of a strand over a stationary layer becomes larger. The area representing the pneumatic conveying of granular materials in the form of low-velocity slug-flow in the state diagram becomes smaller.

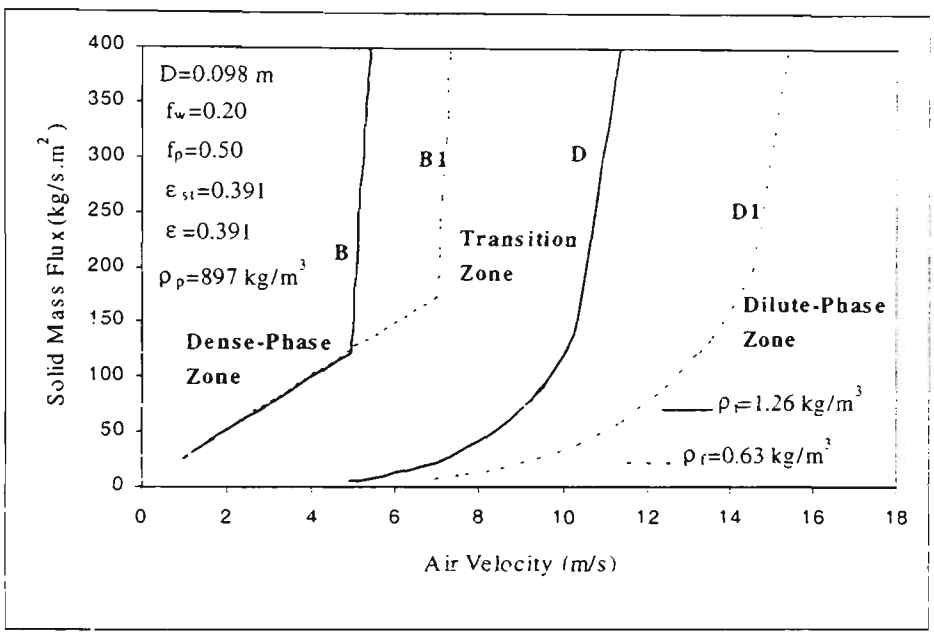

Figure 6.7.4 Predicted state diagram with respect to air density

In Figure 6.7.4, with air velocity as the abscissa, as the air density decreases, the transition zone in the state diagram becomes larger and moves forwards. The area representing conveying in the flow mode of a strand over a stationary layer becomes larger and so does the gap between boundaries B and D.

CHAPTER 7: CLASSIFICATION OF GRANULAR SOLIDS AND POWDERS

7.1 Introduction

Pneumatic conveying of bulk solid materials has been used successfully for many decades in industry. Numerous materials with dramatically different particle properties are transported through pipeline systems with different configuration and pipe wall properties. In general, for powders and granules, two general forms of conveying characteristic have been observed, as described below.

7.1.1Smooth Transition from Dilute-Phase to Dense-Phase

Typical pneumatic conveying characteristics for materials that can be conveyed smoothly from dilute-phase to dense-phase are shown in Figure 7.1.1.

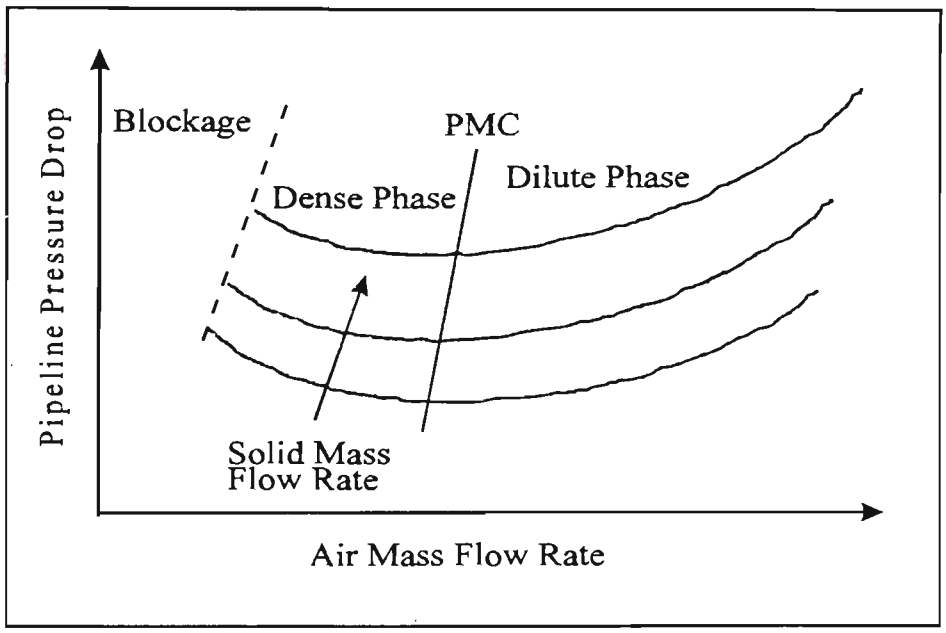

Figure 7.1.1 General form of pneumatic conveying characteristics for materials that displays a smooth transition from dilute-phase to dense-phase

This flow mode is achieved usually for powders (e.g. fly ash, cement and pulverised coal) [80] with low loose-poured bulk density, high bulk voidage and small particle diameter. When the air mass flow rate decreases from high to low and for a constant

solid mass flow rate, the pressure drop across the conveying pipeline also decreases and reaches a minimum point. Conveying at an air mass flow rate higher than this point usually is referred to as dilute-phase pneumatic conveying. Conveying at an air mass flow rate lower than the point, the pressure drop along the pipeline will increase as the air mass flow rate decreases, and the air-solid flow is commonly referred to as dense-phase pneumatic conveying or fluidised dense-phase. For conveying at a low solids mass flow rate, during the transition from the dilute-phase to dense-phase, moving particles will be in form of suspension and/or strand flow over the stationary layer.

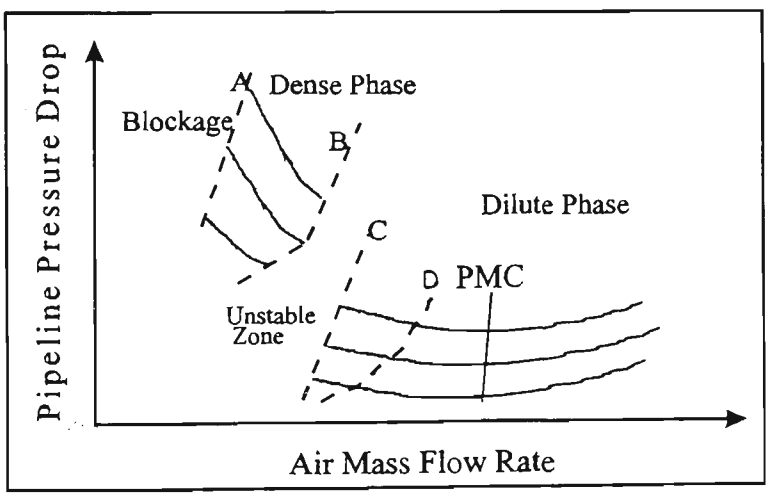

Figure 7.1.2 General form of pneumatic conveying characteristics for the transition from dilute-phase to dense-phase with unstable zone

7.1.2 Transition from Dilute-Phase to Dense-Phase with Unstable Zone or Blockage

This flow mode is usually for granular materials (e.g. plastic pellets, wheat and sand). Figure 7.1.2 shows a typical set of pneumatic conveying characteristics for this flow mode. For conveying of such solid materials in dilute-phase pneumatic, particles move in the form of suspension and/or strand. When conveying at a constant solids mass

flow rate, as the air mass flow rate decreases, the pressure drop across the pipeline will reach a minimum point. This pressure drop minimum point means only that the pneumatic conveying operated at the point can achieve the least pressure drop. It never means the pneumatic conveying is stable or unstable, and is not appropriate for use as the criterion of the minimum conveying velocity of dilute-phase pneumatic conveying even though it is called saltation velocity by some researchers [86, 87, 88]. As the air mass flow rate continues to decrease, a stationary layer or a slowly moving bed will begin to form on the bottom of the pipeline and the air velocity is usually referred as the minimum conveying velocity for the dilute-phase of pneumatic conveying delineated by line D in Figure 7.1.2. As the air mass flow rate further decreases to a certain value delineated by line C in Figure 7.1.2, the air-solid two-phase flow will alternate between a long violent slug flow and a strand over a stationary layer for low solids mass flow rate or slowly moving bed for high solids mass flow rate. Hence the operation enters the unstable zone in the state diagram. As the air mass flow rate increases from the Boundary A shown in Figure 7.1.2, solid materials are moving in the form of low-velocity slug-flow and the pressure drop across the pipeline decreases as air velocity increases. As the air mass flow rate increases further, the point will be reached where low-velocity slug flow can not be maintained and the flow will be in the mode of alternation between a long violent slug flow and a strand over a stationary layer for low solids mass flow rate or slowly moving bed for high solids mass flow rate. This air velocity is considered as the maximum dense-phase conveying velocity for the mode of low-velocity slug-flow and the points mentioned form Boundary B in Figure 7.1.2. Unstable flow with severe pipeline vibrations and pressure fluctuations or blockage may take place when the operation is between Boundaries B and C. Whether pneumatic conveying conducted in the unstable zone will induce blockage of the

pipeline depends on the solid material properties, pipeline properties and the air supply. For some light granular products (e.g. plastic pellet, wheat, and rice) and air supply with steep characteristics or controlled by laval nozzle, conveying in unstable zone will cause pressure fluctuations without blocking the pipeline. While some heavy solid materials, the blockage may happen if the conveying carried out at unstable zone without any further measurement such as bypass pipe to destroy the blockage.

7.2 Review of Classification of Solid Materials for Pneumatic Conveying

It has been demonstrated that solid materials conveyed through the pipeline exhibit different flow modes. An appropriate procedure for assessing the flow mode of solid materials for pneumatic conveying is necessary for the design of industrial applications.

According to the mean surface-volume particle size and density difference, Geldart [27] first classified solid materials into four groups with different fluidisation characteristics. Group A materials generally expand after minimum fluidisation and prior to the commencement of bubbling and retain aeration well. Group B materials usually bubble at minimum fluidisation without expansion and can not retain aeration. Group C materials are very fine and difficult to fluidise. Group D materials are of large size and/or density and spout readily. Geldart's classification was proposed as a method to indicate the potential of materials to be pneumatically conveyed in dense phase but failed to give a reliable prediction of flow mode for pneumatic conveying [57].

Based on Geldart's fluidisation classifications, Dixon [17] developed the slugging diagram for assessing the suitability of solid materials for pneumatic conveying in dense-phase by adjusting the boundaries between four groups of solid materials in the

diagram. Group A powders being pneumatically conveyable at high solid/air loading and not being natural 'sluggers' are the best candidates for dense-phase conveying. Group B powders are not natural 'sluggers' and can not be conveyed at high solid/air loading. They are not likely to be conveyed in dense-phase in a conventional system. Group C has being arguably the worst candidates for dense-phase pneumatic conveying powders. They are cohesive, fine powders that can be difficult to be fluidised. Some materials in group C can be conveyed but many can not be conveyed. Group D particles are large granular pellets that are possible candidates for slug flow. To date Dixon's slugging diagram has been used most commonly for assessing the suitability of materials for dense-phase pneumatic conveying. However, Dixon's work is still imprecise, as his classification has not involved the mechanisms of the air-solid flow through a horizontal pipeline.

Jones and Mills [41] put forward a diagram of powders classification for identifying the suitability for pneumatic conveying in dense-phase according to air retention capability and permeability. The diagram was divided into three groups and the boundaries between the groups are based on experience. Group 1 solid materials have good air retention capacity and particularly low value of vibrated de-aeration constant and permeability. Powders in this group are the best candidates for pneumatic conveying in dense-phase with low velocity and high phase densities through conventional systems. Group 2 solid materials have mid range values of vibrated de-aeration constant, permeability and air retention capacity. Powders in this group are normally not conveyed in dense-phase through conventional systems and can be conveyed in dense-phase through some of the innovative systems available (e.g. bypassing pipe). Group 3 solid materials have good air permeability and poor air retention. Some solid materials in this group can be conveyed in dense-phase. Jones

and Mills' classification of solid materials has still not involved the mechanisms of the air-solid two-phase flow through a horizontal pipeline and the mechanisms for the formation of blockage, so it is still imprecise.

Pan [80] also proposed a diagram of powders classification for identifying the flow modes for pneumatic conveying according to the median particle diameter and loose-poured bulk density of the solid materials. Solid materials were divided into three groups in his diagram. Group PC1 solid materials (e.g. fly ash, cement, pulverised coal) can be transported smoothly and gently from dilute- to fluidised dense-phase. Group PC2 solid materials (e.g. plastic pellets, wheat, barley) can be transported in flow modes of dilute-phase, unstable zone or slug-flow. Group PC3 solid materials (e.g. zircon, coarse sand) can be conveyed in dilute-phase only. Pan's diagram to a certain degree can be considered as the combination of the diagrams of Geldart with Jones and Mills because the loose-poured bulk density of the solid materials used in his diagram is significantly influenced by de-aeration, permeability and air retention capacity of solid materials. Pan's classification has not involved in the mechanisms of air-solid flow through a horizontal pipeline and the mechanisms for the formation of blockage and so it is still imprecise.

7.3 Mechanism for Solids Transported in Different Flow Modes

Two of the most important tasks for pneumatic conveying system design are to determine the system operating boundaries and the total pressure drop across the pipeline. For conveying some powder materials such as fly ash, cement and pulverised coal, the operating boundaries are not taken into account as seriously as that of granular solids because the unstable zone does not exist in the state diagram for conveying many powder materials. It is widely accepted that particle properties such as

particle diameter and its distribution, density, voidage, particle shape, air retention, permeability contribute to the difference between powder and granular solids in the state diagram. The real mechanism involved in air-solid two-phase flow behaviours between dense-phase and dilute-phase pneumatic conveying has not been explored so far. The theoretical model established in Chapter Five provides an approach for determining the mechanism.

As it is discussed in Chapter Six, the Transition Zone in the state diagram for pneumatic conveying of granular materials through a horizontal pipeline consists of upper and lower parts and different flow mechanisms are involved in the air-solid two-phase flow at upper and lower parts of the transition zone in the state diagram. The operating points in the lower part of the transition zone, usually with relatively low solid mass flow rate per unit area, represent air-solid two-phase flow in the mode of a strand flow over a stationary layer. The condition for keeping the flow steady is that the thickness of the stationary layer may grow to increase the air velocity that will also result in an increase of solid mass flow rate per unit area. Since any disturbance in the air-solid two-phase flow may induce the increase of granular solids contained in the conveying pipeline and increase the thickness of the stationary layer, the air velocity naturally increases as the flow channel area across the intersection of the pipeline decreases. Air-solid two-phase flow in such a mode can be kept stable until the air velocity within the flow channel reaches the value that is represented by Type C operating points in state diagram. As discussed in Chapter Six, the area of lower part of the transition zone in the state diagram for the pneumatic conveying of granular solid materials through a horizontal pipeline may vary with particle properties and pipeline properties and air properties, but it never disappears as a result of variation in particle and pipeline properties.

The operating points in the upper part of the transition zone, usually with relatively high solid mass flow rate per unit area, represent air-solid two-phase flow in the mode of a strand flow over a slowly moving bed. To maintain stability in such a flow mode, the friction between the moving strand and the slowly moving bed should be high enough to overcome the friction between the slowly moving bed and pipe wall and push the slowly moving bed to extend forward or lower the thickness of slowly moving bed. The mathematical expression of the force is as follows:

$$f_p \cdot \rho_p \cdot (1-\varepsilon_{st}) \cdot (1-\phi) \cdot (1-\alpha_{cri}) \cdot A \geq f_w \cdot [\rho_p \cdot (1-\varepsilon_{st}) \cdot (1-\phi) \cdot (1-\alpha_{cri}) \cdot A] + f_w \cdot \rho_p \cdot (1-\varepsilon) \cdot \alpha_{cri} \cdot A \quad (7.3.1)$$

Assuming ε_{st} equal to ε when the operation point is very close to the Boundary B, Equation 7.3.1 can be simplified as follows:

$$f_p \geq \left[1.0 + \frac{\alpha_{cri}}{(1.0-\phi)(1.0-\alpha_{cri})}\right] \cdot f_w \quad (7.3.2)$$

Comparing the state diagrams for pneumatic conveying of powder materials and granular materials, it is found that the difference between two state diagrams is that the upper part of the transition zone does not exist or is too narrow to cause any unstable flow behaviours for pneumatic conveying of powder materials. Equation 7.3.2 shows the mechanism that dominates the formation of the upper part of the transition zone in the state diagram for pneumatic conveying through a horizontal pipeline. When the friction between particle and pipeline wall is close to that between particles, the upper part of the transition zone in the state diagram will disappear and there will be no unstable zone between dense-phase and dilute-phase pneumatic conveying in the state

diagram for relatively high solids mass flow rates. Equation 7.3.2 provides the criterion to distinguish between the granular solids and powder. The difference between granular solids and powder seems to be in particle diameter and its distribution, permeability, air retention, compressibility, particle density. Actually what makes powder and granular solids exhibit different flow modes in pneumatic conveying is that for granular solids, f_w is much lower than f_p while for powder, f_w is very close or equal to f_p based on the Equation 7.3.2.

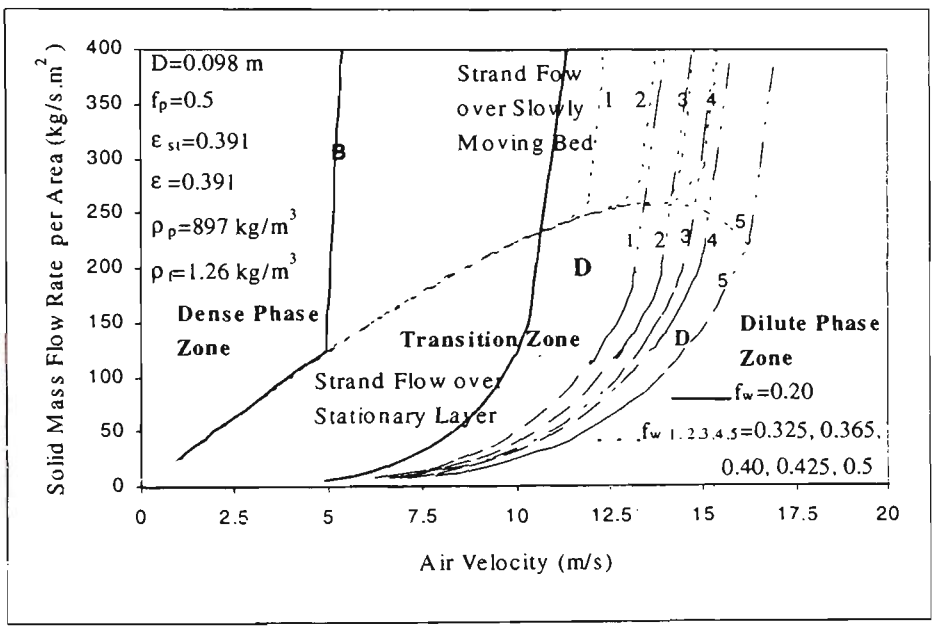

Figure 7.3.1 Variation of transition zone in state diagram with respect to the friction between particle and pipe wall

Figure 7.3.1 shows a variation of the transition zone in the state diagram for pneumatic conveying of granular materials through a horizontal pipeline as the sliding friction between pipe wall and particle approaches the friction between the particles. As f_w is increased from 0.2 to 0.325, the velocity gap between Boundaries B and D at the upper of the transition zone in the state diagram is decreased from about 6.0 m/s to 1.6 m/s. As the f_w is further increased from 0.2 to 0.425, the velocity gap between Boundaries

B and D at the upper of transition zone in state diagram is decreased from about 6.0 m/s to 0.3 m/s. When the upper gap between Boundaries B and D in the state diagram becomes very narrow, it means that the unstable zone tends to decrease in term of air velocity. In most situations with a narrow upper gap between Boundaries B and D in the state diagram, direct transition of the flow mode from dense-phase to dilute-phase pneumatic conveying will take place. Even if a short unstable zone exists, it is not enough to cause pressure fluctuation along the conveying pipeline for high solids mass flow rate

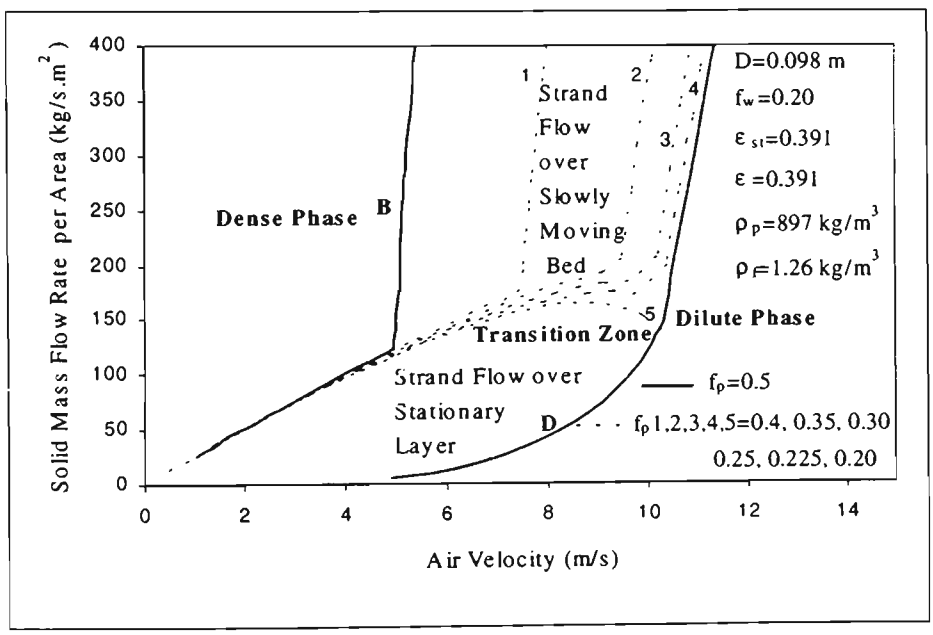

Figure 7.3.2 Variation of transition zone in state diagram with respect to friction between particles approaching friction between particle and pipe wall

Figure 7.3.2 shows variation of transition zone in the state diagram for pneumatic conveying of granular materials through a horizontal pipeline as the friction between particles approaches the sliding friction between pipe wall and particle. As the f_p is decreased from 0.5 to 0.4, the velocity gap between Boundaries B and D in the upper of transition zone in the state diagram is decreased from about 6.3 m/s to 3.4 m/s. As

the f_p is further decreased from 0.4 to 0.3, the velocity gap between Boundaries B and D in the upper of transition zone in the state diagram decreases from about 3.4 m/s to 1.3 m/s. As the f_p is further decreased from 0.3 to 0.225, the velocity gap between Boundaries B and D in the upper of transition zone in the state diagram decreases from about 1.3 m/s to 0.2 m/s. The upper part of the transition zone in the state diagram for pneumatic conveying of particles through a horizontal pipeline almost disappears. Direct transfer from dilute phase to dense-phase pneumatic conveying for high solid mass flow rate as f_p is close to f_w is clearly demonstrated in Figure 7.3.2.

CHAPTER 8: EXPLANATION AND DISCUSSION OF THE STATE DIAGRAM FOR POWDER MATERIALS

8.1 Introduction

In general, powder and granular solids exhibit two basic flow modes in the state diagram for pneumatic conveying. The boundaries of transition zone in state diagram for pneumatic conveying of granular solid materials have been addressed in Chapter Six based on the model established in Chapter Five. So far very little attention has been paid to the boundaries of the transition zone in the state diagram for pneumatic conveying of powder materials. The main reason is that smooth transition from dense-phase to dilute-phase for the conveying powders can be achieved without causing instability of the conveying system (if the solid mass flow rate is not too low). But for conveying powder materials with high particle density, lower voidage and strong friction between particles, a full assessment of the boundaries of the transition zone in the state diagram and correct design of conveying velocity and solid mass flow rate must be obtained. Serious consequences such as the blockage of the pipeline system may be induced if this is not done.

For the dilute-phase pneumatic conveying of powder materials in the form of strand flow through a horizontal conveying pipe, the friction between the moving strand and pipe wall surface differs from that of granular solids. Actually the strand of powder almost does not directly contact with the surface of the pipe wall, so the friction between the moving strand and the pipe wall should be considered as the friction between the particles in strand and particles on the pipe wall. The change of wall friction can be further explained as follows: first, the fine powders tend to adhere to the pipe wall surface because of the static electricity and/or the adhesion of the fine powder and the force of the adhesion between fine particles and the pipe wall surface usually strongly resists the movement; second, fine powders adapt themselves to the rough surface of the pipe wall and take advantage of their position to resist the drag

force of the strand. As a result, the direct friction between the particles in the strand and the wall surface will be higher than that between the powders in strand and powders on the wall surface. To make the model established at Chapter Five applicable for discussion of pneumatic conveying of powder materials in the state diagram, it is assumed that the friction between particle and the pipe wall is equal to that between particles. Also the internal friction factor substitutes for friction between particles for powder materials in the discussion here. In order to have a comparison with the experimental results of conveying PVC powder, all the factors or parameters have been kept constant and are equal to those of PVC powder at experimental condition. The particle density is 1500 kg/m^3, pipeline inner diameters were 105 mm, the voidage of the powder was 0.65 and f_w=0.7, f_p=0.7.

8.2 State Diagram for Pneumatic Conveying of Powder Materials through a Horizontal Pipeline

Based on the model established in Chapter Five, the state diagram of pneumatic conveying of powder materials through a horizontal pipeline is shown in Figure 8.2.1. The state diagram is separated into dense-phase, dilute-phase and transition zones by Lines B and D. Line D in the state diagram is calculated from the model to separate the operating points representing the conveying of powder materials without a stationary layer deposit on the bottom of the conveying pipeline from those representing the flow over a stationary layer or dense-phase flow in the state diagram. Line B, which is the intersection points of curves **F** and **E** for different thickness of stationary layers discussed in Chapter Five, separates the operating points depicting the flow mode of dense-phase pneumatic conveying of powder materials from those depicting the flow mode of a strand over a stationary layer. Line A separating the operating points representing the flow in dense-phase from those representing the flow in fixed-bed

mode in the state diagram and determined by particle properties, pipe wall properties, fluid properties (e.g. air density), structure of feeding design and the length of the pipeline will not be discussed in this chapter.

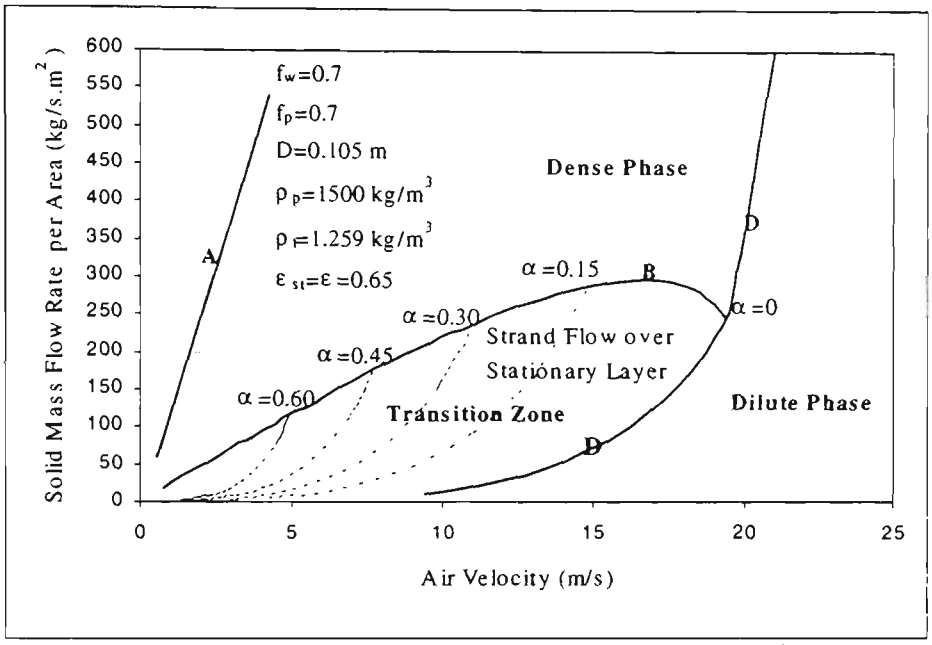

Figure 8.2.1 State diagram for pneumatic conveying of powder materials through horizontal pipeline

Unlike the transition zone in the state diagram for pneumatic conveying of granular materials, the operation in the transition zone in the state diagram for powder materials has only one mode of flow, namely a strand flow over a stationary layer. Any point in the transition zone in the state diagram represents an operation of the pneumatic conveying of power materials with certain air velocity, solids mass flow rate and the thickness of the stationary layer and the area of transition zone may be very large or very small according to the particle properties that will be further discussed later. Operation in the dense-phase zone in the state diagram may in the mode of plug flow or fluidised dense-phase flow but never low-velocity slug flow according to the particle properties. Since the friction between particles for powder materials is higher,

a relatively higher air velocity is demanded for dilute-phase pneumatic conveying of powder materials without a stationary layer on the bottom of conveying pipeline. The point of the intersection of Lines D and B in the state diagram also has particular meaning in that it may transfer into any of three different flow modes if a little variation in the operating condition takes place. With increase or decrease in solid mass flow rate, the flow mode may alternate between dense-phase and dilute phase; with increase or decrease in air mass flow rate, the flow mode may alternate between a strand flow over a stationary layer and a flow over the pipe wall.

For pneumatic conveying of powder in a pipeline free of stationary layer on the bottom, high conveying air velocity is necessary and this causes high pressure drop, high energy consumption and pipe wall wear especially at the bends. Since there is a very wide air velocity range between the two boundaries of the transition zone for conveying with a certain solid mass flow rate, it is still possible for the operation in the transition zone to be steady over a long distance of pipeline without a plug forming near the entrance of the pipeline and extend forward along the pipeline. If this plug forms at the inlet of conveying pipeline, it becomes long and results in a sudden pressure drop increase and pipeline blockage. Nevertheless, many industrial applications of conveying of powder materials such as pulverised coal have operated successfully in the transition zone in the state diagram with a stationary layer on the bottom of conveying pipeline [82].

8.3 Influence of Pipeline Diameter on Boundaries of Transition Zone in State Diagram for Powder

To convey powder with high particle density, lower voidage, strong friction between particles and low solid mass flow rate and avoid high pressure fluctuation and the blockage of the pipeline system, it is important to fully assess the operating boundaries

of the transition zone in the state diagram and correctly design the conveying air velocity and solid mass flow rate. There is a wide variation in pipeline diameter as the amount of solid materials to be conveyed and the conveying distances vary. In most conditions, pipe diameters of the pilot scale test unit are smaller than those of industrial applications. Hence, it is necessary to predict the operating boundaries of the transition zone in the state diagram accurately and reliably in order to ensure that the conveying systems are operated steadily and stably.

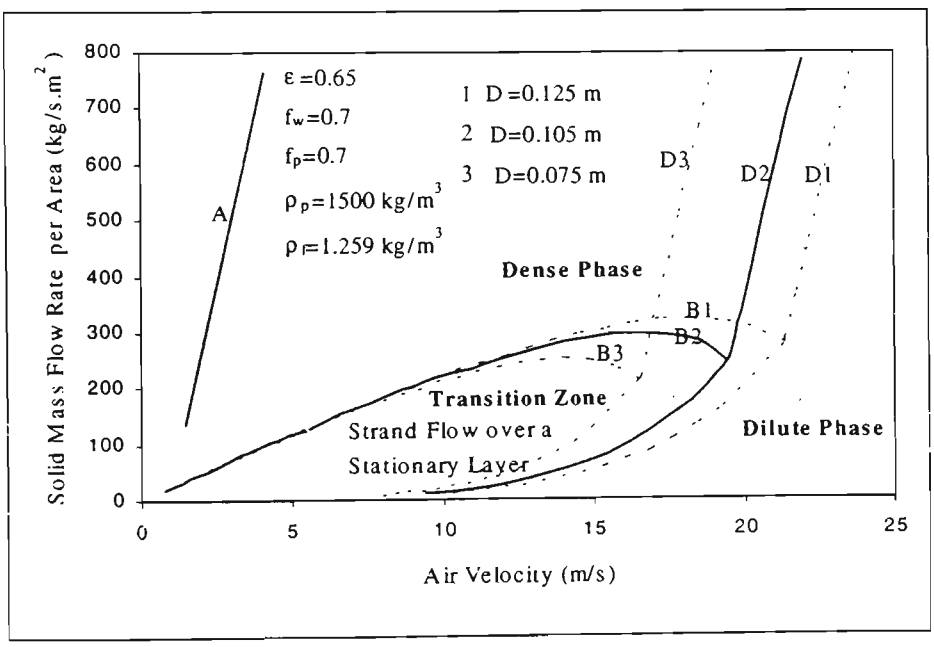

Figure 8.3.1 Predicted state diagram for pneumatic conveying of powder materials with respect to pipeline diameter

Figure 8.3.1 shows a comparison of transition zones in the state diagram for pneumatic conveying of powder materials through horizontal pipelines with diameters of 75, 100 and 125 mm. From Figure 8.3.1 it is clear that as the pipeline diameter increases, Boundary D (representing the minimum conveying velocity defined as the lowest air velocity for conveying without a stationary layer on the bottom of the pipeline) and line B move forward and the transition zone area in the state diagram enlarges. This

means that there is a wider air velocity range in the transition zone for a given solids mass flow rate and higher solid mass flow rate per unit area for a direct transformation of conveying from dilute-phase to dense-phase for the larger pipe bore.

8.4 Influence of Friction between Particles on Boundaries of Transition Zone in State Diagram for Powder Materials

It is assumed that the friction between particle and pipe wall is equal to that between particles and according to the established model, the influence of the factor of friction between particles on the boundaries of transition zone in the state diagram should be discussed.

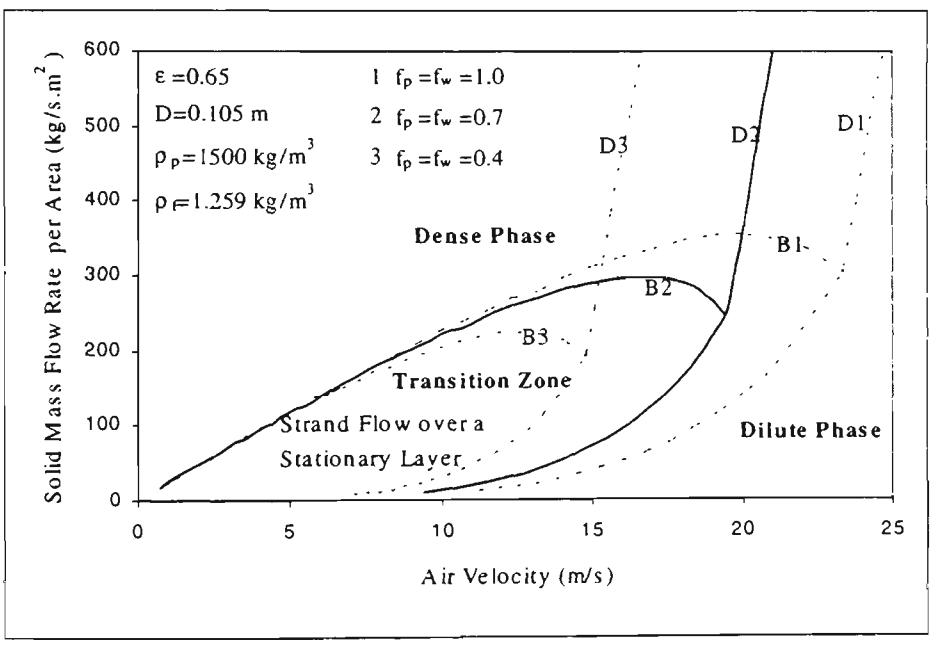

Figure 8.4.1 Predicted state diagram for pneumatic conveying of powder materials with respect to friction between particles

Figure 8.4.1 shows a comparison of the boundaries of the transition zones in the state diagram for pneumatic conveying of three powders with different particle-particle friction factors through a horizontal pipeline. As the particle-particle friction factor increases in value, the boundaries of the transition zone move forward and the area of

the transition zone in the state diagram is enlarged. Hence, for pneumatic conveying of powder materials with bigger particle-particle friction factor, there is a wider air velocity gap between the two boundaries of the transition zone where the flow in the mode of a strand flow over the stationary layer is demonstrated. A higher solid mass flow rate for the direct transition between dilute-phase and dense-phase pneumatic conveying will be observed as the air mass flow rate is decreasing.

8.5 Influence of Bulk Voidage on Boundaries of Transition Zone in State Diagram for Powders

The voidage of the powder is one of the key factors in determining the transition zone in the state diagram according to the model established in Chapter Five. The prediction of the transition zone in the state diagram for pneumatic conveying of powder materials under the influence of powder voidage is shown in Figure 8.5.1.

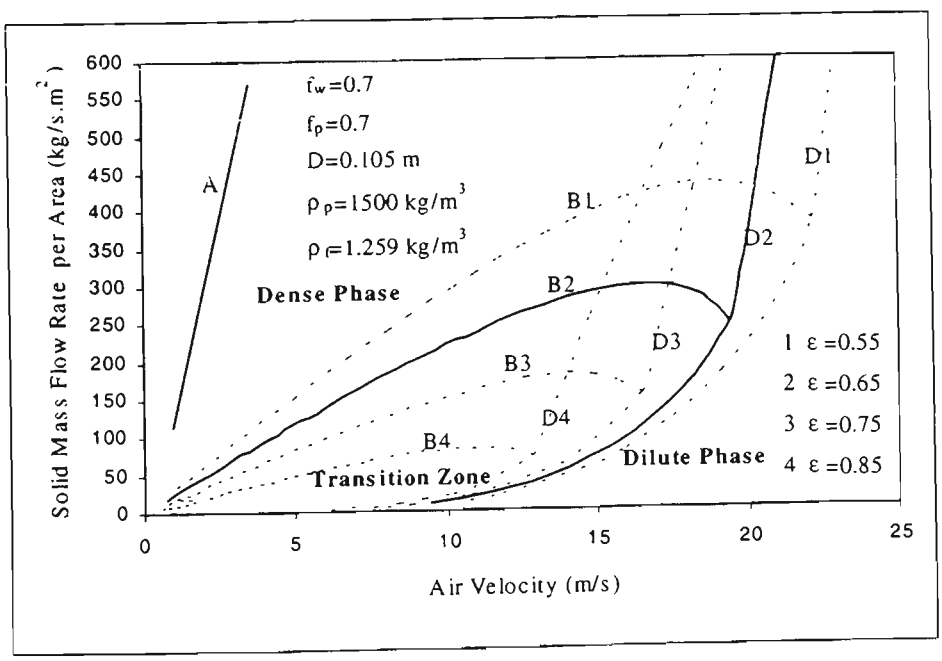

Figure 8.5.1 Predicted state diagram for pneumatic conveying of powder materials with respect to voidage of powder

Figure 8.5.1 shows that as the voidage of powder decreases, the boundaries of the transition zone move forward and the area of the transition zone in the state diagram enlarges dramatically. As well, a wider air velocity gap exists between the two boundaries of the transition zone where the flow is in the mode of a strand flow over a stationary layer, and the solid mass flow rate for direct transition between dilute-phase and dense-phase pneumatic conveying as the air mass flow rate decreases will be higher. The flow mode of a strand flow over a stationary layer will be hard to detect as the air mass flow rate decreases if the powder materials with a high voidage.

8.6 Influence of Particle Density on Boundaries of Transition Zone in State Diagram for Powders

Powder materials with dramatically different particle properties are being transported through pipelines. Particle density is a very important parameter for the design of pneumatic conveying systems

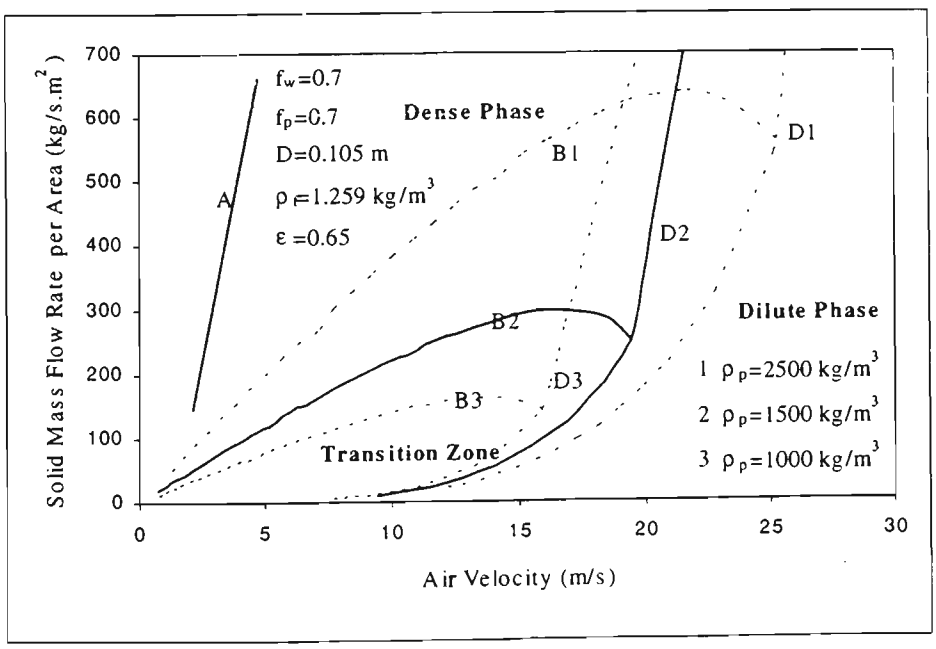

Figure 8.6.1 Predicted state diagram for pneumatic conveying of powder materials with respect to particle density of powder

Figure 8.6.1 shows a comparison in the transition zone in the state diagram of pneumatic conveying of three granular materials with particle density 2500 kg/m^3, 1500 kg/m^3 and 1000kg/m^3 respectively. As the density of the powder increases, the boundaries of the transition zone move forward and the area of transition zone in the state diagram enlarges dramatically. A wider air velocity gap develops between the two boundaries of the transition zone where the flow is in the mode of a strand flow over a stationary layer. The solid mass flow rate for direct transition between dilute-phase and dense-phase pneumatic conveying as the air mass flow rate decreases will be higher

It is worthy to note that particle properties such as particle density, bulk density, particle diameter can not solely decide the flow mode of pneumatic conveying. The mode of air-solid two-phase flow through the horizontal pipeline also relates to pipeline properties and fluid properties. This concept will be reinforced as this research goes on.

8.7 Influence of Air Pressure on Boundaries of Transition Zone in State Diagram for Powder

In many cases pneumatic conveying of powder materials is over a long distance and uses pressured air as a fluid medium or operates in a state of vacuum. It is necessary to understand the variation of the transition zone in the state diagram with different air pressures.

Figure 8.7.1 shows a comparison of the transition zone in the state diagram for pneumatic conveying of powder materials with different air pressures or different air density. As the air density increases (pressure increases), the boundaries of transition zone (in air velocity) move backward and the area of the transition zone shrinks. A

narrower air velocity gap then exists between the two boundaries of the transition zone where the flow is in the mode of a strand flow over the stationary layer and the solid mass flow rate becomes lower for directly transition between dilute-phase and dense-phase pneumatic conveying as the air mass flow rate decreases.

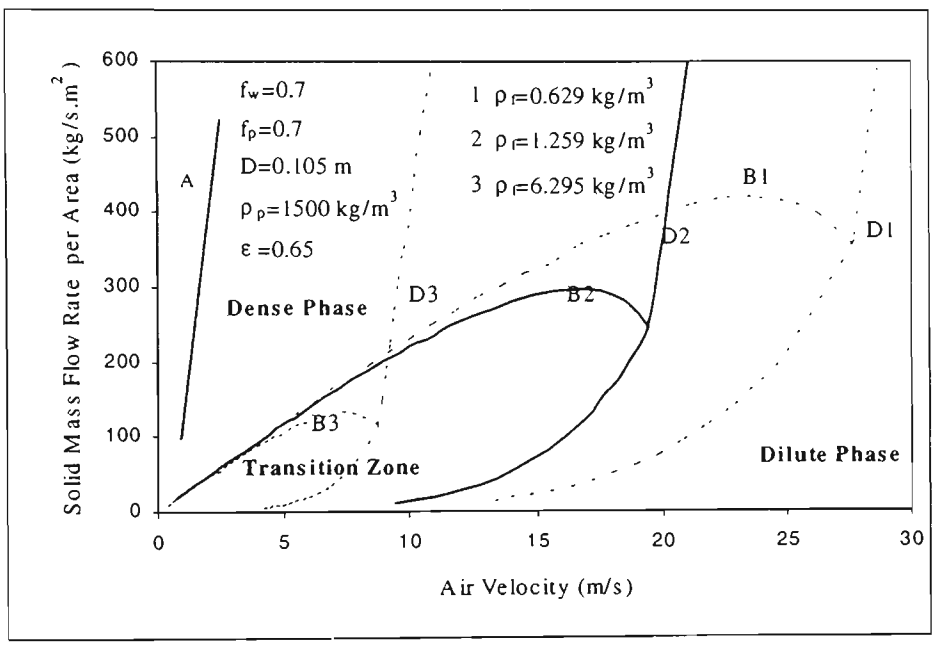

Figure 8.7.1 Predicted state diagram for pneumatic conveying of powder materials with respect to air pressure.

CHAPTER 9: MEASUREMENT OF SLIDING FRICTION FACTOR

9.1 Introduction

Since it was first invented in the late 1960s and came into industry in the mid 1970s, dense phase pneumatic conveying of bulk solid materials has been successfully used in industry. It is now considered as an effective technique for moving solid materials, having the advantages of high capacity, lower energy consumption, less product degradation and less pipeline wear. To locate operating boundaries and predict overall pressure drop reliably are still the main tasks for engineers and researchers in this area. The pipe wall sliding friction factor (given as f_w), which is related to the ratio of the wall shear stress or friction force to wall vertical stress, is the key parameter in many models for prediction of pressure drop of conveying pipeline systems and also in determining the operating boundaries in the state diagram in this thesis.

The wall sliding friction factor is usually determined experimentally and the most common rig for it is the Jenike Direct Shearing Tester. A test for measuring wall-sliding friction with the Jenike Shearing Rig is carried out by applying a certain vertical force and a shearing force on the shearing ring, which is put on the plate made of the pipe wall materials. Failure occurs as soon as the shearing force reaches a particular value. By repeating the shearing test for the sample with different vertical forces, a curve in the vertical force and shearing force co-ordinate system presenting the relationship between the vertical force and the shearing force is obtained. The angle between the curve and horizontal axis is called the wall friction angle (for cohesionless plastic pellets used in this thesis). Sliding friction factors also had been tested by shearing the plate with the sample particles evenly gluing on it over plate made of pipe material with different weight on the top plate [98]. The curving surface properties of the inner pipe wall are usually not exactly the same as those of the flat plate even though they are made of the same material. Sometimes it is difficult to have

a flat plate made of the same materials as the pipeline, the testing results of two sliding friction testing approaches are by no means perfect. Testing sliding friction factors for different solid particles was done by gluing solid particles on to the cylindrical surface of a brass pipe and by checking the titling angle for cessation of motion of that piece of brass inside an inclined glass pipe [67]. This method measured the sliding friction between the particle and the glass pipe wall surface. Normally the glass surface is much smoother than those made of steel, stainless steel, brass and aluminium materials.

To achieve an accurate sliding friction factor for predicting operating boundaries in the state diagram and total pressure drop over the conveying system, a novel technique and test rig was developed to overcome the disadvantages of the testing approach established by the other researchers.

9.2 Objectives and Structure of Design of Sliding Friction Test Rig

The objective of the design of the sliding friction test rig is to ensure that sliding friction force can be measured accurately and the testing results represent the sliding friction between the sliding particles and the actual inner wall of the pipeline without disturbance from both subjective and testing systems. To realise such an objective, the sliding test must be conducted on the inner wall of the pipeline that is used for pneumatic conveying of the solid materials and the friction force is directly measured during the movement of sliding. According to the requirement of the sliding friction test, a novel test rig for such purposes had to be developed and the sketch of the test rig is shown in Figure 9.1

The sliding friction test rig consists of four parts. The case is used to contain particle materials by which the weight block is supported. The blocks are used for adjusting the

vertical force acting on the sliding particles by changing the number of the block and the first block is screwed to the testing case after the setting up is completed. During the sliding test, the weight of the case is added to the block by the strong screwed connection and acts on the upper surface of the sample particles. The set-up supporters are used during the setting up to support the case and install a gap between the case and the pipe wall in order to prevent the case from touching the pipe wall during sliding. The gap or distance between the sliding test case and the pipe wall surface, which is initiated by the set-up supporters, is very sensitive to sliding friction experiment as the lower gap may induce the sliding test case to meet the pipe wall and higher gap may result in the particles running out of the sliding test case. A string connecting the case and a force meter that is used to measure the putting force is for keeping the case moving steadily. The force meter is dragged by a multi-speed motor and moves at the same speed of testing case. The influence of moving speeds on the sliding friction force can be measured by adjusting the speed of the motor. If the setting-up is not done well, the sliding test case will usually meet the wall surface while moving through the pipeline and then the sliding test fails. Such failure can be notified easily from significant increase of the output of the force meter.

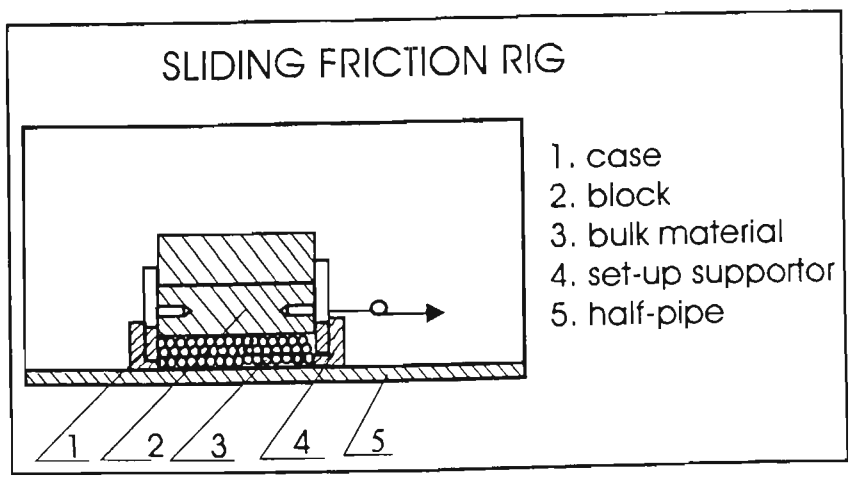

Figure 9.1 Configuration of the sliding friction rig

9.3 Procedure for Sliding Friction Test

To conduct the sliding friction test with the test rig developed in this thesis, the steps can be summarised as follows:

(i) Turn on the power of the force meter and warm it up for fifteen minutes before the test is carried out. Clean the surface of the section of the pipe for the test as powders or grease sticking on the pipe wall surface may affect the test results. Start the multi-speed motor and select a suitable running speed for the sliding friction test at the lowest position of the section of the pipe.

(ii) Undertake the setting-up for the sliding friction test on a short section of half-pipe.

- Put the testing case on the supporters and adjust the position of the testing case. Ensure that the axial line of the testing case is parallel to that of the pipe and the pulling direction of the motor.

- Weigh a certain amount of sample particles to fill one-third of the volume of the testing case and put it carefully into the testing case standing on the case supporters. Make sure the upper surface of the sample particles is even.

- Put the weight block into the testing case carefully and make sure that the block sits evenly on the sample particle in the testing case. Screw the weight block to the testing case and then take off the case supporters.

(iii) Move the testing case with sample and weight block slowly into the testing section of the pipe by pulling the string after aligning the half-pipe section with the testing pipe section.

(iv) Start the multi-speed motor and begin the sliding friction test. Ensure that the force meter, testing case and pulling motor are on one line and record the output of the force meter.

(v) Pull the testing case back to the start point with the string by hand and change the weight block and repeat the sliding friction test.

9.4 Sliding Friction Testing Results and Discussion

The sliding friction tests were conducted on the same stainless steel pipe for the pneumatic conveying of solid materials in the laboratory. The inner diameters of pipes were 60.1 mm and 98.3 mm. The friction forces were read from the output of the force meter and the results are shown in the Table 9.4.1 and Table 9.4.2.

For the sliding friction tests conducted on the stainless steel pipe wall, the conclusions are as follows:

(i) Since the accuracy of the force meter is 1 (g), the precision of every data is 1 (g)

(ii) The length of the sliding friction test pipe is 400 mm and the speed of the test case is within 1.0 cm/s to 3.0 cm/s and makes very little difference in the reading of the force meter.

(iii) The sliding friction factors for two stainless steel pipes are almost the same.

(iv)Since the pipe wall surface properties vary with the location of the pipe wall and the whole surface is not even, the results of the measurement on the sliding friction force are the average value of the output of the force meter.

(v) Any slight damage on the surface of the pipe wall will influence the value of the sliding friction force.

Table 9.4.1: The sliding friction test results for ID 60.3 mm stainless steel pipe

The weight of testing case +block +sample = 180 (g)								
Reading No.	1	2	3	4	5	6	7	8
Friction force (g)	34	35	36	37	35	34	36	33
f_w	0.19	0.19	0.20	0.20	0.19	0.19	0.20	0.18
The weight of testing case +block +sample = 295 (g)								
Reading No.	1	2	3	4	5	6	7	8
Friction force (g)	57	59	58	56	59	58	56	58
f_w	0.19	0.20	0.20	0.19	0.20	0.20	0.19	0.20

Table 9.4.2: The sliding friction test results for ID 98.4 mm stainless steel pipe

The weight of testing case +block +sample = 181 (g)								
Reading No.	1	2	3	4	5	6	7	8
Friction force (g)	35	36	34	32	35	36	34	35
f_w	0.19	0.20	0.19	0.18	0.19	0.20	0.19	0.19

The weight of testing case +block +sample = 293 (g)								
Reading No.	1	2	3	4	5	6	7	8
Friction force (g)	56	58	53	56	59	55	54	58
f_w	0.19	0.20	0.18	0.19	0.20	0.19	0.18	0.20

CHAPTER 10: MEASUREMENT OF STRESS TRANSMISSION COEFFICIENT

10.1 Introduction

The advantages of dense phase pneumatic conveying of bulk solid materials mainly lie in low power consumption, less product degradation and pipe wear. To predict pressure drop across the whole conveying pipeline reliably in the terms of particle properties, pipe line properties and operating conditions is still a major consideration for researchers and engineers in this area even though some models have been developed for this purpose using different approaches and taking account of various forces acting on the solid materials being conveyed. The models developed by using the methods of powder mechanics have been found to perform best in the prediction of the slug flow behaviour [48]. A term relating the lateral wall stress to axial stress called a stress transmission coefficient K_w plays an important role in the analysis of the forces acting on the moving slugs and model development.

From the relationship between the Mohr's failure envelope and the wall yield locus of the particle materials, K_w can be deduced as follows:

$$K_w = \frac{1.0 + \sin\phi_s \cdot \cos(\omega + \phi_w)}{1.0 - \sin\phi_s \cdot \cos(\omega + \phi_w)} \qquad \text{for the passive situation.} \qquad (10.1.1)$$

$$K_w = \frac{1.0 - \sin\phi_s \cdot \cos(\omega - \phi_w)}{1.0 + \sin\phi_s \cdot \cos(\omega - \phi_w)} \qquad \text{for the active situation} \qquad (10.1.2)$$

and ω is given as follow:

$$\sin\omega = \frac{\sin\phi_w}{\sin\phi_s} \qquad (10.1.3)$$

Later ϕ_s was modified by Mi [63, 64] and expressed as below:

$$\phi_S = \frac{4}{3} \cdot \phi_W \cdot \gamma_b^{1/3} \qquad (10.1.4)$$

Here γ_b is the bulk specific gravity with respect to water at 4.0 °C.

From observations of slugs moving through the pipeline, it is believed there is no failure occurring between the particles in the slug. Hence the Equations 10.1.1 and 10.1.2 do not represent the real relationship between lateral wall stress and axial stress and this is further confirmed by the modification of Mi [63, 64]. Mi measured the lateral stress on the pipe wall of the slugs of plastic pellet, wheat and barley passing the conveying pipeline. The axial stress is not measured experimentally but calculated by the equation below:

$$\sigma_f = \alpha \cdot \rho_b \cdot U_s^2 \qquad (10.1.5)$$

Though the K_w provided by Mi's modification is better fitted for the model of pressure prediction, this modification is based on the results of the experimental measurement of the lateral stress created by the moving slug of four different bulk solid materials while its corresponding axial stresses are not from the experimental measurement. Hence it still needs more experimental support before it is widely applied. Also the connection between the modified ϕ_S and the gravity term indicates that the "gravitational" location of tests will vary the test results of K_w and this makes no sense (as ϕ_S is a fundamental particle property).

Actually, K_w as an important parameter in the models for the pressure drop prediction has never been directly and experimentally measured. To obtain K_w easily, reliably and accurately has great significance to the applications of dense phase pneumatic conveying of granular materials in industry.

10.2 Objectives and Structure of Design of Stress Transmission Rig

The objective of the design of the stress transmission rig is to measure K_w more directly and accurately and this measurement represents the real relationship between lateral wall stress and axial stress of a slug in the conveying pipeline. To realise this objective, a novel test rig was developed and a sketch of the test rig is shown in Figure 10.2.1.

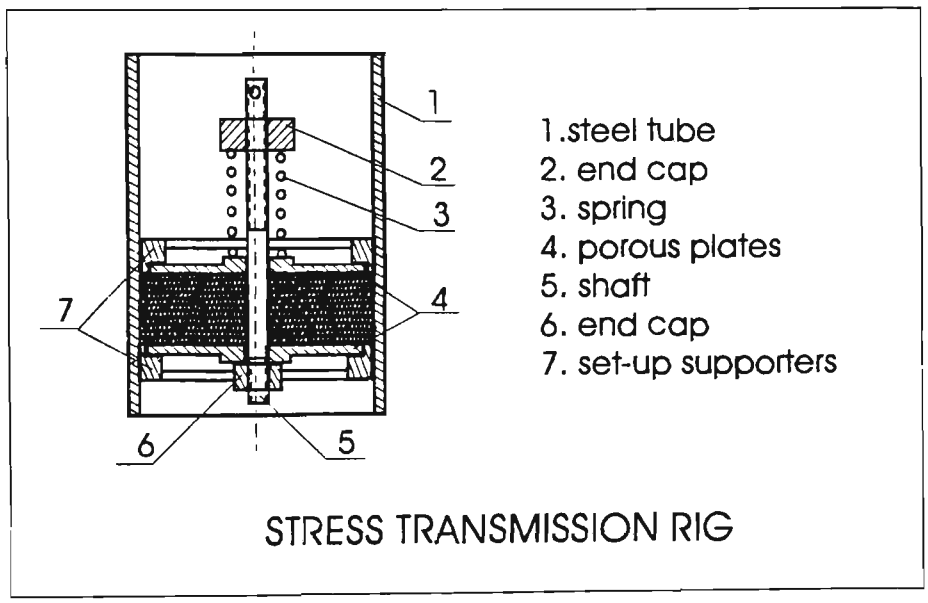

Figure 10.2.1 Configuration of the stress transmission rig

The stress transmission rig consists of six parts. A 400 mm long steel tube is cut from the conveying pipeline and the stress transmission coefficient test is conducted within the tube. The set-up supporters are used to hold the porous plates at the centre of the tube without meeting the pipe wall during the setting up of a short slug unit in the tube. The space between the two porous plates contains the sample solid materials for the test of K_w and the distance between two plates or the length of the slug unit is adjustable. The gap between the porous plates and the inner wall of the tube is very sensitive and is critical to success of the test. The sample particles partially filling the

gap create an extra friction force beyond the lateral stress and it will be further addressed in the discussion of stress transmission test results. The spring is designed to apply a certain amount of force on the porous plate and create an adjustable axial stress on the sample particles. By turning the end cap along the shaft with a screw thread at both ends, the length of the spring can be adjusted to a certain value and generate a desired axial stress on the test sample. The lateral stress is calculated from the pulling force for keeping the slug unit moving vertically and deducting the weight of the moving parts of the rig.

10.3 Principle of Stress Transmission Rig

During stress transmission tests, the slug unit containing the sample particles is pulled upward by a multi-speed motor with a force meter in between. The spring normally acting at the top of the slug unit creates an axial stress that is measured according the length of the spring and other additional weight from the parts of the test unit also attributes to the axial stress. The thickness of the slug unit is designed to ensure the axial stress can be kept constant along the axis of the slug and also stable during the tests. The lateral stress is not directly measured by the wall stress gauge but deducted from the direct measurement of the friction between the moving slug unit and the testing section of the pipeline. In the following force balance analysis, the spring is assumed to act on the top and bottom of the slug unit and the corresponding boundary conditions are also given. Analysis of the forces acting on an element of slug unit in the stress transmission test rig is shown in Figure 10.3.1.

From an equilibrium analysis of the element slice in Figure 10.3.1, the following differential equation may be derived:

$$\frac{\pi}{4}\cdot D^2\cdot[(P_z+dP_z)-P_z]-\frac{\pi}{4}\cdot D^2\cdot\rho_b\cdot g\cdot d_z-\pi\cdot D\cdot d_z\cdot P_z\cdot K_w\cdot f_w=0 \qquad (10.3.1)$$

Solving Equation 10.3.1 yield:

$$P_z=c\cdot\exp\left(\frac{4f_w\cdot K_w\cdot Z}{D}\right)-\frac{\rho_b\cdot g\cdot D}{4f_w\cdot K_w} \qquad (10.3.2)$$

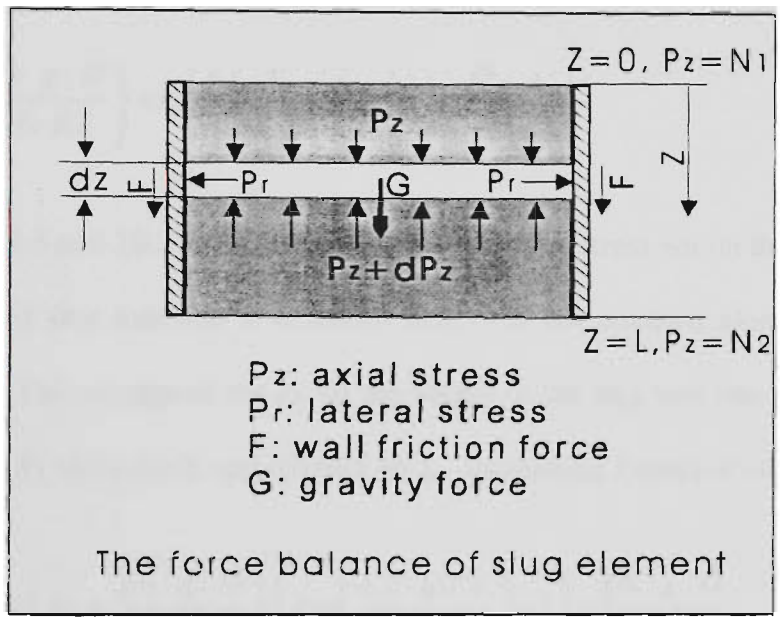

Figure 10.3.1 Analysis of forces on the element of slug

Inserting the boundary condition that the spring acting at the position (top) of Z=0, then $P_z=N_1$, therefore

$$c=\left(N_1+\frac{\rho_b\cdot g\cdot D}{4f_w\cdot K_w}\right) \qquad (10.3.3)$$

Insertion of Equation 10.3.3 into Equation 10.3.2 yields:

$$P_z=\left(N_1+\frac{\rho_b\cdot g\cdot D}{4f_w\cdot K_w}\right)\cdot\exp\left(\frac{4f_w\cdot K_w\cdot Z}{D}\right)-\frac{\rho_b\cdot g\cdot D}{4f_w\cdot K_w} \qquad (10.3.4)$$

For the boundary condition that the spring acting at the position (bottom), $P_z|_{z=L} = N_2$, insert the boundary condition to Equation 10.3.2 to yield:

$$c = \left(N_2 + \frac{\rho_b \cdot g \cdot D}{4 f_w \cdot K_w} \right) \exp\left(- \frac{4 f_w \cdot K_w \cdot L}{D} \right) \tag{10.3.5}$$

Insertion of Equation 10.3.5 to Equation 10.3.2 yields:

$$P_z = \left(N_2 + \frac{\rho_b \cdot g \cdot D}{4 f_w \cdot K_w} \right) \cdot \exp\left(\frac{4 f_w \cdot K_w \cdot (Z - L)}{D} \right) - \frac{\rho_b \cdot g \cdot D}{4 f_w \cdot K_w} \tag{10.3.6}$$

Equations 10.3.4 and 10.3.6 are for calculating the axial stress within the slug unit at a specific slice of slug unit and it is shown that P_z is not constant along the L and it varies with Z. The average of the P_z for the height of the slug unit can be obtained by integrating the P_z along the L and divided by L. Integrating Equation 10.3.4 yields:

$$\overline{P_z} = \frac{D}{4 f_w \cdot K_w \cdot L} \left(N_1 + \frac{\rho_b \cdot g \cdot D}{4 f_w \cdot K_w} \right) \cdot \left(\exp\left(\frac{4 f_w \cdot K_w \cdot L}{D} \right) - 1 \right) - \frac{\rho_b \cdot g \cdot D}{4 f_w \cdot K_w} \tag{10.3.7}$$

Integrating Equation 10.3.6 along L yields:

$$\overline{P_z} = \frac{D}{4 f_w \cdot K_w \cdot L} \left(N_2 + \frac{\rho_b \cdot g \cdot D}{4 f_w \cdot K_w} \right) \cdot \left(1 - \exp\left(- \frac{4 f_w \cdot K_w \cdot L}{D} \right) \right) - \frac{\rho_b \cdot g \cdot D}{4 f_w \cdot K_w} \tag{10.3.8}$$

Here the exponential function can be represented by progression as follows:

$$\exp\left(\pm \frac{4 f_w \cdot K_w \cdot L}{D} \right) = 1 + \left(\pm \frac{4 f_w \cdot K_w \cdot L}{D} \right) + \frac{1}{2!} \left(\pm \frac{4 f_w \cdot K_w \cdot L}{D} \right)^2 + \cdots \tag{10.3.9}$$

Since L in the stress transmission test is relatively small, two terms at the beginning of the progression have been selected. Then Equation 10.3.7 and Equation 10.3.8 can be simplified as follow:

For Equation 10.3.7

$$\overline{P_z} = \left(1 + \frac{2 \cdot f_w \cdot K_w \cdot L}{D}\right) N_1 + \frac{L \rho_b \cdot g}{2} \qquad (10.3.10)$$

For Equation 10.3.8

$$\overline{P_z} = \left(1 - \frac{2 \cdot f_w \cdot K_w \cdot L}{D}\right) N_2 - \frac{L \rho_b \cdot g}{2} \qquad (10.3.11)$$

The deviation caused by the simplification to Equations 10.3.10 and 10.3.11 is estimated to be less than 5 percent for a 4.0cm height slug unit and 1.5 percent for a 2.0cm height slug unit for pipeline inner diameter of 60 mm, less than 2 percent for a 4.0cm height slug unit and 0.6 percent for a 2.0cm height slug unit for pipeline inner diameter of in 98 mm. The relation between the lateral stress and the axial stress within the slug unit is represented as follows:

$$\overline{P_r} = K_w \cdot \overline{P_z} \qquad (10.3.12)$$

The friction force between the slug unit and the wall of tube is given below:

$$F = \pi \cdot D \cdot L \cdot f_w \cdot \overline{P_r} \qquad (10.3.13)$$

The friction between the tube wall and slug unit and the weight of the slug unit contributing to the output of the force meter during the test are as follows.

$$F_{meter} = F + W_{slug} \qquad (10.3.14)$$

Combining Equations 10.3.12, 10.3.13 and 10.3.14 yields:

$$\overline{P_z} = \frac{F_{meter} - W_{slug}}{\pi \cdot D \cdot L \cdot f_w \cdot K_w} \tag{10.3.14}$$

Inserting Equation 10.3.14 into Equation 10.3.10 and Equation 10.3.11 yields:

$$K_w^2 + \left(\frac{2D \cdot N_1 + D \cdot L \cdot \rho_b \cdot g}{4 f_w \cdot L \cdot N_1} \right) K_w - \frac{(F_{meter} - W_{slug})}{2\pi \cdot L^2 \cdot f_w^2 \cdot N_1} = 0 \tag{10.3.15}$$

for the condition of the spring acting on the top of the slug unit, and:

$$K_w^2 - \left(\frac{2D \cdot N_1 - D \cdot L \cdot \rho_b \cdot g}{4 f_w \cdot L \cdot N_2} \right) K_w + \frac{(F_{meter} - W_{slug})}{2\pi \cdot L^2 \cdot f_w^2 \cdot N_2} = 0 \tag{10.3.16}$$

for the condition of the spring acting at the bottom of the slug unit.

Since the force acting on the top or bottom of the slug by the spring is obtained by measuring the length of the spring, N_1 and N_2 as the boundary conditions can be deduced from the following equations:

$$N_1 = \frac{K_{spring} \cdot (l_0 - l) + W_{plate}}{0.25\pi \cdot D^2} \tag{10.3.17}$$

$$N_2 = \frac{K_{spring} \cdot (l_0 - l) - W_{plate}}{0.25\pi \cdot D^2} \tag{10.3.18}$$

Here l_0 is the length of the spring at free condition and l is the length of spring with force acting on the porous plate. The weight of the porous plate is W_{plate} and the weight of the spring is neglected. Pipe diameter D, wall friction factor f_w, Length of the unit slug L, weight of slug W_{slug} are provided. F_{meter} is the output of the force meter. By solving the Equations 10.3.15 or 10.3.16, K_w can be achieved.

10.4 Procedure for Stress Transmission Coefficient Test

To conduct the stress transmission test with the test rig developed in this thesis, the steps can be summarised as follows:

(i) Turn on the power of the force meter and warm it up for fifteen minutes before the test is carried out. Clean the surface of the test section of the tube for the stress transmission test and be aware that powders or grease sticking on the tube wall surface may change the testing results. Start the multi-speed motor and select a suitable running speed for the sliding friction test. Prepare a certain amount of particles for the slug unit and ensure that a proper thickness of the slug unit is obtained for the stress transmission test

(ii) Undertake the setting-up procedure to prepare a slug unit for the stress transmission test on a test tube.

- Prepare a section of supporting pipe about 20 mm less than testing tube in diameter and 80 mm less than testing tube in length. Stand the test tube vertically on a table and put the supporting pipe inside the test tube. Put in the porous plate supporter of the testing rig over the supporting pipe inside the test tube.

- Lay the porous plate with an end cap and shaft on the porous plate supporter inside the test tube and then put the sample particles into the test tube. Even out the upper surface of the sample particles in the tube and then lay the upper porous plate over the sample particle. Cover the upper porous plate with the other porous plate supporter

- Put the spring on the shaft of the test rig and screw on the end cap to make the slug unit under a certain stress.

- Remove the upper porous plate supporter and then remove the supporting pipe standing inside the testing tube off. Remove the lower porous plate supporter at the bottom of the slug unit.

(iii) Adjust the length of the spring to obtain a certain value of axial stress on the slug unit. Adjust the location of the slug unit inside the testing tube standing on the table ready for test.

(iv) Start the multi-speed motor, move the slug unit inside the test tube and begin the stress transmission test. Ensure that the force meter, slug unit and pulling motor are on one line and record the data of the force meter.

(v) Change the spring length, push the slug unit back to a low part of the test tube and conduct the test under another axial stress. Record the data of force meter output

(vi) Change the amount of sample particles to adjust the height of the slug unit and repeat steps (I), (ii), (iii), (iv), (v).

10.5 Wedging Effect on the Stress Transmission Test

During the stress transmission tests, as the axial stress is reduced by adjusting the length of spring, the friction between the slug unit and the tube wall decreases. When the force acting on the porous plate caused by the spring reaches zero, the friction force from the force meter F_{meter} with weight of slug unit and the rig deducted is higher than friction caused by the weight of sample particles in the slug unit. This extra force during the stress transmission test is called the wedging force and the mechanism of the forming of the wedging force is shown in Figure 10.5.1. For example, with a 6.0

cm long slug unit in the 98mm tube, the wedging force may be 0.85 N compared to test unit weight of 3.93 N.

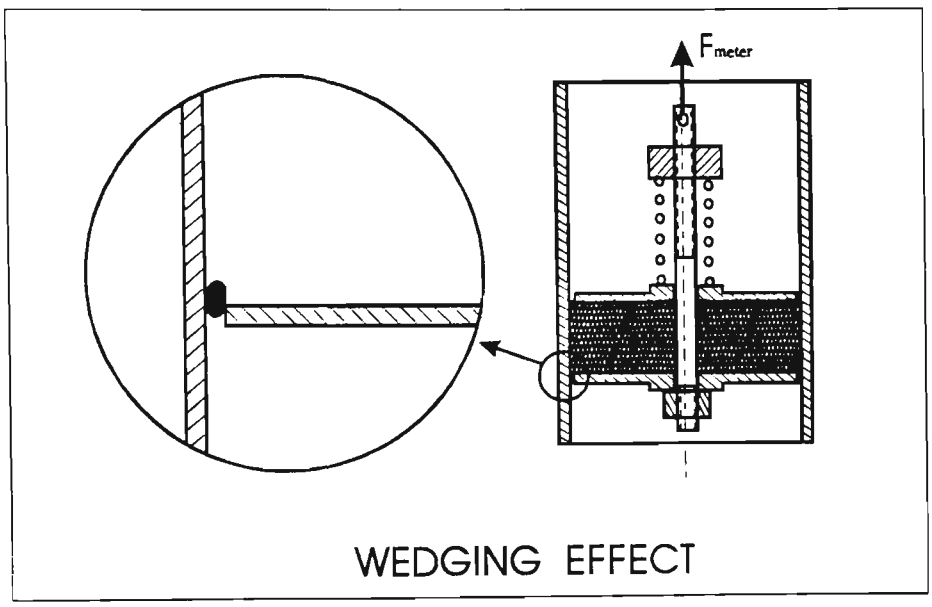

Figure 10.5.1 Configuration of the wedging effect

The particle properties and the design of the stress transmission rig are mainly attributed to the formation of wedging effect. As there is a particle diameter distribution and different shapes for the testing sample particles, the gap between the edge of the porous plate and the wall of the tube makes it difficult to prevent from the effect of wedging by some particles. To minimise the wedging effect, it is normally required to have the diameter of the sample particles equal and decrease the gap between the edge of the porous plate and the wall of the tube. The gap is difficult to determine because the edge of porous plate may contact the inner wall of the tube during the test if the gap is too small. Since the test is to measure the stress transmission coefficient, the friction force that is not caused by the axial stress transmission should be deducted during data processing.

10.6 Stress Transmission Test Results and Discussion

The stress transmission coefficient of plastic pellets with 897 kg/m^3 particle density, 4.7 mm in diameter and 566 kg/m^3 bulk density was tested with the stress transmission rig developed for this study. The heights of the slug unit were selected as 2.0 cm and 4.0 cm and the test tube inner diameters were 60.3 mm and 98.4 mm. The test results for different slug unit heights and tube inner diameters are shown in Figure 10.6.1.

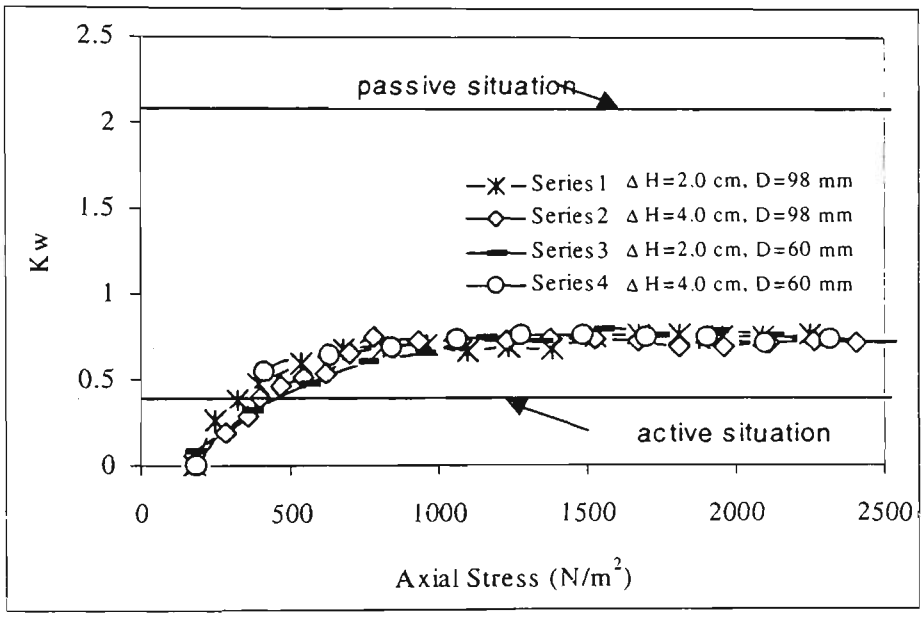

Figure 10.6.1 Test results of K_w with respect to axial stress

The test results of stress transmission coefficient in Figure 10.6.1 show that K_w is kept constant for a certain particle material when the axial stress is higher than a certain value. When the axial stress is lower than a certain value, it will not create any stress in the lateral direction and the value of K_w is zero. Between the two certain values mentioned, K_w varies with the axial stress and increases very quickly as the axial stress is increased. The test results of stress transmission coefficient in Figure 10.6.1 also show that pipe diameter will not influence the value of K_w and the height of slug unit within a certain range will not change the test results.

CHAPTER 11: CONTRIBUTION OF WEIGHT OF SLUG TO WALL STRESS IN HORIZONTAL PIPE

11.1 Introduction

In force balance analysis for the slug moving through a horizontal conveying pipeline, it is generally accepted that the friction resistance between the moving slug and the pipe wall created by the weight of the slug itself should not be neglected in determining the total resistances to the moving slug. But the significance of the weight of the slug itself to the total pressure drop across the slug still lacks positive assessment. In modelling the pressure gradient for dense phase pneumatic conveying of solid materials, the approach for determining the contribution of the weight of the slug to the total friction force on the pipe wall follows the method first proposed by Wilson et al [103] and then adopted by Konrad et al [49] as hydrostatic pressure. It was also assumed that the stress on the pipe wall caused by the weight of slug can be added to that caused by axial stress based on Janssen analysis. The radial stress caused by the weight of the slug was represented by the equation below (see Figure 11.1.1):

$$P_r = \left(1.0 + \cos\theta\right) \cdot \frac{D}{2} \cdot g \cdot \rho_b \qquad (0 \le \theta \le 2\pi) \qquad (11.1.1)$$

Where P_r is the normal stress on the wall due to hydrostatic pressure.

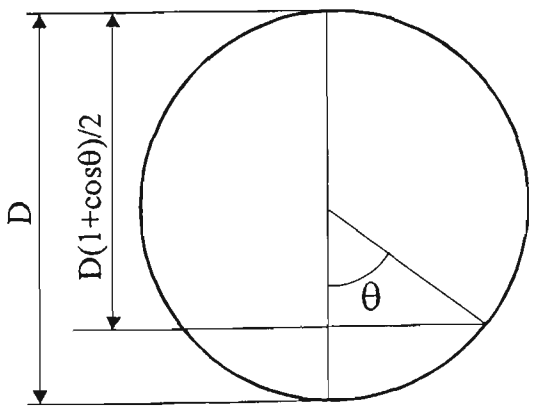

Figure 11.1.1 Cross-section of a slug

The friction caused by the weight of the slug per unit length in the horizontal pipeline was integrated around the circle of the intersection of the conveying pipeline and represented by the equation:

$$F = \int_0^{2\pi} \frac{D}{2} \cdot g \cdot f_w \cdot \rho_b \cdot \left(1.0 + \cos\theta\right) \cdot \frac{D}{2} d\theta$$

$$= \frac{\pi \cdot g \cdot f_w \cdot \rho_b \cdot D^2}{2} \qquad (11.1.2)$$

However, the radial stress acting on the pipe wall by gravity of particles is actually:

$$P_r = D \cdot g \cdot \rho_b \cdot \cos^2\theta \quad \left(-\frac{\pi}{2} \le \theta \le \frac{\pi}{2}\right) \qquad (11.1.3)$$

The friction force caused by the weight of slug per unit length in the horizontal conveying pipeline can be integrated along the lower half circle of the cross-section of the conveying pipeline as shown below:

$$F = \int_{-\frac{\pi}{2}}^{\frac{\pi}{2}} D \cdot g \cdot f_w \cdot \rho_b \cdot \cos^2\theta \cdot \frac{D}{2} d\theta$$

$$= \frac{\pi \cdot g \cdot f_w \cdot \rho_b \cdot D^2}{4} \qquad (11.1.4)$$

Comparison between Equations 11.1.2 and 11.1.4 shows that the weight of slug in the horizontal pipeline when treated as hydrostatic pressure is twice as that when treated as weight of particle contact in the pipeline.

The conclusion that gravity of a slug creates a hydrostatic pressure on the wall of a horizontal conveying pipeline is widely accepted by researchers and adopted in their models for low-velocity slug flow pressure prediction without any experimental

approval. This can be attributed to the fact that compared to the total resistance forces acting on the moving slug, the friction caused by the weight of the slug itself is relatively small especially when the slug velocity is relatively high. With the stress transmission rig developed in this thesis, an opportunity is provided to investigate the contribution of the weight of the slug to the wall stress in the conveying pipeline experimentally by comparing the wall friction acting on the slug unit in a horizontal and a vertical tube.

11.2 Analysis of Force Balance of a Slug Unit

Analysis of the force balance of a slug unit in the vertical tube is conducted in Chapter Ten and represented by Equations 10.3.7 and 10.3.8 and need not be repeated here. An analysis of the forces on a slug unit in a horizontal tube is sketched in Figure 11.2.1.

From a force equilibrium analysis of the element slice in Figure 11.2.1 in an axial direction, the following differential equation may be derived for stress on the wall due to the weight of the slug treated as hydrostatic pressure:

$$\frac{\pi}{4}\cdot D^2\cdot\left[(P_z+dP_z)-P_z\right]-\frac{\pi}{2}\cdot D^2\cdot\rho_b'\cdot g\cdot f_w\cdot d_z-\pi\cdot D\cdot d_z\cdot P_z\cdot K_w\cdot f_w=0 \quad (11.2.1)$$

For stress on the wall due to the weight of the slug treated as that created by piling particles:

$$\frac{\pi}{4}\cdot D^2\cdot\left[(P_z+dP_z)-P_z\right]-\frac{\pi}{4}\cdot D^2\cdot\rho_b'\cdot g\cdot f_w\cdot d_z-\pi\cdot D\cdot d_z\cdot P_z\cdot K_w\cdot f_w=0 \quad (11.2.2)$$

Because of the weight of part of test rig added to the unit slug, it is assumed that:

$$\frac{\pi}{4}\cdot D^2\cdot g\cdot\rho_b'=\frac{\pi}{4}\cdot D^2\cdot g\cdot\rho_b+W_{rig} \quad (11.2.3)$$

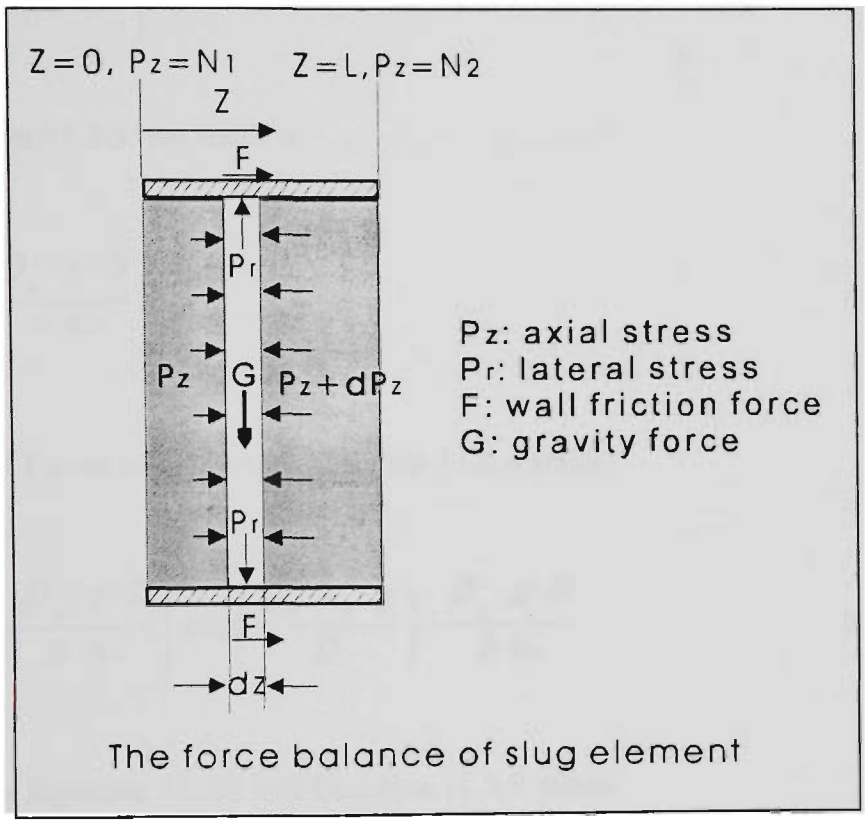

Figure 11.2.1 Analysis of forces on element of slug

Solving Equation 11.2.1 yields:

$$P_z = c \cdot \exp\left(\frac{4 f_w \cdot K_w \cdot Z}{D}\right) - \frac{\rho_b' \cdot g \cdot D}{2K_w} \tag{11.2.4}$$

Solving Equation 11.2.2 yields:

$$P_z = c \cdot \exp\left(\frac{4 f_w \cdot K_w \cdot Z}{D}\right) - \frac{\rho_b' \cdot g \cdot D}{4K_w} \tag{11.2.5}$$

Here the spring force acting at top or front is considered as the boundary condition such that if Z=0, then $P_z=N_1$, for Equation 11.2.4 yielding:

$$c = \left(N_1 + \frac{\rho_b' \cdot g \cdot D}{2 \cdot K_w} \right) \tag{11.2.6}$$

For Equation 11.2.5, the result is:

$$c = \left(N_1 + \frac{\rho_b' \cdot g \cdot D}{4 \cdot K_w} \right) \tag{11.2.7}$$

Insertion of Equation 11.2.6 into Equation 11.2.4 yields:

$$P_z = \left(N_1 + \frac{\rho_b' \cdot g \cdot D}{2 \cdot K_w} \right) \cdot exp\left(\frac{4 f_w \cdot K_w \cdot Z}{D} \right) - \frac{\rho_b' \cdot g \cdot D}{2 \cdot K_w} \tag{11.2.8}$$

Insertion of Equation 11.2.7 into Equation 11.2.5 yields:

$$P_z = \left(N_1 + \frac{\rho_b' \cdot g \cdot D}{4 \cdot K_w} \right) \cdot exp\left(\frac{4 f_w \cdot K_w \cdot Z}{D} \right) - \frac{\rho_b' \cdot g \cdot D}{4 \cdot K_w} \tag{11.2.9}$$

Equations 11.2.8 and 11.2.9 are for calculating the axial stress within the slug unit at a specific slice within the slug unit. The average of the P_z for the slug unit can be obtained by integrating the P_z along L and divided by L. Integrating Equations 11.2.8 and 11.2.9 yields:

$$\overline{P_z} = \frac{D}{4 f_w \cdot K_w \cdot L} \left(N_1 + \frac{\rho_b' \cdot g \cdot D}{2 \cdot K_w} \right) \cdot \left(exp\left(\frac{4 f_w \cdot K_w \cdot L}{D} \right) - 1 \right) - \frac{\rho_b' \cdot g \cdot D}{2 \cdot K_w} \tag{11.2.10}$$

$$\overline{P_z} = \frac{D}{4 f_w \cdot K_w \cdot L}\left(N_1 + \frac{\rho_b' \cdot g \cdot D}{4 \cdot K_w}\right)\cdot\left(\exp\left(\frac{4 f_w \cdot K_w \cdot L}{D}\right) - 1\right) - \frac{\rho_b' \cdot g \cdot D}{4 \cdot K_w} \qquad (11.2.11)$$

For the slug unit, the wall friction can be given as follow:

$$F_{friction} = \pi \cdot D \cdot L \cdot f_w \cdot K_w \cdot \overline{P_z} \qquad (11.2.12)$$

Insertion of Equations 11.2.10 and 11.2.11 into 11.2.12 yields:

$$F_{friction} = \frac{\pi \cdot D^2}{4}\left(N_1 + \frac{\rho_b' \cdot g \cdot D}{2 \cdot K_w}\right)\cdot\left(exp\left(\frac{4 f_w \cdot K_w \cdot L}{D}\right) - 1\right) - \frac{\pi \cdot \rho_b' \cdot g \cdot f_w \cdot D^2 \cdot L}{2} \qquad (11.2.13)$$

For piling solid materials:

$$F_{friction} = \frac{\pi D^2}{4}\left(N_1 + \frac{\rho_b' \cdot g \cdot D}{4 \cdot K_w}\right)\cdot\left(exp\left(\frac{4 f_w \cdot K_w \cdot L}{D}\right) - 1\right) - \frac{\pi \cdot \rho_b' \cdot g \cdot f_w \cdot D^2 \cdot L}{4} \qquad (11.2.14)$$

Equations 11.2.13 and 11.2.14 are used for the calculation of the total wall friction of the whole slug unit moving in the tube with different axial stresses. Comparison of two approaches to treating the weight of the slug is presented in Figure 11.2.2. It is shown that as the axial stress increases, the difference between the friction forces in the two approaches for treating the slug weight becomes less significant. When the axial stress is lower, corresponding to the slug moving slowly in the horizontal conveying pipeline, the difference in wall friction made by the approaches for slug weight

treatment is not negligible. The better approach for treating the slug weight will show the real contribution of the weight of the slug unit to the wall friction. This should be verified under low axial stress within the slug unit according the comparison in Figure 11.2.2.

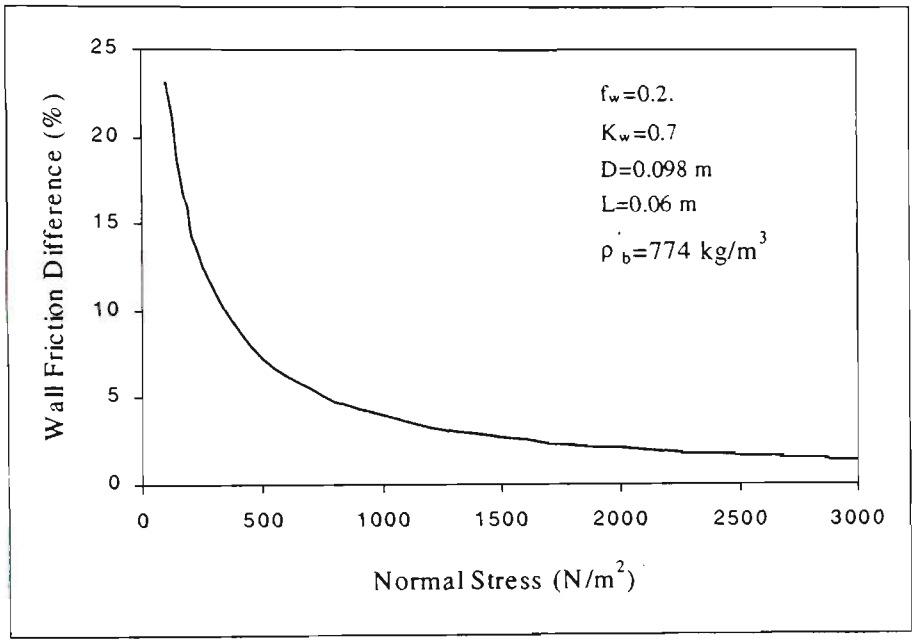

Figure 11.2.2 Comparison between Equations 11.2.13 and 11.2.14

11.3 Test of the Contribution of Slug Weight to Wall Friction

To measure the wall friction force of the slug unit effectively, it is suggested that the axial stress added by the spring be designed to be very low. This will allow the wall friction caused by the weight of the slug to be expressed at the same time as the axial stress, which should be high enough to keep the shape of the slug stable within the tube especially for the horizontal tube. According to Chapter Ten, K_w will be zero when the axial stress is kept less than 200 N/m^2. Hence 1.5 N force from the spring is added to the porous plate in order to prevent the slug unit from breaking through the horizontal tube with 98 mm ID.

For the slug unit in the vertical tube with the axial force due only to the weight of the porous plate and particles (spring fully extended), the output of the force meter while the slug unit is moving upward should be equal to the weight of the slug unit plus the force caused by the wedging effect. Since the weight of the slug unit is given, the force caused by wedging effect can be obtained by deducting the weight of the slug unit from the output of the force meter that is shown in Table 11.3.1.

Table 11.3.1: The results of sliding friction tests on a 6.0 cm slug unit in a vertical tube

The weight of slug unit = 3.93 (N), Vertical sliding test results								
Reading No.	1	2	3	4	5	6	7	8
Force meter (N)	4.70	4.75	4.63	4.64	4.74	4.80	4.61	4.72
Force of wedging effect (N)	0.77	0.82	0.70	0.71	0.81	0.87	0.68	0.79
The average friction force caused by wedging effect =0.77 (N)								

A slug unit sliding through a horizontal tube with an axial force less than 1.5 N is caused by the spring acting on the front. The output of the force meter should be equal to the friction between the slug unit and the pipe wall caused by the gravity of the slug unit plus the force caused by the wedging effect. The results of sliding friction tests on a 6.0 cm slug unit through a horizontal tube are presented in Table 11.3.2. According to the test results in Table 11.3.2, it appears that the contribution of slug weight to wall friction is not properly recognised by hydrostatic approach which has been accepted by some researchers since Konard et al [49] employed it in his model for pressure

prediction of slug flow. The approach of treating the slug in the horizontal conveying pipeline as weight of particle contact seems to be more reasonable. It is necessary to mention that sliding friction tests with very low axial stress must be conducted very carefully. The porous plates of the slug unit may easily meet the pipe wall, and the axes of the slug unit and the tube may no longer be paralleled so that inaccurate or wrong testing results ensue.

Table 11.3.2: The results of sliding friction tests on a 6.0 cm slug unit in a horizontal tube

The weight of slug unit = 3.93 (N). Horizontal sliding test results.

The average friction force caused by wedging effect =0.77 (N) (assumed from vertical tests)

Hydrostatic approach friction=2×3.93×0.2=1.57 (N):

Weight of particle contact approach friction=3.93×0.2=0.79 (N)

Reading No.	1	2	3	4	5	6	7	8
Force meter (N)	1.70	1.65	1.68	1.56	1.60	1.63	1.58	1.71
Force meter output deducting wedging effect (N)	0.93	0.88	0.91	0.79	0.83	0.86	0.81	0.94

CHAPTER 12: MODEL FOR PRESSURE DROP PREDICTION OF LOW-VELOCITY SLUG-FLOW

12.1 Introduction

Modelling the pressure drop for low-velocity slug-flow pneumatic conveying of granular materials is pursued through a wide range of approaches and normally begins with some simple assumptions. In general it is found that the model employing the principles of powder mechanics performs best for low-velocity slug-flow behaviour [48]. For Konrad-like models, the following relationships must be established/used:

(i) The relationship between the axial stress and lateral stress along the slug.

(ii) The relationship between frontal stress and other model parameters such as slug velocity, the thickness of the layer.

(iii) The relationship between the thickness of the stationary layer and model parameters such as slug velocity.

(iv) The relationship between the slug velocity and superficial air velocity.

(v) The relationship between friction resistance and the weight of slug.

The basic concept that an axial stress can transmit in a lateral direction and create a lateral stress to the moving slug was first employed in establishing the model for the pressure drop prediction of low-velocity slug-flow pneumatic conveying of granular materials by Konrad et al in 1980 [49]. This was done according to the principles of powder mechanics and provides an effective approach for the analysis of the force balance within a moving slug through a horizontal conveying pipeline. Actually K_w that is deduced from the relationship between the Mohr failure envelope and the wall yield locus of the bulk solid does not represent the real relationship between lateral wall stress and axial stress. This is further confirmed by the modification of Mi [63,

64]. Mi had modified the correlation for K_w by measuring the lateral stress on the pipe wall of the slugs of plastic pellet, wheat and barley passing through the conveying pipeline. However, the axial stress or frontal stress has not measured experimentally but was calculated from the equation, which is found later to be incorrect. Though the concept of K_w was proposed by Konrad et al in 1980 and modified by Bo Mi in 1994, the true relationship between the axial stress and lateral stress within a slug has not been well explored.

The relationship between frontal stress and other model parameters is also one of the most important equations of pressure drop prediction for low-velocity slug-flow pneumatic conveying. In both the Konrad and Mi's models, the frontal stress is only created from a momentum balance of stationary layer in front of a slug. A simple test in this chapter will confirm that not only the momentum balance of the stationary layer in front of a slug creates a frontal stress, the stationary layer itself also creates a stress on the front of a slug as it resists the trend of movement.

The relationship between the thickness of the stationary layer and model parameters was established by the application of a gas/liquid analogy in Konrad's model and was established by experiment in Mi's model. Two equations for predicting the thickness of a stationary layer are the same while the meaning is different because the slug velocity is equal to the particle velocity within a slug in Mi's model.

The relationship between slug velocity and air velocity was created by application of the Ergun Equation in Konrad's model [49]. Pan endeavoured to establish this relationship by experiment for irregular granular materials [79]. An empirical correlation relating slug velocity and air velocity was put forward by regressing the

experiment results of pneumatic conveying of plastic pellets, wheat and barley in Mi's model.

The relationship between friction resistance and the weight of slug was incorrectly established in both Konrad and Mi's models and this matter has been fully discussed in Chapter Eleven.

The original nature of the model established in this thesis for pressure drop prediction in low-velocity slug-flow pneumatic conveying of granular materials through a horizontal pipeline includes the following aspects which will be fully addressed and explored in this chapter:

(i) K_w is measured through the stress transmission rig developed for this study reported in this thesis.

(ii) The frontal stress of a slug includes the forces created by the momentum balance of the stationary layer in front of a slug and the force balance of the stationary layer that resists the trend of movement.

(iii)The relationship between wall friction resistance and the weight of a slug is proved by experiment.

12.2 Axial Stress at Front of a Slug Caused by Force Balance of Stationary Layer

When the slug is moving through the conveying pipeline, it is generally accepted that the moving slug picks up the stationary layer that becomes part of the slug in front and deposits the same amount of particles behind, keeping the length of slug constant. Actually the detail of the picking up process and the force balance involved in the picking up has not been well investigated so far, so the front stress caused by the static

friction of the stationary layer in front of a slug to resist the trend of movement has never been considered in analysis of the force balance of the moving slug. As a result, the predictions of former models based on the principles of powder mechanics usually are lower than those from experiment. To make the equations of the model fit the experimental results, the stress transmission factor K_w that was assumed to be higher than its real value as that for the passive situation had been accepted [49].

To constitute a concept of the frontal stress caused by static friction of a stationary layer in front of a slug resisting the trend of movement, a simple test with a 60.3 mm ID glass tube was conducted as shown in Figure 12.3.1.

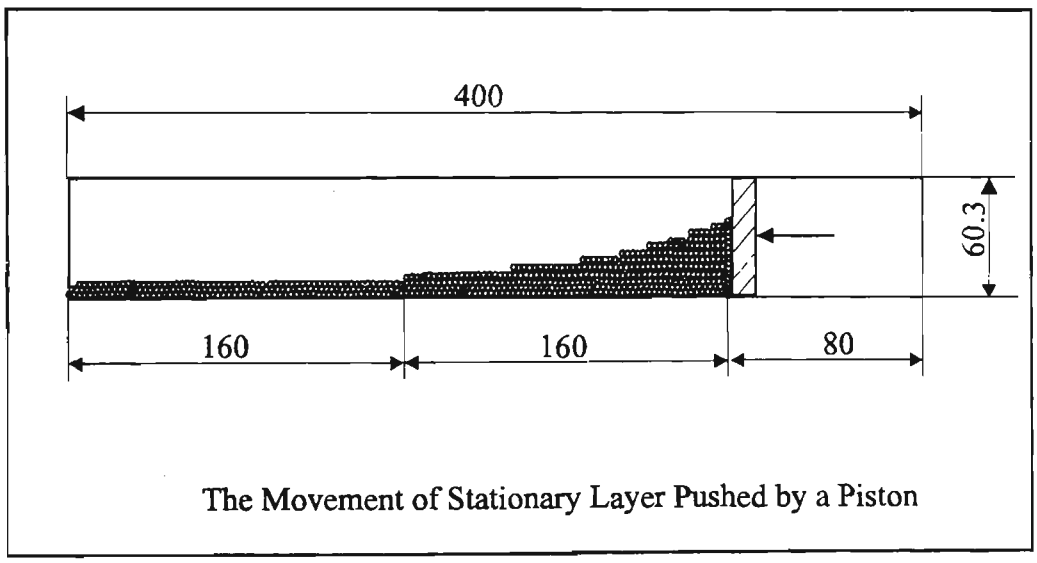

Figure 12.3.1 Configuration for testing static friction force of stationary layer in front of a slug to resist movement

A quantity of plastic pellet with 4.7 mm particle diameter and 897 kg/m^3 particle density was installed in front of the piston to make the stationary layer on the bottom of the tube occupy 10 percent area of the intersection of the tube. Pushing the piston forward from one side of the tube very slowly until the particles at the end of other side of the tube tend to move, it was found that about 160 mm of the stationary layer kept

the same appearance and about 160 mm of the stationary layer increased in thickness as shown in Figure 12.3.1. The significance of the tests is that the force from the piston was transferred to the front of the stationary layer at the end or that the particles in the stationary layer far from the piston were involved in creating a resistance force to the piston. Hence for a moving slug, the frontal stress is not only created by the momentum balance of the stationary layer in front of a slug for accelerating the particles, but also by the stationary layer in front of slug as it resists the movement trend.

As shown in Figure 12.3.2, the process of picking up the stationary layer in front of the moving slug can be separated into two steps. The first step is to raise the particles at the stationary layer up so they can reach the top of the pipeline; the second step is to accelerate the particles to have the same velocity as that in the moving slug, which will be discussed in detail later in this chapter.

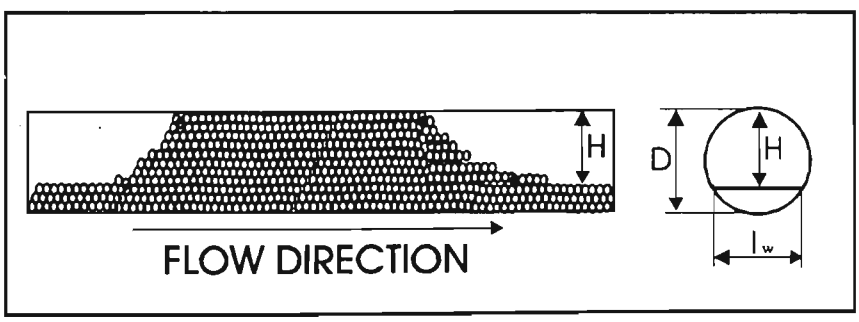

Figure 12.3.2 Configuration of a moving slug

The force to raise up the particles from the surface of the stationary layer to the top of pipeline can be considered to be equal to the lateral stress caused by axial stress transmitted from front surface of moving slug. The relationship between these two stresses is given by the equation below:

$$\sigma_{f1} \cdot K_w = \rho_b \cdot g \cdot H \qquad (12.2.1)$$

The width of the upper surface of the stationary layer within the cross-sectional pipeline area is as follow [67]:

$$l_w = [4 \cdot \alpha \cdot (1-\alpha)]^{1/2} \cdot D \qquad (12.2.2)$$

The relation between H and α the ratio of the area of stationary layer to the area of intersectional pipeline is:

$$H = 0.5 \cdot \left(D - \sqrt{D^2 - l_w^2}\right) \qquad \text{for the condition that } \alpha \le 0.5 \qquad (12.2.3)$$

$$H = 0.5 \cdot \left(D + \sqrt{D^2 - l_w^2}\right) \qquad \text{for the condition that } \alpha \ge 0.5 \qquad (12.2.4)$$

Insertion of Equations 12.2.4, 12.2.3 into Equation 12.2.1 yields:

$$\sigma_{f1} = \rho_b \cdot g \cdot \left(D \pm \sqrt{D^2 - l_w^2}\right) / 2.0 \cdot K_w \qquad (12.2.5)$$

Equation 12.2.5 is for the prediction of the axial stress at the front of the slug caused by the stationary layer in front of slug as it resists the trend of movement.

12.3 Axial Stress at the Front of the Slug Caused by Momentum Balance

When the slug is moving steadily along the horizontal pipeline picking up the stationary layer in front of it and depositing the same amount of particles behind, the velocity of the slug or the front surface of the slug is not equal to the velocity of the particle within the slug. The particle velocity within the slug U_p and the slug velocity U_s have a relationship based on the equation of continuity and the uniformity of the bulk density:

$$U_p = (1-\alpha)\cdot U_{slug} \tag{12.3.1}$$

At the front of the slug, the stationary layer is pushed by the slug and attains a certain momentum. According to the theory of momentum balance, the following equation is obtained:

$$F\cdot\Delta t = \Delta(m\cdot U_p) \tag{12.3.2}$$

Here the force acting at the front of slug can be replaced by axial stress σ_f at the slug front multiplied by the intersection area of the pipeline yields:

$$F\cdot\Delta t = \sigma_{f2}\cdot A\cdot\Delta t \tag{12.3.3}$$

The amount of stationary layer achieving the particle velocity U_p and becoming a part of the slug as the result of momentum balance yields:

$$\begin{aligned}\Delta(m\cdot U_p) &= U_p\cdot(\Delta m)\\ &= (\alpha\cdot A\cdot\rho_b\cdot U_{slug}\cdot\Delta t)\cdot U_p\end{aligned} \tag{12.3.4}$$

Insertion of Equations 12.3.1, 12.3.3 and 12.3.4 into Equation 12.3.2 yields:

$$\sigma_{f2} = \alpha\cdot(1-\alpha)\cdot\rho_b\cdot U_{slug}^2 \tag{12.3.5}$$

Equation 12.3.5 is to estimate axial stress at the front of the slug for accelerating the particles from stationary layer. It is different from that of Bo Mi's model for the pressure drop prediction in low-velocity pneumatic conveying. Hence the total axial stress at the front of slug may be given as:

$$\sigma_f = \sigma_{f1} + \sigma_{f2}$$

$$= \rho_b \cdot g \cdot \left(D \pm \sqrt{D^2 - l_w^2}\right) / 2.0 \cdot K_w + \alpha \cdot (1.0 - \alpha) \cdot \rho_b \cdot U_{slug}^2 \qquad (12.3.6)$$

12.4Thickness of the Stationary Bed

The application of gas/liquid analogy horizontal dense phase conveying suggests that [103]:

$$U_{slug} = U_p + 0.542\sqrt{g \cdot D} \qquad (12.4.1)$$

Combining this with Equation 12.3.1, and eliminating U_{slug} gives:

$$\alpha = 1/\left(1 + U_p/\left(0.542\sqrt{gD}\right)\right) \qquad (12.4.2)$$

Eliminating U_p gives:

$$\alpha = 0.542 \cdot \sqrt{g \cdot D} / U_{slug} \qquad (12.4.3)$$

Note: Equation 12.4.3 may induce an incorrect result if U_{slug} is less than $0.542\sqrt{g \cdot D}$ (i. e. $\alpha > 1.0$) for low air mass flow rates. As a result, the pressure drop prediction from this model may not suitable for the operation close to Boundary A and some modification to Equation 12.4.3 to make up this deficit is suggested for future work.

12.5 Friction Force Caused by the Weight of Slug

The force of slug weight acting on the pipe wall has been addressed in detail in Chapter Eleven. It is given by the equation below:

$$F_{weight} = \frac{\pi}{4} \cdot f_w \cdot \rho_b \cdot g \cdot L_s \cdot D^2 \qquad (12.5.1)$$

12.6 Wall Friction Caused by Axial Stress Transmission

For solid materials in a vertical silo, each element slice of thickness of the solid materials adds the force of its weight to the element below and the configuration of the axial stress is shown in Figure 12.6.1.

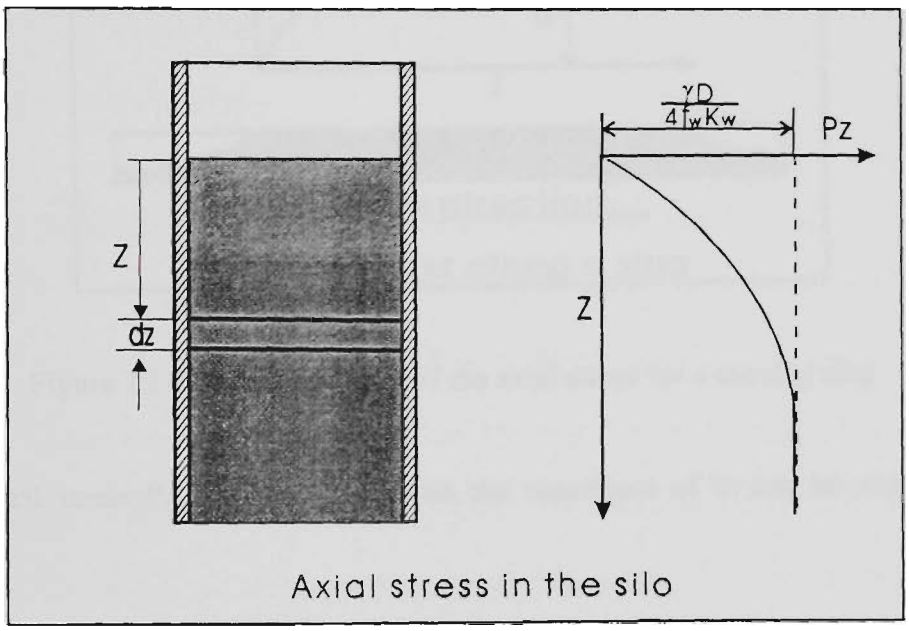

Figure 12.6.1 Configuration of the axial stress in a silo

According to the Janssen Equation [37], the normal stress P_z along the silo can be expressed by the equation:

$$P_z = \frac{\gamma_b \cdot D}{4 \cdot f_w \cdot K_w}\left(1 - e^{\frac{-4 \cdot f_w \cdot K_w \cdot Z}{D}}\right) \qquad (12.6.1)$$

Where γ_b specific weight of the bulk solids.

For a slug moving at an even velocity (without acceleration), having the same thickness of layer in front and behind, with the air penetrating through its voidage and adding drag force to each single particle, eliminating the friction caused by the weight

of the bulk solid, the situation can be analogous to the gravity acting on each single particle at the silo as shown in Figure 12.6.2.

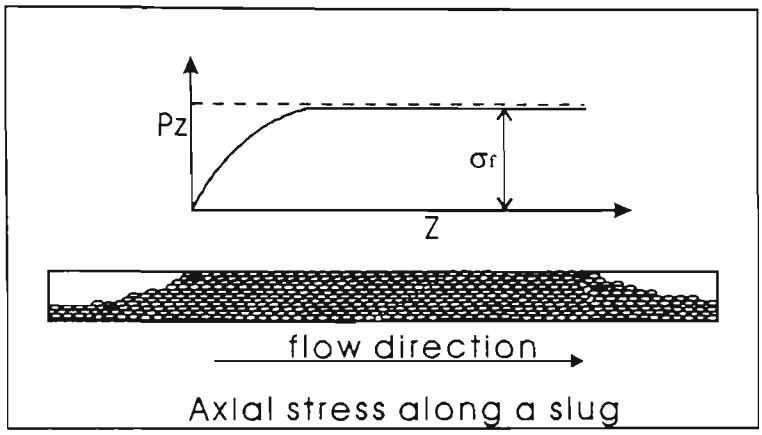

Figure 12.6.2 Configuration of the axial stress for a moving slug

The normal stress P_z along the slug with the maximum of σ_f can be expressed as below:

$$P_z = \sigma_f \cdot \left(1 - e^{\frac{-4 \cdot f_w \cdot K_w \cdot Z}{D}} \right) \tag{12.6.2}$$

Insertion of Equation 12.3.6 into Equation 12.6.2 yields:

$$P_z = \left(\rho_b \cdot g \cdot \left(D \pm \sqrt{D^2 - l_w^2} \right) \Big/ 2.0 \cdot K_w + \alpha \cdot (1-\alpha) \cdot \rho_b \cdot U_{slug}^2 \right) \cdot \left(1 - e^{\frac{-4 \cdot f_w \cdot K_w \cdot Z}{D}} \right) \tag{12.6.3}$$

Then, the wall friction caused by the lateral stress transmitted from axial stress is:

$$F_{lateral} = \int_0^{L_s} \pi \cdot D \cdot f_w \cdot K_w \cdot P_z \cdot dz \tag{12.6.4}$$

Since $L_s >> D$, insertion of Equation 12.6.3 into 12.6.4 yields:

$$F_{lateral} = \pi \cdot D \cdot f_w \cdot K_w \cdot [\rho_b \cdot g \cdot \left(D \pm \sqrt{D^2 - l_w^2}\right) / 2.0 \cdot K_w + \alpha \cdot (1.0 - \alpha) \cdot \rho_b \cdot U_{slug}^2] \cdot \left(L_s - \frac{D}{4 \cdot f_w \cdot K_w}\right) \tag{12.6.5}$$

Note: for some solid materials with a high value of $D/(4 \cdot f_w \cdot K_w)$, Equation 12.6.5 may cause incorrect results.

12.7 Total Resistant Force for the Moving Slug along the Horizontal Pipeline

For a single slug moving along a horizontal pipeline, picking up the stationary layer at the bottom of the pipe and depositing the same amount of the solids as the stationary layer behind, the driving force comes from the drag of air penetrating the slug and is balanced by a resistance which has three parts. The first part comes from the friction caused by the weight of the slug, the second part is the front stress caused by the stationary layer in front of the slug and the third part is the friction force caused by the axial stress along the slug. So the total resistance to a moving slug can be expressed by the following equation:

$$F_{slug} = F_{weight} + F_{lateral} + \sigma_f \cdot A \tag{12.7.1}$$

Insertion of Equations 12.3.6, 12.5.1 and 12.6.5 into Equation 12.7.1 yields:

$$F_{slug} = \pi \cdot D \cdot f_w \cdot K_w \cdot L_s \cdot [\rho_b \cdot g \cdot \left(D \pm \sqrt{D^2 - l_w^2}\right) / 2.0 \cdot K_w + \alpha \cdot (1 - \alpha) \cdot \rho_b \cdot U_{slug}^2] + \frac{\pi}{4} \cdot f_w \cdot \rho_b \cdot g \cdot L_s \cdot D^2 \tag{12.7.2}$$

For low-velocity slug-flow pneumatic conveying of particle materials at a certain solid mass flow rate and air mass flow rate through the pipeline with a length L_t, the total length of the slugs L_{st} is given by the following equation according to the mass balance within the conveying pipeline [63]:

$$L_{st} = \frac{m_s \cdot L_t}{A \cdot (1-\alpha) \cdot \rho_b \cdot U_{slug}} \tag{12.7.3}$$

Hence the number of moving slugs in the conveying pipeline for conveying with a certain solid mass flow rate and air mass flow rate is equal to the total length of the slugs divided by the length of a single slug and is given by the equation below:

$$N_{slug} = \frac{L_{st}}{L_s} = \frac{m_s \cdot L_t}{A \cdot (1-\alpha) \cdot \rho_b \cdot L_s \cdot U_{slug}} \tag{12.7.4}$$

As a result, the total pressure drop caused by the moving slugs in the horizontal conveying pipeline is equal to the pressure drop of a single slug multiplied by the number of slugs contained the conveying pipeline and is as follow:

$$\begin{aligned} \Delta P \cdot A &= N_{slug} \cdot F_{slug} \\ &= \{\pi \cdot D \cdot f_w \cdot K_w \cdot [\rho_b \cdot g \cdot \left(D \pm \sqrt{D^2 - l_w^2}\right) / 2.0 \cdot K_w + \alpha \cdot (1-\alpha) \cdot \rho_b \cdot U_{slug}^2] \\ &\quad + \frac{\pi}{4} \cdot f_w \cdot \rho_b \cdot g \cdot D^2\} \left\{ \frac{m_s \cdot L_t}{A \cdot (1-\alpha) \cdot \rho_b \cdot U_{slug}} \right\} \end{aligned} \tag{12.7.5}$$

Equation 12.7.5 shows that the total pressure drop across a horizontal conveying pipeline for low-velocity slug-flow is independent of the length of a single slug.

12.8 Relationship between Pressure Drop and U_p or U_f by Ergun Equation

At any location of the pipeline across the intersection, when the solid-air two-phase flow is in steady state, irrespective of the steady incompressible flow or steady compressible flow, the volumetric flow through a cross-section should be constant at one location and not change with time. Hence the following equation can be achieved:

$$\frac{m_f}{A \cdot \rho_f} = (1-\varepsilon) \cdot U_p + \varepsilon \cdot U_{gp} \tag{12.8.1}$$

U_p is the particle velocity and U_{gp} is the interstitial air velocity. The superficial slip velocity for the Ergun Equation is given by the equation below:

$$(U_{gp} - U_p) \cdot \varepsilon = U_{slip} \tag{12.8.2}$$

Insertion of Equation 12.8.2 into Equation 12.8.1 yields:

$$\frac{m_f}{A \cdot \rho_f} = U_p + U_{slip} \tag{12.8.3}$$

To establish the relationship between the pressure drop and air velocity, the Ergun Equation is applied and expressed as follow [20, 21]:

$$\frac{\Delta P}{\Delta L} = 150 \frac{(1-\varepsilon)^2 \cdot \eta \cdot U_{slip})}{\varepsilon^3 \cdot d_p^2} + 1.75 \frac{(1-\varepsilon) \cdot \rho_g \cdot U_{slip}^2}{\varepsilon^3 d_p} \tag{12.8.4}$$

For irregular shape bulk materials, since the d_p is hard to measure and the voidage of the bulk materials is constant, Equation 12.8.4 can be transformed into the equation as follows:

$$\frac{\Delta P}{\Delta L} = C_1 \cdot U_{slip} + C_2 \cdot \rho_g \cdot U_{slip}^2 \tag{12.8.4}$$

Constant C_1 and C_2 can be determined experimentally by measuring the pressure drop across a packed bed filled with the materials and the air mass flow rate [79].

12.9 Procedure for Pressure Drop Prediction in the Horizontal Pipeline

For low-velocity slug flow pneumatic conveying of granular materials, particle properties such as particle density ρ_p, particle diameter d_p, bulk voidage ε, stress transmission factor K_w, pipeline properties such as pipe diameter D, pipe wall sliding friction factor f_w and operating condition such as solid mass flow rate m_s and air mass flow rate m_f should be given and the procedure for calculating the pressure across a horizontal conveying pipeline is given below:

(i) Assume an initial value for U_{slug}.

(ii) Calculate ΔP using Equations 12.4.3 and 12.7.5.

(iii) Calculate U_{slug} using Equations 12.4.1, 12.8.3 and 12.8.4.

(iv) Compare U_{slug} calculated with U_{slug} assumed. Using calculated U_{slug} instead of U_{slug} assumed, repeat step (ii) and (iii) onwards until convergence is achieved.

Using above procedure, the pressure drop across a horizontal pipeline with certain operating condition can be predicted. For a long conveying pipeline, it can be separated into certain number of segments and pressure drop prediction for the whole pipeline can be conducted from the outlet to inlet step by step.

12.10 Comparison of Experimental and Predicted Pressure Drop Results

Comparison of the model prediction of pressure drop across a horizontal conveying pipeline 21m in length with the experimental results of low-velocity slug-flow pneumatic conveying of plastic pellets through the test rig described in Chapter Four is

shown in Figures 12.10.1 and 12.10.2. The input data required for the model include the particle diameter (4.7 mm), the particle density (897 kg m^{-3}), the voidage of the bulk solid (0.391), the coefficient of friction between the particles and wall (0.2), the coefficient of particle internal friction (0.5) and pipeline diameters (98 mm; 60.3 mm). The agreements between the modelling results and the experimental data are very good both for the 60.3 mm and 98 mm stainless steel pipelines and better for 98mm pipeline. It is necessary to mention that the model established in this thesis provides more accurate predictions for the pressure drop of low-velocity slug-flow pneumatic conveying. However it is not suitable for the operations that are very close to Boundary A in the state diagram and for the solid materials with a high value of $D/(4 \cdot f_w \cdot K_w)$ as indicated previously in Equation 12.6.5.

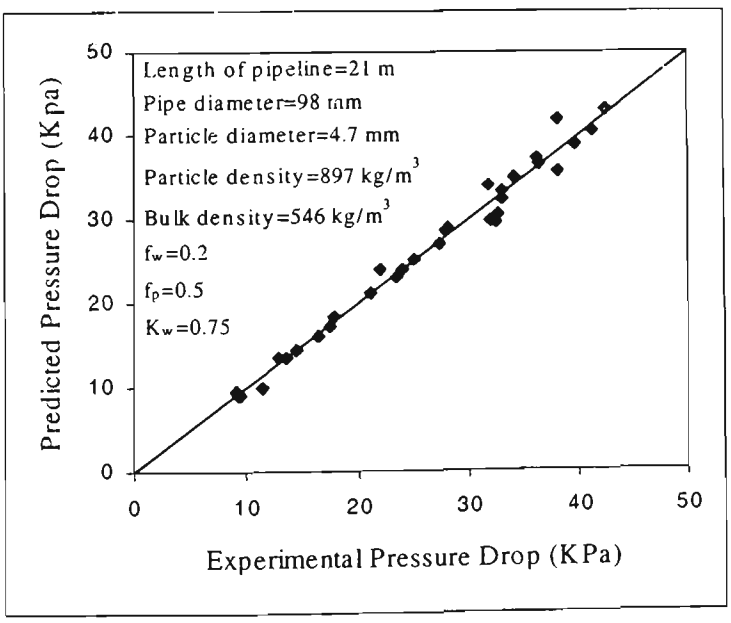

Figure 12.10.1 Comparison of pressure drop for 98mm ID pipeline

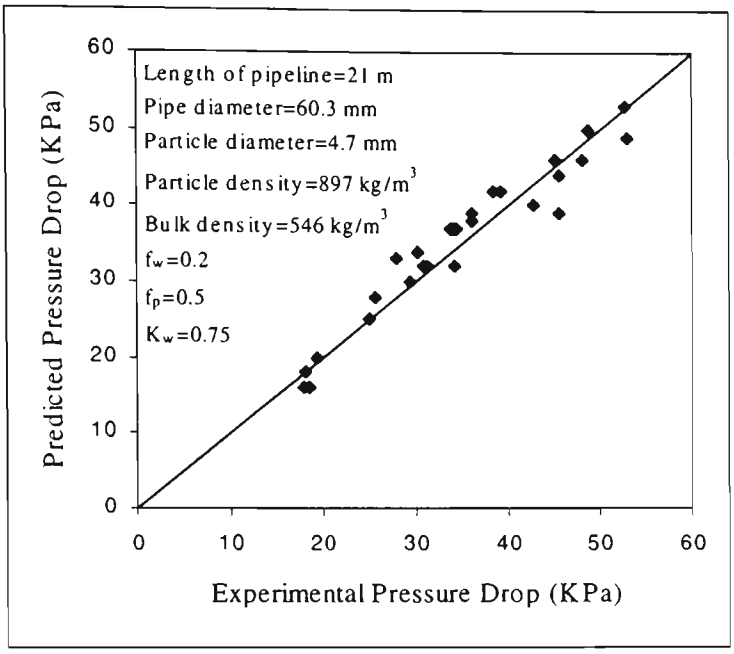

Figure 12.10.2 Comparison of pressure drop for 60.3mm ID pipeline

A comparison of the model prediction of pressure drop across a horizontal conveying pipeline 21m in length with the experimental results of low-velocity slug-flow pneumatic conveying of plastic pellets through the test rig described in Chapter Four in the form of table is shown in Tables 12.10.1 and 12.10.2

Table 12.10.1 Experimental and predicted pressure drop through 98mm ID, 21m horizontal pipeline

Test No	Solids Mass Flow Rate (kg/s)	Air Mass Flow Rate (kg/s)	Experimental Pressure Drop (KPa)	Predicted Pressure Drop (KPa)	Deviation (%)
84	1.75	0.0542	27.8	28.5	2.5
113	2.095	0.0518	33.9	34.8	2.4
93	1.77	0.0506	32.3	29.4	-8.9
85	1.73	0.0408	32.9	32.2	-2.1

114	1.85	0.0389	38	35.5	-6.3
86	1.76	0.0331	36.1	37.2	2.9
87	1.67	0.0269	41.2	40.5	-1.6
116	1.6	0.0267	39.6	38.9	-1.7
64	1.43	0.0539	23.4	22.9	-1.7
95	1.41	0.0436	25	25	0.1
65	1.45	0.0356	28	28.9	3.2
66	1.5	0.0293	31.7	33.9	7.1
67	1.43	0.021	38.1	41.7	9.5
88	1.4	0.0198	42.5	42.9	1.1
36	1.07	0.0454	17.7	18.4	3.9
37	1.12	0.038	21.2	21.2	0
38	1.13	0.0317	23.9	23.8	-0.1
39	1.09	0.0249	27.3	27	-0.8
40	0.94	0.0149	36.3	36.6	0.8
47	0.74	0.04	12.8	13.4	4.9
48	0.74	0.0349	14.5	14.4	0
49	0.72	0.028	16.3	16.1	-1

99	0.7	0.0246	17.5	17.1	-2.1
50	0.74	0.0175	22	23.9	8.7
89	0.78	0.0146	32.6	30.4	-6.7
118	0.77	0.0147	31.9	29.7	-6.7
68	0.82	0.0142	33	33.1	0.4
103	0.38	0.0234	9.4	9.1	-2.9
104	0.37	0.0234	9.1	9.4	3.6
102	0.36	0.0225	9.4	9.1	-2.3
100	0.36	0.0217	9.2	9.4	2.5
19	0.36	0.0204	11.4	9.8	-13.2
20	0.39	0.0156	13.5	13.5	0.2

Table 12.10.2 Experimental and predicted pressure drop through 60.3mm ID, 21m horizontal pipeline

Test No	Solids Mass Flow Rate (kg/s)	Air Mass Flow Rate (kg/s)	Experimental Pressure Drop (KPa)	Predicted Pressure Drop (KPa)	Deviation (%)
41	0.934	0.0161	52.6	53.6	1.91
42	0.868	0.0147	48.6	50.8	4.62
67	0.861	0.019	45.6	44.8	-1.65

66	0.86	0.0152	52.9	49.5	-6.41
68	0.786	0.02	45.6	39.8	-12.51
43	0.771	0.0135	45.2	46.7	3.47
65	0.77	0.0178	42.9	40.9	-4.58
64	0.744	0.0129	48	46.1	-3.86
26	0.726	0.0192	33.7	37.2	10.66
27	0.704	0.0158	36	39.2	8.98
28	0.638	0.0112	38.4	42.4	10.6
44	0.636	0.011	39.3	42.8	8.93
63	0.59	0.0163	34.1	32.1	-5.81
49	0.584	0.0113	36.1	38.3	6.32
51	0.52	0.0123	31.3	32.2	3.09
62	0.508	0.0111	27.8	33.4	20.16
50	0.486	0.0089	34.3	37	7.92
52	0.48	0.0087	34.5	37.1	7.71
54	0.445	0.0101	29.4	30.7	4.69
53	0.439	0.0142	25	25.1	0.4
29	0.389	0.0073	30.2	34.1	13.07

45	0.367	0.0071	30.9	32.8	6.29
13	0.367	0.0086	25.6	28	9.48
12	0.361	0.0143	19.3	20.4	5.81
58	0.298	0.0145	18.4	16.6	-9.49
55	0.279	0.01	18	18.9	5.19
57	0.278	0.0125	17.9	16.6	-7.04

12.11 Comparison of Experimental and Predicted PCC Diagram and Boundaries

With the model for pressure drop and boundaries prediction established, a comparison of the PCC with the theoretical prediction of boundaries B and D for pneumatic conveying of plastic pellets and that from experimental test rig is shown in Figures 12.11.1 and 12.11.2. The input data required for the models include the particle density (897 kg m^{-3}), the voidage of the bulk solid (0.391), the coefficient of friction between the particles and wall (0.2), the coefficient of particle internal friction (0.5), pipeline diameters (98 mm; 60.3 mm) and stress transmission factor K_w (0.75). The agreement between the modeling results and the experimental data is very good. Since the model to predict the pressure drop for pneumatic conveying of granular particles in the form of a strand flow over a stationary layer or slowly moving bed has not been developed, boundary C in both Figures 12.11.1 and 12.11.2 is drawn according to the test results. Also as boundary A which was discovered towards latter stage of this thesis and there was insufficient time to develop model, boundary A is also from test results.

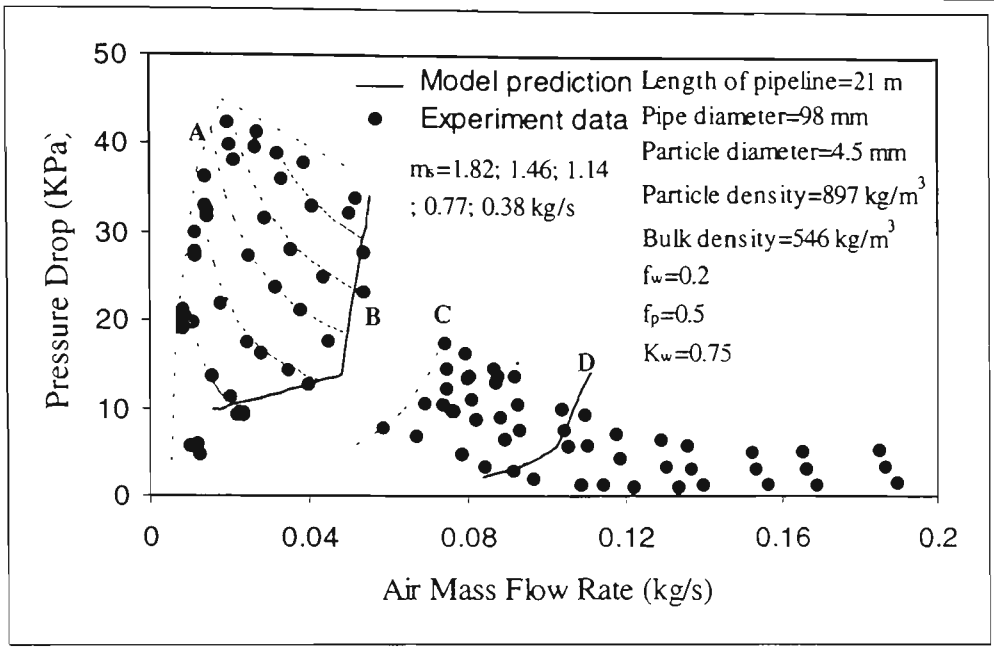

Figure 12.11.1 Comparison of experimental and model predicted PCC with boundaries B and D for 98 mm ID stainless steel pipeline

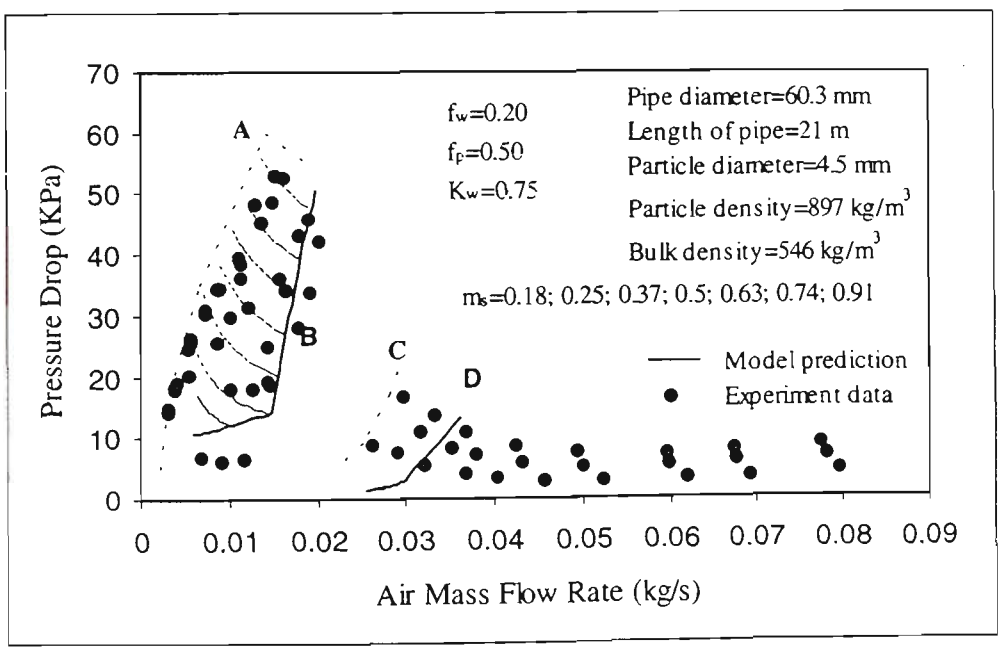

Figure 12.11.2 Comparison of experimental and model predicted PCC with boundaries B and D for 60.3 mm ID stainless steel pipeline

CHAPTER 13: CONCLUSION AND SUGGESTIONS FOR FUTURE WORK

13.1 Conclusions

This thesis was aimed at developing the understanding of the mechanisms involved in the formation of unstable flow during the transition from dilute-phase to dense phase and establishing a model to predict the operating boundaries for pneumatic conveying of granular materials through a horizontal pipeline. The operating boundaries' exploration was extended to powder materials and as the result, classification for powder and granular materials was addressed. Further, a model for prediction of pressure drop for low-velocity slug-flow through a horizontal pipeline also was established. The following conclusions are based on the investigation and finding of this thesis.

13.1.1 Mechanism for Formation of Unstable Flow for Pneumatic Conveying of Granular Solid Materials

Based on conveying tests conducted in this thesis, the following conclusions concerning the formation of unstable flow for pneumatic conveying of granular materials through a horizontal pipeline are listed as follows:

(i) Pneumatic conveying of granular solid materials exhibit different flow modes: low-velocity slug flow, dilute-phase flow with suspended particles and/or strands, strand flow over a layer (stationary layer for low solids mass flow rate or slowly moving layer for high solids mass flow rate).

(ii) Solids mass flow rate has an important influence on the air-solid flow behaviour when the operation is in transition zone. The layers under the strand flow are subjected to different conditions at the bottom of the conveying pipeline: either strand flow over a stationary layer for low solids mass flow rates or strand flow over a slowly moving bed for high solid mass flow rates.

(iii) The pressure fluctuations within the unstable zone result from the flow mode transition from strand flow over a stationary layer (or slowly moving bed) to slug flow starting at the inlet due to a decrease in air velocity. The first slug moves quickly at a relatively high velocity and picks up a relatively thick stationary layer in front of it but only deposits a small amount of the material behind it. The increase in slug length and large increase in pressure cause severe pressure fluctuations and pipeline vibrations.

(iv) The transition between dilute-phase flow with suspended particles and/or strands and strand flow over a stationary or a slowly moving bed as a consequence of increasing air velocity along the conveying pipeline from inlet to exit causes a pulsating flow as the results of material eroded away from the end of the stationary layer or slowly moving bed.

13.1.2 Model for Boundary Predictions

Based on the mass balance, force balance, momentum balance and the unstable zone forming mechanism, a theoretical model for the prediction of the transition zone boundaries in the state diagram has been established.

The formation of Boundary B for pneumatic conveying of granular materials with high and low solids mass flow rate is involved in different mechanism. For the conveying of granular materials with relatively high solids mass flow rate, the formation of a slug will be induced if the friction force from the strand flow is not high enough to move layer or the thickness of the layer is greater than α_{cri}. For a conveying with relative low solids mass flow rate, the formation of a slug will be induced if the thickness of the layer is kept increasing and the air-solid flow eventually reaches Boundary B in the

state diagram where type A operating points turn into type C operating points and the friction between the strand and the layer is not high enough to move the layer.

The boundary predicted by the model has been found to agree very well with experimental data. The influence of particle and bulk properties of the material and pipe wall properties on the boundaries of transition zone had been explored and the exploration had been extended to powder materials. The traditional principle for the design of low-velocity slug flow pneumatic conveying (air velocity within 1.0 m/s to 4.0 m/s) had been improved or upgraded by model prediction based on particle and bulk properties of the material, pipe wall properties, fluid properties and operating condition.

13.1.3 Classification for Powder and Granular Materials

In general, two general forms of P.C.C. have been observed for pneumatic conveying of solids through a horizontal pipeline: the mode of pneumatic conveying characteristics for materials that displays a smooth transition from dilute-phase to dense-phase and the mode of pneumatic conveying characteristics for the transition from dilute-phase to dense-phase with unstable zone.

The difference between two modes is that the upper part of the transition zone in the state diagrams does not exist or is too narrow to cause any unstable flow behaviours for pneumatic conveying of solids. The mechanism that dominates the formation of the upper part of the transition zone in the state diagram is that: when the friction between particle and pipeline wall is close to that between particles, the upper part of the transition zone in the state diagram will contract and disappear. An equation has been developed to provide the criterion for distinguishing granular solids and powders.

13.1.4 Model for Pressure Drop Prediction of Low-Velocity Slug Flow

This thesis presents a new approach for the direct measurement of stress transmission factor and its results were used in a model for low-velocity slug-flow pressure drop prediction. The main differences between this model and previous ones include:

(i) Stress transmission factor is determined by using a new bench-scale test rig;

(ii) Using this new rig, effect of the weight of the granular material in the slug on pressure drop is taken into account;

(iii) A modified equation for the frontal stress on the moving slug allowing for a momentum balance of collecting particles from the stationary layer and the additional force needed to move/expand the stationary material just ahead of the slug (as found by slow-motion analysis) has been established.

The modelling predictions agree very well with test results obtained on poly pellets conveyed through 98 mm and 60.3 mm ID horizontal stainless steel pipelines, each 21 m in length.

13.2 Suggestions for Future Work

It is believed that research conducted in this thesis provides a new viewpoint for research on air-solid flow through a horizontal pipeline and has important theoretical significance and high value for industrial application. Also it is very clear that not all work can be done in this thesis with the approach developed in this study and even the following suggestions are still part of the work to be done after the submission of this thesis.

13.2.1 Operating Boundaries for Vertical Pipe, Inclined Pipe, Bend and Stepped-Bore Line

The work completed in this thesis is concerned with the operating boundaries for pneumatic conveying of solid materials through a horizontal pipeline. However, vertical pipes, inclined pipes, bends and stepped-bore pipes are also widely employed in the industrial application. Whether there is any unstable zone in the state diagram for pneumatic conveying of solid materials through vertical pipes, inclined pipes, bends and stepped-bore pipes and how the particle properties, pipe wall properties and operating condition influence the boundaries of unstable zone is still a question. Also the exploration for the operating boundaries of vertical pipes, inclined pipes, bends and stepped-bore pipes will enhance and richen the theory of transport boundary developed in this thesis.

13.2.2 Experimental Work to Verify Model Predictions

One of aspects to be improved of this thesis is that many predictions from the model have not been confirmed by the experimental work. Two important predictions to be verified include:

(i) A strand flow over a slowly moving layer will be substituted for low-velocity slug-flow if the friction between particles and pipe wall decreases to a certain value.

(ii) A strand flow over a stationary layer will exist only for very low solids mass flow rate if the friction between particles and pipe wall decreases to a certain value.

(iii) Granular materials will displace the flow mode of powder if the roughness of the pipe wall increases to a certain value.

13.2.3 Experimental Work on Transition Behaviour from Dilute-Phase to Dense-Phase for Powder Materials

In discussion on the boundaries of pneumatic conveying of powder materials, it is assumed that the applicability of the model can be extended to the powder materials. So far there is still not enough experimental evidence to confirm and modify the model predictions. Experiment tests on the powders with a wide range variation in particle properties are needed to ensure the modelling results correct.

13.2.4 Improve Pressure Drop Model

The model established in this thesis for low-velocity slug-flow pressure drop produces good results for conveying plastic pellets. It still needs more experimental work covering a wide range of particle properties to verify or modify the existing model and improve its applicability.

13.2.5 Improve Experimental Method to Measure K_w

A test rig was developed in this thesis to directly measure stress transmission coefficient and the results made the pressure drop model work well for plastic pellets. The existing K_w test rig has two shortages as not suitable for small particle measurement and the testing procedure is a little bit complicated. A simple and reliable method or rig is needed to be developed for pressure drop prediction of industrial applications.

CHAPTER 14: REFERENCE

1 Agarwal V. K, Bharathi M. D. and Mills D., The Influence of Conveying Distance on Low-Velocity Pneumatic Conveying of Flyash, Powder Handling & Processing, Vol. 11, No. 1, 1999, pp 57-60.

2 Albright C. W., Holden J. H., Simon H. H. and Schmigt L. D., Pressure Drop in Flow of Dense Coal-Air Mixture, Industrial and Engineering Chemistry, Vol. 43, 1951, pp 1837-1840.

3 Arnold P. C. and Wypych P. W., The Development of Pneumatic Conveying in Australia, Bulk Solids Handling, Vol. 11, 1991, pp 85-91.

4 Arnold P. C., Reed A. R. and Wypych P. W., Advances in the Design of Pneumatic Transport Systems, Powder Handling and Processing, Vol. 6, No. 1, 1994, pp 9-21.

5 Baker J. D. and Klinzing G. E., Optimal Performance of Pneumatic Transport Systems, Powder Technology, Vol. 104, 1999, pp 240-247.

6 Barker C. G. and Geldart D., An Investigation into the Slugging Characteristics of Large Particles, Powder Technology, Vol. 19, 1978, pp 177-187.

7 Beeckmans J. M., Usta B. and Zhu J., Effect of tap spacing on observed differential pressure fluctuations in a pneumatic transport line, Canadian Journal of Chemical Engineering, Vol. 74, 1996, pp 834-839.

8 Bharathi M. D., Agarwal V. K. and Mills D., The Influence of Particle Size Range on the Pneumatic Conveying of Flyash, Powder Handling & Processing, Vol. 11, No. 2, 1999, pp 197-200.

9 Cabrejos F. J. and Klinzing G. E., Minimum Conveying Velocity in Horizontal Pneumatic Transport and the Pickup and Saltation Mechanisms of Solid Particles, Bulk Solids handling, Vol. 14, No. 3, 1994, pp 544-550.

10 Cabrejos F. J. and Klinzing G. E., Pickup and Saltation Mechanisms of Solid Particles in Horizontal Pneumatic Transport, Powder Technology, Vol. 79, 1994, pp 173-186.

11 Cabrejos F. J. and Klinzing G. E., Characteristics of Dilute Gas -Solids Flow Using the Rescaled Range Analysis, Powder Technology, Vol. 84, 1995, pp 139-156.

12 Cabrejos F. J. and Klinzing G. E., Some Observation on Pickup and Saltation Velocity in Pneumatic Conveying, Powder Handling & Processing, Vol. 5, No. 1, 1993, pp 13-14.

13 Collado F. J. and Muñoz M., New Considerations on the Mass and Energy Balances in One-Dimensional Two-Phase Flow at Steady State, Powder Technology, Vol. 92, 1997, pp 195-204.

14 Cook D. and Hurworth N. R., Recent Research on Pulverised Fuel Settlement in Power Station Pipelines and the Significance of "Roping", Pneumotransport 5, 5th International Conference on the Pneumatic Transportation of Solids in Pipes, April 16-18, 1980, London, UK, pp 289-308.

15 Datta B. K. and Basu A. K., Estimation of Limited Deposit Velocity in Dilute Phase Pneumatic Conveying, Powder Handling & Processing, Vol. 8, No. 3, 1996, pp235-239.

16 Davidson J. F. and Harrison D., Fluidisation, Academic Press, London and New York, 1971

17 Dixon G., The Impact of Powder Properties on Dense Phase Flow, Proceedings of International Conference on Pneumatic Conveying, January, 1979, UK.

18 Dorst C. V. and Eyck, J. V., Improving Pneumatic Conveying Systems, Powder Handling & Processing, Vol. 11, No. 2, 1999, pp 193-196.

19 Duckworth R. A., The Influence of the Particle and Fluid Properties and the Inclination of the Pipe on the Minimum Transport Velocity, Proc Pneumotransport 3, Bath, England, 7-9 April 1976, pp S5-31-40.

20 Ergun S. and Orning A. A., Fluid Flow through Randomly Packed Columns and Fluidised Bed. Industrial and Engineering Chemistry, Vol. 41. No. 6, 1949, pp 1179-1184.

21 Ergun S., Fluid Flow through Packed Columns, Chemical Engineering Progress, Vol. 48, 1952, pp 89-94.

22 Flatt W. and Blumer P., Low Velocity Conveying, Pneumatech 1, First International Conference on Pneumatic Conveying Technology, May 3-5, 1982, Stratford-Upon-Avon, UK, pp 1-4.

23 Flatt W., Latest Development and Applications of High Density Pneumatic Conveying System, Pneumotransport 3, Third International Conference on the Pneumatic Transport of Solids in Pipes, Apr. 7-9, 1976, England, A 3-21.

24 Flatt W., Low Velocity Pneumatic Conveying of Granulated and Pulverised Products, Criteria for Selecting the Optimal Pneumatic Conveying System, Pneumotransport 5, Fifth International Conference on the Pneumatic Transport of Solids in Pipes, Apr. 16-18, London, UK, pp 409-418.

25 Flatt W., Today's Possibilities for Low Velocity Conveying of Carbon Black and Pigments with New Conveying Technology, International Conference on Pneumatic Conveying Technology, Sep. 4-6, 1984, Canterbury, UK, pp 1-18.

26 Geldart D. and Ling S. J., Saltation in High Pressure Conveying of Fine Coal, Powder Technology, Vol. 69, 1992, pp 157-162.

27 Geldart D., Types of Gas Fluidisation, Powder Technology, Vol. 7, 1973, pp 285-292.

28 Hartman M., The Pros and Cons of Blower and Vacuum Conveying Systems, Powder Handling & Processing, Vol. 4, No.4, 1992, pp 179-184.

29 Heep D., Winkhardt G. and Nijman G., Application and Optimization of a Dense-Phase Carbon Black Conveying System in a Tyre Works, Powder Handling & Process, Vol. 15, No.1, 1995, pp 53-63.

30 Heep D., Winkhardt G. and Heep M., Conveying Air Management the Key to Troublefree Conveyance of Plastic Granulates, Powder Handling and Process, Vol. 11, No.1, 1999, pp 61-64

31 Heep D., Winkhardt G. and Heep M., Conveying Air Management the Key to Troublefree Conveyance of Plastic Granulates, Powder Handling and Process, Vol.11, No.3, 1999, pp 287-291.

32 Heep D. and Winkhardt G., Low Velocity Conveying of Plastic Pellets Technology and Problems, Powder Handling and Process, Vol.10, No.1, 1998, pp 47-53.

33 Herbreteau C. and Bouard R., Experimental study of parameters which influence the energy minimum in horizontal gas-solid conveying, Powder Technology, Vol. 112, 2000, pp 213-220.

34 Hettiaratchi K., Woodhead S. R. and Reed A. R., Comparison between pressure drop in horizontal and vertical pneumatic conveying pipelines, Powder Technology, Vol. 95, 1998, pp 67-73.

35 Holmes M., Raw materials handling for the plastics compounding industry, Plastics, Additives and Compounding, Vol. 2, 2000, pp 30-34.

36 Huber N., Sommerfeld M., Characterization of the Cross-Sectional Particle Concentration Distribution in Pneumatic Conveying Systems, Powder Technology, Vol. 79, 1994, pp 191-210.

37 Janssen H. A., Tests on Grain Pressure Silo, Z. Ver. Dtsch. Ing. Beih. 35, 1895, pp 1045-1049.

38 Legel D and Schwedes J, Investigation of Pneumatic Conveying of Plug of Cohesionless Bulk Solids in Horizontal Pipes, Bulk Solids Handling, Vol. 4, No. 2, 1984, pp 399-405.

39 Jenike A. W. and Hohnson J. R., Bin Loads, Journal of the Structure Division, ASCE, Vol. 96, No. ST4, 1968, pp 1011-1041.

40 Jenike A. W. and Hohnson J. R., On the Theory of Bin Loads, Journal of Engineering for Industry, Transactions of ASME, Series B, Vol. 91, No. 2, 1969, pp 339-344.

41 Jones M. G. and Mills, D., Product Classification for Pneumatic Conveying, Powder handling & Processing, Vol. 2, No. 2, 1990, pp 117-122.

42 Jones P. J. and Leung L. S., A Comparison of Correlations for Saltation Velocity in Horizontal Pneumatic Conveying, Ind Eng Chem Process Des Dev, Vol. 17, No 4, 1978, pp 571-575.

43 Jones P. J. and Leung L. S., Estimation of Saltation Velocity in Horizontal Pneumatic Conveying - A Comparison of Published Correlations, Pneumotransport 4, 4th International Conference on the Pneumatic Transportation of Solids in Pipes, June 26-28, 1978, California, USA, pp C1 1-12.

44 Kafka C. E., Pneumatic Conveying and Minerals Processing Preparing for the 21 Century, Powder Handling & Processing, Vol. 7, No. 3, 1995, pp 207-211.

45 Klintworth J. and Marcus R. D., A Review of Low-Velocity Pneumatic Conveying Systems, Bulk Solids Handling, Vol. 5, No. 4, 1985, pp 747-753.

46 Klinzing G. E., Rohatgi, N. D., Zatash, A. and Myler, C. A., Pneumatic Transport - a Review (Generalised Phase Diagram Approach to Pneumatic Transport), Powder Technology, Vol. 51, 1987, 135-149.

47 Klinzing G. E., Marcus R. D., Rizk F. and Leung L. S., Pneumatic Conveying of Solids, Chapman & Hall, 1997, pp 188-195.

48 Klinzing G.E., Dense Phase (Plug) Conveying - Observations and Projections, The 3rd Israel Conf. For Conveying and Handling of Particulate Solids, 2000, The Dead Sea, Israel, pp 10.1-10.10.

49 Konrad K., Harrison D., Nedderman R. M. and Davison J. F., Prediction of the Pressure Drop for Horizontal Dense Phase Pneumatic Conveying of Particles, Pneumotransport 5, 5th International Conference on the Pneumatic Transportation of Solids in Pipes, April 16-18, 1980, London, UK, pp 225-244.

50 Konrad K., Dense Phase Pneumatic Conveying: A Review, Powder technology, Vol. 49, 1986, pp 1-35.

51 Konrad K., Dense-Phase Pneumatic Conveying through Long Pipelines: Effect of Significantly Compressible Air Flow on Pressure Drop, Powder technology, Vol. 48, 1986, pp 193-203.

52 Kunii D. and Levenspiel O., Fluidisation Engineering, Huntington, New York, 1977.

53 Laouar S. and Molodtsof Y., Experimental characterization of the pressure drop in dense phase pneumatic transport at very low velocity, Powder Technology, Vol. 95, 1998, pp 165-173.

54 Legel D. and Schwedes J., Investigation of Pneumatic Conveying of Plugs of Cohesionless Bulk Solids in Horizontal Pipes, Bulk Solids Handling, Vol. 4, No. 2, 1984, pp 399405.

55 Levy A. and Mason D. J., Two-layer model for non-suspension gas-solids flow in pipes, Powder Technology, Vol. 112, 2000, pp 256-262.

56 Levy A., Two-fluid approach for plug flow simulations in horizontal pneumatic conveying, Powder Technology, Vol. 112, 2000, pp 263-272.

57 Mainwaring, N. J. and Reed, A. R., An Appraisal of Dixons's Slugging Diagram for Assessing the Dense Phase Conveying Potential of Bulk Solid Materials, Pneumatech 4, Fourth International Conference on Pneumatic Conveying Technology, March, 1987, pp221-234.

58 Mason D. J. and Li J., A novel experimental technique for the investigation of gas-solids flow in pipes, Powder Technology, Vol. 112, 2000, pp 203-212.

59 Mason D. J. and Levy A., A model for non-suspension gas-solids flow of fine powders in pipes. International Journal of Multiphase Flow, Vol. 27, 2001, pp 415-435.

60 Mason D. J., Marjanovic P. and Levy A., A simulation system for pneumatic conveying systems, Powder Technology, Vol. 95, 1998, pp 7-14.

61 Matsumoto S., Hara M., Saito S. and Maeda S., Minimum Transport Velocity for Horizontal Pneumatic Conveying, Journal of Chemical Engineering of Japan, Vol. 7, No 6, 1974, pp 425-431.

62 Matsumoto S., Kikuta M. and Maeda S., Effect of Particle Size on the Minimum Transport Velocity for Horizontal Pneumatic Conveying of Solids, Journal of Chemical Engineering of Japan, Vol. 10, No 4, 1977, pp 273-279.

63 Mi B., Wypych P.W., Pressure drop prediction in low-velocity pneumatic conveying, Powder Technology, Vol. 81, 1994, pp 125-137.

64 Mi B., Wypych P.W., Investigations into wall pressure during slug-flow pneumatic conveying, Powder Technology, Vol. 84, 1995, pp 91-98.

65 Mierka O. and Timar P., Energy Optimisation of Pneumatic Transport, Powder Handling & Processing, Vol. 9, No. 3, 1997, pp 221-225.

66 Mills, D., Pneumatic Conveying Design Guide, Butterworth-Heinemann, 1990.

67 Molerus O., Principles of Flow in Disperse Systems, Chapman & Hall, London, New York, 1993.

68 Molerus O., Overview: Pneumatic transport of solids, Powder Technology, Vol. 88, 1996, pp 309-321.

69 Molerus O. and Burschka A., Pneumatic transport of coarse-grained materials, Chemical Engineering and Processing, Vol. 34, 1995, pp 173-184.

70 Munson B. R., Young D. F. and Okiishi T. H., Fundamentals of Fluid Mechanics, John Wiley & Sons Inc., 1994.

71 Myler C. A., Zaltash A., Dhodapkar S. and Klinzing G. E., Phase Equilibria in Horizontal Pneumatic Transport, Powder Technology, Vol. 57, 1989, pp 51-57.

72 Ochi M., Saltation, Velocity of the Gas-Solid Two-Phase Flow in a Horizontal Pipe, ASME, Gas-Solid Flow, Fed-Vol. 121, 1991, pp 163-166.

73 Ochi M., Saltation and Takei M., Minimum Transport Velocity of Gas-Solid Two-Phase Flow in a Vertical Pipe, JSME ICFE, Tokyo, Japan, 13-16 July, pp 817-891.

74 Ostrowski K. L., Luke S. P., Bennett M. A. and Williams R. A., Application of capacitance electrical tomography for on-line and off-line analysis of flow pattern in horizontal pipeline of pneumatic conveyer, Chemical Engineering Journal, Vol. 77, 2000, pp 43-50.

75 Ostrowski K. L., Luke S. P., Bennett M. A. and Williams R. A., Real time visualisation and analysis of dense phase powder conveying, Powder Technology, Vol. 102, 1999, pp 1-13.

76 Ostrowski K. L., Luke S. P. and Williams R. A., Simulation of the performance of electrical capacitance tomography for measurement of dense phase pneumatic conveying, Chemical Engineering Journal, Vol. 68, 1997, pp 197-205.

77 Pan R. and Wypych P. W., Pressure drop and slug velocity in low-velocity pneumatic conveying of bulk solids, Powder Technology, Vol. 94, 1997, pp 123-132.

78 Pan R. and Wypych P. W., Classification of Bulk Solid Materials for Pneumatic Conveying, Pro National Conference on Bulk Materials Handling, Melbourne, Australia, 30 September - 2 October 1996, pp 349-353.

79 Pan R., Simplified Procedure for Pressure Drop Prediction in Low-Velocity Slug-Flow Pneumatic Conveying, Powder Handling & processing, Vol. 10, N0. 4, 1998, pp 367-371.

80 Pan R., Material properties and flow modes in pneumatic conveying, Powder Technology, Vol. 104, 1999, Pages 157-163.

81 Pan R., Long Distance Slug-Flow Pneumatic Conveying, Powder Handling & Process, Vol. 12, 2000, pp 365-369.

82 Patterson R. C., Pulverised Coal Transport through Pipes, Combustion, July, 1958, pp 47-57.

83 Plasynski S., Dhodapkar S. and Klinzing G. E., Comparison of Saltation velocity and Pickup Velocity Correlations for Pneumatic Conveying, AIChE Symposium Series Vol. 87, No 281, 1991, pp 78-90.

34 Pugh F. J. and Wilson K. C., Role of the Interface in Stratified Slurry Flow, Powder Technology, Vol. 104, 1999, pp 221-226.

85 Rhodes M. J., Principles of Powder technology, John Wiley & Sons, Chichester, New York, Brisbane, Toronto, Singapore, 1990.

86 Rizk F., Pneumatic Conveying at Optimal Operation Conditions and a Solution of Barth's Equation $\lambda_Z=\emptyset(\lambda^*_z, \beta)$, Proc Pneumotransport 3, Bath, England, 7-9 April 1976, pp D4-43-58.

87 Rizk F., Pneumatic Transport in Dilute and Dense Phase, Bulk Solids handling, Vol. 2, 1982, pp 235-241.

88 Rizk F., A Comparison between Horizontal and Vertical Pneumatic Conveying Systems Considering the Optimal Operating Conditions, Journal of Powder & Bulk Solids Technology, Vol. 7, 1983, pp 5-11.

89 Rose H. E. and Duckworth R. A., Transport of Solid Particles in Liquids and Gases, The Engineer, Vol. 227, No 5903, 1969, pp 392-396.

90 Rose H. E. and Duckworth R. A., Transport of Solid Particles in Liquids and Gases, The Engineer, Vol. 227, No 5904, 1969, pp 430-434.

91 Rose H. E. and Duckworth R. A.,, Transport of Solid Particles in Liquids and Gases, The Engineer, Vol. 227, No 5905, 1969, pp 478-483.

92 Schade B., Zum Übergang Sprung-Strähnenförderung bei der Horizontalen Pneumatischen Feststoffördrung, Dissertation, University of Karlsruhe, 1987.

93 Sundaresan S., Some outstanding questions in handling of cohesionless particles, Powder Technology, Vol. 115, 2001, pp 2-7.

94 Tashiro H., Peng X. and Tomita Y., Numerical prediction of saltation velocity for gas-solid two-phase flow in a horizontal pipe, Powder Technology, Vol. 91, 1997, pp 141-146.

95 Taylor T., Specific Energy Consumption and Particle Attrition in Pneumatic Conveying, Powder Technology, Vol. 95, 1998, pp 1-6.

96 Tomita Y. and Tateishi K., Pneumatic slug conveying in a horizontal pipeline, Powder Technology, Vol. 94, 1997, pp 229-233.

97 Tsuji Y. and Morikawa, Y., LDV Measurements of an Air- Solid Two Phase Flow in a Horizontal Pipe, J. Fluid Mech., Vol. 120, 1982, pp 385-409.

98 Uematsu T., Tsuchiya K. and Okamura S., Packing and Friction of Coarse Particle (in Japanese), Trans. Jpn. Soc. Mech. Eng. Vol. 17, 1951, pp 171-179.

99 Walter D. M., A theoretical Analysis of Stress in Silos with Vertical Wall, Chemical Engineering Science, Vol. 28, 1973, pp13-21.

100 Wall R. E. and Soo S. L., Measurement of Transport Properties of a Gas-Solid Suspension Using Phase Doppler Anemometer, Powder Technology, Vol. 94, 1997, pp 141-151.

101 Weber M., Principles of Hydraulic and Pneumatic Conveying in Pipes, Bulk Solids Handling, Vol. 1, No 1, February, 1981, pp 57-63.

102 Wen C. Y. and Simons H. P., Flow Characteristics in Horizontal Fluidised Solids Transport, AIChE Journal, Vol. 5, No. 2, 1959, pp 263-267.

103 Wilson K. C., Streat M. and Bantin R. A., Slip Model Correlation of Dense Two-Phase Flow, Proc. Hydrotransport 2, Cranfield, Bedford, U. K. 1972.

104 Wirth K. E., Critical Velocity of Solids Transport through Horizontal Circular Pipeline, Ger. Chem. Eng. Vol. 6, 1983, pp 45-52.

105 Wirth K. E and Molerus O., Critical Solids Transport Velocity with Horizontal Pneumatic Conveying, Journal of Powder & Bulk Solids Technology, Vol. 1, No 9, 1985, pp 17-24.

106 Wirth K. E and Molerus O., The Influence of Pipe Geometry on the Critical Velocity of Horizontal Pneumatic Conveying of Coarse Particles, Powder Technology, Vol. 42, 1985, pp 27-34.

107 Wypych P. W., Pneumatic conveying of powders over long distances and at large capacities, Powder Technology, Vol. 104, 1999, pp 278-286.

108 Yan, Y., Flow Rate Measurement of Bulk Solids in Pneumatic Pipelines Problems and Solutions, Bulk Solids Handling, Vol. 15, No. 3, 1995, pp 447-456.

109 Yi J., Wypych P. W. and Pan R., Evaluation of Existing Correlations for Minimum Conveying Velocity, 6th International Conference on Bulk Materials Storage, Handling and Transportation, Wollongong, Australia, Sept. 28-30, 1998, pp191-198.

110 Yi J., Wypych P. W. and Pan R., Minimum Conveying Velocity in Dilute-Phase Pneumatic Conveying, Powder Handling & Processing, Vol. 10, No. 3, 1998, pp 255-261.

111 Yi J., Wypych PW and Pan R., Effect of Pipe Wall Roughness on Dilute-Phase Minimum Conveying Velocity, Powder Handling & Processing, Vol. 12, No. 3, 2000, pp 235-237.

112 Yi J., and Wypych P. W., Modelling the unstable boundary for low-velocity slug-flow conveying, The 3rd Israel Conf. For Conveying and Handling of Particulate Solids, 2000, The Dead Sea, Israel, pp 10.11-10.17.

113 Yilmaz A. and Levy E. K., Formation and dispersion of ropes in pneumatic conveying, Powder Technology, Vol. 114, 2001, pp 168-185.

114 Yilmaz A. and Levy E. K., Roping phenomena in pulverized coal conveying lines, Powder Technology, Vol. 95, 1998, pp 43-48.

115 Zenz F.A. and Othmer, D. F., Fluidisation and Fluid-Particle System, Reinhold Publishing Corporation, New York, Chapman & Hall, London, 1960.

116 Zenz F.A., Conveyability of Materials of Mixed Particle Size, I & EC Fundamentals, Vol. 3, No 1, 1964, pp 65-75.

APPENDICES

COMPUTER PROGRAMME FOR BOUNDARIES PREDICTION

```
C     THIS PROGRAMME IS FOR THE BOUNDARIES PREICTION OF
PNEUMATIC CONVEYING OF GRANULAR MATERIALS. THE BOUNDARIES
PREDICTION IS COUPLED WITH PRESSURE DROP PREDICTION FOR LOW-
VELOCITY SLUG-FLOW.
C
      EV:    VOIDAGE OF THE GRANUALR MATERIALS
      ROS:   PARTICLE DENSITY
      ROF:   AIR DENSITY
      PK:    FACTOR OF FRICTION BETWEEN PARTICLES
      WK:    FACTOR OF FRICTION BETWEEN PARTICLE AND PIPE WALL
      G:     GRAVITY ACCELERATION
      D:     PIPE DIAMETER
      EVM:   VOIDAGE OF STRAND
      PE:    INITIAL AIR PRESSURE
C
C
      DIMENSION X(30),Y(30),X2(30),Y2(30)
      COMMON HL,EV,ROS,ROF,PK,WK,G,D,EVM,PE
      PE=101325.0
      G=9.8
      HL=0.0826
      D=0.098
      WK=0.20
      PK=0.5
      ROS=897
      EV=0.391
      EVM=0.391
      WRITE(*,*)'D=',D,' WK=',WK,' PK=',PK,' ROS=',ROS,
     *  ' EV=',EV,' EVM=',EVM
      WRITE(*,*)'NO FOR CHANGE, PUT IN 1'
      READ(*,*)YS
      IF(YS.EQ.1) GOTO 2
1     WRITE(*,*)'PUT IN PIPE DIAMETER D (M)'
      READ(*,*)D
      WRITE(*,*)'PUT IN WALL FRICTION WK'
      READ(*,*)WK
      WRITE(*,*)'PUT IN PARTICLE FRICTION PK'
      READ(*,*)PK
      WRITE(*,*)'PUT IN PARTICLE DENSITY ROS (KG/M-3)'
      READ(*,*)ROS
      WRITE(*,*)'PUT IN VOIDAGE EV FOR STRAND'
      READ(*,*)EV
      WRITE(*,*)'PUT IN THE VOIDAGE OF BULK MATERIAL'
      READ(*,*)EVM
      WRITE(*,*)'D=',D,'WK=',WK,'PK=',PK,'ROS=',ROS,'EV=',EV,'EVM=',EVM
      WRITE(*,*)'NO FOR CHANGE, PUT IN 1'
      READ(*,*)YES
      IF(YES.NE.1) GOTO 1
2     WRITE(*,*)'PUT IN PRESSURE OF THE AIR'
      READ(*,*)PRE
```

```
      WRITE(*,*)'PRESSURE=',PRE
      ROF=1.259*PRE
      WRITE(*,*)' TAKE YOUR SELECTION'
      WRITE(*,*)'1=ORIGINAL E AND F;2=EF ONE LINE;3=CROSS
      LINE;4=MOVING'
      READ(*,*)MUM
      IF(MUM.EQ.1)GOTO 3
      IF(MUM.EQ.2)GOTO 4
      IF(MUM.EQ.3)GOTO 5
      IF(MUM.EQ.4)GOTO 16
      GOTO 6
3     CALL TEF
      GOTO 6
4     CALL EF
      GOTO 6
5     CALL CROSS(X,Y,X2,Y2)
      GOTO 6
16    CALL MOVE(X,Y,X2,Y2)
      GOTO 6
6     CONTINUE
      WRITE(*,*)'TO CONTINUE FROM BEGINNING PUT IN 1, FROM
      MIDDLE 2'
      READ(*,*)NUN
      IF(NUN.EQ.1)GOTO 1
      IF(NUN.EQ.2)GOTO 2
      STOP
      END
C     ************************************************
      THIS SUBROUTINE IS FOR CALCAULATING BOUNDARY B. IT MUST
      BE CONDUCTED AFTER THE LOWER PART OF BOUNDARY B HAS
      BEEN OBTAINED BY SUBROUTINE CROSSS
C     ************************************************
       SUBROUTINE MOVE(X1,Y1,PX1,PY1)
      REAL MSF(30),MSS(30),MAF(65),MAS(65),MAP(65)
      DIMENSION PRE(30),ASS(30),X1(30),Y1(30),PX1(30),PY1(30),XR1(2),
      XR2(2),XXR1(2),XXR2(2)
       COMMON HL,EV,ROS,ROF,PK,WK,G,D,EVM,PE
      AA=0.25*3.1416*D**2
       MV=1
      WRITE(*,*)' THIS PROGRAM IS FOR CALCULATING THEBOUNDAYR'
      WRITE(*,*)' BETWEEN STATIONARY LAYER AND MOVING LAYER
      AT LINE E'
       WRITE(*,*)'PLEASE PUT IN THE UPPER AND LOWER AS'
      READ(*,*)ASUP,ASL
      WRITE(*,*)'ASup=',ASUP,'  ASDOWN=',ASL
      DO 10 I=1,30
      RA=I
       ASS(I)=ASUP-RA*(ASUP-ASL)/30.0
       CALL FLM(MV,ASS(I),MSF(I),MSS(I),PRE(I))
       FSM=MSF(I)/(AA*ROF)
```

```
      SSM=MSS(I)/AA
      WRITE(*,11)ASS(I),MSF(I),MSS(I),PRE(I)
11    FORMAT(1X,4(5X,F9.5))
10    CONTINUE
      CALL FIT2(MSF,PRE,PX1,PY1,XR1,XR2,SX,SY)
      WRITE(*,*)'SX=',SX,'  SY=',SY
      CALL FIT2(MSF,MSS,X1,Y1,XXR1,XXR2,SSX,SSY)
      WRITE(*,*)'SSX=',SSX,'  SSY=',SSY
      DO 15 I=1,30
      MAF(I)=MSF(I)
      MAP(I)=PRE(I)
      MAS(I)=MSS(I)
      KK=I-1
      IF(PRE(I).LE.SY)GOTO 16
15    CONTINUE
16    MM=KK+4
      DO 17 I=KK,MM
      MAF(I)=SX
      MAP(I)=SY
17    MAS(I)=SSY
      NN=MM+1
      DO 18 I=1,30
      IF(PY1(I).LT.SY)THEN
      MAF(NN)=PX1(I)
      MAP(NN)=PY1(I)
      MAS(NN)=Y1(I)
      NN=NN+1
      ELSE
      ENDIF
18    CONTINUE
      DO 19 K=1,65,2
      IF(MAP(K).EQ.0.0)GOTO 21
      WRITE(*,20)MAF(K),MAS(K),MAP(K)
20    FORMAT(1X,3(5X,F10.5))
19    CONTINUE
21    CONTINUE
31    WRITE(*,*)'PREDICT PRESSURE PUT IN MSF, TURNING POINT=',SX
      READ(*,*)ZX
      write(*,*)'XR21=',XR2(1),'  XR22=',XR2(2)
      WRITE(*,*)'XR11=',XR1(1),'  XR12=',XR1(2)
      ZFP=XR2(1)+XR2(2)*ZX
      ZEP=XR1(1)+XR1(2)*ZX
      WRITE(*,*)'MORE THAN TURNING PRESSURE1=',ZFP
      WRITE(*,*)'LESS THAN TURNING PRESSURE2=',ZEP
      WRITE(*,*)'PUT IN 1 TO CONTINUE, PUT 2 TO AIR MASS FR
      PREDICTION'
      READ(*,*)MUMM
      IF(MUMM.EQ.1)GOTO 31
      IF(MUMM.EQ.2)GOTO 32
      WRITE(*,*)'TO CONTINUE PUT IN 1'
```

```
      READ(*,*)IJL
      IF(IJL.EQ.1)GOTO 1
      IF(IJL.EQ.1)GOTO 40
32    WRITE(*,*)'PREDICT AIR MASS FLOW RATE PUT IN MSS,
     * TURNING POINT=',SX
      READ(*,*)ZX
      write(*,*)'XXR21=',XXR2(1),'   XXR22=',XXR2(2)
      WRITE(*,*)'XXR11=',XXR1(1),'    XXR12=',XXR1(2)
      ZFP=(ZX-XXR2(1))/XXR2(2)
      ZEP=(ZX-XXR1(1))/XXR1(2)
      WRITE(*,*)'MORE THAN TURNING AIR MASS FR1',ZFP
      WRITE(*,*)'LESS THAN TURNING AIR MASS FR2',ZEP
      WRITE(*,*)'PUT IN 1 TO CONTINUE, PUT 2 TO PRESSURE
      PREDICTION'
      READ(*,*)MUMMM
      IF(MUMMM.EQ.1)GOTO 32
      F(MUMMM.EQ.2)GOTO 31
      WRITE(*,*)'TO CONTINUE FROM MOVE PUT IN 1'
      READ(*,*)IJL
      IF(IJL.EQ.1)GOTO 1
      IF(IJL.EQ.1)GOTO 40
40    CONTINUE
      RETURN
      END
C     ***************************************************************
      THIS SUBROUTINE (FLM) IS FOR CALCAULATING UPPER PART OF
      BOUNDARY B COUPLED WITH PRESSURE DROP PREDICTION. IT
      MUST BE CONDUCTED AFTER THE THICKNESS OF THE LAYER HAS
      BEEN OBTAINED
C
      ***************************************************************
*
      SUBROUTINE FLM(MV,AS,MSF,MSS,PPRESS)
      REAL MSF, MSS,MASF,MASS
      DIMENSION RV(1000),BFRI(1000),RRVF(1000)
      COMMON HL,EV,ROS,ROF,PK,WK,G,D,EVM,PE
      DO 7 II=1,30
      RV(II)=0.0
      BFRI(II)=0.0
7     RRVF(II)=0.0
      MSF=0.0
      MSS=0.0
      XM=(PK/WK)**0.5
      RV1=0.08
      RV2=0.5
      IF(AS.LT.0.01.OR.PK.LE.WK)THEN
      XM=1.0
      FR=WK
      ELSE
      FR=PK
```

```
      ENDIF
      XX=(RV2-RV1)/999.0
      AA=3.14159*D**2/4.0
      CONT1=(FR*(ROS/ROF)*(1.0-(ROF/ROS))*(1.0-EV)*D*G)**0.5
      CONT2=ROS*(1.0-EV)/ROF
      UP=WK*AS*(1.0-EVM)
      DW=(PK*(1.0-AS*ROF/ROS)-WK*(1.0-AS))*(1.0-EV)
      CRIT=UP/DW
      WRITE(*,*)'CRIT=',CRIT
      DO 10 I=1,1000
      KKK=1
      RV(I)=RV1+XX*(I-1)
1     CALL FMM(MV,AS,RV(I),BBB,BDP,RRVF(I))
      BBB1=BBB
      IF(BBB.EQ.0.0)THEN
      BBB=BBB2
      ELSE
      ENDIF
      KKK=KKK+1
      BFRI(I)=BBB*(XM*(1.0-AS))
      MASF=BBB*CONT1*AA*(1.0-AS)*ROF
      MASS=MASF*RRVF(I)*CONT2
      CALL PRIDICT(MASF,MASS,PRESS)
      FPRS1=MASF
      ROF=1.259*PRESS/PE
      CONT1=(FR*(ROS/ROF)*(1.0-(ROF/ROS))*(1.0-EV)*D*G)**0.5
      CONT2=ROS*(1.0-EV)/ROF
      CALL FMM(MV,AS,RV(I),BBB,BDP,RRVF(I))
    BBB2=BBB
    IF(BBB.EQ.0.0)THEN
    BBB=BBB1
    ELSE
    ENDIF
    IF(BBB.EQ.0.0)GOTO 10
    BFRI(I)=BBB*(XM*(1.0-AS))
    MASF=BBB*CONT1*AA*(1.0-AS)*ROF
    MASS=MASF*RRVF(I)*CONT2
    CALL PRIDICT(MASF,MASS,PRESS)
    ROF=1.259*PRESS/PE
    FPRS2=MASF
    DPRE=ABS((FPRS2-FPRS1)/FPRS2)
    IF(DPRE.GT.0.005)GOTO 1
      IF(BDP.GE.CRIT)GOTO 101
10    CONTINUE
      GOTO 102
101   CONTINUE
      MSF=BBB*CONT1*AA*(1.0-AS)*ROF
      MSS=MSF*RRVF(I)*CONT2
      PPRESS=(PRESS-PE)/1000.0
102   CONTINUE
```

```
      RETURN
      END
C     ************************************************************
      THIS SUBROUTINE IS FOR CALCAULATING LOWER PART OF
      BOUNDARY B. IT MUST BE CONDUCTED AFTER TWO THICKNESSES
      OF THE LAYERS HAVE BEEN GIVEN.
C     ************************************************************
      SUBROUTINE CROSS(XXX,YYY,XXX2,YYY2)
      REAL MASS1(30),MASS2(30),MASF1(30),MASF2(30),EFX(30),EFY(30),
     * XR1(3),XR2(2),XXR1(3),XXR2(2),ASS(30),FAM(30),FSM(30),
     * XXX(30),YYY(30),PRE1(30),
     * PRE2(30),PRS1(30),PRS2(30),PEFX(30),PEFY(30),XXX2(30),YYY2(30)
      COMMON HL,EV,ROS,ROF,PK,WK,G,D,EVM,PE
      DO 2 I=1,30
      MASS1(I)=0.0
      MASS2(I)=0.0
      MASF1(I)=0.0
      MASF2(I)=0.0
      EFX(I)=0.0
      EFY(I)=0.0
      ASS(I)=0.0
      FAM(I)=0.0
      PRE1(I)=0.0
      PRE2(I)=0.0
      PRS1(I)=0.0
      PRS2(I)=0.0
      PEFX(I)=0.0
2     PEFY(I)=0.0
      DO 3 I=1,5
      XXX(I)=0.0
      YYY(I)=0.0
      XXX2(I)=0.0
3     YYY2(I)=0.0
      DO 4  I=1,3
      XR1(I)=0.0
4     XXR1(I)=0.0
      DO 5 I=1,2
      XR2(I)=0.0
5     XXR2(I)=0.0
102   WRITE(*,*)'PUT IN THE MINIMUM AS AND MAXIMUM AS'
      READ(*,*)AS1,AS2
      WRITE(*,*)'MINIMUM=',AS1,'      MAXIMUM=',AS2
      write(*,*)'FOR MOVING BED CONDITION PUT IN MV=1'
      READ(*,*)MV
      WRITE(*,*)'MV=',MV
      AA=0.25*3.1416*D**2
      DO 100 I=1,30
      ASS(I)=AS1+I*(AS2-AS1)/15.0
      CALL EL(ASS(I),MASF1,MASS1,FAM,FSM,PRS1)
      CALL FL(1,ASS(I),MASF2,MASS2,PRS2)
```

```
      DO 10 LL=1,30
      PRE1(LL)=(PRS1(LL)-PE)/10000.0
      PRE2(LL)=(PRS2(LL)-PE)/10000.0
10    CONTINUE
      CALL FIT(MASF1,MASS1,MASF2,MASS2,XR1,XR2,EFX(I),EFY(I))
100   CALL FIT(MASF1,PRE1,MASF2,PRE2,XXR1,XXR2,PEFX(I),PEFY(I))
      WRITE(*,*)'FOR VELOCITY IN M/S PUT IN 1'
      WRITE(*,*)' FOR MASS FLOW RATE KG/S PUT IN 2'
      READ(*,*)ME
      WRITE(*,*)' YOU PUT IN=',ME
      IF(ME.EQ.1) GOTO 91
      DO 203 I=1,30
      WEFX=EFX(31-I)
      WEFY=EFY(31-I)
      PWEFX=PEFX(31-I)
      PWEFY=PEFY(31-I)*10.0
      WRITE(*,201)WEFX,WEFY,PWEFX,PWEFY,I
201   FORMAT(F8.4,3(5X,F8.4),I4)
203   CONTINUE
      GOTO 103
91    CONTINUE
      DO 204 I=1,30
      WEFX=EFX(31-I)/(AA*ROF)
      WEFY=EFY(31-I)/AA
      PWEFX=PEFX(31-I)
      PWEFY=PEFY(31-I)*10.0
      WRITE(*,101)WEFX,WEFY,PWEFX,PWEFY,I
101   FORMAT(F8.4,3(5X,F8.4),I2)
204   CONTINUE
103   CONTINUE
      DO 104 I=1,30
      XXX(I)=EFX(I)
      YYY(I)=EFY(I)
      XXX2(I)=PEFX(I)
104   YYY2(I)=PEFY(I)*10.0
      WRITE(*,*)'TO CONTINUE PUT IN 1'
      READ(*,*)MY
      IF(MY.EQ.1)GOTO 102
      RETURN
      END
C     ************************************************
C     THIS SUBROUTINE IS FOR CALCAULATING E-LINE AND F-LINE
      SEPARATELY FOR ANY GIVEN THICKNESS OF LAYERS. LINE F
      WILL NOT EXIST IF THE THICKNESS OF LAYER DOES NOT REACH
      CERTAIN VALUE. PUT IN MV=1 FOR ANY F-LINE WITHOUT
      CONSIDERATION ON THE THICKNESS OF LAYER
C     ********************************************** *
      SUBROUTINE TEF
      REAL MXSS1(30),MXSS2(30),MXSF1(30),MXSF2(30),PRE1(30)
     *  ,PRE2(30)
```

```
      COMMON HL,EV,ROS,ROF,PK,WK,G,D,EVM,PE
301   DO 302 J=1,30
      MXSS1(J)=0.0
      MXSS2(J)=0.0
      MXSF1(J)=0.0
302   MXSF2(J)=0.0
      WRITE(*,*)'PUT IN AS '
      READ(*,*)AS
      WRITE(*,*)'AS=',AS
      WRITE(*,*)'PUT IN MV MV=1 MOVING LAYER MAINTAINED'
      READ(*,*)MV
      WRITE(*,*)' MV=',MV
      CALL EL(AS,MXSF1,MXSS1,MXSF2,MXSS2,PRE1)
      WRITE(*,*)'ENTER FL'
      CALL FL(MV,AS,MXSF2,MXSS2,PRE2)
      WRITE(*,*)'OUT  FL'
      WRITE(*,*)'MASF1=,   MASS1=, PRESSURE MASF2= MASS2=
      PRESSURE'
      DO 201 I=1,30
      PRS1=(PRE1(I)-PE)/1000.0
      PRS2=(PRE2(I)-PE)/1000.0
      WRITE(*,101)MXSF1(I),MXSS1(I),PRS1,MXSF2(I),MXSS2(I),PRS2
101   FORMAT(1X,F8.4,5(5X,F8.4))
201   CONTINUE
      WRITE(*,*)'TO CONTINUE PUT IN 1'
      READ(*,*)MY
      IF(MY.EQ.1)GOTO 301
      RETURN
      END
C     ************************************************************
C
C     THIS SUBROUTINE IS FOR CALCAULATING E-LINE AND F-LINE
      SEPARATELY FOR ANY GIVEN THICKNESS OF LAYERS. AND THEN
      PUT TWO LINE TOGETHER FOR A GIVEN THICKNESS OF LAYER

C     ************************************************************
      SUBROUTINE EF
      REAL MZSS1(30),MZSS2(30),MZSF1(30),MZSF2(30),EFX(60),EFY(60),
     *  XR1(3),XR2(2),MF(30),MS(30),PRE1(30),PRE2(30),PRE(30),
     *  PPRE1(30),PPRE2(30),XXR1(3),XXR2(2)
      COMMON HL,EV,ROS,ROF,PK,WK,G,D,EVM,PE
      AA=0.25*3.1416*D**2
131   DO 132 MI=1,30
      PRE1(MI)=0.0
      PRE2(MI)=0.0
      PRE(MI)=0.0
      PPRE1(MI)=0.0
      PPRE2(MI)=0.0
      MZSS1(MI)=0.0
      MZSS2(MI)=0.0
```

```
      MZSF1(MI)=0.0
132   MZSF2(MI)=0.0
      DO 133 MJ=1,60
      EFX(MJ)=0.0
133   EFY(MJ)=0.0
      DO 134 III=1,3
      XR1(III)=0.0
134   XXR1(III)=0.0
      DO 135 JJJ=1,2
      XR2(JJJ)=0.0
135   XXR2(JJJ)=0.0
      WRITE(*,*)'PLEASE PUT IN AS'
      READ(*,*)AS
      WRITE(*,*)'FOR MOVING BED PUT IN MV=1'
      READ(*,*)MV
      WRITE(*,*)' TWO LINE INTO ONE     MV=',MV
      CALL EL(AS,MZSF1,MZSS1,MF,MS,PRE1)
      CALL FL(MV,AS,MZSF2,MZSS2,PRE2)
      CALL  FIT(MZSF1,MZSS1,MZSF2,MZSS2,XR1,XR2,SX,SY)
      DO 141 I=1,30
      PPRE1(I)=(PRE1(I)-PE)/10000.0
141   PPRE2(I)=(PRE2(I)-PE)/10000.0
C     WRITE(*,*)'P-E=',PPRE1(I),'  P-F=',PPRE2(I)
      write(*,*)'enter fit'
      CALL  FIT(MZSF1,PPRE1,MZSF2,PPRE2,XXR1,XXR2,SSX,SSY)
      WRITE(*,*)'X=',SX,'  Y=',SY,'  Z=',SSY
      DO 301 KK=1,60
      IF(MZSF1(KK).LT.SX)THEN
      EFX(KK)=MZSF1(KK)
      EFY(KK)=MZSS1(KK)
      PRE(KK)=PPRE1(KK)
      ELSE
      EFX(KK)=SX
      EFY(KK)=SY
      PRE(KK)=SSY
      NK=KK+1
      GOTO 302
      ENDIF
301   CONTINUE
302   CONTINUE
      DO 303 JK=1,30
      IF(MZSF2(JK).LT.SX)THEN
      NJ=JK
      ELSE
      GOTO 304
      ENDIF
303   CONTINUE
304   DO 305 MM=NK,60
      EFX(MM)=MZSF2(NJ+1)
      EFY(MM)=MZSS2(NJ+1)
```

```
      PRE(MM)=PPRE2(NJ+1)
      NJ=NJ+1
      IF(NJ.EQ.31)GOTO 306
305   CONTINUE
306   WRITE(*,*)'MASF=     MASS=     PRESSURE='
      WRITE(*,*)'FOR VELOCITY IN M/S PUT IN 1'
      WRITE(*,*)' FOR MASS FLOW RATE KG/S PUT IN 2'
      READ(*,*)ME
      WRITE(*,*)' YOU PUT IN=',ME
      IF(ME.EQ.1) GOTO 91
      DO 408 III=1,60,3
      WEFX=EFX(III)
      WEFY=EFY(III)
      PRESS=PRE(III)*10.0
      WRITE(*,407)WEFX,WEFY,PRESS
407   FORMAT(1X,F9.5,2(10X,F9.5))
408   CONTINUE
      GOTO 308
91    CONTINUE
      DO 309 III=1,60,3
      WEFX=EFX(III)/(AA*ROF)
      WEFY=EFY(III)/AA
      PRESS=PRE(III)*10.0
      WRITE(*,307)WEFX,WEFY,PRESS
307   FORMAT(1X,F9.5,10X,F9.5)
309   CONTINUE
308   CONTINUE
      WRITE(*,*)'TO CONTINUE PUT IN 1'
      READ(*,*)MY
      IF(MY.EQ.1)GOTO 131
      RETURN
      END
C     ************************************************************
C     THIS SUBROUTINE IS FOR CALCULATING THE LINE-E WITH ANY
      GIVEN THICKNESS OF LAYER AND COUPLING WITH AIR PRESSURE
      PREDICTION. THE E-LINE IS LOCATED WITHIN TWO RATIOS OF
      VOLUMETRIC FLOW
      RVF1: THE MINIMUM RATIO OF VOLUMETRIC FLOW
      RVF2: THE MAXIMUM RATIO OF VOLUMETRIC FLOW

      RV:   RATIOS OF VOLUMETRIC FLOW
C     ************************************************************
      SUBROUTINE EL(AS,MSF,MSS,MSF2,MSS2,PRE)
      REAL MASS(100),MASF(100),MASS2(100),MASF2(100),
     *MSF(30),MSS(30),MSF2(30),MSS2(30)
      DIMENSION RVF(100),RV(100),BDP(100),BFRI(100),BDP2(100)
     *,BFRI2(100),PRE(30),PRS1(100)
      COMMON HL,EV,ROS,ROF,PK,WK,G,D,EVM,PE
      DO 21 K=1,30
      MSF(k)=0.0
```

```
      MSS(K)=0.0
      MSF2(K)=0.0
21    MSS2(K)=0.0
      DO 22 J1=1,100
      MASS(J1)=0.0
      MASF(J1)=0.0
      MASS2(J1)=0.0
      MASF2(J1)=0.0
      RVF(J1)=0.0
      RV(J1)=0.0
      BDP2(J1)=0.0
      BFRI2(J1)=0.0
      BDP(J1)=0.0
22    BFRI(J1)=0.0
     XX=0.99
     M=1
      IF(AS.GT.0.2)THEN
     RVF1=0.01*(AS+AS*AS+2.0*AS*AS*AS)
      ELSE
      RVF1=0.002
      ENDIF
      RVF2=0.1
     IF(AS.LT.0.01)THEN
     FR=WK
     BBC=1.0
     ELSE
     BBC=(PK/WK)**0.5
     FR=PK
     ENDIF
     XX=EXP((LOG(RVF2)-1.0*LOG(RVF1))/99.0)
     DO 10 I=1,100
     RVF(I)=RVF1*XX**(I-1)
C    RV(I) HERE IS TO DETERMINE THE INITIAL VALUE OF RV FOR
C    FURTHER CALCULATION BELOW
     RV(I)=0.99-(RVF(I)-0.001)*3.6
     AA=3.14159*D**2/4.0
     CONT1=(FR*(ROS/ROF)*(1.0-(ROF/ROS))*(1.0-EV)*D*G)**0.5
     CONT2=ROS*(1.0-EV)/ROF
1    CALL EMM(AS,RVF(I),RV(I),BBB,BDP(I),BBB2,BDP2(I))
     IF(BBB.LE.0.0)GOTO 10
     BFRI(I)=BBB*(1.0-AS)*BBC
     MASF(I)=BBB*CONT1*AA*(1.0-AS)*ROF
     MASS(I)=MASF(I)*RVF(I)*CONT2
     CALL PRIDICT(MASF(I),MASS(I),PRS1(I))
     FPRS1=MASF(I)
     ROF=1.259*PRS1(I)/PE
     CONT1=(FR*(ROS/ROF)*(1.0-(ROF/ROS))*(1.0-EV)*D*G)**0.5
     CONT2=ROS*(1.0-EV)/ROF
     CALL EMM(AS,RVF(I),RV(I),BBB,BDP(I),BBB2,BDP2(I))
     IF(BBB.LE.0)GOTO 10
```

```
      BFRI(I)=BBB*(XM*(1.0-AS))
      MASF(I)=BBB*CONT1*AA*(1.0-AS)*ROF
      MASS(I)=MASF(I)*RVF(I)*CONT2
      CALL PRIDICT(MASF(I),MASS(I),PRS1(I))
      FPRS2=MASF(I)
      ROF=1.259*PRS1(I)/PE
      DPRE=ABS((FPRS2-FPRS1)/FPRS2)
      IF(DPRE.GT.0.005)GOTO 1
      BFRI2(I)=BBB2*(1.0-AS)*BBC
      MASF2(I)=BBB2*CONT1*AA*(1.0-AS)*ROF
      MASS2(I)=MASF2(I)*RVF(I)*CONT2
10    CONTINUE
      DO 11 JIK=1,100
      IF(MASF(JIK).LT.0.0005.AND.MASF(JIK+1).LT.0.0005.
     *  AND.MASF(JIK+3).LT.0.0005)THEN
      NNN=JIK-1
      GOTO 17
      ELSE
      ENDIF
11    CONTINUE
17    L=1
12    DO 13 KK=1,NNN-10,4
      IF(MASF(KK).NE.0.0)THEN
      MSF(L)=MASF(KK)
      MSS(L)=MASS(KK)
      PRE(L)=PRS1(KK)
      L=L+1
      ELSE
      ENDIF
13    CONTINUE
      III=0
      DO 15 II=1,20
      IF(MASF(NNN+1-II-III).EQ.0)THEN
      III=III+1
      ELSE
      ENDIF
      IF(MASF(NNN+1-II-III).EQ.0)THEN
      III=III+1
      ELSE
      ENDIF
      IF(MSF(31-II).EQ.0)THEN
      MSF(31-II)=MASF(NNN+1-II-III)
      MSS(31-II)=MASS(NNN+1-II-III)
      PRE(31-II)=PRS1(NNN+1-II-III)
      ELSE
      GOTO 217
      ENDIF
15    CONTINUE
217   CONTINUE
      DO 31 JN=1,100
```

```
      IF(MASF2(JN).GT.0.001)GOTO 32
31    CONTINUE
32    MJ=JN
      DO 33 JJN=MJ,100
      IF(MASF2(JJN).LT.0.001)GOTO 34
33    CONTINUE
34    MK=JJN
      MM=MK-MJ
      IF(MM.LE.30)GOTO 41
      IF(MM.LE.60)GOTO 42
      IF(MM.LE.90)GOTO 43
41    DO 44 I=1,30
      MSF2(I)=MASF2(MJ-1+I)
44    MSS2(I)=MASS2(MJ-1+I)
      RETURN
42    DO 45 I=1,30
      MSF2(I)=MASF2(MJ-1+I*2)
45    MSS2(I)=MASS2(MJ-1+I*2)
      RETURN
43    DO 46 I=1,30
      MSF2(I)=MASF2(MJ-2+I*3)
46    MSS2(I)=MASS2(MJ-2+I*3)
      RETURN
      END
C     ************************************************************
      THIS SUBROUTINE IS FOR LOCATING A NARROW REGIME ALONG
      THE CURVE OF A CONSTANT RATIO OF VOLUMETRIC FLOW AND
      THEN BY CALLING DEE TO DETERMINE SINGLE POINT OF LINE E.
C     ************************************************************
      SUBROUTINE EMM(AS,RVF,BRV.BFRI1,BDP1,BFRI2,BDP2)
      DIMENSION BDP(3),BFRI(3)
      COMMON HL,EV,ROS,ROF,PK,WK,G,D,EVM,PE
      XX=0.99
      M=1
      DO 99 I=1,3
      BDP(I)=0.0
99    BFRI(I)=0.0
      DF1=0
      BDP1=0
      BFRI1=0
      SFI=1.0-1.0/(1.0+BRV*(1.0/RVF-EV))
      DDP=1.0-SFI
      SFRI=FT1(AS,RVF,SFI)
      IF(PK.LE.WK)THEN
      DPMAX=0.99
      GOTO 315
      ELSE
      ENDIF
      IF(AS.LT.0.01)THEN
      DPMAX=0.99
```

```
      ELSE
      DPMAX=WK*AS/((1.0-AS)*(PK-WK))
      ENDIF
      IF(DPMAX.GE.1.0)THEN
      DPMAX=0.99
      ELSE
      ENDIF
  315 CONTINUE
      XX=EXP((LOG(DPMAX)-1.0*LOG(DDP))/100.0)
      M=1
      X1=DDP
      X2=DDP*xx
      Y1=FT1(AS,RVF,(1.0-X1))
      Y2=FT1(AS,RVF,(1.0-X2))
      SLOP1=(Y2-Y1)/(X2-X1)
      DO 1 I=2,100
      X3=DDP*XX**I
      Y3=FT1(AS,RVF,(1.0-X3))
      SLOP2=(Y3-Y2)/(X3-X2)
      IF((SLOP1*SLOP2).LT.0)THEN
      CALL DEE(AS,X3,X1,RVF,WFRI,WDP)
      BDP(M)=WDP
      BFRI(M)=WFRI
      M=M+1
      ELSE
      ENDIF
      X1=X2
      X2=X3
      Y1=Y2
      Y2=Y3
      SLOP1=SLOP2
    1 CONTINUE
      BFRI1=BFRI(1)
      BFRI2=BFRI(2)
      BDP1=BDP(1)
      BDP2=BDP(2)
      RETURN
      END
C     ************************************************************
C     THIS SUBROUTINE IS FOR DETERMINING A SINGLE POINT OF LINE
      E ALONG THE CURVE OF A CONSTANT RATIO OF VOLUMETRIC
      FLOW WITHIN A VERY NARROW REGIME OF Fri. THE LIMITATIONS
      OF THE REGIME ARE ALREADY KNOWN AND AS THE INPUT FOR
      THIS SUBROUTINE
C     ************************************************************
      SUBROUTINE DEE(AS,DPMAX,DPMIN,RVF,BFRI,BDP)
      COMMON HL,EV,ROS,ROF,PK,WK,G,D,EVM,PE
      XX=EXP((LOG(DPMAX)-1.0*LOG(DPMIN))/100.0)
      X1=DPMIN
      X2=DPMIN*XX
```

```
      Y1=FT1(AS,RVF,(1.0-X1))
      Y2=FT1(AS,RVF,(1.0-X2))
      SLOP1=(Y2-Y1)/(X2-X1)
      DO 1 I=2,100
      X3=DPMIN*XX**I
      Y3=FT1(AS,RVF,(1.0-X3))
      SLOP2=(Y3-Y2)/(X3-X2)
      IF((SLOP1*SLOP2).LT.0)THEN
      BDP=X2
      BFRI=Y2
      GOTO 2
      ELSE
      ENDIF
      X1=X2
      X2=X3
      Y1=Y2
      Y2=Y3
      SLOP1=SLOP2
1     CONTINUE
2     CONTINUE
      RETURN
      END
C       ************************************************
C       ************************************************
C       ************************************************
      FUNCTION FT1(AS,RVF,FI)
      COMMON HL,EV,ROS,ROF,PK,WK,G,D,EVM
      RV=(FI/(1.0-FI))/(1.0/RVF-EV)
      IF(RV.GT.1.0)THEN
      RV=0.999
      ELSE
      ENDIF
      IF(AS.LT.0.01)GOTO 10
      A=3.1416*(1.0-AS)/(4.0*HL)
      B1=(1.0-FI)*FI**3
      B2=(4.0*(1.0-AS)*FI*(1.0-FI*(1.0-AS)))
      B=B1/B2**0.333
      C=1.0/(1-RV)
      DD=1.0/(1.0-RVF*EV)
      FT1=(A*B*C*DD)**0.5
      RETURN
10    A=3.1416/(4.0*HL)
      B=(1.0-FI)*FI**3/(4.0*FI*(1.0-FI))**0.333
      C=1.0/(1-RV)
      DD=1.0/(1.0-RVF*EV)
      FT1=(A*B*C*DD)**0.5
      RETURN
      END
C       ************************************************************
```

```
C     THIS SUBROUTINE IS FOR CALCULATING THE LINE-F WITH ANY
      GIVEN THICKNESS OF LAYER AND COUPLING WITH AIR PRESSURE
      PREDICTION. THE F-LINE IS LOCATED WITHIN TWO RATIOS OF
      STRAND VELOCITY TO SUSPENSION VELOCITY
      RV1: THE MINIMUM RATIO OF STRAND VELOCITY TO SUSPENSION
      VELOCITY.
      RV2: THE MAXIMUM RATIO OF STRAND VELOCITY TO
      SUSPENSION VELOCITY
      RV:  RATIOS OF STRAND VELOCITY TO SUSPENSION VELOCITY
C     ************************************************************
      SUBROUTINE FL(MV,AS,MASF,MASS,PRESS)
      REAL MASS(30),MASF(30),PRESS(30)
      DIMENSION RV(30),BDP(30),BFRI(30),RRVF(30)
      COMMON HL,EV,ROS,ROF,PK,WK,G,D,EVM,PE
      DO 7 II=1,30
      RV(II)=0.0
      BDP(II)=0.0
      BFRI(II)=0.0
      RRVF(II)=0.0
      MASS(II)=0.0
7     MASF(II)=0.0
      XM=(PK/WK)**0.5
      RV1=0.065
      RV2=0.5
      IF(AS.LT.0.001.OR.PK.LE.WK)THEN
      XM=1.0
      FR=WK
      ELSE
      FR=PK
      ENDIF
      XX=(RV2-RV1)/29.0
      A=3.14159*D**2/4.0
      CONT1=(FR*(ROS/ROF)*(1.0-(ROF/ROS))*(1.0-EV)*D*G)**0.5
      CONT2=ROS*(1.0-EV)/ROF
      DO 10 I=1,30
      RV(I)=RV1+XX*(I-1)
      KKK=1
1     CONTINUE
      CALL FMM(MV,AS,RV(I),BBB,BDP(I),RRVF(I))
      BBB1=BBB
      IF(BBB.EQ.0.0)THEN
      BBB=BBB2
      ELSE
      ENDIF
      KKK=KKK+1
      BFRI(I)=BBB*(XM*(1.0-AS))
      MASF(I)=BBB*CONT1*AA*(1.0-AS)*ROF
      MASS(I)=MASF(I)*RRVF(I)*CONT2
      IF(BBB.EQ.0.0)THEN
      PRESS(I)=PE
```

```
      ELSE
      CALL PRIDICT(MASF(I),MASS(I),PRESS(I))
      ENDIF
      FPRS1=MASF(I)
      ROF=1.259*PRESS(I)/PE
      CONT1=(FR*(ROS/ROF)*(1.0-(ROF/ROS))*(1.0-EV)*D*G)**0.5
      CONT2=ROS*(1.0-EV)/ROF
      CALL FMM(MV,AS,RV(I),BBB,BDP(I),RRVF(I))
      BBB2=BBB
      IF(BBB.EQ.0.0)THEN
      BBB=BBB1
      ELSE
      ENDIF
      IF(BBB.EQ.0.0)GOTO 10
      BFRI(I)=BBB*(XM*(1.0-AS))
      MASF(I)=BBB*CONT1*AA*(1.0-AS)*ROF
      MASS(I)=MASF(I)*RRVF(I)*CONT2
      IF(BBB.EQ.0.0)GOTO 10
      CALL PRIDICT(MASF(I),MASS(I),PRESS(I))
      ROF=1.259*PRESS(I)/PE
      FPRS2=MASF(I)
      DPRE=ABS((FPRS2-FPRS1)/FPRS2)
      IF(KKK.GT.20)GOTO 10
      IF(DPRE.GT.0.005)GOTO 1
      CONTINUE
10    RETURN
      END
C     ****************************************************************
      THIS SUBROUTINE IS FOR DETERMINING A NARROW REGIME
      ALONG THE CURVE OF A CONSTANT RATIO OF STRAND VELOCITY
      TO SUSPENSION AIR VELOCITY WHERE A POINT OF LINE F MAY
      LOCATED IN. BY CALLING THE SUBROUTINE DFF THE POINT ON
      LINE F WITH A CERTAIN VALUE OF THE RATIO OF STRAND
      VELOCITY TO SUSPENSION AIR VELOCITY CAN BE FINALLY
      ACHIEVED
c     ****************************************************************
      SUBROUTINE FMM(MV,AS,RV,BFRI1,BDP1,RRVF)
      DIMENSION BDP(3),BFRI(3),RVFF(3)
      COMMON HL,EV,ROS,ROF,PK,WK,G,D,EVM,PE
      XX=0.99
      M=1
      X4=0
      DDP=0.1
      IF(PK.LE.WK)THEN
      DPMAX=0.99
      ELSE
      ENDIF
      IF(AS.LT.0.005)THEN
      DPMAX=0.99
      ELSE
```

```
C      **************  *************  ********
      UP=WK*AS*(1.0-EVM)
      DW=(PK*(1.0-AS*ROF/ROS)-WK*(1.0-AS))*(1.0-EV)
      DPMAX=UP/DW
C      *********   **********   ****************
      ENDIF
      IF(DPMAX.GE.1.0)THEN
      WRITE(*,*)'DOMAX=',DPMAX
      DPMAX=0.99
      ELSE
      ENDIF
C      ************************************************
      IF(MV.EQ.1)THEN
      DPMAX=0.99
      ELSE
      ENDIF
C      ************************************************
114   CONTINUE
      DO 99 I=1,3
      BDP(I)=0.0
99    BFRI(I)=0.0
      DTP=(DPMAX-DDP)/199.0
      XX1=DDP
      XX2=DDP+DTP
      YY1=FT(AS,RV,(1.0-XX1))
      YY2=FT(AS,RV,(1.0-XX2))
      SLOP1=(YY2-YY1)/(XX2-XX1)
      DO 10 I=2,200
      XX3=DDP+I*DTP
      YY3=FT(AS,RV,(1.0-XX3))
      SLOP2=(YY3-YY2)/(XX3-XX2)
      IF((SLOP1*SLOP2).LT.0)THEN
      CALL  DFF(AS,RV,XX3,XX1,FRRI,DDPP,RVVF)
      BDP(M)=DDPP
      BFRI(M)=FRRI
      RVFF(M)=RVVF
      M=M+1
      GOTO 101
      ELSE
      ENDIF
      SLOP1=SLOP2
      XX1=XX2
      XX2=XX3
      YY1=YY2
      YY2=YY3
10    CONTINUE
101   CONTINUE
      BDP1=BDP(1)
      BFRI1=BFRI(1)
      RRVF=RVFF(1)
```

```
      RETURN
      END
C     ************************************************************
      THIS SUBROUTINE IS FOR DETERMINING A SINGLE POINT OF LINE
      F ALONG THE CURVE OF A CONSTANT RATIO OF STRAND
      VELOCITY TO SUSPENSION AIR VELOCITY WITHIN A VERY
      NARROW REGIME OF Fri. THE LIMITATIONS OF THE REGIME ARE
      ALREADY KNOWN AND AS THE INPUT FOR THIS SUBROUTINE.
C     ************************************************************
      SUBROUTINE DFF(AS,RV,DMAX,DMIN,FRI,DP,RVF)
      COMMON HL,EV,ROS,ROF,PK,WK,G,D,EVM,PE
      DTP=(DMAX-DMIN)/199.0
      XX1=DMIN
      XX2=DMIN+DTP
      YY1=FT(AS,RV,(1.0-XX1))
      YY2=FT(AS,RV,(1.0-XX2))
      SLOP1=(YY2-YY1)/(XX2-XX1)
      DO 10 I=2,200
      XX3=DMIN+I*DTP
      YY3=FT(AS,RV,(1.0-XX3))
      SLOP2=(YY3-YY2)/(XX3-XX2)
      IF((SLOP1*SLOP2).LT.0)THEN
      DP=XX2
      FRI=YY2
      X4=1.0-XX2
      RVF=1.0/(EV+X4/((1.0-X4)*RV))
      GOTO 1
      ELSE
      ENDIF
      SLOP1=SLOP2
      XX1=XX2
      XX2=XX3
      YY1=YY2
      YY2=YY3
10    CONTINUE
1     CONTINUE
      RETURN
      END
C     ************************************************************
C     ************************************************************
C     ************************************************************
      FUNCTION FT(AS,RV,FI)
      COMMON HL,EV,ROS,ROF,PK,WK,G,D,EVM,PE
      RVF=1.0/(EV+FI/((1.0-FI)*RV))
      IF(AS.LT.0.01)GOTO 10
      A=3.1416*(1.0-AS)/(4.0*HL)
      B=(1.0-FI)*FI**3/(4.0*(1.0-AS)*FI*(1.0-FI*(1.0-AS)))**0.333
      C=1.0/(1-RV)
      DD=1.0/(1.0-RVF*EV)
      FT=(A*B*C*DD)**0.5
```

```
      RETURN
10    A=3.1416/(4.0*HL)
      B=(1.0-FI)*FI**3/(4.0*FI*(1.0-FI))**0.333
      C=1.0/(1-RV)
      DD=1.0/(1.0-RVF*EV)
      FT=(A*B*C*DD)**0.5
      RETURN
      END

C     ************************************************************
C     THIS SUBROUTINE IS DIRECTLY FOR CALCULATING THE
      CROSSING POINT OF TWO SEGMENTS OF BOUNDARY B.
      SX:   AIR MASS FLOW RATE OF THE CROSSING POINT
      SY:   SOLIDS MASS FLOW RATE OF THE CROSSING POINT
C     ************************************************************
      SUBROUTINE FIT(SF1,SS1,SF2,SS2,XR1,XR2,SX,SY)
      DIMENSION X1(10),Y1(10),X2(10),Y2(10),AC1(3,3),AC2(3,3),
     *  B1(3),B2(3),XR1(3),XR2(3),SF1(30),SS1(30),SF2(30),SS2(30)
      DOUBLE PRECISION AC1,AC2
      DO 2 J=1,10
      X1(J)=0.0
      Y1(J)=0.0
      X2(J)=0.0
2     Y2(J)=0.0
      DO 3 JJ=1,3
      B1(JJ)=0.0
      B2(JJ)=0.0
      XR1(JJ)=0.0
3     XR2(JJ)=0.0
      DO 4 M=1,3
      DO 4 N=1,3
      AC1(M,N)=0.0
4     AC2(M,N)=0.0
      DO 1 I=1,10
      X1(I)=SF1(19+I)
      Y1(I)=SS1(19+I)
      X2(I)=SF2(I+2)
      Y2(I)=SS2(I+2)
1     CONTINUE
      CALL LSSQ(X1,Y1,10,2,AC1,B1)
      CALL LSSQ(X2,Y2,10,1,AC2,B2)
      CALL GAUSS(AC1,B1,XR1,3,3,DEP1)
      CALL GAUSS(AC2,B2,XR2,2,2,DEP2)
      A=XR1(3)
      B=XR1(2)-XR2(2)
      C=XR1(1)-XR2(1)
      SX=(-(B*B-4.0*A*C)**0.5-B)/(2.0*A)
      SY=XR2(1)+XR2(2)*SX
      WRITE(*,*)'SX=',SX,'     SY=',SY
      RETURN
```

```
      END
C     ************************************************************
C     THIS SUBROUTINE IS DIRECTLY FOR CALCULATING THE
      CROSSING POINT OF TWO SEGMENTS OF BOUNDARY B.
      SX:   AIR MASS FLOW RATE OF THE CROSSING POINT
      SY:   SOLIDS MASS FLOW RATE OF THE CROSSING POINT
C     ************************************************************
      SUBROUTINE FIT2(SF1,SS1,SF2,SS2,XR1,XR2,SX,SY)
      DIMENSION X1(10),Y1(10),X2(10),Y2(10),AC1(3,3),AC2(3,3),
     * B1(3),B2(3),XR1(3),XR2(3),SF1(30),SS1(30),SF2(30),SS2(30)
      DOUBLE PRECISION AC1,AC2
      DO 2 J=1,10
      X1(J)=0.0
      Y1(J)=0.0
      X2(J)=0.0
2     Y2(J)=0.0
      DO 3 JJ=1,3
      B1(JJ)=0.0
      B2(JJ)=0.0
      XR1(JJ)=0.0
3     XR2(JJ)=0.0
      DO 4 M=1,3
      DO 4 N=1,3
      AC1(M,N)=0.0
4     AC2(M,N)=0.0
      DO 1 I=1,10
      X1(I)=SF1(19+I)
      Y1(I)=SS1(19+I)
      X2(I)=SF2(I+2)
      Y2(I)=SS2(I+2)
1     CONTINUE
      CALL LSSQ(X1,Y1,10,1,AC1,B1)
      CALL LSSQ(X2,Y2,10,1,AC2,B2)
      CALL GAUSS(AC1,B1,XR1,2,2,DEP1)
      CALL GAUSS(AC2,B2,XR2,2,2,DEP2)
      SX=-(XR2(1)-XR1(1))/(XR2(2)-XR1(2))
      SY=XR2(1)+XR2(2)*SX
      WRITE(*,*)'SX=',SX,'     SY=',SY
      RETURN
      END
C     ************************************************************
      THIS SUBROUTINE IS FOR CALCULATING THE CROSS POINT OF
      TWO SEGMENTS OF BOUNDARY B WHICH ARE REPRESENTED BY
      TWO POLYNOMIAL EQUATIONS BY THE GAUSS-JORDAN METHOD.
C     ************************************************************
C     A( )----COEFFICIENT MATRIX
C     B( )----RIGHT SIDE VECTOR
C     X( )----SOLUTION VECTOR
C     ND------SIZE OF ARRAY A( )
C     N-------SIZE OF THE ARRAY IN GAUSS ND > OR =N
```

```
c     ************************************************
      SUBROUTINE GAUSS(A,B,X,ND,N,DEP)
      INTEGER ND,N,IPV
      DOUBLE PRECISION A(3,3),C(3)
      REAL B(3),X(3),DET,PIVOT,FCTR
      DO 30 K=1,3
      C(K)=0.0
30    X(K)=0.0
      DO 10 IPV=1,N
      DO 2 I=1,N
      C(I)=A(I,IPV)
      B(I)=B(I)/(100.0*C(I))
      B(I)=100.0*B(I)
      DO 2 J=1,N
      A(I,J)=A(I,J)/(C(I)*100.0)
      A(I,J)=A(I,J)*100.0
2     CONTINUE
      DO 3 I=1,N
      IF(I.EQ.IPV)THEN
      CONT=0.0
      ELSE
      CONT=1.0
      ENDIF
      B(I)=B(I)-B(IPV)*CONT
      DO 3 J=IPV,N
      A(I,J)=A(I,J)-A(IPV,J)*CONT
3     CONTINUE
10    CONTINUE
      DO 20 I=1,N
      X(I)=B(I)/A(I,I)
20    CONTINUE
      RETURN
      END
C     ************************************************************
        THIS SUBROUTINE IS FOR A POLYNOMIAL LEAST SQUARES CURVE
        FIT. WHEN CALCULATING THE BOUNDARY B WHICH CONSISTS OF
        TWO PARTS AND WANT TO KNOW THE CROSSING PONT OF TWO
        PARTS. THE TWO PARTS ARE TRANSFORMED INTO TWO
        POLYNOMIALS. THEN THE CROSSING PONT CAN BE OBTAINED BY
        SOLUTING TWO POLYNOMIAL EQUATIONS.
c     x( ),y(0)------EXPERIMENTAL DATA          INPUT
C     NDATA----------NUMBER OF DATA POINTS      INPUT
C     NP-------------DEGREE OF POLYNOMIAL FIT   INPUT
C     AC( )----------COEFFICIENT MATRIX
C     B( )-----------RIGHT SIDE VECTOR OF SUM[X**N*Y]
C     D( )-----------ELEMENTS OF AC
C     ************************************************
      SUBROUTINE LSSQ(XX,YY,NDATA,NP,AC,B)
      INTEGER NDATA,NP,FAIL
      DOUBLE PRECISION AC(3,3),DXY(20),X(10),Y(10)
```

```
      REAL XX(NDATA),YY(NDATA),B(3),DET
C     ******* COMPUTE THE ELEMENTS OF THE D ARRAY *******
        DO 20 I=1,10
        X(I)=0.0
20      Y(I)=0.0
        DO 21 I=1,20
21      DXY(I)=0.0
        DO 22 I=1,3
22      B(I)=0.0
        DO 24 M=1,3
        DO 24 N=1,3
24      AC(M,N)=0.0
      DO 119 I=1,10
      X(I)=XX(I)
119     Y(I)=YY(I)
      FAIL=0.0
      DO 2 K=1,2*NP
      DXY(K)=0.0
      DO 1 I=1,NDATA
      DXY(K)=DXY(K)+X(I)**K
1     CONTINUE
2     CONTINUE
C     **** ASSIGN VALUES TO THE AC ARRAY *************
      SOS=NDATA
      AC(1,1)=SOS
      DO 3 I=1,NP+1
      DO 3 J=1,NP+1
      K=I+J-2
      IF(K.NE.0)THEN
      AC(I,J)=DXY(K)
      ELSE
      AC(I,J)=SOS
      ENDIF
3     CONTINUE
C     ****** RIGHT SIDE VECTOR IS OF SUM[X(I)**N*Y] ******
      DO 5 K=1,NP+1
      B(K)=0
      DO 4 I=1,NDATA
      TERM=Y(I)*X(I)**(K-1)
      B(K)=B(K)+TERM
4     CONTINUE
5     CONTINUE
      RETURN
      END
C       ***************************************************************C
        THIS SUBROUTINE IS FOR PRESSURE DROP PREDICTION FOR THE
        PIPELINE 21M IN LENGTH. THE WHOLE PIPE IS SEPARATED INTO
        TEN SEGMENTS AND THE CALCAULATION IS CONDUCTED FROM
        THE OUTLET TO INLET STEP BY STEP. IF THE LENGTH OF THE
```

```
      PIPELINE CHANGED, OTHER PARAMETERS ALL SHOULD BE
      CHANGED.

      AF:     RATIO OF THE AREA OCCUPIED BY LAYER
      DL:     THE LENGTH OF A SEGMENT
      DD:     PARTICLE DIAMETER
      LT:     THE LENGTH OF THE WHOLE PIPELINE
      LS:     LENGTH OF A SLUG
      KW:     STRESS TRANSMISSION COEFFICIENT
      US:     SLUG VELOCITY
      UP:     PARTICLE VELOCITY
      MSF:    AIR MASS FLOW RATE
      MSS:    SOLIDS MASS FLOW RATE
      PRESS: PRESSURE DROP ACROSS THE PIPELINE

C
C     *************   PRESSURE DROP   ***********************

C     ************************************************************
      SUBROUTINE PRIDICT(MSF,MSS,PRESS)
      REAL KW,LS,MSF,MSS,LT
      DIMENSION USS(11),PPD(11)
      COMMON HL,EV,ROS,ROF,PK,WK,G,D,EVM,PE
      IF(MSF.EQ.0.0.OR.MSS.EQ.0.0)THEN
      PRESS=PE
        GOTO 1
      ELSE
        ENDIF
      ROSS=ROS*(1.0-EV)
      DL=2.1
      LT=21.0
      ET=1.81E-5
      DD=0.0045
      A=0.25*3.1416*D*D
      ROF1=1.259
      PE=101325
      LS=1.0
      KW=0.4
C     ********************************************************
C     ****   ****   ****   ****  ***  ****   ****
C     ********************************************************
      USS(1)=3.5
      PPD(1)=PE
      DO 100 I=2,11
      US=USS(I-1)
      PD=PPD(I-1)
10     CALL FRICT(LS,US,DL,MSS,DP,DTP,ROSS,ET,DD,A,ROF1,KW)
      P=PD+DTP
      CALL ERGUN(MSF,P,DP,US1,ROSS,ET,DD,A,ROF1)
      DT=ABS((US1-US)/US1)
```

```
      IF(DT.GT.0.002)THEN
      US=US1
      GOTO 10
      ELSE
      USS(I)=US1
      PPD(I)=P
      ENDIF
100   CONTINUE
      PRESS=PPD(11)
1     CONTINUE
      RETURN
      END
      SUBROUTINE FRICT(LS,US,DL,MSS,DP,DTP,ROSS,ET,DD,A,ROF1,KW)
      REAL KW,LS,MSF,MSS,LT
      COMMON HL,EV,ROS,ROF,PK,WK,G,D,EVM,PE
      AF=0.542*(G*D)**0.5/US
      IF(AF.GT.0.99)THEN
      AF=0.99
      RETURN
      ELSE
      ENDIF
C     ****************************************
      IF(AF.LT.0.50)THEN
      Z=-1.0
      ELSE
      Z=1.0
      ENDIF
      S=D*(4.0*AF*(1.0-AF))**0.3333
      HH=(D+Z*(D*D-S*S)**0.5)/2.0
C     ************************************
      WF=WK*ROSS*G*A*LS
      FF1=AF*(1.0-AF)*ROSS*US*US+(D-HH)*ROSS*G/KW
      RKW=FKW(FF1)
      FF1=AF*(1.0-AF)*ROSS*US*US+(D-HH)*ROSS*G/RKW
      RKW=FKW(FF1)
      FF1=AF*(1.0-AF)*ROSS*US*US+(D-HH)*ROSS*G/RKW
      RKW=FKW(FF1)
      FF1=AF*(1.0-AF)*ROSS*US*US+(D-HH)*ROSS*G/RKW
      FF3=3.1415*D*WK*RKW*FF1*(LS-D/(4.0*WK*RKW))
      PER=MSS/(A*(1-AF)*ROSS*US)
      DP=(WF+FF1*A+FF3)/(LS*A)
      DTP=PER*DL*DP
      RETURN
      END
      SUBROUTINE ERGUN(MSF,P,DP,US,ROSS,ET,DD,A,ROF1)
      REAL LS,MSF,MSS,LT
      COMMON HL,EV,ROS,ROF,PK,WK,G,D,EVM,PE
      PP=P+DP
      ROF=ROF1*PP/PE
      AROF=(P+0.5*DP)*ROF1/PE
```

```
A1=1.75*(1.0-EV)*AROF/(DD*EV**3)
B1=150*ET*(1-EV)**2/(DD*DD*EV**3)
C1=-DP
USL=((B1*B1-4*A1*C1)**0.5-B1)/(2.0*A1)
UP=MSF/(A*ROF)-USL
US=UP+0.542*(G*D)**0.5
RETURN
  END
FUNCTION FKW(S)
A=0.75
B=1.2E-3
C=1.6E-6
W=-B*(S-150.0)-C*(S-150.0)**2
FKW=A*(1.0-EXP(W))
RETURN
END
```

PUBLICATIONS WHILE PHD CANDIDATE

1 J Yi, PW Wypych and R Pan: Evaluation of Existing Correlations for Minimum Conveying Velocity, 6th International Conference on Bulk Materials Storage, Handling and Transportation, Wollongong, Australia, Sept. 28-30, 1998, pp191-198.

2 R Pan, PW Wypych and J Yi: Design of Low-Velocity Slug-Flow Pneumatic Conveying Systems, 6th International Conference on Bulk Materials Storage, Handling and Transportation, Wollongong, Australia , Sept. 28-30, 1998, pp211-218.

3 J Yi, PW Wypych and R Pan: Minimum Conveying Velocity in Dilute-Phase Pneumatic Conveying, Powder Handling & Processing, Vol. 10, No. 3, 1998, pp 255-261.

4 J Yi, PW Wypych and R Pan: Effect of Pipe Wall Roughness on Dilute-Phase Minimum Conveying Velocity, Powder Handling & Processing, Vol. 12, No. 3, 2000, pp 235-237.

5 J Yi, and PW Wypych: Modelling the unstable boundary for low-velocity slug-flow conveying, The 3rd Israel Conf. For Conveying and Handling of Particulate Solids, 2000, The Dead Sea, Israel, pp 10.11-10.17.

6 PW Wypych and J Yi: Dense-Phase Pneumatic Conveying of Poly Granules, The 6th World Congress of Chemical Engineering, Melbourne, Australia, Sept. 23-27, 2001.

7 J Yi, PW Wypych and DB Hastie: Mechanism for Unstable Pneumatic Conveying of Granular Materials through Horizontal Pipe, The 7th International Conference on Bulk Materials, Storage, Handling and Transportation, Newcastle, Australia, Oct. 3-5, 2001.

8 J Yi, and PW Wypych: Management of Air Mass Flow Rate for Low-Velocity Slug Flow, The 7th International Conference on Bulk Materials, Storage, Handling and Transportation, Newcastle, Australia, Oct. 3-5, 2001.

9 J Yi, and PW Wypych: Stress Transmission Factor and Pressure Drop Prediction for Low-Velocity Slug Flow, The 7th International Conference on Bulk Materials, Storage, Handling and Transportation, Newcastle, Australia, Oct. 3-5, 2001.

10 PW Wypych, DB Hastie and J Yi, Using Low-Velocity Pneumatic Conveying for Fragile Particle, Australian Bulk Handling Review, August/September, 2001, pp58-63.